



Universidad de Valladolid

ESCUELA DE INGENIERÍA INDUSTRIALES

DEPARTAMENTO DE INGENIERÍA QUÍMICA Y
TECNOLOGÍA DEL MEDIO AMBIENTE

TESIS DOCTORAL:

STUDY OF THE IMPROVEMENT OF
CELLULOSE PROCESSING IN IONIC
LIQUID BY USING CARBON DIOXIDE

Presentada por Joana Maria Cristóvão Lopes
para optar al grado de
doctora con mención internacional por la
Universidad de Valladolid

Dirigida por:
Doctora María Dolores Bermejo Roda
Profesora Doctora María José Cocero Alonso

UNIVERSIDAD DE VALLADOLID

ESCUELA DE INGENIERÍAS INDUSTRIALES

Secretaría

La presente tesis doctoral queda registrada en el folio N° _____
del correspondiente Libro de Registro con el N° _____

Valladolid, a _____ de _____ de 2016

Fdo. El encargado del Registro

María Dolores Bermejo Roda

Investigadora Ramón y Cajal del Departamento de Ingeniería Química

y Tecnología del Medio Ambiente

Universidad de Valladolid

y

María José Cocero Alonso

Catedrática del Departamento de Ingeniería Química

y Tecnología del Medio Ambiente

Universidad de Valladolid

CERTIFICAN QUE:

JOANA MARIA CRISTÓVÃO LOPES ha realizado bajo su dirección el trabajo ***“STUDY OF THE IMPROVEMENT OF CELLULOSE PROCESSING IN IONIC LIQUID BY USING CARBON DIOXIDE”***, en el Departamento de Ingeniería Química y Tecnología del Medio Ambiente de la Escuela de Ingenierías Industriales de la Universidad de Valladolid. Considerando que dicho trabajo reúne los requisitos para ser presentado como Tesis Doctoral expresan su conformidad con dicha presentación.

Valladolid a ____ de _____ de 2016.

Fdo. María José Cocero Alonso

Fdo. María Dolores Bermejo Roda

Reunido el tribunal que ha juzgado la tesis doctoral "**STUDY OF THE IMPROVEMENT OF CELLULOSE PROCESSING IN IONIC LIQUID BY USING CARBON DIOXIDE**" presentada por Joana Maria Cristóvão Lopes y en cumplimiento con lo establecido por el Real Decreto 861/2010 (BOE 28.01.2011) ha acordado conceder por _____ la calificación de _____.

Valladolid, a de de 2016

PRESIDENTE

SECRETARIO

1^{er} Vocal

2^{do} Vocal

3^{er} Vocal

Content

Introduction, objectives and summary	11
Part I. State of the art.....	15
Chapter 1. Ionic liquid as reaction media for the production of cellulose-derived polymers from cellulosic biomass byproducts.....	17
Part II. Thermodynamic properties of mixtures of ionic liquid + CO ₂	69
Chapter 2. Melting Point Depression Effect with CO ₂ in High Melting Temperature Cellulose Dissolving Ionic Liquids. Modeling with Group Contribution Equation of State	71
Chapter 3. Experimental determination of viscosities and densities of mixtures carbon dioxide + 1-allyl-3-methylimidazolium chloride.....	113
Part III. Influence of CO ₂ as reaction media in dissolution and acetylation of cellulose.....	127
Chapter 4. Analysis of the synthesis of cellulose acetate in ionic liquids. Experimental study, modeling and use of additives and co-solvents	129
Part IV. Recovery of valuable products	165
Chapter 5. Cellulose aerogels regenerated from microcrystalline cellulose + ionic liquid solution: properties and drug loading capacity study.....	167
Conclusions and Future Work	187
Resumen.....	193
Acknowledgements	205
About the author.....	207

Contenido

Introducción, objetivos y resumen	11
Parte I. Estado del Arte.....	15
Capitulo 1. Líquido iónico como medio de reacción para la producción de polímeros derivados de la celulosa de la biomasa celulósica por productos.....	17
Parte II. Propiedades termodinámicas de las mezclas de líquido iónico + CO ₂	69
Capitulo 2. Efecto de CO ₂ en la disminución del punto de fusión en líquidos iónicos con alta temperatura de fusión capaces de disolver celulosa. Modelado con la ecuación de estado de contribución de grupos	71
Capitulo 3. Determinación experimental de viscosidades y densidades de mezclas dióxido de carbono + cloruro de + 1-alil-3-metilimidazolio	113
Parte III. Influencia de CO ₂ en la disolución y la acetilación de celulosa en líquidos iónicos.....	127
Capitulo 4. Análisis de la síntesis de acetato de celulosa en líquidos iónicos. Estudio experimental, el modelado y el uso de aditivos y codisolventes	129
Parte IV. La recuperación de productos valiosos	165
Capitulo 5. Aerogeles de celulosa regenerada a partir de celulosa microcristalina disuelta en líquidos iónicos. Propiedades y estudio de la capacidad de carga de fármaco	167
Conclusiones y trabajo futuro	187
Resumen.....	193
Agradecimientos	207
Sobre la autora	209

Introduction, objectives and summary

Study of the improvement of cellulose processing in ionic liquid by using carbon dioxide

The capacity of the ionic liquids (ILs) of dissolving high concentrations of cellulose and/or lignin at relatively low temperatures makes them promising solvents for the processing of lignocellulosic biomass waste. Many applications have been proposed over the years: pre-treatment for fermentation processes, chemical transformations for obtaining chemical or biofuels and substitution reaction for obtaining cellulose derived polymers among others. The use of ionic liquids has a number of advantages determined by the unique combination of their properties. Ionic liquids are a group of salts that exist as liquids at relatively low temperatures (<100 °C). Their properties can be tuned by appropriate selection of cation and anion, and they have an immeasurably low vapor pressure that makes them to be considered as green solvents.

Several aspects of cellulose processing in ILs have been reviewed and analyzed in State of the Art. The advantages and disadvantages of using ILs in cellulose derivatization were discussed for esterification and etherification of cellulose. The main limitation of these processes is the high viscosity that is highly increased when ILs dissolve cellulose. It is known that when the ILs dissolves small amounts of molecular solvents their viscosity is drastically decreased. Carbon dioxide presents high solubilities in ILs even at low pressures thus, influencing their thermophysical properties and cellulose substitution reactions.

Carbon dioxide presents as a promising co-solvent for the ionic liquid processing of lignocellulose as it is an inert gas without environmental limitation that, and can be easily separated of the mixture by depressurization.

The aim of this work is study how CO₂ can improve different aspects of biomass processing using ionic liquids. To accomplish the aim of this thesis several aspects have been taken into account

- 1) Effect of the CO₂ in the properties of mixtures CO₂ + ILs: phase equilibrium, melting points, viscosities and densities.
- 2) Analysis of the influence of CO₂ in reaction processes, specifically in substitution reactions in order to produce cellulose-derived polymers. To do so the well known synthesis of cellulose acetate is chosen as model reaction.
- 3) Study the application of CO₂ in recovering valuable materials derived from cellulose. To accomplish this objective the preparation of cellulose aerogels from ionic liquids by supercritical drying will be obtained.

In order to achieve the objectives the work was structured in four parts.

In the first part the state of the art is reviewed in chapter 1 where subjects of the mechanism of dissolution of cellulose, the use of ionic liquids in pretreatment and substitution reactions are thoroughly revised. In additions other subjects not so directly related as toxicity and recyclability of ILs are considered because there are important for the commercial development of these processes

In the second part properties of the mixtures CO₂ + cellulose dissolving ionic liquids are studied. This part has two chapters:

In Chapter 2 “Melting point depression effect with CO₂ in high melting temperature cellulose dissolving ionic liquids. Modeling with Group Contribution Equation of State” the effect of pressurized carbon dioxide on the melting point depression (MPD) of some ILs able to dissolve biopolymers was experimentally determined by observation of the first sign of melt on the solid surface. Five different ILs were studied in contact with carbon dioxide using a high-pressure visual cell, up to 10 MPa. To correlate the MPD of imidazolium chloride ILs the parameters for the Group Contribution Equation of State of Skold-Jorgensen were adjusted using literature data of liquid vapour and activity coefficient and infinite dilution. In this way a predictive correlation for calculating the solubility of CO₂ in different ILs of the alkylimidazolium chloride family was obtained.

In Chapter 3 “Experimental determination of viscosities and densities of mixtures carbon dioxide + 1-allyl-3-methylimidazolium chloride. Viscosity correlation” the study of the effect of CO₂ on the viscosity and density of the ionic liquid [Amim][Cl] is presented. Viscosities were correlated as a function of temperature and CO₂ molar fractions. The viscosities of other mixtures CO₂ + ILs were also correlated for other ILs. In general [Amim][Cl] and the other ILs present a linear decrease of viscosity with CO₂ molar fractions up to around 0.5 mol that more pronounced at lower temperatures and depends of each ionic liquid, and can reach between 60-100% viscosity reduction with respect the viscosity of the pure ionic liquid.

In the third part of the thesis, the focus is made in the acetylation reaction of cellulose in imidazolium chloride ILs. It consists of chapter 4 “Analysis of the synthesis of cellulose acetate in ionic liquids. Experimental study, modeling and use of additives and co-solvents” where the synthesis of cellulose acetate in ILs is analyzed. To do so the degree of substitution of acetylated cellulose have been experimentally measured for 40, 60 and 80°C and residence times between 1 and 24 h in the ILs [Amim][Cl], comprising in this way a temperature range (lower than 60°C) scarcely studied in literature. In addition the influences of additive of scandium III triflate and CO₂ were investigated. Other factors as the used of ILs of different suppliers and the water content were also analysed. A mathematical model was developed using both literature and experimental data and kinetics parameters are adjusted.

The last part of the thesis is dedicated to the obtaining valuable materials from the cellulose processing. It consists of chapter 5 “Cellulose aerogels regenerated from microcrystalline cellulose + ionic liquid solution: properties and drug loading capacity study” where the study on the influence of the ILs, dissolution temperature and coagulation bath on surface area, volume size and pore size in cellulose aerogel production by supercritical CO₂ drying is presented. Cellulose aerogels from cellulose/ionic liquid solutions were prepared with five different alkylmethylimidazolium-based ILs. Optimal cellulose concentrations in aerogel preparation are 1-2% w/w. The aerogel was loaded with phytol as a model compound obtaining loads of around 50% w/w. The drug loading capacity of the cellulose aerogels was positively influenced by their pore volume and size and resulted to be much better than aerogels of different materials.

Part I. State of the art

Chapter 1. Ionic liquid as reaction media for the production of cellulose-derived polymers from cellulosic biomass byproducts

Abstract

The most abundant natural polymer on Earth is cellulose that is present together with lignin and hemicellulose in vegetal biomass. Cellulose is a promising sustainable source of chemicals, fuels and materials. Nevertheless only 0.3% of cellulose is processed nowadays due to the difficulty in dissolving it, and only a small proportion is used as starting material for the production of synthetic cellulosic fibres especially esters and other cellulose derivatives, normally in extremely polluting processes. The efficient dissolution of cellulose is a long-standing goal in cellulose research and development. Ionic liquids (ILs) are considered “green” solvent due to their negligible vapour pressure that prevents them of passing to the environment. In addition, these molten salts present advantages in process intensification that makes that more than 70 patents in lignocellulosic biomass in ILs had been published since 2005, most of them related with the production of cellulose derived polymers, e.g. acetates, benzoates, sulfates, fluorates, phthalates, succinates, tritylates or silylates. In this work, the use of ILs for the production of cellulose derived polymers is thoroughly studied. To do so, in first place a brief summary of the state of the art in cellulose derivatives production is presented, as well as the main features of ILs in cellulose processing application. Later the main results in the production of cellulose derivatives using ILs are presented followed by an analysis of the industrial viability of the process considering aspects such as, environmental concerns and ILs recyclability.

1. Introduction

Cellulose is a natural biopolymer being the most common organic polymer and main component of cell wall in plants. Natural global production is about 40 billion tons per year of which three-tenth of a percent is used by the pulp industry [1]. Cellulose is a homopolysaccharide of $\beta(1\rightarrow4)$ D glucosyl residues resulting in a linear chain polymer composed of Anhydrous Glucose Units (AGU) (Fig. 1) each one containing three hydroxyl groups [2] able to form hydrogen bonding. As a result of this hydrogen bonding and of the van der Waals forces, cellulose molecules align together in a highly ordered state to form crystalline regions, whereas the less ordered molecules constitute the amorphous part [3]. The proportion of ordered to disordered regions (index of cristallinity, I_c) of cellulose varies with its origin [4] and chemical or physical treatment [5]. The chain length is expressed by the number of AGUs that is called degree of polymerization (DP). Therefore, cellulose of different origin, DP and I_c is expected to require different dissolution/reaction conditions due to the effect of these parameters on the accessibility to hydroxyl groups.

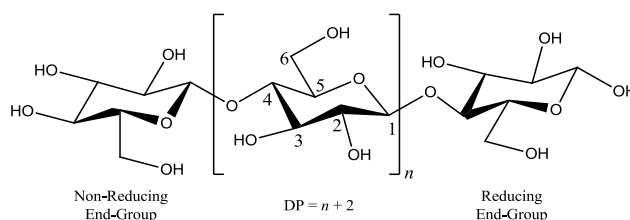


Fig. 1 Cellulose structure

In nature, cellulose can be found as a part of lignocellulose that it is mainly composed of three fractions: cellulose (30-60%), hemicellulose (20-40%) and lignin (10-30%) [6]. While cellulose and hemicellulose are composed of covalently linked and hydrogen bonded carbohydrate polymers, lignin consists of a net of phenolic polymers, forming a substance insoluble in water and common solvents.

The main cellulose resources are forestry, agriculture crops, industrial, food and garden waste [7]. Nevertheless, wood pulp remains the most important raw material source for the processing of cellulose being most of it used for the production of paper and cardboard after partial removal of the non-cellulosic constituents from its original fibre form [8]. The use of organic solvents (e.g. ethanol, methanol, ethylene glycol, acetic acid, formic acid) for cellulose isolation and processing [9] is associated to higher pretreatment temperature, use of catalysts, toxicity and inflammability issues. Thus, for its realistic use as an extensive raw matter, it will be necessary the development of a technology platform using this natural polymer for the production of environmentally friendly and biocompatible products [10]. Therefore, development of alternative solvents for the efficient dissolution and transformation of lignocellulose into value-added products is necessary. Promising solvents for cellulose processing are the ionic liquids (ILs) [11-14].

2. Dissolution of cellulose in ionic liquids

2.1. Ionic Liquids

ILs are molten organic salts containing only ions that can be fluid at room temperature (usually defined as fluid below or around 100°C) [15]. They are considered green solvents due to their negligible vapour pressure below their decomposition temperature. Due to this property they cannot pollute the environment by evaporation, unlike the organic solvents [16]. However, the label “green solvents” does not mean that all ILs are nontoxic [17]. This question will be analyzed later on this review.

Different ILs with tunable properties can be synthesized by selection of their anion and the cation. The solvent properties can be adjusted by the variation of the size chain of the cation and variation of anion due to the changing polarity and size [18]. Different synthesis methods (e.g. direct quaternization, reaction of halide with Lewis acid, anion exchange) have been reviewed by Wasserscheid and Keim [19]. More recent reviews on synthesis can be found in literature, e.g. biocompatible ILs [20], ether and alcohol functionalized ILs [21], or poly(ionic liquid)s [22]. ILs present high solvation properties for a number of substances, e.g. water, methanol, acetone, chloroform, acetic anhydride, toluene, both polar and apolar, and even polymeric substances such as cellulose. Many ILs present catalytic activity and are able to stabilize catalysts and enzymes [23]. An update on ILs use as solvents in synthesis and catalysis has been published by Hallett and Welton [24] and very recently by Steinrück and Wasserscheid [25].

Furthermore, most ILs are non-flammable and ILs have relatively high thermal stability, compared with organic solvents [26]. A number of extensive revisions about the properties of the ionic liquids can be found in literature [27-30].

The structures of the main cations and anions described in literature [31] are shown in Fig. 2. Salts based on the dialkylimidazolium, pyrrolidinium and pyridinium cations have gained attention because of the wide spectrum of physicochemical properties [32-36] such as melting points, viscosities, densities, surface tension, refractive indices and miscibilities with polar and nonpolar solvent. These properties can be affected by water, halides and metals which are the most prevalent impurities present in ILs [37]. The presence of water can occur due to hygroscopicity and other impurities mainly come from the mode of preparation of the IL. Thus, identically reactions performed with ionic liquids provided by different supplier can give different results, due to the presence of small amounts of different impurities [38]. Methods for preparation of ILs and purity determination (in most cases by ^1H and ^{13}C NMR) are proposed in literature [39]. Additionally, methods for producing large quantities of high quality ILs propose simple techniques to determine the purity of the final product e.g. UV-Vis spectroscopy for optical purity [40] and colorimetric determination of 1-methylimidazole in the range 0-3 mol% [41]. Recently real time monitoring of 1-methylimidazole concentration through LED-based optical sensor and photodiode detectors was achieved with detection limit of 4 mol% [42].

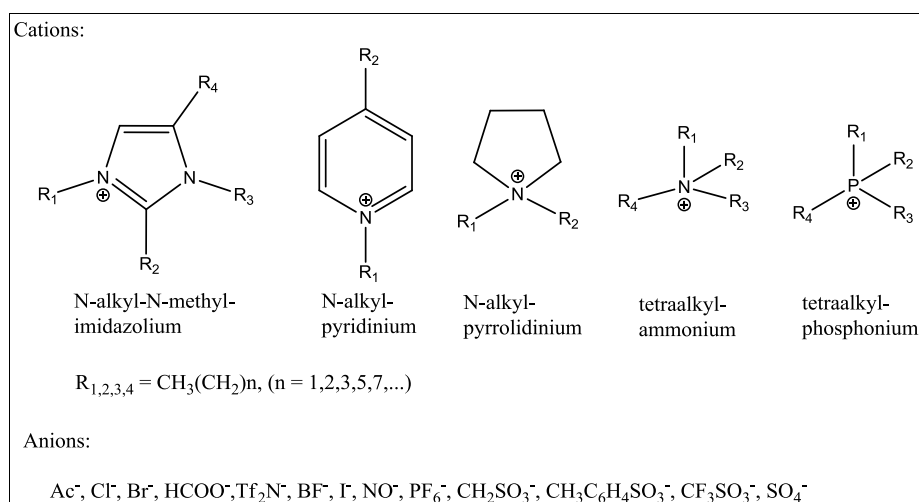


Fig. 2 Main cations and anions described in literature from Olivier-Bourdigou et al.(Olivier 2010)

2.2. Mechanism of cellulose dissolution

The discovery of the dissolution of cellulose in ILs by Swatloski et al. [43] provided new opportunities for the processing of this and other biopolymers such as lignin [44-46] or chitin [47, 48]. It was demonstrated that cellulose can be dissolved at high concentrations of 25% (w/w) in imidazolium-based ILs with chloride anions. Since then, a number of ILs have been found to be able to dissolve cellulose [49-53]. The most successful cations for cellulose dissolution are based on the imidazolium, pyridinium and pyrrolidinium cores, with allyl-, ethyl-, or butyl- side chains and the most promising anions, apart from chloride, are acetate, formate and alkylphosphate. However, chloride-based ILs with longer chain substituted imidazolium cations are less efficient in cellulose dissolution [43].

Cellulose dissolution results from the solvent ability to eliminate the inter and intramolecular hydrogen bonds among biopolymer molecule. The predominant mechanism of this dissolution process is found to be the formation of hydrogen bonds between the anions of the ILs and the hydroxyl groups of the biopolymer with no specific role for the cation [54-57]. However, it can also be found that the driving force of cellulose dissolution should be a result of the joint interactions of anions and cations with cellulose [58-60]. Computer simulations were carried out to support this [61].

Cellulose maintains its original chemical structure or forms a complex with the solvent only by intermolecular interactions (no covalent interactions occur) [62], thus, ILs are part of the so called non-derivatizing solvents [63] that include for example aqueous solution of sodium hydroxide [64], N,N-dimethylacetamide/lithium chloride (DMA/LiCl) [65, 66], dimethyl sulfoxide in combination with ammonium fluorides [67-70], and N-methylmorpholine-N-oxide (NMMO) [71]. There are a number of derivatizing solvents (able to dissolve cellulose with substitution forming new covalent bonds) e.g. trifluoroacetic acid (TFA) [72], sodium hydroxide/Carbon disulfide (NaOH/CS_2) [73] and N,N-dimethylformamide/Dinitrogen tetroxide ($\text{DMF}/\text{N}_2\text{O}_4$) [74].

A number of works including several reviews [75-80] have been already published on the cellulose dissolution process in ILs. Thus this subject will not be discussed in depth in this review. However, for an effective understanding of the dissolution of cellulose in ILs in relation with its industrial application, it is important to mention the solvent properties: hydrogen bond basicity, viscosity and water content.

3. Hydrogen bond basicity of cellulose dissolving ionic liquids

ILs of high hydrogen bond basicity (the ability to form hydrogen bonds) weaken the inter- and intra- molecular hydrogen bonds of the cellulose causing its dissolution [81]. Thus, the efficiency of these processes is usually improved with increased basicity of the ILs. The hydrogen bonding ability can be quantified by the Kamlet-Taft parameters [82] which specify three distinct polarities: hydrogen-bonding acidity (α), hydrogen-bonding basicity (β), and dipolarity/polarizability (π^*). All three protons of the imidazolium ring are acidic being the 2-position proton the one that contributes more to the hydrogen-bonding acidity [83]. A study [84] on imidazolium-based ILs reported π^* variation with both anion and cation, α dependence mainly on the cation and β value in general affected mainly by the nature of the anion species. β values of ILs with the same cations vary with the anion structure as shown in

Table 1. Chloride-based ILs are potential solvents for cellulose (e.g. $\beta_{[\text{Bmim}][\text{Cl}]}=0.95$) as the chloride anion is a strong proton acceptor in interaction between hydroxyl groups of cellulose. Nevertheless, the high melting temperature and high viscosity makes their use expensive and inefficient. As an alternative to conventional ILs, polar ILs with low melting points and relatively low viscosities such as dialkylimidazolium salts with phosphate-, acetate- and formate-derived anions have been studied [85]. Some [Bmim]-based ILs containing carboxylic anions (Ac and HCO₂) were reported [86] to show stronger hydrogen-bonding basicity ($\beta_{[\text{Bmim}][\text{Ac}]}=1.09$, $\beta_{[\text{Bmim}][\text{HCO}_2]}=1.01$) than chloride anion. The methylphosphonate anion salts with stronger hydrogen bond basicity than conventional ILs are able to dissolve 2.0 wt% of cellulose powder within 3h at room temperature [86] (25°C) and within 30 min at 45°C [87]. In general, polar ILs are very hygroscopic, however almost no correlation has been found between π^* and hygroscopicity of [mim]-based ILs [88]. Ionic liquids with other anions presenting low basicity such those with bromide ($\beta_{[\text{Emim}][\text{Br}]}=0.87$), trifluoroacetate ($\beta_{[\text{Emim}][\text{CF}_3\text{CO}_2]}=0.74$), thiocyanate ($\beta_{[\text{Emim}][\text{SCN}]}=0.71$), methanesulfonate ($\beta_{[\text{Emim}][\text{MeSO}_3]}=0.70$) or tetrafluoroborate ($\beta_{[\text{Bmim}][\text{BF}_4]}=0.38$) anions show [81] cellulose solubilities < 1% in mass.

Table 1 Ionic liquids capable of dissolving cellulose modified from literature ([81] and molecular-microscopic properties measured at 25°C: hydrogen-bonding acidity (α), hydrogen-bonding basicity (β), dipolarity/polarizability (π^*) and physical properties: viscosity at 25°C (η), melting temperature (T_m), decomposition temperature (T_{dec}) found in the literature.

ILs (cellulose solubility >1%) ^a	η (mPa·s)	T_m (°C)	T_{dec} (°C)	Kamlet-Taft parameters ^b			Ref.	ILs (cellulose solubility <1%)	β	Ref.
				β	α	π^*				
[Amim][Cl]	2090		256	0.83	0.46	1.17	[85]	[Bmim][BF ₄]	0.38	[84]
[Emim][HCO ₂]		52	212				[85]	[Bmim][PF ₆]	0.21	[84]
[Prmim][HCO ₂]	117			0.99	0.48	1.08	[85]	[Emim][MeOSO ₃]	0.61	[87]
[Amim][HCO ₂]	66		205	0.99	0.48	1.08	[85]	[Emim][MeSO ₃]	0.70	[87]
[Bmim][Ac]				1.09	0.55	0.99	[86]	[Emim][CF ₃ CO ₂]	0.74	[89] ^d
[Bmim][Cl]		66	254	0.95	0.47	1.10	[89]	[Emim][SCN]	0.71	[89]
[Bmim][HCO ₂]				1.01	0.56	1.03	[86]	[Emim][BF ₄]	0.55 ^c	[89, 90]
[Emim][(MeO) ₂ PO ₂]	265	21	289	1.00	0.51	1.06	[87]	[Emim][N(CN) ₂]	0.64	[89]
[Emim][(MeO)HPO ₂] ^c	107		275	1.00	0.52	1.06	[87]	[Emim][I]	0.75	[89]
[Emim][(MeO)MePO ₂]	510		262	1.07	0.50	1.04	[87]	[Emim][PF ₆]	0.44	[89]
[Emim][(EtO) ₂ PO ₂]						1.00	[87]	[Bmim][CH ₃ SO ₃]	0.85	[89]
[Emim][(MeO)HPO ₂] ^c	107		278	1.00	0.52	1.06	[91]	[Bmim][Br]	0.87	[89]
[Emim][H ₂ PO ₂]		17	260	0.97	0.52	1.09	[91]	[Emim][OTs]		
[Amim][(MeO)HPO ₂]	123		265	0.99	0.51	1.06	[91]	[Amim][Br]		
[Prmim][(MeO)HPO ₂]	219		277	1.00	0.54	1.02	[91]	[Admim][Br]		
[Bmim][(MeO)HPO ₂]	287		277	1.02	0.52	1.01	[91]	[Bdmim][Br]		
[Emim][Cl]		89	285				[90]	[MeOEmim][Br]		
[Emim][Ac]	162			0.95	0.40	1.09	[92, 93] ^{e,f}	[EdmimM][Br]		

^aSolubility conditions: 2-8 wt% of cellulose in ionic liquid, temperature of dissolution from 100°C to 130°; ^bKamlet-Taft parameters values measured at 25°C using a single set of dyes: Reichardt's dye, 4-nitroaniline and N,N-diethyl-4-nitroaniline; ^cSolubility conditions: 5 wt% of cellulose in ionic liquid, temperature of dissolution 50°C; ^d β value obtained using the 3-(4-amino-3-methylphenyl)-7-phenyl-benzo-[1,2-*b*:4,5-*b'*]-difuran-2,6-di-one dye; ^eKamlet-Taft parameters measured using Reichardt's dye 2,6-Diphenyl-4-(2,4,6-triphenyl-*N*-pyridino) phenolate; ^fViscosity measured at 20°C

The β parameter is considered an excellent predictor of lignocellulosic biomass pretreatment efficacy [94]. Cellulose dissolving ILs present β values between 0.83 and 1.09 while non cellulose dissolving ILs β values range from 0.21 to 0.87., as shown in

Table 1. Strong hydrogen-bonding basicity alkyl methylimidazolium-based ILs can be designed using various anions: Ac, (MeO)MePO₂, (MeO)HPO₂, HCO₂, (MeO)₂PO₂, Cl, H₂PO₂. Furthermore, the dipolarity/polarizability studied [95] as a function of cation-anion interaction strength indicates an increase with stronger ion pairing effect i.e., the resulting cation effect on π^* is different with weakly coordinating anion compared to the strongly coordinating anion (e.g. chloride). It is expected that 1-alkyl-3-methylimidazolium cations show larger values of π^* [96], even when compared with different cations sharing the same anion such that imidazolium > pyridinium > pyrrolidinium [97]

4. Viscosity of concentrated cellulose solutions in ILs

The viscosity of ILs depends on the molecular structure and interactions between ions: electrostatic, van der Waals and hydrogen bonds [98]. It is normally associated with melting point. ILs with high melting points normally are the most viscous ILs. To obtain low viscosity low melting point ILs we must choose asymmetrical cations and anions (irregular packing) or increase their size increasing in this way the distance between the cation and anion, which makes the ionic interaction weaker [99]. In ILs having a common anion and a similar alkyl chain length on the cation, the viscosity increases with cation size following the order: imidazolium < pyridinium < pyrrolidinium [100]. Viscosities generally increase with increasing number and length of alkyl substituents on the cation, with the pyridinium salts typically being slightly more viscous than the equivalent imidazolium compounds [101] as shown in Table 2.

Table 2 Viscosity (η), density (ρ) and water content (wt %) of ionic liquids

Ionic Liquid	T (°C)	η (mPa·s)	ρ (kg/m ³)	Water (wt %)	Ref.
<i>Methylimidazolium</i>					
[Bmim][Ac]	20	646		1.100	[101]
[Bmim][CF ₃ CO ₂]	20	89		0.225	[101]
ECOENG 41M	20	1676		0.083	[101]
[Bmim][Ac]	20	429	1055	0.085	[102]
[Bmim][Cl]	25		1080	0.220	[103]
[Amim][Cl]	25	821	1166	0.180	[104]
[Emim][Ac]	20	202	1102	0.124	[105]
[Emim][CH ₃ OHPO ₂]	20	286	1212	0.078	[105]
[Emim][CH ₃ SO ₃]	20	232	1246	0.029	[105]
[Emim][CF ₃ SO ₃]	20	52	1390	0.002	[105]
[Emim][N(CN) ₂]	20	19	1107	0.006	[105]
[Emim][SCN]	20	29	1120	0.027	[105]
[Emim][Tos]	30	1417	1223	0.056	[105]
[Emim][(OCH ₃) ₂ PO ₂]	30	193	1214	0.014	[105]
[Emim][EtSO ₄]	20	125	1240	0.105	[106]
<i>Pyridinium</i>					
[Empy][EtSO ₄]	20	204		0.026	[101]
[Epy][EtSO ₄]	20	183		0.068	[101]
[EEpy][EtSO ₄]	25	325	1220	< 0.08	[107]
[Mpy][CH ₃ SO ₄]	25	116	1345	< 0.06	[107]
[MMpy][CH ₃ SO ₄]	25	129	1302	< 0.06	[107]
[EMpy][CH ₃ SO ₄]	25	456	1285	< 0.08	[107]
<i>Pyrrolidinium</i>					

[Bmpyr][Ac]	25	107	1021	0.070	[102]
[Bmpyr][CF ₃ SO ₃]	20	222	1256	0.072	[98]
[Bmpyr][BtOHPO ₂]	25	321	1082	0.025	[108]
[Empyr][EtOHPO ₂]	25	320	1123	0.021	[108]

From the alkylmethylimidazolium-based ILs viscosities, it is clear that chloride anion increases the value of that property as reported in literature [109]. In addition, even the presence of very low concentrations of chloride as an impurity in non-chloride-based alkylimidazolium ILs increases the viscosity. Seddon et al. [109] related this increase to an increase in the cohesive forces via hydrogen bonding between the chloride and the protons of the imidazolium ring. In the same work, it was also concluded that the presence of water and other molecular co-solvents reduces the viscosity of ILs. For example, viscosities of binary mixtures [110] of water + [Amim][Cl] and ethanol + [Amim][Cl] measured in the range of 20-60°C with water molar fraction up to 0.8 and ethanol of 0.55 are up 85% lower than the viscosity of the pure IL.

While the addition of molecular solvents to an IL decreases the solution viscosity, the addition of cellulose increases drastically the viscosity of the mixture. Concentrated cellulose/IL solutions show non-Newtonian behaviour. The Newtonian behaviour is lost progressively with increasing polymer concentration [111] explained by the increase of interactions between polymer chains and restriction of the motion of individual chains. The zero shear viscosity of concentrated cellulose solutions in [Amim][Cl] in the range of 10 to 25 wt% at 100°C presents values between 2209 and 125700 Pa·s [111]. These values represent a problem for cellulose processing with highly viscous-high melting point ILs. The viscosities of mixtures IL+cellulose were compared at 85°C by Kosan [112] which were found to increase in the following order: [Emim][Ac] (2281 Pa·s) < [Bmim][Ac] (9690 Pa·s) < [Emim][Cl] (24900 Pa·s) < [Bmim][Cl] (47540 Pa·s) < [Bdmim][Cl] (188400 Pa·s) with cellulose concentrations between 12.8% to 15.8%. The viscosity of solutions of 4 and 8 wt% cellulose fibres (DP = 650) in [Amim][Cl] at 80°C reported by Zhang et al [58] was respectively 110 and 1480 Pa·s. In order to improve the processability of cellulose, a co-solvent can be added to reduce the viscosity of the solution, but the co-solvent must be chosen in order that it does not reduce the solubility of cellulose in water. The most frequent co-solvent used in cellulose processing is DMSO. The maximal amount of cellulose dissolved in [Emim][Ac] + 10 wt% DMSO is five times higher than at [Emim][Ac] + 10 wt% water [113]. The cellulose intrinsic viscosity of the solution does not depend on DMSO content but the addition of water higher than 10-15% in cellulose-[Emim][Ac] solution leads to cellulose coagulation [113]. Although, cellulose/IL/DMSO solutions behave as Newtonian fluids at very low cellulose concentration (< 0.80 wt%), while the solution viscosity increases with concentration, and exhibits a shear-thinning behaviour at higher shear rates [114]. Additionally, shear thinning behaviour can be detected as well with DMAc and DMF (co-solvents) at high fractions of IL [115]. As an alternative to water or organic solvents, viscosity reduction can be provided by carbon dioxide (CO₂) [116]. Using CO₂ as a co-solvent has the advantages of being non-toxic, cheap, and can be easily separated of the IL by depressurization. ILs and CO₂ are considered to be a promising media for the development of "green" technology [117]. In biphasic mixtures IL-CO₂ at moderate or high pressure, CO₂ can dissolve significantly into the IL-rich liquid phase, up to concentrations round 30-40% in mol [117] in the case of imidazolium chloride ILs. CO₂ it is not causing the precipitation of cellulose except in ILs with acetate anion in which a reversible carboxylate reaction occurs that causes cellulose precipitation [118, 119].

So far, only a few viscosity data of mixtures carbon dioxide + IL can be found in literature [120-122] for non cellulose dissolving ILs and of the mixture CO₂ + [Amim][Cl] [123]. In general, the decrease in viscosity is between 85 and 45% at moderate pressures of 10-12 MPa, but with molar fractions as low as 10% of CO₂ decrease of 30-40% of the pure IL viscosity is already observed. In all cases the effect in viscosity reduction with CO₂ is more remarkable at lower temperatures the viscosities are higher and CO₂ solubilities are also more elevated.

The effect of CO₂ in IL + cellulose mixtures was only studied by Iguchi et al [124], with and acetate anion IL using low concentrations of cellulose to avoid its precipitation with CO₂. At 40 bar and 39°C, viscosity can be reduced of 1.2 wt% cellulose + [Bmim][Ac] solution by about 80%.

5. Water effect on the anion interaction with cellulose

The presence of water or alcohol in an IL decreases the solubility of cellulose, so those can precipitate cellulose from IL solutions being a serious challenge for the cellulose processing in ILs, because, even partially water-immiscible ILs are hygroscopic and are able to absorb up to 1% by weight of water from the environment [125]. Absorbed water interacts with the anions of the ILs, and these interactions lead to changes in the structure of water [126]. Cammarata et al. [127] showed that for low coordinating anion (low basicity) water is associated with the anion of the ILs via hydrogen bonding instead of being self-associated. In those cases, the concentrations of the dissolved water are typically in the range of 0.2±1.0 mol/L. In ILs with strongly coordinating anion (highly basic, that is, those able to dissolve cellulose) water molecules can self-associate, being able to dissolve much higher water amounts that may exceed 1.0 mol/L.

Adding water to the solution cellulose/IL means that the water-anion interactions saturate the hydrogen-bonding ability of the anions, allowing the water molecules to form hydrogen bonds with cellulose [128] meanwhile the cations are maintained in a second solvation shell of cellulose due to strong interactions with anions. Computer simulations [129] using 1-alkyl-3-methylimidazolium cations (n=1, 2, 3, 4, 5) paired with chloride, acetate or dimethylphosphate showed that water crowds the hydrogen-accepting sites of the anions, preventing interactions with cellulose.

6. Biomass pretreatments for cellulose isolation

Lignocellulosic materials are attractive feedstocks for both use of cellulose fibres or fermentation of cellulose or/and hemicelluloses in order to obtain bioethanol [130]. Some methods have been developed in order to isolate cellulose fibres from the other biomass components [131]. In general, the pretreatment of biomass consists of changing and improving the accessibility of biomass fractions: structure (pore size and volume, particle size and specific surface area), modifying its chemical composition (lignin, hemicelluloses, and acetyl group), and changing the cellulose structure (crystallinity and degree of polymerization) [131]. Possible physicochemical pretreatments include steam explosion, lime, wet oxidative, ammonia fibre explosion (AFEX), organosolv, NMMO and IL. Conventional chemical pretreatments comprehend alkali, acid, oxidizing agents and organic solvents [130]. Some examples of biomass pretreatment are summarized in Table 3 including IL pretreatment processes for various feedstocks.

Table 3 Physicochemical and chemical pretreatments for bioconversion of lignocellulosic biomass

Biomass	Pretreatment	Chemical composition after pretreatment (%)	Ref.
<i>NMMO, acid, alkaline, steam explosion, lime, wet oxidation, ammonia fibre explosion (AFEX), organosolv process</i>			
softwood spruce	85% NMMO, 90 - 130°C, 1 – 3 h	42.1±2.1 (glucan); 5.4±0.7 (xylan); 13.8±1.1 (mannan); 29.6±0.7 (acid-insoluble lignin); 0.58±0.11 (acid-soluble lignin)	[132]
hardwood oak	85% NMMO, 90 - 130°C, 1 – 3 h	44.0±2.5 (glucan); 19.5±1.2 (xylan); 4.1±0.5 (mannan); 18.8±0.3 (acid-insoluble lignin); 3.4±0.2 (acid-soluble lignin)	[132]
sugarcane bagasse	NMMO, 5% (w/w) biomass, 130°C, 1 h	38.1 (cellulose); 28.8 (hemicellulose); 12.1 (acid-soluble lignin); 20.3 (acid-insoluble lignin)	[133]
switchgrass	acid (0.1% H ₂ SO ₄ , 60°C, 12 h) and dry steam (100, 125 and 145°C, 1h)	36.03±0.25 (glucan); 22.69±0.06 (xylan); 3.85±0.03 (arabinan); 19.00±0.04 (total lignin)	[134]
lespedeza crytobotrya	steam explosion (15-25 kg/m ² , 4 min) and alkaline (60% aq. ethanol +1% NaOH)	49.6 - 65.5 (cellulose rich fractions)	[135]
corn stover	acid catalysis (3% SO ₂ w/w dry weight) and steam (170°C, 9 min)	46.1 (glucan); 16.6 (xylan); 23.9 (acid-insoluble lignin)	[136]
rice straw	alkaline (1 M NaOH, 30°C, 18h)	30.7 (hemicelluloses); 6.9 (acid-insoluble lignin); 1.1 (acid-soluble lignin)	[137]
corn stover	lime (0.5 g Ca(OH) ₂ /g biomass, 55°C, 4 weeks with aeration)	91.3 (glucan); 51.8 (xylan)	[138]
sugar bagasse	alkali alkali + ultrasonic irradiation acid + 10% KOH acid+ 10% NaOH 80% acetic acid - 70% nitric acid	45.5 (cellulose), 7.2 (hemi), 3.9 (lignin) 44.7 (cellulose), 6.0 (hemi), 3.4 (lignin) 44.7 (cellulose), 5.7 (hemi), 1.6 (lignin) 44.2 (cellulose), 3.7 (hemi), 1.5 (lignin) 43.6 (cellulose), 4.3 (hemi), 0.6 (lignin)	[139]

wheat straw	alkaline wet oxidation 60 gL ⁻¹ straw, 195°C, 10 min, 12 bar of O ₂ , 6.5 gL ⁻¹ Na ₂ CO ₃	96.0 (cellulose); 68.0 (hemicellulose); 35 (lignin)	[140]
poplar wood	organosolv process (2- PrOH/H ₂ O (7:3, v/v), 180°C)	79 (glucan); 11(xylan); 7 (lignin) ^a	[141]
corn stover	AFEX (60% biomass, NH ₃ (1:1), 120°C, 30 min, 200 psi)	34.8 (glucan); 21.4 (xylan); 20.5 (lignin)	[142]
<i>Ionic Liquids</i>			
corn stover	[Emim][Ac], 3% (w/w) biomass, 160°C, 3 h, 14.7 psi	62.1 (glucan); 4.3 (xylan); 6.6 (lignin)	[142]
maple wood flour	[Emim][Ac], 5% (w/w) biomass, 50-130°C, 90 min	52-60 (cellulose); 29-31 (xylan); 8.8-17 (lignin)	[143]
spruce sawdust	[Amim][Cl], 4% biomass, 110°C, 120 h	45 (lignin)	[144]
switchgrass	[Me(OEt)3-Et3N]Ac	36 (cellulose); 20 (xylan); 24 (insoluble lignin); 2 (acid-soluble lignin)	[145]
switchgrass	[Emim][Ac], 3% (w/w) biomass, 160°C, 3 h	67.7 (glucan); 7.6 (xylan); 2.1 (arabinan); 2.1 (galactan); 10.8 (klason lignin); 2.8 (acid-soluble lignin); 3.6 (ashes)	[146]
bran	[Emim]MeHPO ₃ , [Amim]MeHPO ₃ , [Prmim]MeHPO ₃ , [Bmim]MeHPO ₃ , [Emim]H ₂ PO ₂ , 25-50°C, 120-300 min	11 - 42 (cellulose + other polysaccharides)	[91]
corn stover	5 g [Emim][Ac], 4.8 - 50 % (w/w) biomass, 125°C, 1h	37.4 - 42.2 (cellulose); 21.9 - 25.9 (hemicellulose); 13.3 - 18.6 (lignin)	[147]
sugarcane bagasse	[Bmim]MeSO ₄ , 7% (w/w) H ₂ SO ₄ , 10 %(w/w) biomass, 100°C, 0 - 240 min	38-40 (glucose); 5-24 (xylose); 12-19 (lignin)	[148]

The sugar yields from hemicellulose and cellulose are critical parameters for an economically feasible ethanol production process however, these pretreatment processes involve severe operation conditions such as high temperature, pressure, acids, bases and organic solvents. The composition of the materials is changed with dilute acid [134] or sodium hydroxide [137] by removing hemicelluloses and lignin. Sulfuric acid and acetic acid/nitric acid [139] are used as well for lignocellulosic pre-treatment. The most common alkaline pretreatments make use of sodium hydroxide and lime (calcium hydroxide) [138], although combination of alkali delignification with ultrasonic irradiation [139] or steam explosion [135] are also used to increase the accessibility of the exposed surface to enzymatic hydrolysis. Isolated fractions from biomass can be obtained as well through severe steam + acid catalyst (sulfur dioxide) pretreatment at high temperature to produce ethanol [136]. NMMO and ILs are considered to be advantageous compared to conventional pretreatments (acid, alkali and thermal) due to the milder operation conditions and direct cellulose dissolution [130]. NMMO patented by Johnson [149] is able to dissolve high concentrations of cellulose (up to 23%) and overcome environmental issues in regenerated cellulose fibres production [150]. In the example showed in Table 3 sugarcane bagasse NMMO pretreatment [133] enhanced enzymatic hydrolysis at least twofold as compared to untreated bagasse although with 10% loss of the initial weight after regeneration. In the case of ILs pretreatment [146], [Emim][Ac] removed three times more lignin (69.2% of total lignin) than dilute acid pretreatment (22.4%), reduced the total process time to produce high yields of sugar from the recovered product and produced less degradation of monosaccharides. Li et al. [142] compared AFEX and IL pretreatment, founding that in contrast

to AFEX the biomass crystal structure treated with IL was significantly disrupted and when enzymatic hydrolysis was tested the IL treated biomass required less enzyme loading and shorter hydrolysis time. Therefore, NMMO and ILs are claimed to be more efficient than conventional solvents for biomass pretreatment.

Although ILs viscosity is a limitation in biomass processing, different alkyimidazolium-based ILs such as [Mmim][MeSO₄], [Bmim][CF₃SO₃], [Emim][Ac], [Amim][Cl], [Bmim][Cl], and [Bzmim]Cl, were reported [91] to be good solvents for lignin dissolution and selective extraction. Biomass dispersibility showed to be easier in lower viscosity ILs, and in general the less viscous ILs as dialkyl phosphates and acetates present higher solubility even under mild conditions and in short times [91]. However, some limitations of IL pretreatment have to be taken in consideration. High solid biomass loading require longer retention times [151] because ILs high viscosity and non-Newtonian behaviour causes difficulties in stirring which significantly decreases the biomass accessibility to the salt. Additionally, cellulose loss can occur during IL pretreatment (e.g. with [Bmim][Cl] between 4-9%) that could be caused by cellulose degradation or incomplete recovery [151]. It has been proposed to improve IL pretreatment by reducing biomass particle size through preparatory milling [152]. For example, wood direct dissolution in [Amim][Cl] and [Bmim][Cl] [153], without prior isolation of its individual components was highly dependent of the particle size of the wood sample: ball-milled wood powder > sawdust > thermomechanical pulp > wood chips. As an alternative, the addition of alcohol to biomass/[Emim][Ac] solution in order to dissolve the lignocellulosic biomass in the different fractions has been investigated with ethanol [154] and methanol [155].

Another effect of pretreatment apart from improving cellulose accessibility is reducing cellulose DP. Altering DP is always accompanied by change of crystallinity. Naturally occurring cellulose can have a DP around 15000 AGU and after the pretreatment process, technical cellulose can present DPs between 100 and 3000 [156], depending on the pretreatment technique. The Table 4 shows some examples of biomass conventional acid and IL treatments and the DP before and after treatment.

Table 4 Degree of polymerization (DP) before and after biomass acid and ILs treatment with respective DP determination method

Lignocellulosic biomass (DP) ^a	Treatment conditions	DP after treatment	DP determination method ^b	Reference
<i>Acid</i>				
Avicel PH-101 (330)	H ₃ PO ₄ , r.t., 3 weeks	DPw = 35	SEC	[156]
Avicel PH-101 (153)	H ₃ PO ₄ , r.t., 30 min and 55°C, 20h	DPw = 14.6	GPC (DMSO)	[157]
Avicel PH-101 (309) Whatman #4 filter paper (2046)	acid-chorite, r.t., 2h	DPw = 294 DPw = 1347	GPC	[158]
Avicel PH 105 (212) SigmaCell 20 (209) Whatman CC41 (212) Fibrous cellulose SigmaCell 101 (257) Whatman #1 filter paper (2085)	H ₃ PO ₄ 75% (w/v)	DPn = 208 DPn = 215 DPn = 199 DPn = 263 DPn = 1850	Phenol-H ₂ SO ₄ BCA	[159]
<i>Ionic Liquids</i>				
Mycrocrystalline cellulose (300) α-cellulose fibres (1050)	[Bmim][Cl] and Amberlist 15 dry, 1h	DP = 100 DP = 150	GPC	[160]
Wheat straw (580) Steam exploded wheat straw (500)	[Bmim][Cl], microwave, 10 min	DP = 320 DP = 260	n.d.	[161]
Cotton-ramie pulp (576)	[Emim][DEP], 90°C, 11 min [Mmim]DMP, 90°C, 300 min	DPv = 448 DPv = 380	Ubbelohde viscometer (Cuen)	[162]
Mycrocrystalline cellulose (1740) Filter paper (2310) Cotton fabrics (2730)	[Amim][Cl], 110°C, 1h	DPv = 1430 DPv = 1720 DPv = 2140	Ubbelohde viscometer (LiCl/DMAc)	[163]
Cellulose (580)	[Bmim][Cl], 70°C, 40h [Bmim][Cl], 90°C, 2h [Bmim][Cl], 130°C, 6h	DPv = 556 DPv = 470 DPv = 260	Ubbelohde viscometer (Cuen)	[164]
^a DP, degree of polymerization: DPw (weight-average degree of polymerization), DPv (viscosity-average degree of polymerization), DPn (number-average degree of				

polymerization); ^bDP determination methods: GPC (gel permeation chromatography), Cuen (Cupriethylenediamine hydroxide solution), SEC (size-exclusion chromatography), Phenol-H₂SO₄ (phenol-sulfuric acid), BCA (2,2'-bicinchoninate), n.d. (not defined in the article)

Phosphoric acid is able to reduce microcrystalline cellulose (MCC) DP even to a low molecular weight (cellodextrines) e.g. down to 15 [156] or 7.5 [157]. The acid-chlorite treatment [158] is also an effective way to reduce the DP, e.g. Avicel samples can be reduced by nearly 5% during 2h treatment. However, like in the case of cellulose/IL solution, different crystallinity between cellulose samples determines the accessibility to the reagents contributing to different levels of degradation. The same acid-chlorite treatment could reduce the DP from Whatman filter paper by 34% and through phosphoric acid treatment by 11% [159]. Additionally, [Bmim][Cl] treatment shows very high DP reduction when the feedstock is MCC or α -cellulose, due to the addition of Amberlyst, a sulfonated resin for the production of reducing sugars [160]. However, in the case of [Bmim][Cl] + microwave treatment of wheat straw [161], a steam explosion pretreatment on the biomass indeed enhanced the DP reduction. Furthermore, a treatment only with [Bmim][Cl] could reduce the DP, e.g. from 4% to 55% just increasing the temperature [164]. The IL [Emim][DEP] was proven to be an excellent cellulose treatment reagent owing to its low viscosity, the potential for accelerating enzymatic hydrolysis, and recyclability [162]. The cotton treatment shows that [Emim][DEP] features are an advantage when compared to [Amim][Cl] treatment [163] once the same DP reduction of cotton (22%) is achieved in 11 min at 90°C and 1h at 110°C respectively. ILs have demonstrated advantageous as solvents for cellulose depolymerization allowing the use of milder treatment conditions such as temperature and time.

7. Industrial cellulose derivatives production methods

Fibres are divided into two groups: natural fibres and chemical fibres (man-made fibres). Natural materials are dissolved to make cellulose fibres such as wood pulp or cellulose. The market is focusing on using cellulose fibres through renewable sources [165]. Cotton represents 30% of the total volume (89 million tons) of the global fibre market in 2014 and man-made cellulose fibres approximately 7 % with a predicted growth of about 9% per year [166]. Cotton still is the dominating cellulose fibre in the textile industry, but the need of fertilizers, artificial irrigation and land priority for food production will create environmental problems and will not allow the cover of the demand for cellulose fibres. Unlike cotton, man-made cellulose fibres derive from natural raw material wood and can be manufactured with partially better properties than cotton [167]. Most man-made fibres made from cellulose derivatives with high molecular weight compounds are produced by replacing the hydrogen atoms of hydroxyl groups in the AGUs of cellulose with alkyl or substituted alkyl groups [168]. Cellulose derivatives can be cellulose esters and ethers. They are generally synthesized by esterification of cellulose with inorganic or organic acids or by etherification or Michael addition in heterogeneous or homogeneous media respectively [168]. Cellulose derivatives production mechanism using ILs is schematized in Fig. 3.

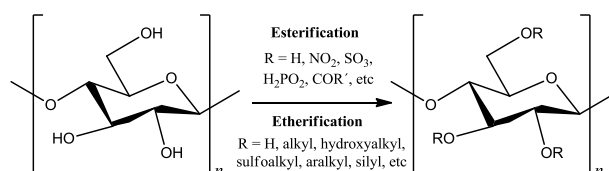


Fig. 3 Synthesis of cellulose esters and ethers [168]

Depending on the number of hydroxyl groups substituted, cellulose derivatives may have low or high degree of substitution (DS). The DS is a measure of the average number of hydroxyl groups on each AGU unit which are derivatized by substituent groups. As each AGU has three hydroxyl groups available for substitution the maximum possible DS is 3. Cellulose contains 31.48% by weight of hydroxyl groups (one primary and two secondary per AGU) and the reactivity of these hydroxyl groups varies according to the reaction medium in which functionalization is done [169].

Since 1944 cellulose esters have been produced [170] by a simple heterogeneous process consisting on pouring a mixture containing the acetylation agent into water, filtering, washing and drying. The polymers have been produced in different shapes: films, fibres, plastics and coating applications. Various types of organic cellulose esters have been used in commercial products or in pharmaceutical investigations such as cellulose acetate (CA), cellulose acetate phthalate (CAP), cellulose acetate butyrate (CAB), and cellulose esters based on inorganic acids, e.g. cellulose nitrate, silylated celluloses such as trimethylcellulose and others [171].

The following table presents the applications of some commercially marketed cellulose acetates [172]. In general cellulose esters have versatile applications. Besides their traditional applications as additives in the food industry, in coatings, printing, cosmetic, textile and in the pharmaceuticals industry, new cellulose derivatives have also been investigated for their applications such as drug delivery systems [173], in chiral separation and recognition [174], as photoactive materials [175], as antioxidant agents [176], in memory of electronic devices [177], and graft copolymers [178].

Table 5 Commercially marketed cellulose acetates and their applications [172]

Cellulose derivatives	Solubility	Applications
Cellulose acetate butyrate	- Soluble and compatible with resins and plasticizers - Alcohols	- Wood finishes - Automotive topcoats - Rubber and plastic coatings - Cloth coatings - Glass coatings - Flexographic, gravure and screen-printing inks - Hot melts Adhesives
Cellulose acetate propionate	- Alcohol-water mixtures	- Inks - Overprint varnishes - Plastic coatings - Paper coatings - Reprographic processes
Cellulose acetate	- Acetone - Methyl ethyl ketone - Ethyl acetate	Solvent- and grease- resistant coatings for paper products, wire and cloth - Dopes and cements for models airplanes - Lacquers for industrial insulation and for manufacture of capacitors - Barrier and release coatings for pressure-sensitive tapes - Protective coating s for plastic items - Film former for coating wire screening for greenhouse windows, poultry, runs and similar structures

The properties of cellulose ethers important for their commercialization are determined by their molecular weights, chemical structure and distribution of the substituent groups, degree of substitution and molar substitution [179]. Examples of mostly used cellulose ethers are: methyl cellulose (MC), ethyl cellulose (EC), hydroxyethyl cellulose (HEC), hydroxypropyl cellulose (HPC), hydroxypropylmethyl cellulose (HPMC) and carboxymethyl cellulose (CMC). Cellulose ethers act as thickeners, binders, film formers and water retention agents in construction applications although, they function as well as suspension aids, surfactants, lubricants, protective colloids and emulsifiers [180]. HPC and HEC in particular have been investigated for production of antibiotics [181].

Natural cellulose contains highly crystalline regions, and the highly branched hydrogen bonding network makes it insoluble in water and many organic solvents, sometimes even after following a pretreatment methods such as the ones described in the previous section. This explains that standard commercial methods for preparation of cellulose derivatives begin as heterogeneous reactions, involving in the case of esters a subsequent back-hydrolysis reaction [182]. In the case of cellulose ethers an activation of the cellulose previous to the heterogeneous etherification is required and the produced cellulose ethers exhibit non-uniform mixtures [183]. Cellulose must be activated to disrupt its crystallinity prior to etherification to obtain a soluble product. A common method to activate cellulose is to mercerize it with NaOH [184].

Cellulose derivatives synthesized in homogeneous reaction media could have different properties from those of cellulose derivatives synthesized in heterogeneous media with similar chemical compositions. When carrying out reactions in homogeneous solutions, the

regioselectivity of the reaction is determined by the reactivity differences among the free hydroxyl groups on the cellulose molecules [185], not by their accessibility [186].

Suitable non-derivatizing solvents for homogeneous dissolution of cellulose under lab scale were mentioned before e.g. DMSO/TBAF and DMAc/LiCl. These solvents are able to dissolve cellulose with a DP as high as 650 in short period of time however, they have the disadvantages such as being slightly explosive with heat and contain a certain amount of water which leads to lower DS in acetylation with acetic anhydride due to fast hydrolysis [187]. Examples of cellulose acetylation in the presence of DMAc/LiCl and DMSO/TBAF are shown in Table 6.

Table 6 Experimental results from acetylation reactions in DMAc/LiCl and DMSO/TBAF available in literature

Biomass (DP) ^a	wt% ^b	Reagent	Reaction conditions ^c	DS	Ref.
<i>Dimethylacetamide/Lithium chloride (DMAc/LiCl)</i>					
MCC (260)	7.5	Acetyl chloride	5:1, 80°C, 2h	2.96	[188]
Sisal (650) Cotton (410)	5 - 7	Acetic anhydride	2:1, 110°C, 4h	1.5	[189]
MCC, sisal	5 - 9	Acetic anhydride	3:1, 110°C, 1 - 4h	1.6	[190]
<i>Dimethylsulfoxide/tetrabutylammonium fluoride trihydrate (DMSO/TBAF)</i>					
Avicel (330)	11	Acetic anhydride	11:1, 60°C, 3h	1.2	[67]
MCC (260)	11	Acyl-1H-benzotriazole	3:1, 60°C, 3h	1.07 – 1.89	[68]
Cotton	15	Succinic anhydride/DMAP	20:1, R.T., 24h	2.5 – 2.6	[191]
^a DP is degree of polymerization of biomass; ^b wt% is weight percentage of solvent; ^c Reaction conditions: ratio reagent/AGU, reaction temperature (°C) and reaction time (h)					

The degree of substitution (DS) can vary with the nature of the cellulose and the conditions of solubilization and acetylation. Homogenous acetylation of cellulose dissolved in DMAc/LiCl with acetyl chloride and a base [188] leads to DS decrease and less preferred substitution in position 6. Moreover, LiCl leaves OH groups of the cellulose available for substitution reactions. Thereby lower concentrations of LiCl (5% and 6%) in DMAc could prevent totally uniform acetylation [189]. Shorter chains in microcrystalline cellulose (MCC) favours aggregation leaving less hydroxyls available for acetylation, thus the necessary amount of LiCl is higher in the case of MCC in comparison to sugarcane bagasse or sisal [190]. The choice of the derivatizing agent and molar ratio (mol/mol of AGU) is also very important for a good control of the DS. As mentioned above acetic anhydride has high tendency towards hydrolysis, as the solvent contains a high amount of water, thus very low DS could be obtained e.g. acetylation of sisal dissolved in DMSO/TBAF with acetic anhydride [67]. Acyl-1H-benzotriazole and succinic anhydride show better results with the same solvent [68, 191].

The most prominent example for the utilisation of a derivatizing cellulose solvent is the viscose process [192]. Viscose fibre is a cellulose fibre obtained by the viscose process. It is known as rayon fibre in the USA. Viscose fibres are made from cellulose from wood pulp. The cellulose is derivatized in NaOH/CS₂ and submitted to wet spinning. Wet-spinning is based on precipitation, where the polymer is drawn through a spinneret into a non-solvent. However, the viscose process has several drawbacks due to the use of highly toxic CS₂ and precipitate formation owing to chemical degradation of polysaccharides [193]. The process to make Lyocell [194] fibres is a solvent spinning process (dry-jet wet spinning) developed to replace viscose technology. The cellulose is directly dissolved in the solvent NMMO/water or ionic liquids (Iocell-F fibres) such as [Bmim][Cl], [Bmim]Ac, [Emim][Cl], [Emim][Ac] and [DBNH]Ac [195], spun through an air gap and precipitated in water. Thus, this fibre is composed of cellulose

because it has not suffered substitution reactions. The comparison of the structure and properties of the viscose fibre to NMMO fibre can be found in literature [150]. The Table 7 shows mechanical properties of cellulose fibres prepared from ILs.

Table 7 Mechanical properties of cellulose fibres modified from Röder [196]

Fibre/solvent	Cross section shape	titre (dtex)	Tenacity cond. (cN/tex)	Elongation cond. (%)	Tenacity wet (cN/tex)	Elongation wet (%)	BISF A modulus (cN/tex/5%)	Modulus cond. (cN/tex/%)	Commercial/experimental fibre
Viscose ^a	Lobate	1.3	22		12				Commercial
NMMO	Round	1.3	40.2	13.0	37.5	18.4	10.8	8.8	Commercial
[Emim][Cl]	Round	1.7	43.0	9.6	35.9	11.6	14.0	8.1	Experimental
[Bmim][Cl]	Round	1.5	50.1	9.3	39.4	10.4	17.8		Experimental
[Emim][Ac]	Round	1.8	44.7	10.4	38.1	11.9	13.2	10.0	Experimental

^aFibre data from [150]

Fibre characterisation is normally done by measuring the tenacity and the elongation at break. Furthermore, titre, modulus and cross-section can be determined [196]. The level of stretching determines the tenacity and elongation level. A high degree of stretching results in a relatively tear-resistant and low strain fibre. A higher elastic modulus means a higher resistance of the fibre against deformation. The same cross section can be obtained for different solvent systems assuming the use of similar spinnerets. NMMO and ILs present fibre properties in the same range (Table 7) and the same cross section (round). Higher tenacity, crystallinity and molecular weight can be obtained using the Lyocell process [197]. Degradation during the Lyocell process should be less than 10%, thus similar fibre properties of Lyocell fibres spun from ILs compared to NMMO suggest similar solution structures of cellulose [197]. Additionally, the mechanical properties of the regenerated fibres such as tensile strength and elongation at break can be strongly dependent on the DP of the original cellulose [163]. Despite many advantages, the Lyocell process still produces fibres with severe fibrillation. Fibrillation is the peeling away of fibrils of the fibre surface by applying mechanical stress to fibres which are swollen in water [198]. This is undesired for especially in the processing from fibre to fabric. Methods for fibrillation reduction have been published [199-201]. The use of NMMO which is a thermally unstable solvent could lead to uncontrolled thermal degradation. From the thermodynamic point of view the state of a thermal explosion is reached that requires a major investment in safety technology [202]. Additionally, the use of high melting point alkylmethylimidazolium based ILs shows spinning dopes containing high cellulose concentration (e.g. 16.5 wt %) however, the decomposition and the viscosity remain a challenge [203]. A novel cellulose spinning solvent consisting of a superbase -based ionic liquid, [DBNH]Ac have been reported with high dissolution power and a low viscosity [195] producing high tenacity fibres (over 50 cN/tex).

It has been demonstrated that chemical modification of cellulose may be carried out under homogenous conditions using ILs in a commercial scale towards high-value cellulose derivatives as published in a patents review [204]. The substitution reaction using ILs does not require an inorganic base in order to activate cellulose [205]. The performance of the homogeneous reaction in ionic liquid media presents a number of advantages, being the main one the existence of different options in introducing functional groups and the better control of the DP and in the degree of substitution (DS). Several experimental methods have been developed in the field of biomass processing using ILs in substitution reaction to obtain cellulose derivatives. Some of them are shown in Table 8.

Table 8 Reaction conditions of cellulose esters production and the respective degree of substitution

Ionic liquid	Co-solvent Catalyst Base	(wt%) ^a	Reagent	Reaction conditions ^b	DS ^c	Ref.
[Amim][Cl]	DMAP, DMF	4	Propionic anhydride, butyric anhydride	1:1 - 5:1; 2 - 180 min; 20 - 100°C	Prop: 0.89-2.89, But: 0.91-2.76	[205]
[Amim][Cl]		4	Propionic anhydride/acetic anhydride, butyric anhydride	5:1, 9:1, 13:1; 60 - 300 min; 80 -100°C	Prop: 0.93-2.46, But: 0.86-2.07	[206]
[Bmim][Cl]	Pyridine	11	Acetyl chloride	3:1, 5:1, 10:1; 2 h; 80°C	Ac < 3.00	[207]
[Amim][Cl]	Pyridine, Triethylamine	10	Acetic anhydride, tosyl chloride	3:1, 8:1; 48 h, r.t.	Ac: 2.99, Tos: 0.84	[208]
[Emim][Ac]	Imidazole	3	Tosyl chloride	2:1; 300 min; 7°C	Tos: 0.55	[209]
Bmim]Cl,	Pyridine, DMF,	11	Tosyl chloride	1:1 - 5:1; 1 -	Tos: 1.14, Cl:	[210]

[Amim][Cl], [Emim][DEP]	DMI			48 h; 25°C	0.16	
[Bmim][Cl]	Pyridine	11	2-furoyl chloride	1:1, 3:1, 5:1; 0.5 – 17 h; 65°C	0.46-3.00	[211]
[Bmim][Cl] [Emim][Cl] [Bdmim]Cl [Admim]Br	Pyridine	11	Acetyl chloride Lauroyl chloride Phenyl isocyanate	3:1, 5:1, 10:1; 15 - 120 min; 80°C	Ac: 2.81 - 3.0 Lau: 0.34 - 1.54 Carb:0.26 - 3.0	[212]
[Bmim][Cl]		6	Phenyl isocyanate Acetic anhydride	1:1 – 10:1; 120 - 240 min; 80°C	Carb: 0.29 - 3.0 Ac: 0.69 - 3.0	[213]
[Bmim][Cl]		3	Choroacetyl chloride	3:1, 5:1; 60 – 300 min; 30 - 50°C	0.33 - 1.87	[214]
[Amim][Cl]	DMF	4	2-bromopropionyl bromide	5:1; 480 min; r.t.	0.7	[215]
[Amim][Cl]		3 - 7	Benzoyl chloride, 4-toluoyl chloride, 4-chlorobenzoyl chloride, 4- nitrobenzoyl chloride	2:1 – 10:1; 60 – 240 min; 40 – 100°C	1 - 3.0	[216]
[Bmim][Cl]		10 - 12	Acetic anhydride, Propionic anhydride, Butyric anhydride, Pentanoic anhydride, Hexanoic anhydride	1:1, 3:1, 5:1; 2 h; 80°C	0.4 – 3.0	[217]
[Bmim][Cl], [Amim][Cl], [Emim][Ac]	Pyridine, DMF	11	Sulfur trioxide, chlorosulfonic acid	1.3:1 - 3:1; 120 - 240 min; 25°C	0.22 - 0.89	[218]
[Bmim][Cl]		2.35	Phthalic anhydride	2:1 - 10:1; 20 - 120 min; 85 - 105°C	0.12 - 2.54	[219]
[Bmim][Cl]		2	Succinic anhydride	1:1 - 12:1; 5 - 120 min; 85 - 105°C	0.037 - 0.53	[220]
[Bmim][Cl]	DMSO <i>N</i> - bromosuccinimi de	2	Succinic anhydride	4:1; 30 - 240 min; 90 - 120°C	0.24 - 2.31	[221]
[Bmim][Cl]	DMAP	2	Succinic anhydride	4:1; 30 - 120 min; 60 - 110°C	0.24 - 2.34	[222]
[Bmim][Cl]	Iodine		Succinic anhydride	4:1; 30 - 120 min; 85 - 110°C	0.56 - 1.54	[223]
Patents						
[Bmim]Ac [Bmim][Cl] [Bmim]OPr			Carboxylic anhydrides, carboxylic acid halides, diketene, or acetoacetic acid esters	< 0.2 (molar ratio)	0.1-3.0	[224]
d	Aprotic solvents, protic solvents, acids		Ci to C20 straight- or branched-chain		0.1-3.0	[225]

			alkyl or aryl carboxylic anhydrides, carboxylic acid halides, diketene, or acetoacetic acid esters			
e			Acetic anhydride, Propionic anhydride, Butyric anhydride, 2-ethylhexanoic anhydride, Nonanoic anhydrid		≤ 3.0	[226]
Carboxylated ILs						[227]
d		0.1 - 50	Thionyl chloride, Methanesulfonyl chloride, Chlorodimethylim inium chloride, Phosphoryl chloride, Tosyl chloride	30 – 150°C	0.5 - 3.0	[228]
d	Pyridine	5 - 10	Chlorosulfonic acid, Sulfur trioxide, Sulphuric acid, Sulfamic acid	1:1 - 6:1; 1 – 720 min; 130°C	0.05-2.5	[229]
^a Concentration of cellulose in ionic liquid during dissolution by weight; ^b Molar ratio of reagent per mol of anhydroglucose unit (AGU) in cellulose; Reaction time; Reaction temperature; ^c Range of degrees of substitution (DS); ^d Cation: imidazolium, pyrazolium, oxazolium, 1,2,4-triazolium, 1,2,3-triazolium, and/or thiazolium, quinolinium, isoquinolinium, piperdinium, pyrrolidinium, pyridazinium, pyrimidinium, pyrazinium, pyrazolinium; Anion: C1 to C20 straight- or branched-chain carboxylate or substituted carbolyate, or alkylphosphates (e.g. chloride, formate, acetate, propionate, butyrate, valorate, hexanoate, lactate, oxalate, chloro-, bromo-, fluoro- substituted acetate, propionate and butyrate); ^e Carboxylated ionic liquids containing sulfur, halide or transition metals						

7.1. Esterification

Conversion of cellulose, dissolved in different ILs, with carboxylic acid chlorides or anhydrides is very efficient for the preparation of cellulose esters (Table 8). General synthesis route and molecular structure of cellulose esters homogeneously prepared in ILs were thoroughly reviewed elsewhere [230].

Cellulose acetate butyrate and cellulose acetate propionate can be prepared homogeneously in [Amim][Cl] from sugarcane bagasse [206]. The cellulose acetates content was affected by reaction temperature, reaction time, and molar ratio reagent/AGUs. With propionic anhydride the DS obtained was between 0.89 and 2.89, and with butyric anhydride was from 0.91 to 2.76. The most common methods for determination of DS include ¹H NMR, ¹³C NMR in DMSO-*d*₆, CDCl₃ or D₂O.

Heinze et al [207] used [Bmim][Cl] as reaction medium and synthesized cellulose acetates with high DS values in good yield (85.9%) within a short time (2h). DS was controlled by the amount of reagent added. The acetylating reagent acetic anhydride proved to be less effective than acetyl chloride. Cellulose fluorates can be synthesized with yields of 84,4% and 90,2% and with a DS range of 0.46 - 3.0; thus, as [Bmim][Cl]

is a very efficient medium for reaction, short reaction times and low amounts of acylation reagent are needed [211]. Cellulose benzoates with different moieties at the aromatic ring are prepared homogeneously in [Amim][Cl] by conversion of cellulose with the corresponding benzoyl chlorides [216]. An excess of reagent of 5 mol per mol of AGU leads to completely substituted cellulose derivatives [217] such as cellulose pentanoates, cellulose hexanoates, with DS above 0.9 soluble in DMSO and for DS of 2.3 soluble in DMSO, acetone and chloroform. Comparing these DS data to that presented in Table 5 from homogeneous acetylation reactions using organic solvents it is clear that the DS is higher with use of ILs. In addition, the reaction temperature also decreases with ILs from the range 40-110°C to 25-80°C.

Cellulose sulfates were prepared through homogeneous conversion of cellulose with different sulfating reagents in [Bmim][Cl], [Amim][Cl] and [Emim][Ac] is performed using DMF as dipolar aprotic co-solvent [218]. The sulfation of cellulose in [Bmim][Cl] proceeded in 30 min and the prolongation of the reaction time to 2h did not change the DS values significantly. In contrast, after 24h, the DS of the products decreased from 0.83 to 0.66, which is most likely due to acidic cleavage of the sulphate ester bond. The sulfation was investigated at 25°C and higher temperature. The results show that sulfation at higher temperature does not give the desired DS, indicating decomposition of polymer chain. Production of cellulose sulfates with DS up to 2.5 was patented by Procter & Gamble Company [229].

The *p*-toluenesulfonic acid esters of cellulose, commonly referred to as cellulose tosylates, are versatile intermediates for the preparation of various cellulose derivatives. Homogeneous reaction yielding tosylated cellulose can be carried out in [Amim][Cl] and aspects such as the degree of tosylation, the reaction temperature and the base can be varied, e.g., trimethylamine is not fully mixed with [Amim][Cl], however, pyridine works efficiently [208]. The homogeneous reaction leads to a predominant conversion of primary hydroxyl groups at DS values up to 1 [209, 210]. However, derivatization with tosyl chloride generates additional chloride as a second reaction product, thus chlorination of cellulose occurs due to chloride ions present in the reaction media Fig. 4. Additionally, a tosylated AGU may also react with hydroxyl groups of the same or another cellulose chain, which would result in cross linking and thus, insoluble products. In order to prevent these side reactions, temperature is usually kept around 8-10°C [210].

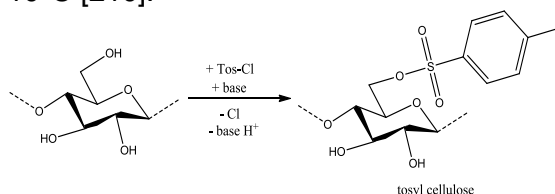


Fig. 4 Tosylation of cellulose with tosyl chloride [210]

Preparation of cellulose carbanilates with DS up to 3.0 could be prepared in [Bmim][Cl]. The synthesis of cellulose carbanilates was carried out without any catalysts. Higher DS were accessible by increasing molar ratio and reaction time. Heinze [212] and Schluffer [213] showed that bacterial cellulose with DP~ 6500 could be efficiently converted with phenyl isocyanate under homogeneous reaction conditions. Heinze and co-workers have investigated the acylation of cellulose in four kinds of ILs with fatty acid chloride (lauroyl chloride), leading to cellulose laurates with DS from 0.34 to 1.54. The reaction was found to start homogeneously and then continue heterogeneously. DS values slightly increased with addition of a base such as pyridine and with shorter reaction time (2h). Additionally, the acetates were soluble in DMSO but not in acetone and for DS higher than 2.85 were soluble in chloroform. Schluffer compared DS of acetylated bacterial cellulose (BC) to the DS from the reaction with cellulose from plants (lower DP) a lower reactivity was found. Highly substituted BC phenyl urethanes were soluble in DMSO, DMF and in THF depending on the DS.

Cellulose chloroacetates and bromoacetates, were synthesized by acylation of cellulose with chloroacetyl chloride and 2-bromopropionyl bromide under mild conditions in [Bmim][Cl] and [Amim][Cl] respectively [214, 215]. The cellulose acetates (macroinitiators) have been applied for subsequent preparation of methacrylate graft copolymers by atom transfer radical polymerization (ATRP).

[Bmim][Cl] have been also applied as reaction media for the homogeneous preparation of dicarboxylic acid esters such as cellulose phthalates. A series of phthalated cellulosic derivatives [219] can be prepared with moderate DS (ranging from 0.12 to 2.54). DS increases with reaction temperature from 85 to 100°C, molar ratio of phthalic anhydride/AGU in cellulose from 2:1 to 10:1 and reaction time from 20 to 120 min. Cellulose succinates are produced through succinylation of cellulose with succinic anhydride and [Bmim][Cl] (DS up to 2.18) [220] and with addition of catalysts: N-bromosuccinimide (DS up to 2.31) [221], 4-dimethylaminopyridine (DS up to 2.34) [222] and iodide (DS up to 1.54) [223].

Various patents have been published by Eastman Chemical Company that describe the homogeneous preparation of cellulose esters and mixed esters, and the recycling of the ILs by evaporation of precipitation agent and residues of the volatile acylation reagents [224-227]. In some of these inventions, the produced cellulose esters were used as protective and compensation films for liquid crystalline displays. A patent for chlorinating polysaccharides with DS up to 3 is also found in literature [228].

7.2. Etherification

In Millymaki and Aksela [231] invention of a method for preparing cellulose ethers, the derivatives have been divided into aliphatic cellulose ethers, comprising alkyl ethers, substituted alkyl ethers, hydroxyalkyl ethers and mixed aliphatic ethers of cellulose. The second group comprises aryl and aralkyl ethers of cellulose and the third group silyl ethers of cellulose. Table 9 presents some examples of etherification reactions of cellulose dissolved in different ILs.

Table 9 Reaction conditions of cellulose ethers production and the respective degree of substitution

Ionic liquid	Co-solvent Catalyst Base	(wt%) ^a	Reagent	Reaction conditions ^b	DS ^c	Ref.
[Emim][Ac], [Emim][Cl]	DMSO, DMA		Hexamethyldisilazane	3:1, 5:1, 8:1; 1 h; 80°C	1.6 - 2.9	[217]
[Emim][Cl], [Bmim][Cl], [Emim]SCN, [Bmim]SCN, [Emim][Ac], [Bmim]Ac, [Bmim]PrO, [Bmim]Bz	Saccharine, Toluene	10	Hexamethyldisilazane	1.8:1 - 9.2:1; 16 h, 80 - 120°C	1.2 - 2.9	[232]
[Bmim][Cl]	Pyridine	11	Trityl chloride	1 - 14 h, 100°C	0.80- 1.37	[233]
[Amim][Cl]	Pyridine		4-methoxytrityl chloride	3:1, 6 h, 60°C	~ 2	[234]
[Amim][Cl]	Pyridine or 1- butylimidazole	10	Trityl chloride	3:1, 6:1; 1 - 20 h; 90°C	0.02 - 0.95	[235]
[Emim][Ac]	DMSO	4 - 11.5	Propylene oxide, ethylene oxide	5:1 - 50:1; 19 h; 80°C	0.09 - 1.34	[236]
Patents						
Cations: [Bmim] ⁺ , [Emim] ⁺ Anions: Ac, Cl, Bz, SCN, OPr, (C ₂ H ₅ O) ₂ PO ₂	ethers, ketones, hydrocarbons		Trimethylsilyls (e.g. hexamethyldisilazane, trimethylsilyldiethylamine or N,O bis(trimethylsilyl)acetamide		0.4- 2.6	[237]
[Emim][Ac], [Bmim][Cl]	H ₂ O, DMSO, DMF, DME, CHCl ₃		Propylene oxide, ethylene oxide, 1- allyloxy-2,3-epoxypropane, 2,3- epoxypropyl isopropyl, etherepichlorohydrine, 2,3- epoxypropyltrimethylammonium chloride, phenylglycidylether, 2,3- epoxypropyl isopropyl ether	5:1, 10:1, 30:1; 3 - 72 h; 21 - 100°C	0.09 - 2.16 ^d	[238]
[Bmim][Cl]		1 - 35	hexamethyldisilazane	30 - 210 h; 125°C	< 0.9	[239]
^a Concentration of cellulose in ionic liquid during dissolution by weight; ^b Molar ratio of reagent per mol of anhydroglucose unit (AGU) in cellulose; reaction time; reaction temperature; ^c Range of degrees of substitution (DS); ^d Molar substitution (MS).						

Homogenous silylation of cellulose has been reported under mild conditions, within short reaction time at low temperature (1h, 80°C) and low excess of reagent [217]. Trimethylsilyl cellulose was obtained through reaction of cellulose dissolved in [Emim][Ac] and [Emim][Cl] with etherifying reagent hexamethyldisilazane (HMDS). [Emim][Ac] is more efficient than [Emim][Cl] in this reaction. It has been reported [232] that carboxylate and diethylphosphate counter-ions give better results than chloride. Furthermore, the solubility of HMDS in the IL increases with the increasing extent of CH_x groups in the anion. Additionally, because of HMDS insolubility in the IL trimethylsilyl cellulose precipitates thus the reaction starts homogeneously and ends heterogeneously. To keep it homogenous a solvent is added (DMSO or DMAc).

Tritylation of cellulose with trityl chloride is an effective protecting group strategy for synthesizing regioselectively modified cellulose derivatives [235]. Homogeneous tritylation of cellulose in [Amim][Cl] with trityl chloride (TrCl) showed that DS can be influenced by the type of base used in the reaction (pyridine or 1-butylimidazole). The reaction with pyridine started heterogeneously then changed to homogeneous finishing heterogeneous and produced trityl cellulose with higher DS ~ 1. Despite the homogeneous reaction in the presence of 1-butylimidazole (BIM) the higher DS was 0.22. BIM is not considered suitable for tritylation of cellulose in ILs.

Köhler [236] reported the homogeneous hydroxyalkylation of cellulose without additional inorganic bases under completely homogeneous reaction conditions in [Emim][Ac] at 80°C for 19h. The reagents propylene oxide and ethylene oxide produced derivatives with a DS from 0.09 to 1.34. Addition of co-solvent (dimethylsulfoxide) to a higher concentrated solution of cellulose/IL changed the DS to higher value.

The Invention [238] of homogeneous reaction without addition of organic or inorganic bases with lower IL load and in which high DP (from 1000 to 6500) cellulose can be applied. The cellulose ethers produced by this invention include 2-hydroxyethyl cellulose, 2-hydroxypropyl cellulose, 2-hydroxybutyl cellulose, 2-hydroxy-3-isopropoxypropyl cellulose, 3-allyloxy-2-hydroxypropyl cellulose, 3-chloro-2-hydroxypropyl cellulose, (2-hydroxy-3-trimethylammoniumpropyl)-cellulose chloride and 2-hydroxy-3-phenoxypropyl cellulose. These products are soluble in H₂O and DMSO depending on the molar substitution (MS). MS values of hydroxyalkyl celluloses were determined by the method of Zeisel. Homogeneous synthesis of cellulose ethers [238] has been patented by Tylose GmbH & Co. in ILs such as [Bmim][Cl], [Emim][Ac] and co-solvents: dimethylsulfoxide, dimethylformamide, dimethoxyethane and chloroform.

An example of cellulose etherification process carried out under heterogeneous reactions conditions [239] was introduced in Table 9 for comparison. On the contrary to homogeneous process the heterogeneous etherification method described require an activation of the cellulose previous to the etherification. Trimethylsilylcellulose was produced by reaction from microcrystalline cellulose using [Bmim][Cl] and silylating agent HMDS (mol reagent/molAGU up to 4.5) at high temperature (125°C) with low DS up to 0.9. Suitable reaction times were found to be from 30 min to 3.5 h.

Commercially available hydroxyalkyl celluloses are prepared heterogeneously. This process requires activation of the cellulose which is a cause for higher costs and energy consumption. Additionally, because of the solid state of cellulose and intermediates the product quality depends on the quality of the stirring and geometry of the reaction vessel [240]. In contrast, homogeneous production of cellulose derivatives allows the development of methods for synthesis of cellulose ethers without activation of cellulose and high yields of products with new and better properties.

8. Cellulose precipitation

Regeneration of cellulose from ILs systems occurs by contact of the cellulose solution with a coagulation bath of protic polar solvents such as water or alcohols. Cellulose regeneration mechanisms for selected solvents have been reviewed elsewhere [241]. The yield of regenerated wood and the yield of recycled IL are affected by the choice of anti-solvent. Regeneration of 8 wt% solution of wood dissolved in [Amim][Cl] yielded > 95% (weight percent from the original amount of wood) and practically all the IL could be recovered (under vacuum at 40°C) using water as anti-solvent. Moreover, the yield of regenerated wood with water was reported higher than that of methanol at the same number of IL recycles uses (up to 3). Conventional precipitation can be achieved with anti-solvents such as water (e.g. water concentration in ionic liquid > 20% [113]), ethanol, methanol and acetonitrile show high yields above 90%. Precipitation with compressed CO₂ has been reported as a “greener” alternative [242]. Precipitation of cellulose dissolved in ionic liquid with acetate anion is produced by CO₂ addition because the CO₂ reacts with the acetate anion forming another compound, a carboxylate zwitterion. With the formation of that compound the bonds between cellulose and the acetate anion are broken causing cellulose precipitation. The ionic liquids can be regenerated by adding water in stoichiometric proportion, which destroys the zwitterion. The cellulose precipitated by this method presents a decrease of crystallinity and stability. At pressures between 60 - 180 bar of CO₂ 60% of the cellulose dissolved in [Bmim]Ac is precipitated resulting in relatively low yield compared to that of protic solvent. Despite the low yield, CO₂ could be a sustainable method to regenerate cellulose from ILs.

The cellulose can be regenerated in the shape of powder, fibers or films, but these last two forms are especially interesting. The fabrication of regenerated cellulose fibre/film involves two steps: dissolution of cellulose in IL to make the spinning dope and extrusion of the spinning dope to form regenerated cellulose fibre and film. The influence of spinning conditions on cellulose crystallization taken place during fibre/film precipitation with water, of great importance in fibre and film processing, has been studied in several works

Sun and coworkers [243] studied the crystalline characteristics of regeneration of cellulose fibre, extrudate, and film from 6 % cellulose/[Bmim][Cl] solution with different spinning conditions. The degree of crystallinity, crystal size and crystallite orientation of the regenerated cellulose fibre and film, were evaluated using wide angle X-ray diffraction (WAXD).

WAXD data showed that cellulose regenerated from [Bmim][Cl] solution was transformed from Cellulose I to Cellulose II structure, and amorphous regions increased in the regenerated cellulose. Crystalline characteristics of regenerated cellulose are affected by the die shapes. A reduction of die diameter does not cause a significant change in fibre crystallinity, but results in an increase in crystallite size and crystal orientation factor. Additionally, fibre drawing speed was showed to be a main effect to improve fibre crystal orientation.

Airgap- and wet spinning of Eucalypt dissolving grade pulp in [Emim][Ac] and methylimidazole (MIM) was investigated by Olsson et al. [244]. Pure [Emim][Ac]/cellulose solution was spun at 2.8 m min⁻¹ through 150 µm capillaries. For samples with co-solvent MIM an 80 µm holes spinneret was used due to lower viscosity. Coagulation took place in water, and fibres were drawn by rotating take-off rollers to desired extent. The fibres were then immersed in pure water for 1 week before drying at 105°C for 1h. The crystallinity of the fibre with only [Emim][Ac] as solvent is lower than for fibres with co-solvent. However, fibres with higher tenacity cannot be achieved with high amount of co-solvent i.e., $x_{IL} = 0.5$ in 15% pulp solutions.

Michud and coworkers [245] produced regenerated cellulose fibres by dry-jet spinning from cellulose/[DBNH]Ac solutions to study the influence of cellulose molecular

structure on the spinnability and the mechanical properties of the resulting fibres. The solutions were extruded through a multi-hole spinneret (36 holes, diameter of 100 μm , and capillary length of 20 μm) via 1 cm air gap into a cold (10 - 15°C) aqueous coagulation bath at constant extrusion velocity 16 cm^3/min . High spinnability with high stretching was found for a proportion of cellulose chain having DP > 2000 larger than 20 wt% and DP < 100 between 5 and 10 wt%. The final properties of the fibres are directly affected by the draw of the fluid filaments in the air gap.

The effect of altering the coagulation medium during regeneration of cellulose dissolved in [Emim][Ac] was also studied [246]. 4 wt% cellulose solutions were coagulated in water, ethanol and 1-propanol. For films coagulated in water a higher degree of cellulose II was found compared to the films coagulated in alcohols. The decreased preference of [Emim][Ac] to diffuse into the coagulation bath could explain the lower conversion to cellulose II in alcohols.

Diffusion of [Bmim][Cl] from cellulose filament during coagulation process was studied [247] and the factors affecting it: polymer concentration, concentration and temperature of the coagulation bath. The diffusion rate of [Bmim][Cl] decreased with increasing polymer content (5, 8, 10 and 12 wt%) in the spinning solution and the initial concentration of [Bmim][Cl] in the coagulation bath (0 - 20 wt%), while the diffusion coefficients increased largely with the coagulation temperature becoming higher (5 - 70°C).

9. Recycling of ILs after cellulose processing

In general, synthesis of ILs is a polluting and energy intensive process that frequently involves the use of halide and/or sulfur intermediates, conventional organic solvents or the uses of metal oxide catalysts. Chlorinated organic compounds are in general undesired, especially in processes at technical scale, due to the difficulties and safety issues in waste disposal. For environmental conservation and economy of processes, it is required and important to recover and recycle ILs after the regeneration or derivatization of cellulose [248]. If these solvents are efficiently recycled, the overall waste production of the process will be decreased.

Methods used for recovery and recycling of ILs such as distillation, extraction, adsorption, induced phase separation and membrane-based methods were thoroughly reviewed elsewhere [249]. Thus, only a few considerations about this point will be treated here.

In cellulose processing the most frequent impurities in ILs at the end of the process are heavy impurities due to the decomposition or incomplete precipitation of cellulose, and volatile impurities such as water or alcohols used to cause cellulose precipitation. Due to the negligible vapour pressure of ILs volatile impurities can be removed from the IL mixture by evaporation without loss of the ILs. Nevertheless, this process can be energy intensive. Traditional methods like evaporation and extraction were applied to remove the impurities from [Emim][Ac] which had been previously used as medium for cellulose acetylation [250]. Impurities like ethyl acetate, *n*-propyl acetate, isopropyl acetate, and tetrahydrofuran (THF) could be reduced from 40 wt % to 5 wt % within less than 1h using these methods. However, acetic acid was found not to be easily removed from [Emim][Ac] or [Emim][Cl] by evaporation, and a residual level of about 20 % and 8 % was respectively achieved, due to the high normal boiling point of acetic acid (118°C). Liquid-liquid extraction for acetic acid removal was also unsuccessful due to the slow mass transfer despite the extraction ability for acetic acid of the tested solvents. Esterification of acetic acid with alcohol in large excess at elevated temperature and pressure with subsequent distillation was found to be the best method to purify [Emim][Ac]. Molecular distillation was used to recover [Amim][Cl] used in homogeneous cellulose acetylation [251]. The IL was recovered with combination of

two techniques: conventional vacuum to remove most of the water and then the small amounts of acetic acid and water (less than 10% by mass) that are difficult to remove were disposed through molecular distillation. The IL was recycled and reused 5 times in the reaction and the purity of recycled IL the 5th time reached 99.56%.

In theory ILs, can be reused, but after many cycles heavy impurities can be accumulated or degradation can be suffered by the ILs. Moreover, in derivatization processes the use of organic or inorganic bases and the addition of stabilizers results in degradation of the biopolymer and exhibits an enormous drawback for ILs recycling and its repeated application [226]. An object of further investigation in cellulose processing is to develop a simple process for the preparation of cellulose derivatives which does not require the addition of any organic and/or inorganic bases and which reduces the salt load and were the IL can be easily recycled and reused after purification.

10. Evaluation of ILs toxicity

Dissolution of cellulose with ionic liquids allows the combination of two major green chemistry principles: using environmentally preferable solvents and bio-renewable feed-stocks. Imidazolium and cellulose are part of the Safer Chemical Ingredients List that meets the criteria of the Design for the Environment (DfE) Safer Product Labeling Program [252]. Nevertheless, some ionic liquids show hazard potential for man and the environment. The “greenness” of IL strongly depends on its substructure (anion, head group and side chain of the cation) [253].

ILs are in general considered green solvents because in general they do not evaporate and pass to the atmosphere unlike the organic solvents. Thus, waste water streams most likely represent the main entrance pathways of ILs into the environment and their potential effects on aquatic ecosystems are largely unknown. In Table 10 are reported EC₅₀ values (concentration at which 50% of the exposed organisms are either immobilized or killed) of different ILs. The data represents possible hazard potentials that ILs might exert when coming into contact with organisms.

Table 10 Ecotoxicological data of ILs from UFT Ionic Liquids Biological Effects Database [253]

Entry	Compound	Citotoxicity EC ₅₀ ^a ($\mu\text{mol}\cdot\text{L}^{-1}$)	Ecotoxicity EC ₅₀ ^b ($\mu\text{mol}\cdot\text{L}^{-1}$)
1	1-ethyl-3-methyl-1H-imidazolium acetate	16800	
2	1-ethyl-3-methyl-1H-imidazolium methyl sulfate	15700	
3	1-ethyl-3-methyl-1H-imidazolium chloride	9900	770 ^c
4	1-ethyl-3-propyl-1H-imidazolium bromide	>2000	
5	1-butyl-3-methyl-1H-imidazolium chloride	3580	84.7 ^c
6	1-butyl-3-methyl-1H-imidazolium methyl sulfate	1630	
7	1-butyl-3-methyl-1H-imidazolium 1,1,1-trifluoromethanesulfonate	1050	233 ^d , 3950 ^e
8	1-butyl-3-methyl-1H-imidazolium iodide	3030	3910 ^e
9	1-butyl-3-methyl-1H-imidazolium	1250	70.1 ^c , 182 ^d , 3270 ^e

	hexafluorophosphate		
10	1-butylpyridinium hexafluorophosphate	7100	
11	1-(2-hydroxyethyl)-3-methyl-1H-imidazolium tetrafluoroborate(1-)	3040	
12	1-(4-hydroxybutyl)-3-methyl-1H-imidazolium chloride	>3000	
13	1-(3-carboxypropyl)-3-methyl-1H-imidazolium chloride	>3000	
14	1-(3-hydroxypropyl)-3-methyl-1H-imidazolium chloride	>20000	3350 ^d
15	1-(2-hydroxyethyl)-3-methyl-1H-imidazolium iodide	>20000	1650 ^d , 7710 ^e
16	1-decyl-3-methyl-1H-imidazolium chloride	21.8	0.586 ^e
^a Viability of IPC-81 leukemia cells; ^b Growth inhibition: assessment according to empirical data (rough classification of cytotoxicity towards ^c water flea <i>Daphnia magna</i> ; ^d aquatic plant <i>Lemna minor</i> ; ^e marine bacteria <i>Vibrio fischeri</i>); < 1 $\mu\text{mol}\cdot\text{L}^{-1}$: very high cytotoxicity; 1 - 100 $\mu\text{mol}\cdot\text{L}^{-1}$: high cytotoxicity; 100 - 5000 $\mu\text{mol}\cdot\text{L}^{-1}$: moderate cytotoxicity; > 5000 $\mu\text{mol}\cdot\text{L}^{-1}$: low cytotoxicity			

It is known that in general ILs with longer alkylic substituent have their hydrophobicity increased as well as its toxicity. The impact of aromaticity on the toxicity of different cations (pyridinium, piperidinium, pyrrolidinium and imidazolium) and hydrophobic anions has been studied [254]. For example changing from imidazolium to pyridinium cation and keeping the same anion decreases the toxicity (entry 9 and 10 of Table 12). The acute effects of room-temperature ILs on survival of the crustacean *Daphnia magna* was studied were toxicity appeared to be related to the imidazolium cation and not to the various anions (e.g., Cl^- , Br^- , PF_6^- , and BF_4^-) [255]. Imidazolium cations representing lower toxicity would be the ones with a hydroxyl group in the alkyl chain (entries 11 to 15) followed by those with short alkyl substituents 1-ethyl-3-methyl-1H-imidazolium (entries 1 to 3) and 1-butyl-3-methyl-1H-imidazolium cations (entries 5 to 9)

In what respects to the effect of the different cations, the phosphonium-based ILs seem to be more toxic when compared to the analog imidazolium-based ILs (with the same anion and alkyl chains). The toxicity of five guanidinium-, six phosphonium-, and six imidazolium-based ILs, towards the luminescent marine bacteria *Vibrio fischeri* was studied [256]. These results showed that guanidinium-, unlike the imidazolium- and phosphonium-based ILs, do not follow the trend of increasing toxicity with the increase in the alkyl chain length (entry 16). Toxicity of ILs tends to decrease for organisms (e.g. *Lemna minor*) when short functionalised side chains replace non-polar alkyl chains [257]. The effect of ILs was assessed on the growth of *Lemna minor*, a common aquatic vascular plant [258] and in general, 1-alkyl-3-methylimidazolium chemicals with longer alkyl chains were more toxic to *Lemna minor* than those with short alkyl chain lengths. The concentration that produced a 50% reduction (the EC_{50}) in root growth was higher when a butyl chain was present than when an octyl chain was substituted (i.e., much more toxic). Butyl-substituted 3-methylpyridinium and 3-methylimidazolium cations had similar toxicity, whereas a tetrabutyl ammonium cation was considerably less toxic.

Significant uncertainty still exists regarding the toxicity and potential impact of ILs on the environment. In general, ILs used in cellulose dissolution and derivatization present

a relatively low toxicity (e.g. [Emim][Ac] and [Bmim][Cl]). Nevertheless, in their use as solvents in cellulose industry, the toxicity and safety to human health should be further evaluated, because of possible trace residual ILs in the final regenerated cellulose materials and cellulose derivatives.

11. Conclusions

Several aspects of cellulose processing in ILs have been reviewed. Cellulose has strong inter- and intramolecular hydrogen bonds, which limits the efficient application of this bio-polymer. The advantages and disadvantages of using ILs in cellulose derivatization were discussed for esterification and etherification of cellulose. However, key problems such as the high cost and high viscosity of ILs have been delaying their use in industrial cellulose processing. Additionally, effective recyclability and reuse of ILs are also required for industrial application. Most ionic liquids used for cellulose processing present low or moderate toxicity and ecotoxicity, but further studies must be made because of possible traces residual in the regenerated cellulose materials and derivatives.

Abbreviations

AGU	Anhydrous Glucose Unit
[Amim][Cl]	1-Allyl-3-methylimidazolium chloride
[Admim]Br	1-Allyl-2,3-methylimidazolium bromide
[Amim]HCO ₂	1-Allyl-3-methylimidazolium formate
[Bmim]CH ₃ SO ₃	1-Butyl-3-methylimidazolium methanesulfonate
[Bmim][Cl]	1-Butyl-3-methylimidazolium chloride
[Bmim]BF ₄	1-Butyl-3-methylimidazolium tetrafluoroborate
[Bmim]NO ₃	1-Butyl-3-methylimidazolium nitrate
[Bmim]PF ₆	1-Butyl-3-methylimidazolium hexafluorophosphate
[Bmim]Tf ₂ N	1-Butyl-3-methylimidazolium bis(trifluoromethylsulfonyl)imide
[Bmim]I	1-Butyl-3-methylimidazolium iodide
[Bmim]Ac	1-Butyl-3-methylimidazolium acetate
[Bmim]C ₂ H ₅ CO ₂	1-Butyl-3-methylimidazolium propionate
[Bdmim]Cl	1-Butyl-2,3-methylimidazolium chloride
[Bmim]MeSO ₄	1-Butyl-3-methylimidazolium methylsulfate
[bdta]Cl	Benzyltrimethyltetradecylammonium chloride
[Bmpyr]Cl	1-Butyl-1-methylpyrrolidinium chloride
[Bmpyr]CF ₃ SO ₃	1-Butyl-1-methylpyrrolidinium trifluoromethanesulfonate
CH ₃ C ₆ H ₄ SO ₃ [Tos]	Tosylate
CF ₃ SO ₃	Trifluoromethanesulfonate
CH ₃ (CH ₂) ₂ C ₂	Butyrate
CP	Cellulose propionate
CA	Cellulose acetate
CB	Cellulose butyrate
CAP	Cellulose acetate phthalate
CAB	Cellulose acetate butyrate
CMC	Carboxymethyl cellulose
CS ₂	Carbon disulphide
DP	Degree of polymerization
DS	Degree of substitution
DMF/N ₂ O ₄	N,N-Dimethylformamide/Dinitrogen tetroxide
DMAc/LiCl	N,N-Dimethylacetamide/Lithium chloride

DMSO/TBAF	Dimethylsulfoxide/tetrabutylammonium fluoride
DMSO	Dimethylsulfoxide
DMAP	4-Dimethylaminopyridine
[DBNH]Ac	1,5-diaza-bicyclo[4.3.0]non-5-enium acetate;;
DMI	1,3-Dimethyl-2-imidazolidinone
DME	Dimethoxyethane
[Emim]Br	1-Ethyl-3-methylimidazolium bromide
Emim]CF ₃ CO ₂	1-Ethyl-3-methylimidazolium trifluoroacetate;
[Emim]SCN	1-Ethyl-3-methylimidazolium thiocyanate
[Emim]N(CN) ₂	1-Ethyl-3-methylimidazolium dicyanamide
[Edmim]Br	1-Ethyl-2,3-methylimidazolium bromide
[Emim]Tf ₂ N	1-Ethyl-3-methylimidazolium bis(trifluoromethylsulfonyl)imide
[Emim]BF ₄	1-Ethyl-3-methylimidazolium tetrafluoroborate
[Emim]I	1-Ethyl-3-methylimidazolium iodide
[Emim][Cl]	1-Ethyl-3-methylimidazolium chloride
[Emim]CH ₂ SO ₃	1-Ethyl-3-methylimidazolium ethanesulfonate
[Emim]CH ₃ SO ₃	1-Ethyl-3-methylimidazolium methanesulfonate
[Emim](C ₂ H ₅ O) ₂ PO ₂	1-Ethyl-3-methylimidazolium diethylphosphate
[Emim](OCH ₃) ₂ PO ₂	1-Ethyl-3-methylimidazolium dimethylphosphate
[Emim]HCO ₂	1-Ethyl-3-methylimidazolium formate
[Emim]CH ₃ OHPO ₂	1-Ethyl-3-methylimidazolium methylphosphonate
[Me(OEt) ₃ -Et ₃ N] Ac	Triethyl(2-(2-methoxyethoxy)ethoxy)ethylammonium acetate
ECOENG 41M	1-Butyl-3-methylimidazolium 2-(2-methoxyethoxy)-ethylsulfate
[Empy]EtSO ₄	1-Ethyl-3-methylpyridinium ethylsulfate
[Epy]EtSO ₄	1-Ethylpyridinium ethylsulfate
[EEpy]EtSO ₄	1,2-Diethylpyridinium ethylsulfate
[EMpy]CH ₃ SO ₄	2-ethyl-1-methylpyridinium methylsulfate
EC	Ethyl cellulose
HEC	Hydroxyethyl cellulose
HPC	Hydroxypropyl cellulose
HPMC	Hydroxypropylmethyl cellulose
H ₃ PO ₄	Phosphoric acid
H ₂ SO ₄	Sulfuric acid
KOH	Potassium hydroxide
[Mpy]CH ₃ SO ₄	1-methylpyridinium methylsulfate
MMpy]CH ₃ SO ₄	1,3-Dimethylpyridinium methylsulfate
MC	Methyl cellulose
NaOH	Sodium hydroxide
NMMO	N-Methylmorpholine-N-oxide
NBS	N-Bromosuccinimide
[P6,6,6,14](C ₂ F ₅) ₃ PF ₃	Trihexyl(tetradecyl)phosphoniumtris(pentafluoroethyl) trifluorophosphate
2-PrOH	2-Propanol
THF	Tetrahydrofuran

Acknowledgments

Authors thank the Marie Curie Program for the Project DoHip “Training program for the design of resource and energy efficient products for high pressure process”, and the Junta de Castilla y León for funding through the project VA295U14. MDB thank the Spanish Ministry of Economy and Competitiveness for the Ramón y Cajal research fellowship.

References

1. Lenzing. Focus Sustainability. 2008 [cited 2016 10 May]; 2008:[Sustainability in Lenzing Group]. Available from:

http://www.lenzing.com/fileadmin/template/pdf/konzern/nachhaltigkeit/Sustainability_Brochure_2008_EN.pdf.

2. Gardner, K.H. and J. Blackwell, The structure of native cellulose. *Biopolymers*, 1974. 13(10): p. 1975-2001.
3. Nishiyama, Y., J. Sugiyama, H. Chanzy and P. Langan, Crystal Structure and Hydrogen Bonding System in Cellulose Ia from Synchrotron X-ray and Neutron Fiber Diffraction. *Journal of the American Chemical Society*, 2003. 125(47): p. 14300-14306.
4. Thygesen, A., J. Oddershede, H. Lilholt, B.A. Thomsen and K. Ståhl, On the determination of crystallinity and cellulose content in plant fibres. *Cellulose*, 2005. 12(6): p. 563-576.
5. Oh, S.Y., D.I. Yoo, Y. Shin, H.C. Kim, H.Y. Kim, Y.S. Chung, W.H. Park and J.H. Youk, Crystalline structure analysis of cellulose treated with sodium hydroxide and carbon dioxide by means of X-ray diffraction and FTIR spectroscopy. *Carbohydrate Research*, 2005. 340(15): p. 2376-2391.
6. Behera, S., R. Arora, N. Nandhagopal and S. Kumar, Importance of chemical pretreatment for bioconversion of lignocellulosic biomass. *Renewable and Sustainable Energy Reviews*, 2014. 36: p. 91-106.
7. Searle, S. and C. Malins. Availability of Cellulosic residues in the EU. 2013; Available from: http://theicct.org/sites/default/files/publications/ICCT_EUcellulosic-waste-residues_20131022.pdf.
8. Klemm, D., B. Heublein, H.-P. Fink and A. Bohn, Cellulose: Fascinating Biopolymer and Sustainable Raw Material. *Angewandte Chemie International Edition*, 2005. 44(22): p. 3358-3393.
9. Zhang, K., Z. Pei and D. Wang, Organic solvent pretreatment of lignocellulosic biomass for biofuels and biochemicals: A review. *Bioresource Technology*, 2016. 199: p. 21-33.
10. The European Bioeconomy in 2030. [cited 2016 10 May]; Available from: <http://www.epsoweb.org/file/560>.
11. Bagheri, M., H. Rodríguez, R.P. Swatloski, S.K. Spear, D.T. Daly and R.D. Rogers, Ionic Liquid-Based Preparation of Cellulose–Dendrimer Films as Solid Supports for Enzyme Immobilization. *Biomacromolecules*, 2008. 9(1): p. 381-387.
12. Brennan, T.C.R., S. Datta, H.W. Blanch, B.A. Simmons and B.M. Holmes, Recovery of Sugars from Ionic Liquid Biomass Liquor by Solvent Extraction. *BioEnergy Research*, 2010. 3(2): p. 123-133.

13. Dibble, D.C., A. Cheng and A. George, Novel compositions and methods useful for ionic liquid treatment of biomass. 2011: United States.
14. Mikkola, J.-P., A. Kirilin, J.-C. Tuuf, A. Pranovich, B. Holmbom, L.M. Kustov, D.Y. Murzin and T. Salmi, Ultrasound enhancement of cellulose processing in ionic liquids: from dissolution towards functionalization. *Green Chemistry*, 2007. 9(11): p. 1229-1237.
15. Welton, T., Room-Temperature Ionic Liquids. Solvents for Synthesis and Catalysis. *Chemical Reviews*, 1999. 99(8): p. 2071-2084.
16. Earle, M. and K. Seddon, Ionic liquids. Green solvents for the future, in Workshop on Sustainable Chemistry. 2000, Pure and Applied Chemistry: Venice, Italy. p. 1391-1398.
17. Thuy Pham, T.P., C.-W. Cho and Y.-S. Yun, Environmental fate and toxicity of ionic liquids: A review. *Water Research*, 2010. 44(2): p. 352-372.
18. Olivier-Bourbigou, H. and L. Magna, Ionic liquids: perspectives for organic and catalytic reactions. *Journal of Molecular Catalysis A: Chemical*, 2002. 182–183: p. 419-437.
19. Wasserscheid, P. and W. Keim, Ionic Liquids—New “Solutions” for Transition Metal Catalysis. *Angewandte Chemie International Edition*, 2000. 39(21): p. 3772-3789.
20. Petkovic, M., J.L. Ferguson, H.Q.N. Gunaratne, R. Ferreira, M.C. Leitao, K.R. Seddon, L.P.N. Rebelo and C.S. Pereira, Novel biocompatible cholinium-based ionic liquids-toxicity and biodegradability. *Green Chemistry*, 2010. 12(4): p. 643-649.
21. Tang, S., G.A. Baker and H. Zhao, Ether- and alcohol-functionalized task-specific ionic liquids: attractive properties and applications. *Chemical Society Reviews*, 2012. 41(10): p. 4030-4066.
22. Yuan, J., D. Mecerreyes and M. Antonietti, Poly(ionic liquid)s: An update. *Progress in Polymer Science*, 2013. 38(7): p. 1009-1036.
23. Zhao, D., M. Wu, Y. Kou and E. Min, Ionic liquids: applications in catalysis. *Catalysis Today*, 2002. 74(1–2): p. 157-189.
24. Hallett, J.P. and T. Welton, Room-Temperature Ionic Liquids: Solvents for Synthesis and Catalysis. 2. *Chemical Reviews*, 2011. 111(5): p. 3508-3576.
25. Steinrück, H.-P. and P. Wasserscheid, Ionic Liquids in Catalysis. *Catalysis Letters*, 2015. 145(1): p. 380-397.
26. Poole, C.F. and S.K. Poole, Extraction of organic compounds with room temperature ionic liquids. *Journal of Chromatography A*, 2010. 1217(16): p. 2268-2286.
27. Marsh, K.N., J.A. Boxall and R. Lichtenthaler, Room temperature ionic liquids and their mixtures—a review. *Fluid Phase Equilibria*, 2004. 219(1): p. 93-98.
28. Galiński, M., A. Lewandowski and I. Stępnik, Ionic liquids as electrolytes. *Electrochimica Acta*, 2006. 51(26): p. 5567-5580.

29. Welton, T., Ionic liquids in catalysis. *Coordination Chemistry Reviews*, 2004. 248(21–24): p. 2459-2477.
30. Torimoto, T., T. Tsuda, K.-i. Okazaki and S. Kuwabata, New Frontiers in Materials Science Opened by Ionic Liquids. *Advanced Materials*, 2010. 22(11): p. 1196-1221.
31. Olivier-Bourbigou, H., L. Magna and D. Morvan, Ionic liquids and catalysis: Recent progress from knowledge to applications. *Applied Catalysis A: General*, 2010. 373(1–2): p. 1-56.
32. Anderson, J.L., R. Ding, A. Ellern and D.W. Armstrong, Structure and Properties of High Stability Geminal Dicationic Ionic Liquids. *Journal of the American Chemical Society*, 2005. 127(2): p. 593-604.
33. Gardas, R.L., H.F. Costa, M.G. Freire, P.J. Carvalho, I.M. Marrucho, I.M.A. Fonseca, A.G.M. Ferreira and J.A.P. Coutinho, Densities and Derived Thermodynamic Properties of Imidazolium-, Pyridinium-, Pyrrolidinium-, and Piperidinium-Based Ionic Liquids. *Journal of Chemical & Engineering Data*, 2008. 53(3): p. 805-811.
34. Pádua, A.A.H., M.F. Costa Gomes and J.N.A. Canongia Lopes, Molecular Solutes in Ionic Liquids: A Structural Perspective. *Accounts of Chemical Research*, 2007. 40(11): p. 1087-1096.
35. Gardas, R.L., M.G. Freire, P.J. Carvalho, I.M. Marrucho, I.M.A. Fonseca, A.G.M. Ferreira and J.A.P. Coutinho, High-Pressure Densities and Derived Thermodynamic Properties of Imidazolium-Based Ionic Liquids. *Journal of Chemical & Engineering Data*, 2007. 52(1): p. 80-88.
36. Tokuda, H., K. Hayamizu, K. Ishii, M.A.B.H. Susan and M. Watanabe, Physicochemical Properties and Structures of Room Temperature Ionic Liquids. 2. Variation of Alkyl Chain Length in Imidazolium Cation. *The Journal of Physical Chemistry B*, 2005. 109(13): p. 6103-6110.
37. Chiappe, C. and D. Pieraccini, Ionic liquids: solvent properties and organic reactivity. *Journal of Physical Organic Chemistry*, 2005. 18(4): p. 275-297.
38. Lazarus, L.L., C.T. Riche, N. Malmstadt and R.L. Brutchey, Effect of Ionic Liquid Impurities on the Synthesis of Silver Nanoparticles. *Langmuir*, 2012. 28(45): p. 15987-15993.
39. Cassol, C.C., G. Ebeling, B. Ferrera and J. Dupont, A Simple and Practical Method for the Preparation and Purity Determination of Halide-Free Imidazolium Ionic Liquids. *Advanced Synthesis & Catalysis*, 2006. 348(1-2): p. 243-248.
40. Burrell, A.K., R.E.D. Sesto, S.N. Baker, T.M. McCleskey and G.A. Baker, The large scale synthesis of pure imidazolium and pyrrolidinium ionic liquids. *Green Chemistry*, 2007. 9(5): p. 449-454.
41. Holbrey, J.D., K.R. Seddon and R. Wareing, A simple colorimetric method for the quality control of 1-alkyl-3-methylimidazolium ionic liquid precursors. *Green Chemistry*, 2001. 3(1): p. 33-36.

42. Wheeler, J.L., C.B. Dreyer, J. Poshusta, J.L. Martin and J.M. Porter, Real-time monitoring of room-temperature ionic liquid purity through optical diode-based sensing. *Sensors and Actuators B: Chemical*, 2015. 220: p. 309-313.
43. Swatloski, R.P., S.K. Spear, J.D. Holbrey and R.D. Rogers, Dissolution of Cellulose with Ionic Liquids. *Journal of the American Chemical Society*, 2002. 124(18): p. 4974-4975.
44. Pu, Y., N. Jiang and A.J. Ragauskas, Ionic Liquid as a Green Solvent for Lignin. *Journal of Wood Chemistry and Technology*, 2007. 27(1): p. 23-33.
45. Pinkert, A., D.F. Goeke, K.N. Marsh and S. Pang, Extracting wood lignin without dissolving or degrading cellulose: investigations on the use of food additive-derived ionic liquids. *Green Chemistry*, 2011. 13(11): p. 3124-3136.
46. Chatel, G. and R.D. Rogers, Review: Oxidation of Lignin Using Ionic Liquids—An Innovative Strategy To Produce Renewable Chemicals. *ACS Sustainable Chemistry & Engineering*, 2014. 2(3): p. 322-339.
47. Qin, Y., X. Lu, N. Sun and R.D. Rogers, Dissolution or extraction of crustacean shells using ionic liquids to obtain high molecular weight purified chitin and direct production of chitin films and fibers. *Green Chemistry*, 2010. 12(6): p. 968-971.
48. Wu, Y., T. Sasaki, S. Irie and K. Sakurai, A novel biomass-ionic liquid platform for the utilization of native chitin. *Polymer*, 2008. 49(9): p. 2321-2327.
49. Xu, A., Y. Zhang, Y. Zhao and J. Wang, Cellulose dissolution at ambient temperature: Role of preferential solvation of cations of ionic liquids by a cosolvent. *Carbohydrate Polymers*, 2013. 92(1): p. 540-544.
50. Ma, H., B. Zhou, H.-S. Li, Y.-Q. Li and S.-Y. Ou, Green composite films composed of nanocrystalline cellulose and a cellulose matrix regenerated from functionalized ionic liquid solution. *Carbohydrate Polymers*, 2011. 84(1): p. 383-389.
51. Ohno, E. and H. Miyafuji, Reaction behavior of cellulose in an ionic liquid, 1-ethyl-3-methylimidazolium chloride. *Journal of Wood Science*, 2013. 59(3): p. 221-228.
52. Wang, X., H. Li, Y. Cao and Q. Tang, Cellulose extraction from wood chip in an ionic liquid 1-allyl-3-methylimidazolium chloride (AmimCl). *Bioresource Technology*, 2011. 102(17): p. 7959-7965.
53. Hameed, N. and Q. Guo, Blend films of natural wool and cellulose prepared from an ionic liquid. *Cellulose*, 2010. 17(4): p. 803-813.
54. Ding, Z.-D., Z. Chi, W.-X. Gu, S.-M. Gu, J.-H. Liu and H.-J. Wang, Theoretical and experimental investigation on dissolution and regeneration of cellulose in ionic liquid. *Carbohydrate Polymers*, 2012. 89(1): p. 7-16.
55. Du, H. and X. Qian, The effects of acetate anion on cellulose dissolution and reaction in imidazolium ionic liquids. *Carbohydrate Research*, 2011. 346(13): p. 1985-1990.

56. Remsing, R.C., G. Hernandez, R.P. Swatoski, W.W. Masefski, R.D. Rogers and G. Moyna, Solvation of Carbohydrates in N,N'-Dialkylimidazolium Ionic Liquids: A Multinuclear NMR Spectroscopy Study. *The Journal of Physical Chemistry B*, 2008. 112(35): p. 11071-11078.
57. Guo, J., D. Zhang, C. Duan and C. Liu, Probing anion–cellulose interactions in imidazolium-based room temperature ionic liquids: a density functional study. *Carbohydrate Research*, 2010. 345(15): p. 2201-2205.
58. Zhang, H., J. Wu, J. Zhang and J. He, 1-Allyl-3-methylimidazolium Chloride Room Temperature Ionic Liquid: A New and Powerful Nonderivatizing Solvent for Cellulose. *Macromolecules*, 2005. 38(20): p. 8272-8277.
59. Youngs, T.G.A., C. Hardacre and J.D. Holbrey, Glucose Solvation by the Ionic Liquid 1,3-Dimethylimidazolium Chloride: A Simulation Study. *The Journal of Physical Chemistry B*, 2007. 111(49): p. 13765-13774.
60. Liu, D.-t., K.-f. Xia, W.-h. Cai, R.-d. Yang, L.-q. Wang and B. Wang, Investigations about dissolution of cellulose in the 1-allyl-3-alkylimidazolium chloride ionic liquids. *Carbohydrate Polymers*, 2012. 87(2): p. 1058-1064.
61. Liu, H., K.L. Sale, B.M. Holmes, B.A. Simmons and S. Singh, Understanding the Interactions of Cellulose with Ionic Liquids: A Molecular Dynamics Study. *The Journal of Physical Chemistry B*, 2010. 114(12): p. 4293-4301.
62. Lindman, B., G. Karlström and L. Stigsson, On the mechanism of dissolution of cellulose. *Journal of Molecular Liquids*, 2010. 156(1): p. 76-81.
63. Wu, J., J. Zhang, H. Zhang, J. He, Q. Ren and M. Guo, Homogeneous Acetylation of Cellulose in a New Ionic Liquid. *Biomacromolecules*, 2004. 5(2): p. 266-268.
64. Isogai, A. and R.H. Atalla, Dissolution of Cellulose in Aqueous NaOH Solutions. *Cellulose*, 1998. 5(4): p. 309-319.
65. El Seoud, O.A., G.A. Marson, G.T. Ciacco and E. Frollini, An efficient, one-pot acylation of cellulose under homogeneous reaction conditions. *Macromolecular Chemistry and Physics*, 2000. 201(8): p. 882-889.
66. Heinze, T., T. Liebert, P. Klüfers and F. Meister, Carboxymethylation of cellulose in unconventional media. *Cellulose*, 1999. 6(2): p. 153-165.
67. Ciacco, G.T., T.F. Liebert, E. Frollini and T.J. Heinze, Application of the solvent dimethyl sulfoxide/tetrabutyl-ammonium fluoride trihydrate as reaction medium for the homogeneous acylation of Sisal cellulose. *Cellulose*, 2003. 10(2): p. 125-132.
68. Nagel, M.C.V. and T. Heinze, Esterification of cellulose with acyl-1H-benzotriazole. *Polymer Bulletin*, 2010. 65(9): p. 873-881.
69. Hussain, M.A., T. Liebert and T. Heinze, Acylation of Cellulose with N,N'-Carbonyldiimidazole-Activated Acids in the Novel Solvent Dimethyl Sulfoxide/Tetrabutylammonium Fluoride. *Macromolecular Rapid Communications*, 2004. 25(9): p. 916-920.

70. Köhler, S. and T. Heinze, New Solvents for Cellulose: Dimethyl Sulfoxide/Ammonium Fluorides. *Macromolecular Bioscience*, 2007. 7(3): p. 307-314.
71. Jeihanipour, A., K. Karimi and M.J. Taherzadeh, Enhancement of ethanol and biogas production from high-crystalline cellulose by different modes of NMO pretreatment. *Biotechnology and Bioengineering*, 2010. 105(3): p. 469-476.
72. Yuan, H., Y. Nishiyama and S. Kuga, Surface Esterification of Cellulose by Vapor-Phase Treatment With Trifluoroacetic Anhydride. *Cellulose*, 2005. 12(5): p. 543-549.
73. Kim, H.-T. and K. Lee, Application of insoluble cellulose xanthate for the removal of heavy metals from aqueous solution. *Korean Journal of Chemical Engineering*, 1999. 16(3): p. 298-302.
74. Brewer, R., Process for preparing cellulose sulfate esters. 1984: United States.
75. Pinkert, A., K.N. Marsh, S. Pang and M.P. Staiger, Ionic Liquids and Their Interaction with Cellulose. *Chemical Reviews*, 2009. 109(12): p. 6712-6728.
76. Zhu, S., Y. Wu, Q. Chen, Z. Yu, C. Wang, S. Jin, Y. Ding and G. Wu, Dissolution of cellulose with ionic liquids and its application: a mini-review. *Green Chemistry*, 2006. 8(4): p. 325-327.
77. Mäki-Arvela, P., I. Anugwom, P. Virtanen, R. Sjöholm and J.P. Mikkola, Dissolution of lignocellulosic materials and its constituents using ionic liquids—A review. *Industrial Crops and Products*, 2010. 32(3): p. 175-201.
78. Isik, M., H. Sardon and D. Mecerreyes, Ionic Liquids and Cellulose: Dissolution, Chemical Modification and Preparation of New Cellulosic Materials. *International Journal of Molecular Sciences*, 2014. 15(7): p. 11922.
79. El Seoud, O.A., A. Koschella, L.C. Fidale, S. Dorn and T. Heinze, Applications of Ionic Liquids in Carbohydrate Chemistry: A Window of Opportunities. *Biomacromolecules*, 2007. 8(9): p. 2629-2647.
80. Wang, H., G. Gurau and R.D. Rogers, Ionic liquid processing of cellulose. *Chemical Society Reviews*, 2012. 41(4): p. 1519-1537.
81. Stark, A., M. Sellin, B. Ondruschka and K. Massonne, The effect of hydrogen bond acceptor properties of ionic liquids on their cellulose solubility. *Science China Chemistry*, 2012. 55(8): p. 1663-1670.
82. Kamlet, M.J. and R.W. Taft, The solvatochromic comparison method. I. The .beta.-scale of solvent hydrogen-bond acceptor (HBA) basicities. *Journal of the American Chemical Society*, 1976. 98(2): p. 377-383.
83. Avent, A.G., P.A. Chaloner, M.P. Day, K.R. Seddon and T. Welton, Evidence for hydrogen bonding in solutions of 1-ethyl-3-methylimidazolium halides, and its implications for room-temperature halogenoaluminate(III) ionic liquids. *Journal of the Chemical Society, Dalton Transactions*, 1994(23): p. 3405-3413.

84. Crowhurst, L., P.R. Mawdsley, J.M. Perez-Arlandis, P.A. Salter and T. Welton, Solvent-solute interactions in ionic liquids. *Physical Chemistry Chemical Physics*, 2003. 5(13): p. 2790-2794.
85. Fukaya, Y., A. Sugimoto and H. Ohno, Superior Solubility of Polysaccharides in Low Viscosity, Polar, and Halogen-Free 1,3-Dialkylimidazolium Formates. *Biomacromolecules*, 2006. 7(12): p. 3295-3297.
86. Ohno, H. and Y. Fukaya, Task specific ionic liquids for cellulose technology. *Chemistry Letters*, 2009. 38(1): p. 2-7.
87. Fukaya, Y., K. Hayashi, M. Wada and H. Ohno, Cellulose dissolution with polar ionic liquids under mild conditions: required factors for anions. *Green Chemistry*, 2008. 10(1): p. 44-46.
88. Cao, Y., Y. Chen, X. Wang and T. Mu, Predicting the hygroscopicity of imidazolium-based ILs varying in anion by hydrogen-bonding basicity and acidity. *RSC Advances*, 2014. 4(10): p. 5169-5176.
89. Lungwitz, R. and S. Spange, A hydrogen bond accepting (HBA) scale for anions, including room temperature ionic liquids. *New Journal of Chemistry*, 2008. 32(3): p. 392-394.
90. Ngo, H.L., K. LeCompte, L. Hargens and A.B. McEwen, Thermal properties of imidazolium ionic liquids. *Thermochimica Acta*, 2000. 357–358: p. 97-102.
91. Abe, M., Y. Fukaya and H. Ohno, Extraction of polysaccharides from bran with phosphonate or phosphinate-derived ionic liquids under short mixing time and low temperature. *Green Chemistry*, 2010. 12(7): p. 1274-1280.
92. Bonhôte, P., A.-P. Dias, N. Papageorgiou, K. Kalyanasundaram and M. Grätzel, Hydrophobic, Highly Conductive Ambient-Temperature Molten Salts. *Inorganic Chemistry*, 1996. 35(5): p. 1168-1178.
93. Zhang, S., X. Qi, X. Ma, L. Lu, Q. Zhang and Y. Deng, Investigation of cation–anion interaction in 1-(2-hydroxyethyl)-3-methylimidazolium-based ion pairs by density functional theory calculations and experiments. *Journal of Physical Organic Chemistry*, 2012. 25(3): p. 248-257.
94. Doherty, T.V., M. Mora-Pale, S.E. Foley, R.J. Linhardt and J.S. Dordick, Ionic liquid solvent properties as predictors of lignocellulose pretreatment efficacy. *Green Chemistry*, 2010. 12(11): p. 1967-1975.
95. Lungwitz, R., V. Strehmel and S. Spange, The dipolarity/polarisability of 1-alkyl-3-methylimidazolium ionic liquids as function of anion structure and the alkyl chain length. *New Journal of Chemistry*, 2010. 34(6): p. 1135-1140.
96. Oehlke, A., K. Hofmann and S. Spange, New aspects on polarity of 1-alkyl-3-methylimidazolium salts as measured by solvatochromic probes. *New Journal of Chemistry*, 2006. 30(4): p. 533-536.
97. Ab Rani, M.A., A. Brant, L. Crowhurst, A. Dolan, M. Lui, N.H. Hassan, J.P. Hallett, P.A. Hunt, H. Niedermeyer, J.M. Perez-Arlandis, M. Schrems, T. Welton, and R. Wilding, Understanding the polarity of ionic liquids. *Physical Chemistry Chemical Physics*, 2011. 13(37): p. 16831-16840.

98. Gaciño, F.M., T. Regueira, L. Lugo, M.J.P. Comuñas and J. Fernández, Influence of Molecular Structure on Densities and Viscosities of Several Ionic Liquids. *Journal of Chemical & Engineering Data*, 2011. 56(12): p. 4984-4999.
99. Tokuda, H., K. Ishii, M.A.B.H. Susan, S. Tsuzuki, K. Hayamizu and M. Watanabe, Physicochemical Properties and Structures of Room-Temperature Ionic Liquids. 3. Variation of Cationic Structures. *The Journal of Physical Chemistry B*, 2006. 110(6): p. 2833-2839.
100. Gardas, R.L. and J.A.P. Coutinho, Group contribution methods for the prediction of thermophysical and transport properties of ionic liquids. *AIChE Journal*, 2009. 55(5): p. 1274-1290.
101. Crosthwaite, J.M., M.J. Muldoon, J.K. Dixon, J.L. Anderson and J.F. Brennecke, Phase transition and decomposition temperatures, heat capacities and viscosities of pyridinium ionic liquids. *The Journal of Chemical Thermodynamics*, 2005. 37(6): p. 559-568.
102. Almeida, H.F.D., H. Passos, J.A. Lopes-da-Silva, A.M. Fernandes, M.G. Freire and J.A.P. Coutinho, Thermophysical Properties of Five Acetate-Based Ionic Liquids. *Journal of Chemical & Engineering Data*, 2012. 57(11): p. 3005-3013.
103. Huddleston, J.G., A.E. Visser, W.M. Reichert, H.D. Willauer, G.A. Broker and R.D. Rogers, Characterization and comparison of hydrophilic and hydrophobic room temperature ionic liquids incorporating the imidazolium cation. *Green Chemistry*, 2001. 3(4): p. 156-164.
104. Wu, D., B. Wu, Y.M. Zhang and H.P. Wang, Density, Viscosity, Refractive Index and Conductivity of 1-Allyl-3-methylimidazolium Chloride + Water Mixture. *Journal of Chemical & Engineering Data*, 2010. 55(2): p. 621-624.
105. Freire, M.G., A.R.R. Teles, M.A.A. Rocha, B. Schröder, C.M.S.S. Neves, P.J. Carvalho, D.V. Evtuguin, L.M.N.B.F. Santos and J.A.P. Coutinho, Thermophysical Characterization of Ionic Liquids Able To Dissolve Biomass. *Journal of Chemical & Engineering Data*, 2011. 56(12): p. 4813-4822.
106. Fröba, A.P., H. Kremer and A. Leipertz, Density, Refractive Index, Interfacial Tension, and Viscosity of Ionic Liquids [EMIM][EtSO₄], [EMIM][NTf₂], [EMIM][N(CN)₂], and [OMA][NTf₂] in Dependence on Temperature at Atmospheric Pressure. *The Journal of Physical Chemistry B*, 2008. 112(39): p. 12420-12430.
107. Gómez, E., N. Calvar, Á. Domínguez and E.A. Macedo, Synthesis and temperature dependence of physical properties of four pyridinium-based ionic liquids: Influence of the size of the cation. *The Journal of Chemical Thermodynamics*, 2010. 42(11): p. 1324-1329.
108. Zarrougui, R., N. Raouafi and D. Lemordant, New Series of Green Cyclic Ammonium-Based Room Temperature Ionic Liquids with Alkylphosphite-Containing Anion: Synthesis and Physicochemical Characterization. *Journal of Chemical & Engineering Data*, 2014. 59(4): p. 1193-1201.
109. Seddon, K., A. Stark and M. Torres, Influence of chloride, water, and organic solvents on the physical properties of ionic liquids in 15th International Conference on Physical Organic Chemistry (ICPOC 15). 2000, INT UNION PURE APPLIED CHEMISTRY: GOTHENBURG, SWEDEN. p. 2275-2287.

110. Xu, H., D. Zhao, P. Xu, F. Liu and G. Gao, Conductivity and Viscosity of 1-Allyl-3-methyl-imidazolium Chloride + Water and + Ethanol from 293.15 K to 333.15 K. *Journal of Chemical & Engineering Data*, 2005. 50(1): p. 133-135.
111. Lu, F., B. Cheng, J. Song and Y. Liang, Rheological characterization of concentrated cellulose solutions in 1-allyl-3-methylimidazolium chloride. *Journal of Applied Polymer Science*, 2012. 124(4): p. 3419-3425.
112. Kosan, B., C. Michels and F. Meister, Dissolution and forming of cellulose with ionic liquids. *Cellulose*, 2008. 15(1): p. 59-66.
113. Le, K.A., C. Rudaz and T. Budtova, Phase diagram, solubility limit and hydrodynamic properties of cellulose in binary solvents with ionic liquid. *Carbohydrate Polymers*, 2014. 105: p. 237-243.
114. Lv, Y., J. Wu, J. Zhang, Y. Niu, C.-Y. Liu, J. He and J. Zhang, Rheological properties of cellulose/ionic liquid/dimethylsulfoxide (DMSO) solutions. *Polymer*, 2012. 53(12): p. 2524-2531.
115. Härdelin, L., J. Thunberg, E. Perzon, G. Westman, P. Walkenström and P. Gatenholm, Electrospinning of cellulose nanofibers from ionic liquids: The effect of different cosolvents. *Journal of Applied Polymer Science*, 2012. 125(3): p. 1901-1909.
116. Ahosseini, A., E. Ortega, B. Sensenich and A.M. Scurto, Viscosity of n-alkyl-3-methyl-imidazolium bis(trifluoromethylsulfonyl)amide ionic liquids saturated with compressed CO₂. *Fluid Phase Equilibria*, 2009. 286(1): p. 72-78.
117. Blanchard, L.A., D. Hancu, E.J. Beckman and J.F. Brennecke, Green processing using ionic liquids and CO₂. *Nature*, 1999. 399(6731): p. 28-29.
118. Sun, X., Y. Chi and T. Mu, Studies on staged precipitation of cellulose from an ionic liquid by compressed carbon dioxide. *Green Chemistry*, 2014. 16(5): p. 2736-2744.
119. Barber, P.S., C.S. Griggs, G. Gurau, Z. Liu, S. Li, Z. Li, X. Lu, S. Zhang and R.D. Rogers, Coagulation of Chitin and Cellulose from 1-Ethyl-3-methylimidazolium Acetate Ionic-Liquid Solutions Using Carbon Dioxide. *Angewandte Chemie International Edition*, 2013. 52(47): p. 12350-12353.
120. Liu, Z., W. Wu, B. Han, Z. Dong, G. Zhao, J. Wang, T. Jiang and G. Yang, Study on the Phase Behaviors, Viscosities, and Thermodynamic Properties of CO₂/[C₄mim][PF₆]/Methanol System at Elevated Pressures. *Chemistry – A European Journal*, 2003. 9(16): p. 3897-3903.
121. Tomida, D., S. Kenmochi, K. Qiao, Q. Bao and C. Yokoyama, Viscosity of ionic liquid mixtures of 1-alkyl-3-methylimidazolium hexafluorophosphate + CO₂. *Fluid Phase Equilibria*, 2011. 307(2): p. 185-189.
122. Tomida, D., A. Kumagai, K. Qiao and C. Yokoyama, Viscosity of 1-Butyl-3-methylimidazolium Hexafluorophosphate + CO₂ Mixture. *Journal of Chemical & Engineering Data*, 2007. 52(5): p. 1638-1640.
123. Lopes, J.M., S. Kareth, M.D. Bermejo, Á. Martín, E. Weidner and M.J. Cocero, Experimental determination of viscosities and densities of mixtures carbon

- dioxide + 1-allyl-3-methylimidazolium chloride. Viscosity correlation. *The Journal of Supercritical Fluids*, 2016. 111: p. 91-96.
124. Iguchi, M., K. Kasuya, Y. Sato, T.M. Aida, M. Watanabe and R.L. Smith, Viscosity reduction of cellulose + 1-butyl-3-methylimidazolium acetate in the presence of CO₂. *Cellulose*, 2013. 20(3): p. 1353-1367.
 125. Visser, A.E., W.M. Reichert, R.P. Swatloski, H.D. Willauer, J.G. Huddleston and R.D. Rogers, Characterization of Hydrophilic and Hydrophobic Ionic Liquids: Alternatives to Volatile Organic Compounds for Liquid-Liquid Separations, in *Ionic Liquids*. 2002, American Chemical Society. p. 289-308.
 126. Tran, C.D., S.H. De Paoli Lacerda and D. Oliveira, Absorption of Water by Room-Temperature Ionic Liquids: Effect of Anions on Concentration and State of Water. *Applied Spectroscopy*, 2003. 57(2): p. 152-157.
 127. Cammarata, L., S.G. Kazarian, P.A. Salter and T. Welton, Molecular states of water in room temperature ionic liquids. *Physical Chemistry Chemical Physics*, 2001. 3(23): p. 5192-5200.
 128. Liu, H., K.L. Sale, B.A. Simmons and S. Singh, Molecular Dynamics Study of Polysaccharides in Binary Solvent Mixtures of an Ionic Liquid and Water. *The Journal of Physical Chemistry B*, 2011. 115(34): p. 10251-10258.
 129. Rabideau, B.D. and A.E. Ismail, Mechanisms of hydrogen bond formation between ionic liquids and cellulose and the influence of water content. *Physical Chemistry Chemical Physics*, 2015. 17(8): p. 5767-5775.
 130. Agbor, V.B., N. Cicek, R. Sparling, A. Berlin and D.B. Levin, Biomass pretreatment: Fundamentals toward application. *Biotechnology Advances*, 2011. 29(6): p. 675-685.
 131. Zhao, X., L. Zhang and D. Liu, Biomass recalcitrance. Part I: the chemical compositions and physical structures affecting the enzymatic hydrolysis of lignocellulose. *Biofuels, Bioproducts and Biorefining*, 2012. 6(4): p. 465-482.
 132. Shafiei, M., K. Karimi and M.J. Taherzadeh, Pretreatment of spruce and oak by N-methylmorpholine-N-oxide (NMMO) for efficient conversion of their cellulose to ethanol. *Bioresource Technology*, 2010. 101(13): p. 4914-4918.
 133. Kuo, C.-H. and C.-K. Lee, Enhanced enzymatic hydrolysis of sugarcane bagasse by N-methylmorpholine-N-oxide pretreatment. *Bioresource Technology*, 2009. 100(2): p. 866-871.
 134. Otieno, D.O. and B.K. Ahring, A thermochemical pretreatment process to produce xylooligosaccharides (XOS), arabinooligosaccharides (AOS) and mannoooligosaccharides (MOS) from lignocellulosic biomasses. *Bioresource Technology*, 2012. 112: p. 285-292.
 135. Wang, K., J.-X. Jiang, F. Xu and R.-C. Sun, Influence of steaming explosion time on the physic-chemical properties of cellulose from *Lespedeza stalks* (*Lespedeza crybotrya*). *Bioresource Technology*, 2009. 100(21): p. 5288-5294.

136. Öhgren, K., R. Bura, J. Saddler and G. Zacchi, Effect of hemicellulose and lignin removal on enzymatic hydrolysis of steam pretreated corn stover. *Bioresource Technology*, 2007. 98(13): p. 2503-2510.
137. Xiao, B., X.F. Sun and R. Sun, Chemical, structural, and thermal characterizations of alkali-soluble lignins and hemicelluloses, and cellulose from maize stems, rye straw, and rice straw. *Polymer Degradation and Stability*, 2001. 74(2): p. 307-319.
138. Kim, S. and M.T. Holtzapfle, Lime pretreatment and enzymatic hydrolysis of corn stover. *Bioresource Technology*, 2005. 96(18): p. 1994-2006.
139. Sun, J.X., X.F. Sun, H. Zhao and R.C. Sun, Isolation and characterization of cellulose from sugarcane bagasse. *Polymer Degradation and Stability*, 2004. 84(2): p. 331-339.
140. Klinke, H.B., B.K. Ahring, A.S. Schmidt and A.B. Thomsen, Characterization of degradation products from alkaline wet oxidation of wheat straw. *Bioresource Technology*, 2002. 82(1): p. 15-26.
141. Ferrini, P. and R. Rinaldi, Catalytic Biorefining of Plant Biomass to Non-Pyrolytic Lignin Bio-Oil and Carbohydrates through Hydrogen Transfer Reactions. *Angewandte Chemie International Edition*, 2014. 53(33): p. 8634-8639.
142. Li, C., G. Cheng, V. Balan, M.S. Kent, M. Ong, S.P.S. Chundawat, L.d. Sousa, Y.B. Melnichenko, B.E. Dale, B.A. Simmons, and S. Singh, Influence of physico-chemical changes on enzymatic digestibility of ionic liquid and AFEX pretreated corn stover. *Bioresource Technology*, 2011. 102(13): p. 6928-6936.
143. Lee, S.H., T.V. Doherty, R.J. Linhardt and J.S. Dordick, Ionic liquid-mediated selective extraction of lignin from wood leading to enhanced enzymatic cellulose hydrolysis. *Biotechnology and Bioengineering*, 2009. 102(5): p. 1368-1376.
144. Leskinen, T., A.W.T. King, I. Kilpeläinen and D.S. Argyropoulos, Fractionation of Lignocellulosic Materials with Ionic Liquids. 1. Effect of Mechanical Treatment. *Industrial & Engineering Chemistry Research*, 2011. 50(22): p. 12349-12357.
145. Zhao, H., G.A. Baker and J.V. Cowins, Fast enzymatic saccharification of switchgrass after pretreatment with ionic liquids. *Biotechnology Progress*, 2010. 26(1): p. 127-133.
146. Li, C., B. Knierim, C. Manisseri, R. Arora, H.V. Scheller, M. Auer, K.P. Vogel, B.A. Simmons and S. Singh, Comparison of dilute acid and ionic liquid pretreatment of switchgrass: Biomass recalcitrance, delignification and enzymatic saccharification. *Bioresource Technology*, 2010. 101(13): p. 4900-4906.
147. Wu, H., M. Mora-Pale, J. Miao, T.V. Doherty, R.J. Linhardt and J.S. Dordick, Facile pretreatment of lignocellulosic biomass at high loadings in room temperature ionic liquids. *Biotechnology and Bioengineering*, 2011. 108(12): p. 2865-2875.
148. Diedericks, D., E.v. Rensburg, M. del Prado García-Aparicio and J.F. Görgens, Enhancing the enzymatic digestibility of sugarcane bagasse through the

- application of an ionic liquid in combination with an acid catalyst. *Biotechnology Progress*, 2012. 28(1): p. 76-84.
149. Johnson, D.L., *Compounds dissolved in cyclic amine oxides*. 1969.
 150. Fink, H.P., P. Weigel, H.J. Purz and J. Ganster, Structure formation of regenerated cellulose materials from NMMO-solutions. *Progress in Polymer Science*, 2001. 26(9): p. 1473-1524.
 151. Tan, H.T. and K.T. Lee, Understanding the impact of ionic liquid pretreatment on biomass and enzymatic hydrolysis. *Chemical Engineering Journal*, 2012. 183: p. 448-458.
 152. Leskinen, T., A.W.T. King, I. Kilpeläinen and D.S. Argyropoulos, Fractionation of Lignocellulosic Materials Using Ionic Liquids: Part 2. Effect of Particle Size on the Mechanisms of Fractionation. *Industrial & Engineering Chemistry Research*, 2013. 52(11): p. 3958-3966.
 153. Kilpeläinen, I., H. Xie, A. King, M. Granstrom, S. Heikkinen and D.S. Argyropoulos, Dissolution of Wood in Ionic Liquids. *Journal of Agricultural and Food Chemistry*, 2007. 55(22): p. 9142-9148.
 154. Castro, M.C., H. Rodríguez, A. Arce and A. Soto, Mixtures of Ethanol and the Ionic Liquid 1-Ethyl-3-methylimidazolium Acetate for the Fractionated Solubility of Biopolymers of Lignocellulosic Biomass. *Industrial & Engineering Chemistry Research*, 2014. 53(29): p. 11850-11861.
 155. Castro, M.C., A. Arce, A. Soto and H. Rodríguez, Influence of Methanol on the Dissolution of Lignocellulose Biopolymers with the Ionic Liquid 1-Ethyl-3-methylimidazolium Acetate. *Industrial & Engineering Chemistry Research*, 2015. 54(39): p. 9605-9614.
 156. Meiland, M., T. Liebert and T. Heinze, Tailoring the Degree of Polymerization of Low Molecular Weight Cellulose. *Macromolecular Materials and Engineering*, 2011. 296(9): p. 802-809.
 157. Liebert, T., M. Seifert and T. Heinze, Efficient Method for the Preparation of Pure, Water-Soluble Cellodextrins. *Macromolecular Symposia*, 2008. 262(1): p. 140-149.
 158. Hubbell, C.A. and A.J. Ragauskas, Effect of acid-chlorite delignification on cellulose degree of polymerization. *Bioresource Technology*, 2010. 101(19): p. 7410-7415.
 159. Zhang, Y.H.P. and L.R. Lynd, Determination of the Number-Average Degree of Polymerization of Cellodextrins and Cellulose with Application to Enzymatic Hydrolysis. *Biomacromolecules*, 2005. 6(3): p. 1510-1515.
 160. Rinaldi, R., R. Palkovits and F. Schüth, Depolymerization of Cellulose Using Solid Catalysts in Ionic Liquids. *Angewandte Chemie International Edition*, 2008. 47(42): p. 8047-8050.
 161. Liu, L. and H. Chen, Enzymatic hydrolysis of cellulose materials treated with ionic liquid [BMIM] Cl. *Chinese Science Bulletin*, 2006. 51(20): p. 2432-2436.

162. Zhao, D., H. Li, J. Zhang, L. Fu, M. Liu, J. Fu and P. Ren, Dissolution of cellulose in phosphate-based ionic liquids. *Carbohydrate Polymers*, 2012. 87(2): p. 1490-1494.
163. Kim, S.-j. and J. Jang, Effect of degree of polymerization on the mechanical properties of regenerated cellulose fibers using synthesized 1-allyl-3-methylimidazolium chloride. *Fibers and Polymers*, 2013. 14(6): p. 909-914.
164. Chen, H.-Z., N. Wang and L.-Y. Liu, Regenerated cellulose membrane prepared with ionic liquid 1-butyl-3-methylimidazolium chloride as solvent using wheat straw. *Journal of Chemical Technology & Biotechnology*, 2012. 87(12): p. 1634-1640.
165. Lenzing. Sustainability report. 2012; Available from: http://www.lenzing.com/fileadmin/template/pdf/konzern/nachhaltigkeit/Sustainability_Report_2012_EN.pdf
166. Lenzing. Responsibility for economic success. 2014 [19/02/2016]; Available from: http://www.lenzing.com/fileadmin/template/pdf/konzern/prasentationen/Press_Conference_Annual_Results_2014_EN.pdf.
167. Lenzing. Sustainability report. 2003 [19/02/2016]; Available from: http://www.lenzing.com/fileadmin/template/pdf/konzern/nachhaltigkeit/Sustainability_Brochure_EN_2003.pdf.
168. Kang, H., R. Liu and Y. Huang, Cellulose derivatives and graft copolymers as blocks for functional materials. *Polymer International*, 2013. 62(3): p. 338-344.
169. Varshney, V.K. and S. Naithani, Chemical Functionalization of Cellulose Derived from Nonconventional Sources, in *Cellulose Fibers: Bio- and Nano-Polymer Composites*, S. Kalia, B.S. Kaith, and I. Kaur, Editors. 2011, Springer: Verlag Berlin Heidelberg. p. 43-60.
170. Seymour, G.W. and B.B. White, Preparation of cellulose esters. 1944.
171. Heinze, T. and T. Liebert, Unconventional methods in cellulose functionalization. *Progress in Polymer Science*, 2001. 26(9): p. 1689-1762.
172. Eastman. Eastman cellulose-based specialty polymers. 2014 [cited 2016; Available from: http://www.eastman.com/Literature_Center/E/E325.pdf.
173. Edgar, K.J., Cellulose esters in drug delivery. *Cellulose*, 2007. 14(1): p. 49-64.
174. Tang, S., X. Li, F. Wang, G. Liu, Y. Li and F. Pan, Synthesis and hplc chiral recognition of regioselectively carbamoylated cellulose derivatives. *Chirality*, 2012. 24(2): p. 167-173.
175. Wondraczek, H., A. Pfeifer and T. Heinze, Water soluble photoactive cellulose derivatives: synthesis and characterization of mixed 2-[(4-methyl-2-oxo-2H-chromen-7-yl)oxy]acetic acid-(3-carboxypropyl)trimethylammonium chloride esters of cellulose. *Cellulose*, 2012. 19(4): p. 1327-1335.
176. Trombino, S., R. Cassano, E. Bloise, R. Muzzalupo, S. Leta, F. Puoci and N. Picci, Design and Synthesis of Cellulose Derivatives with Antioxidant Activity. *Macromolecular Bioscience*, 2008. 8(1): p. 86-95.

177. Karakawa, M., M. Chikamatsu, Y. Yoshida, R. Azumi, K. Yase and C. Nakamoto, Organic Memory Device Based on Carbazole-Substituted Cellulose. *Macromolecular Rapid Communications*, 2007. 28(14): p. 1479-1484.
178. Thakur, V.K., M.K. Thakur and R.K. Gupta, Rapid synthesis of graft copolymers from natural cellulose fibers. *Carbohydrate Polymers*, 2013. 98(1): p. 820-828.
179. Fox, S.C., B. Li, D. Xu and K.J. Edgar, Regioselective Esterification and Etherification of Cellulose: A Review. *Biomacromolecules*, 2011. 12(6): p. 1956-1972.
180. Dow. Cellulose ethers. 2012; Available from: <http://www.dowconstructionchemicals.com/na/en/pdfs/832-00226.pdf>.
181. Amin, M., N.S. Abbas, M.A. Hussain, K.J. Edgar, M.N. Tahir, W. Tremel and M. Sher, Cellulose ether derivatives: a new platform for prodrug formation of fluoroquinolone antibiotics. *Cellulose*, 2015. 22(3): p. 2011-2022.
182. Malm, C. and L. Tanghe, Chemical reactions in the making of cellulose acetate. *Industrial and Engineering Chemistry*, 1955. 47(5): p. 995-999.
183. Hearon, W.M., G.D. Hiatt and C.R. Fordyce, Cellulose Trityl Ether1a. *Journal of the American Chemical Society*, 1943. 65(12): p. 2449-2452.
184. Xia, K., J. Chen, R. Yang, F. Cheng and D. Liu, Green Synthesis and Crystal Structure of Regioselectively Substituting 6-O-tritylcellulose Derivatives. *Journal of Biobased Materials and Bioenergy*, 2014. 8(6): p. 587-593.
185. Marson, G.A. and O.A. El Seoud, A novel, efficient procedure for acylation of cellulose under homogeneous solution conditions. *Journal of Applied Polymer Science*, 1999. 74(6): p. 1355-1360.
186. Sassi, J.-F. and H. Chanzy, Ultrastructural aspects of the acetylation of cellulose. *Cellulose*, 1995. 2(2): p. 111-127.
187. Heinze, T. and A. Koschella, Solvents applied in the field of cellulose chemistry: a mini review. *Polímeros*, 2005. 15: p. 84-90.
188. Heinze, T., T.F. Liebert, K.S. Pfeiffer and M.A. Hussain, Unconventional Cellulose Esters: Synthesis, Characterization and Structure–Property Relations. *Cellulose*, 2003. 10(3): p. 283-296.
189. Ass, B.A.P., G.T. Ciacco and E. Frollini, Cellulose acetates from linters and sisal: Correlation between synthesis conditions in DMAc/LiCl and product properties. *Bioresource Technology*, 2006. 97(14): p. 1696-1702.
190. Ciacco Gabriela, T., A. Ramos Ludmila, E. Frollini and A.P. Ass Beatriz, Sisal, Sugarcane Bagasse and Microcrystalline Celluloses: Influence of the Composition of the Solvent System N,N-Dimethylacetamide /Lithium Chloride on the Solubility and Acetylation of these Polysaccharides. *e-Polymers*, 2008. 8(1): p. 226.
191. Yoshimura, T., K. Matsuo and R. Fujioka, Novel biodegradable superabsorbent hydrogels derived from cotton cellulose and succinic anhydride: Synthesis and

- characterization. *Journal of Applied Polymer Science*, 2006. 99(6): p. 3251-3256.
192. Perepelkin, K.E., Ways of developing chemical fibres based on cellulose: Viscose fibres and their prospects. Part 1. Development of viscose fibre technology. *Alternative hydrated cellulose fibre technology. Fibre Chemistry*, 2008. 40(1): p. 10-23.
 193. Mayr, G., F. Zeppetbauer, T. Zweckmair, D. Bauer, S. Hild, A. Potthast, T. Rosenau and T. Röder, The reactions of cellulose and hemicellulose degradation products in the viscose fibre spin bath. *Lenzinger Berichte*, 2015(92): p. 53-58.
 194. Gannon, J.M., I. Graveson and S.A. Mortimer, *Process for the manufacture of lyocell fibre*. 1998.
 195. Sixta, H., A. Michud, L. Hauru, S. Asaadi, Y. Ma, K.A.W. T., I. Kilpeläinen and M. Hummel, Ioncell-F: A High-strength regenerated cellulose fibre. *Nordic Pulp & Paper Research Journal*, 2015. 30(1): p. 43-57.
 196. Röder, T., J. Moosbauer, G. Kliba, S. Schlader, G. Zuckerstätter and H. Sixta, Comparative characterisation of man-made regenerated cellulose fibres. *Lenzinger Berichte*, 2009(87): p. 98-105.
 197. Röder, T., J. Moosbauer, K. Wöss, S. Schlader and G. Kraft, Man-made cellulose fibres – a comparison based on morphology and mechanical properties. *Lenzinger Berichte*, 2013(91): p. 7-12.
 198. Nemeč, H., Fibrillation of cellulose materials – can previous literature offer a solution? *Lenzinger Berichte*, 1994(9): p. 69-72.
 199. Mortimer, S.A. and A.A. Péguý, Methods for reducing the tendency of lyocell fibers to fibrillate. *Journal of Applied Polymer Science*, 1996. 60(3): p. 305-316.
 200. Zhang, W., S. Okubayashi and T. Bechtold, Fibrillation Tendency of Cellulosic Fibers. Part 1: Effects of Swelling. *Cellulose*, 2005. 12(3): p. 267-273.
 201. Zhang, W., S. Okubayashi and T. Bechtold, Fibrillation tendency of cellulosic fibers—part 3. Effects of alkali pretreatment of lyocell fiber. *Carbohydrate Polymers*, 2005. 59(2): p. 173-179.
 202. Rosenau, T., A. Potthast, H. Sixta and P. Kosma, The chemistry of side reactions and byproduct formation in the system NMMO/cellulose (Lyocell process). *Progress in Polymer Science*, 2001. 26(9): p. 1763-1837.
 203. Hermanutz, F., F. Gähr, E. Uerdingen, F. Meister and B. Kosan, New Developments in Dissolving and Processing of Cellulose in Ionic Liquids. *Macromolecular Symposia*, 2008. 262(1): p. 23-27.
 204. de la Parra, C.J., A. Navarrete, M.D. Bermejo and M.J. Cocero, Patents Review on Lignocellulosic Biomass Processing Using Ionic Liquids. *Recent Patents on Engineering*, 2012. 6(3): p. 159-181.

205. Luan, Y., J. Zhang, M. Zhan, J. Wu, J. Zhang and J. He, Highly efficient propionylation and butyralation of cellulose in an ionic liquid catalyzed by 4-dimethyliminopyridine. *Carbohydrate Polymers*, 2013. 92(1): p. 307-311.
206. Huang, K., B. Wang, Y. Cao, H. Li, J. Wang, W. Lin, C. Mu and D. Liao, Homogeneous Preparation of Cellulose Acetate Propionate (CAP) and Cellulose Acetate Butyrate (CAB) from Sugarcane Bagasse Cellulose in Ionic Liquid. *Journal of Agricultural and Food Chemistry*, 2011. 59(10): p. 5376-5381.
207. Heinze, T., K. Schwikal and S. Barthel, Ionic Liquids as Reaction Medium in Cellulose Functionalization. *Macromolecular Bioscience*, 2005. 5(6): p. 520-525.
208. Granström, M., J. Kavakka, A. King, J. Majoinen, V. Mäkelä, J. Helaja, S. Hietala, T. Virtanen, S.-L. Maunu, D.S. Argyropoulos, and I. Kilpeläinen, Tosylation and acylation of cellulose in 1-allyl-3-methylimidazolium chloride. *Cellulose*, 2008. 15(3): p. 481-488.
209. Schöbitz, M., F. Meister and T. Heinze, Unconventional Reactivity of Cellulose Dissolved in Ionic Liquids. *Macromolecular Symposia*, 2009. 280(1): p. 102-111.
210. Gericke, M., J. Schaller, T. Liebert, P. Fardim, F. Meister and T. Heinze, Studies on the tosylation of cellulose in mixtures of ionic liquids and a co-solvent. *Carbohydrate Polymers*, 2012. 89(2): p. 526-536.
211. Köhler, S. and T. Heinze, Efficient synthesis of cellulose furoates in 1-N-butyl-3-methylimidazolium chloride. *Cellulose*, 2007. 14(5): p. 489-495.
212. Barthel, S. and T. Heinze, Acylation and carbanilation of cellulose in ionic liquids. *Green Chemistry*, 2006. 8(3): p. 301-306.
213. Schluffer, K., H.-P. Schmauder, S. Dorn and T. Heinze, Efficient Homogeneous Chemical Modification of Bacterial Cellulose in the Ionic Liquid 1-N-Butyl-3-methylimidazolium Chloride. *Macromolecular Rapid Communications*, 2006. 27(19): p. 1670-1676.
214. Chun-xiang, L., Z. Huai-yu, L. Ming-hua, F. Shi-yu and Z. Jia-jun, Preparation of cellulose graft poly(methyl methacrylate) copolymers by atom transfer radical polymerization in an ionic liquid. *Carbohydrate Polymers*, 2009. 78(3): p. 432-438.
215. Sui, X., J. Yuan, M. Zhou, J. Zhang, H. Yang, W. Yuan, Y. Wei and C. Pan, Synthesis of Cellulose-graft-Poly(N,N-dimethylamino-2-ethyl methacrylate) Copolymers via Homogeneous ATRP and Their Aggregates in Aqueous Media. *Biomacromolecules*, 2008. 9(10): p. 2615-2620.
216. Zhang, J., J. Wu, Y. Cao, S. Sang, J. Zhang and J. He, Synthesis of cellulose benzoates under homogeneous conditions in an ionic liquid. *Cellulose*, 2009. 16(2): p. 299-308.
217. Heinze, T., S. Dorn, M. Schöbitz, T. Liebert, S. Köhler and F. Meister, Interactions of Ionic Liquids with Polysaccharides – 2: Cellulose. *Macromolecular Symposia*, 2008. 262(1): p. 8-22.
218. Gericke, M., T. Liebert and T. Heinze, Interaction of Ionic Liquids with Polysaccharides, 8 – Synthesis of Cellulose Sulfates Suitable for Polyelectrolyte Complex Formation. *Macromolecular Bioscience*, 2009. 9(4): p. 343-353.

219. Liu, C.F., R.C. Sun, A.P. Zhang and J.L. Ren, Preparation of sugarcane bagasse cellulosic phthalate using an ionic liquid as reaction medium. *Carbohydrate Polymers*, 2007. 68(1): p. 17-25.
220. Liu, C.F., R.C. Sun, A.P. Zhang, J.L. Ren and Z.C. Geng, Structural and thermal characterization of sugarcane bagasse cellulose succinates prepared in ionic liquid. *Polymer Degradation and Stability*, 2006. 91(12): p. 3040-3047.
221. Liu, C.-F., A.-P. Zhang, W.-Y. Li, F.-X. Yue and R.-C. Sun, Homogeneous Modification of Cellulose in Ionic Liquid with Succinic Anhydride Using N-Bromosuccinimide as a Catalyst. *Journal of Agricultural and Food Chemistry*, 2009. 57(5): p. 1814-1820.
222. Li, W.Y., A.X. Jin, C.F. Liu, R.C. Sun, A.P. Zhang and J.F. Kennedy, Homogeneous modification of cellulose with succinic anhydride in ionic liquid using 4-dimethylaminopyridine as a catalyst. *Carbohydrate Polymers*, 2009. 78(3): p. 389-395.
223. Liu, C.F., A.P. Zhang, W.Y. Li, F.X. Yue and R.C. Sun, Succinylation of cellulose catalyzed with iodine in ionic liquid. *Industrial Crops and Products*, 2010. 31(2): p. 363-369.
224. Buchanan, C.M., N.L. Buchanan, M.E. Donelson, M.G. Gorbunova, T. Kuo and B. Wang, Regioselectively substituted cellulose esters produced in a halogenated ionic liquid process and products produced therefrom. 2010 Patent no. WO2010019245 A1.
225. Buchanan, C.M., N.L. Buchanan and E. Guzman-Morales, Regioselectively substituted cellulose esters produced in a tetraalkylammonium alkylphosphate ionic liquid process and products produced therefrom. 2010 Patent no. US20100267942 A1
226. Buchanan, C.M., N.L. Buchanan, R.T. Hembre and J.L. Lambert, Cellulose esters and their production in carboxylated ionic liquids. 2012 Patent no. US20120142910 A1
227. Buchanan, C.M. and N.L. Buchanan, Production of cellulose esters in the presence of a cosolvent. 2012 Patent no. US20120238742 A1
228. Granström, M., W. Mormann and P. Frank, Method of chlorinating polysaccharides or oligosaccharides. 2011 Patent no. WO2011086082 A1
229. Scheibel, J.J., C.J. Kenneally, J.A. Menkaus, K.R. Seddon and P. Chwala, Methods for modifying cellulosic polymers in ionic liquids. 2007 Patent no. WO2007112382 A1
230. Zhang, J., W. Chen, Y. Feng, J. Wu, J. Yu, J. He and J. Zhang, Homogeneous esterification of cellulose in room temperature ionic liquids. *Polymer International*, 2015. 64(8): p. 963-970.
231. Myllymaki, V. and R. Aksela, Method for preparing a cellulose ether. 2007 Patent no. US20070112185 A1

232. Mormann, W. and M. Wezstein, Trimethylsilylation of Cellulose in Ionic Liquids. *Macromolecular Bioscience*, 2009. 9(4): p. 369-375.
233. Erdmenger, T., C. Haensch, R. Hoogenboom and U.S. Schubert, Homogeneous Tritylation of Cellulose in 1-Butyl-3-methylimidazolium Chloride. *Macromolecular Bioscience*, 2007. 7(4): p. 440-445.
234. Granström, M., A. Olszewska, V. Mäkelä, S. Heikkinen and I. Kilpeläinen, A new protection group strategy for cellulose in an ionic liquid: simultaneous protection of two sites to yield 2,6-di-O-substituted mono-p-methoxytrityl cellulose. *Tetrahedron Letters*, 2009. 50(15): p. 1744-1747.
235. Lv, Y., Y. Chen, Z. Shao, R. Zhang and L. Zhao, Homogeneous tritylation of cellulose in 1-allyl-3-methylimidazolium chloride and subsequent acetylation: The influence of base. *Carbohydrate Polymers*, 2015. 117: p. 818-824.
236. Köhler, S., T. Liebert, T. Heinze, A. Vollmer, P. Mischnick, E. Möllmann and W. Becker, Interactions of ionic liquids with polysaccharides 9. Hydroxyalkylation of cellulose without additional inorganic bases. *Cellulose*, 2010. 17(2): p. 437-448.
237. Massonne, K., V. Stegmann, G. D'Andola, W. Mormann, M. Wezstein and W. Leng, Process for silylating cellulose. 2009 Patent no. US20090281303 A1
238. Moellmann, E., T. Heinze, T. Liebert and S. Koehler, Homogeneous synthesis of cellulose ethers in ionic liquids. 2013 Patent no. US8541571 B2
239. Lehmann, A. and B. Volkert, Method for producing polysaccharide derivatives. 2012 Patent no. US20120088909 A1
240. Holtkötter, T., S. Michel and G. Sonnenberg, Process and apparatus for the industrial preparation of methylhydroxyalkylcellulose. 2003 Patent no. US6667395 B2
241. Medronho, B. and B. Lindman, Brief overview on cellulose dissolution/regeneration interactions and mechanisms. *Advances in Colloid and Interface Science*, 2015. 222: p. 502-508.
242. Liu, Z., X. Sun, M. Hao, C. Huang, Z. Xue and T. Mu, Preparation and characterization of regenerated cellulose from ionic liquid using different methods. *Carbohydrate Polymers*, 2015. 117: p. 99-105.
243. Sun, L., J.Y. Chen, W. Jiang and V. Lynch, Crystalline characteristics of cellulose fiber and film regenerated from ionic liquid solution. *Carbohydrate Polymers*, 2015. 118: p. 150-155.
244. Olsson, C., A. Hedlund, A. Idström and G. Westman, Effect of methylimidazole on cellulose/ionic liquid solutions and regenerated material therefrom. *Journal of Materials Science*, 2014. 49(9): p. 3423-3433.
245. Michud, A., M. Hummel and H. Sixta, Influence of molar mass distribution on the final properties of fibers regenerated from cellulose dissolved in ionic liquid by dry-jet wet spinning. *Polymer*, 2015. 75: p. 1-9.
246. Östlund, Å., A. Idström, C. Olsson, P.T. Larsson and L. Nordstierna, Modification of crystallinity and pore size distribution in coagulated cellulose films. *Cellulose*, 2013. 20(4): p. 1657-1667.

247. Jiang, G., W. Huang, T. Zhu, C. Zhang, A.K. Kumi, Y. Zhang, H. Wang and L. Hu, Diffusion dynamics of 1-Butyl-3-methylimidazolium chloride from cellulose filament during coagulation process. *Cellulose*, 2011. 18(4): p. 921-928.
248. Li, B., J. Asikkala, I. Filpponen and D.S. Argyropoulos, Factors Affecting Wood Dissolution and Regeneration of Ionic Liquids. *Industrial & Engineering Chemistry Research*, 2010. 49(5): p. 2477-2484.
249. Mai, N.L., K. Ahn and Y.-M. Koo, Methods for recovery of ionic liquids—A review. *Process Biochemistry*, 2014. 49(5): p. 872-881.
250. Shi, J.-z., J. Stein, S. Kabasci and H. Pang, Purification of EMIMOAc Used in the Acetylation of Lignocellulose. *Journal of Chemical & Engineering Data*, 2013. 58(2): p. 197-202.
251. Huang, K., R. Wu, Y. Cao, H. Li and J. Wang, Recycling and Reuse of Ionic Liquid in Homogeneous Cellulose Acetylation. *Chinese Journal of Chemical Engineering*, 2013. 21(5): p. 577-584.
252. Environmental Protection Agency, E. Safer Chemical Ingredients List. 2016 28/06/2016]; Available from: <http://www.epa.gov/dfe/saferingredients.htm>.
253. UFT/Merck. UFT/Merck Ionic Liquids Biological Effects DataBase 2013 11/11/2013]; Available from: <http://www.il-eco.uft.uni-bremen.de/> (currently offline).
254. Ventura, S.P.M., A.M.M. Gonçalves, T. Sintra, J.L. Pereira, F. Gonçalves and J.A.P. Coutinho, Designing ionic liquids: the chemical structure role in the toxicity. *Ecotoxicology*, 2013. 22(1): p. 1-12.
255. Bernot, R.J., M.A. Brueseke, M.A. Evans-White and G.A. Lamberti, Acute and chronic toxicity of imidazolium-based ionic liquids on *Daphnia magna*. *Environmental Toxicology and Chemistry*, 2005. 24(1): p. 87-92.
256. Ventura, S.P.M., C.S. Marques, A.A. Rosatella, C.A.M. Afonso, F. Gonçalves and J.A.P. Coutinho, Toxicity assessment of various ionic liquid families towards *Vibrio fischeri* marine bacteria. *Ecotoxicology and Environmental Safety*, 2012. 76: p. 162-168.
257. Stolte, S., M. Matzke, J. Arning, A. Boschen, W.-R. Pitner, U. Welz-Biermann, B. Jastorff and J. Ranke, Effects of different head groups and functionalised side chains on the aquatic toxicity of ionic liquids. *Green Chemistry*, 2007. 9(11): p. 1170-1179.
258. Larson, J.H., P.C. Frost and G.A. Lamberti, Variable toxicity of ionic liquid-forming chemicals to *Lemna minor* and the influence of dissolved organic matter. *Environmental Toxicology and Chemistry*, 2008. 27(3): p. 676-681.

Part II. Thermodynamic properties of mixtures of ionic liquid + CO₂¹

¹ Part II outcome was published on The Journal of Supercritical Fluids as “Melting point depression effect with CO₂ in high melting temperature cellulose dissolving ionic liquids. Modeling with Group Contribution Equation of State” in collaboration with Planta Piloto de Ingeniería Química (PLAPIQUI-UNS-CONICET) as the thermodynamic modeling was performed by Francisco Sanchez and as “Experimental determination of viscosities and densities of mixtures carbon dioxide + 1-allyl-3-methylimidazolium chloride. Viscosity correlation”. Viscosity and density measurements were performed at Ruhr University Bochum.

Chapter 2. Melting Point Depression Effect with CO₂ in High Melting Temperature Cellulose Dissolving Ionic Liquids. Modeling with Group Contribution Equation of State

Abstract

Ionic liquids of the alkylmethylimidazolium chloride family are able to solubilize high amounts of cellulose and other natural polymers and have very good characteristics for their processing. Nevertheless, they present important disadvantages related to their high melting points and viscosities. Dissolution of carbon dioxide (CO₂) can reduce the melting point of these ionic liquids. In this work, the effect of pressurized carbon dioxide on the melting point depression of some ionic liquids able to dissolve biopolymers was experimentally determined using the first melting point method. Five different ionic liquids were studied using a high-pressure visual cell, up to a pressure of 10 MPa. The ILs studied were four ionic liquids with chloride anion coupled with 1-butyl-3-methylimidazolium cations: [C₄mim]⁺, 1-ethyl-3-methylimidazolium, [C₂mim]⁺, 1-allyl-3-methylimidazolium, [Amim]⁺ and 1-(2-hydroxyethyl)-3-methylimidazolium, [C₂OHmim]⁺ and one ammonium-based cation choline [C₅H₁₄NO]⁺ combined with dihydrogen phosphate anion, [H₂PO₄]⁻. Melting point depression effect observed for these groups of ionic liquids were around 10 K for chloride ILs and went as high as 33.2 K for choline dihydrogen phosphate. To correlate the melting point depression of imidazolium chloride ILs, parameters for the Group Contribution Equation of State (GC-EoS) of Skjold-Jørgensen for the liquid phase plus a fugacity expression for solid phases was employed. Experimental data used for the parameterization includes literature data of binary vapor-liquid, liquid-liquid and solid-liquid equilibria, and activity coefficients at infinite dilution. Melting point depression was calculated with an average deviation of 1.7 K (0.5%) and a maximum deviation of 4.3 K (1.3%).

1. Introduction

Ionic liquids (ILs) are substances composed entirely of ions that generally are fluid around or below 100°C [1]. The unique physicochemical properties of ILs such as low vapour pressure [2], and high solvation ability to dissolve various organic and inorganic substances allows their use as green solvents in several applications. Furthermore, ionic liquids can be easily modified by changing the structure of the cations or anions and, thus also their properties.

One of the most promising application of ionic liquids is cellulose processing. Some ILs have been demonstrated to be highly effective solvents for the dissolution of cellulose in amounts as high as 25% in mass [3], sometimes even at room temperature [4]. Nevertheless the high viscosity of ILs which is greatly increased when they dissolve cellulose is the main limitation for their use in those processes. Imidazolium chlorides, acetates and alkylphosphates can dissolve high amounts of cellulose and other biopolymers, but recently acetates and alkylphosphates has been preferred due to their lower viscosities and melting points [4] caused by their asymmetrical cation and anions. The large size of the anions enlarges the distance between cation and anion, making the ionic interaction weaker. Thus, the imidazolium chlorides present a more regular packing and consequently high melting temperatures and viscosities. For these reasons, these ILs are sometimes set aside in cellulose processing, even though they are more effective than the others in hydrolysis [5] and avoid using strong acids in cellulose acylation reactions.

The melting process of ILs is governed by Van der Waals forces and electrostatic interaction forces and each one plays different roles for different kinds of ILs constituting a very complex behavior [6]. As Bourbigou et al. [7] reviewed, the length of the alkyl chain, the existence of H-bond and the presence of impurities are factors that influence parameters such as dielectric constant values or solvent polarity as well as the competition for the ions between the added species and the counter-ion. The anion Cl⁻ is a good H-bond acceptor and its probable location has been proposed closer to the C(2) of the imidazolium ring. This provides higher charged density, symmetry and a more regular network. Therefore an increase of viscosity and high melting points is related to a growth in the cohesive forces via hydrogen bonding between the chloride and protons of the imidazolium ring. On the other hand, in the crystal structure of (2-hydroxyethyl)trimethylammonium dihydrogen phosphate, [C₅H₁₄NO][H₂PO₄], also known as choline dihydrogen phosphate ([Cho][DHP]) a number of O-H...O hydrogen bonds and C-H...O interactions are present [8]. The high crystallinity gives to this IL an elevated melting point (392 K).

It is known that mixing an IL with molecular solvents allows decreasing its viscosity and its melting point can be decreased. The viscosity of ILs-solvent mixtures is mainly dependent on the mole fraction of added molecular solvents [9]. This is also possible when using carbon dioxide (CO₂) as a co-solvent, which has the advantages of being non-toxic, cheap, and can be easily separated of the IL by depressurization. ILs and CO₂ are considered to be a promising media for the development of "green" technology [10]. In biphasic mixtures IL-CO₂ at high pressure, CO₂ can dissolve significantly into

the IL-rich liquid phase as well at moderate pressures as high as 75% in mol, but no ionic liquid dissolves in the gas phase [10,11]. The first example of CO₂-induced melting point depression (MPD) was reported by Kazarian et al. [12], who investigated an imidazolium salt, 1-hexadecyl-3-methylimidazolium hexafluorophosphate, [C₁₆mim][PF₆] with CO₂. They reported a MPD of 25 K with a CO₂ pressure of 70 bar. Scurto and Leitner tested [13] a quaternary ammonium salt tetra-*n*-butyl-ammonium tetrafluoroborate, [NBu₄][BF₄], and reported a solid-liquid transition temperature depression higher than 100K under 150 bar of CO₂. Later [14], they tested quaternary ammonium and phosphonium cations that showed strong depression as high as 80 K and 120 K. The method generally used was that of first melting point, with the exception of Serbanovic and coworkers that used a different method consisting in introducing a IL in a capillary tube inside a high pressure cell and increasing the temperature till the last solid particle is melted [15]. Selected results from MPD measurements on imidazolium and ammonium-based ILs found in literature are summarized in tables 1 and 2 respectively. In general imidazolium and pyridinium cations showed a much lower MPD in the range of 20 K than ammonium based ILs that can show melting MPD higher than 100 K.

Table 1 Summary of imidazolium-based ionic liquids normal melting point T_m (°C), CO₂ pressure (bar) and MPD (°C) found in literature.

Compound	T_m (K)	P_{CO_2} (bar)	MPD (K)	Ref.
[C ₁₆ mim][PF ₆]	348	70	25	[10]
[C ₄ mim][CH ₃ SO ₃]	345	150	19.6	[11]
[C ₄ mim][Tosyl]	341	150	25.8	[11]
[C ₄ mim][Cl]	342	150	10.2	[12]
[C ₂ mim][PF ₆]	333	147	35	[15]
[C ₅ O ₂ mim][PF ₆]	316	20	20	[15]

Abbreviations: 1-Hexadecyl-3-methylimidazolium hexafluorophosphate, [C₁₆mim][PF₆]; 1-butyl-3-methylimidazolium methanesulfonate, [C₄mim][CH₃SO₃]; 1-butyl-3-methylimidazolium tosylate, [C₄mim][Tosyl]; 1-butyl-3-methylimidazolium chloride, [C₄mim][Cl]; 1-ethyl-3-methylimidazolium hexafluorophosphate, [C₂mim][PF₆]; 1-[2-(2-methoxyethoxy)-ethyl]-3-methylimidazolium hexafluorophosphate, [C₅O₂mim][PF₆].

Table 2 Summary of ammonium-based salts normal melting point T_m (°C), CO₂ pressure (bar) and MPD (°C) found in literature.

Compound	T_m (K)	P_{CO_2} (bar)	MDP (K)	Ref.
$[(C_2H_5)_4N][NTf_2]$	375	35	82	[11]
$[(C_4H_9)_4N][BF_4]$	429	150	120	[12]
$[(C_4H_9)_3(CH_3)N][CF_3SO_3]$	356	50	43	[12]
[AB][CF ₃ SO ₃]	321	40	31	[12]
$[(C_4H_9)_4N][Tosyl]$	345	100	33	[15]

Abbreviations: Tetraethylammonium bis(trifluoromethylsulfonyl)imide, $[(C_2H_5)_4N][NTf_2]$; tetrabutylammonium tetrafluoroborate, $[(C_4H_9)_4N][BF_4]$; methyl tributylammonium trifluoromethanesulfonate $[(C_4H_9)_3(CH_3)N][CF_3SO_3]$; (S)-1-hydroxy-*N,N,N*-trimethylbutan-2-ammonium trifluoromethanesulfonate, [AB][CF₃SO₃]; tetrabutylammonium tosylate, $[(C_4H_9)_4N][Tosyl]$

The solubility of CO₂ in different ILs has been studied together with CO₂ induced MPD. Recently was published a study on ammonium-based ILs tested up to 150 bar was published [16]. The MPD reported was between 25 K and 120 K and the solubility between 0.57 and 0.8 (mole fraction) at 369 K. Nevertheless, no positive correlation was found between the magnitude of the melting point lowering and the solubility of the gas in each liquid. Melting point induced by CO₂ is minor in the case of methylimidazolium-based ILs as observed in Table 1.

In this work an experimental study of the MPD of various ionic liquids (solid at room temperature) was carried out in the presence of pressurized CO₂ up to 100 bar. MPD of imidazolium chloride ILs, were correlated using Group Contribution Equation of State of Skjold-Jørgensen and parameters were adjusted using literature data of CO₂ solubility in the ionic liquid [C₄mim][Cl] available in literature [17] as well as activity coefficient at infinite dilution.

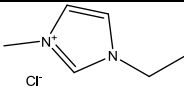
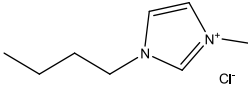
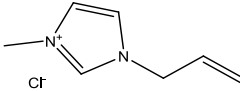
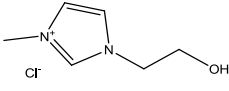
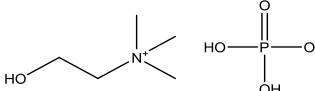
2. Experimental Section

2.1. Materials

The ionic liquids used in this work were 1-ethyl-3-methylimidazolium chloride, [C₂mim][Cl], 1-allyl-3-methylimidazolium chloride, [Amim][Cl], 1-butyl-3-methylimidazolium chloride, [C₄mim][Cl], 1-(2-hydroxyethyl)-3-methylimidazolium chloride, [C₂OHmim][Cl] and (2-hydroxyethyl) trimethylammonium dihydrogen phosphate, [C₅H₁₄NO][H₂PO₄]. The structure of these ILs is shown in Table 3, all of which were purchased from Iolitec (Germany). The water contents were determined by Karl-Fischer coulometric titration (Mettler toledo C20 coulometric KF titrator). Carbon

dioxide (99.5% purity) was supplied by Carbueros Metalicos (Spain) and was used without further purification.

Table 3 Ionic liquids used for experimental melting point depression (MPD) in pressurized CO₂

Abbreviation	Structure
[C ₂ mim][Cl]	
[C ₄ mim][Cl]	
[Amim][Cl]	
[C ₂ OHmim][Cl]	
[Cho][DHP]	

2.2. Apparatus

A schematic diagram of the equipment used for melting point measurements is shown in Fig. 1. The apparatus includes an optical cell (SITEC 740.2120) with an inner volume of 25 mL. Maximum operating temperature is 473 K and pressure is 500 bar. The cell has two opposite quartz windows. A lamp was used to illuminate one end of the view cell. The image was captured by a camcorder and displayed on the computer screen. The internal temperature of the cell was controlled by a PID temperature controller (OMRON E5GN) acting over an electrical jacket. The temperature was measured with a *K* type thermocouple with an accuracy of 1.5 K. The pressure was measured with a membrane relative pressure meter DESIN TPR 18/V2, with an accuracy of 0.2% span (0-400 bar) (accuracy 0.8 bar). The equipment and the methodology used has been described somewhere else [18].

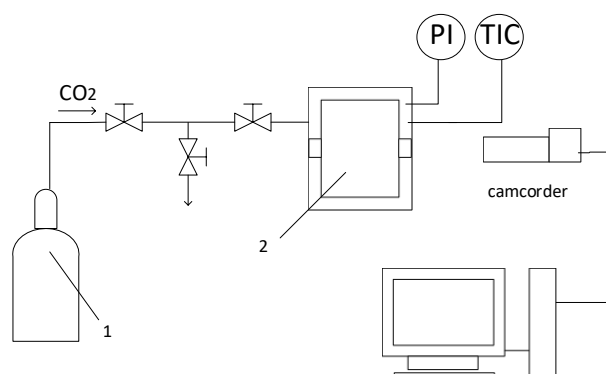


Fig.1 Scheme of the apparatus for melting temperatures measurements: 1, CO₂ supply; 2, optical cell

2.3. Method

The experiment starts with a small amount of ionic liquid in a glass vial introduced in the optical cell. First the cell was kept at vacuum for 15 minutes in order to remove air and volatile impurities. Afterward, the cell was filled with CO₂ and pressurized up to the desired operating pressure. At fixed pressure, and after an equilibration time of about 15 min, the cell was gradually heated at a rate of 5 K/30 min until melting of the ionic liquid sample was observed with the camcorder. The melting point temperature of the ILs was measured when the surface starts to melt, according to the “First Melting Point” method. Each measurement was repeated 3 times to determine the standard deviation in measurements.

2.4. Differential scanning calorimetry

Differential scanning calorimetry (DCS) of the ILs was performed using a DSC 822e Mettler Toledo SAE, with a high sensibility ceramic sensor FSR5 whose characteristics are detailed in Table 4. During the analysis nitrogen of analytical quality was used as purge gas with a flow of 50 cm³/min. Aluminum crucible standard, 40ul with pin (REF: ME-27331. from Mettler Toledo SAE) was used. Samples were weighted under nitrogen in a Balance Mettler. AT-261 with a precision of 0.01 mg. Temperature was increased from 298 to 423 K at 10 K/min.

Table 4 Characteristic of DCS sensor.

T Range (K)	Resolution (μ W)	Enthalpy Range (mW)	Sensibility (μ V/ μ W)
-123- 973	<0.04	\pm 350 (100 K) \pm 250 (300 K) \pm 200 (700 K)	15

3. Results and Discussion

3.1. Normal melting point and fusion enthalpies

Normal fusion temperatures and enthalpies of the ILs were determined by DSC and they are listed in Table 5. DSC curves are shown in Fig. s1 to s4 of supplementary information.

Table 5 DSC results measured in this work.

IL	T_{onset} (K)	T_{peak} (K)	ΔH [DSC] (kJ/mol)
[Amim][Cl]	315.75	324.95	-15.44 ± 0.06
[C ₄ mim][Cl]	335.45	341.35	-20.44 ± 0.09
[C ₂ OHmim][Cl]	360.35	363.35	-22.78 ± 0.12
[Cho][DHP] (Peak 1)	362.15	367.95	-12.957 ± 0.009
[Cho][DHP] (Peak 2)	391.85	395.55	-0.9586 ± 0.0008

Our results are compared to measurements of melting point and fusion enthalpies of other authors in Table 6. In general, important divergences are found in fusion enthalpy and melting temperature among the different authors: for [C₄mim][Cl], our fusion enthalpy is in the range of other author's values, while our melting temperature is also in the range but it is somehow lower than most literature values. In the case of [Amim][Cl] and [C₂OHmim][Cl] very few experimental values are available, existing great divergences among them, and our data present a higher melting temperature than other's author data, existing great divergences among them. In the case of [Cho][DHP], the DSC showed two peaks, being the fusion temperature reported in literature similar to the second peak reported [8].

Table 6 Comparison of different ILs normal melting points and fusion enthalpies

IL	T_m (K)	ΔH_{fus} (kJ/mol)	Method	Purity	Humidity	Ref.
[C ₄ mim][Cl]	335.35	20.44 ± 0.09	DSC	99%	1092 ppm	This work
	338.1 ± 1		DSC	Not stated	Not stated	[19]
	341.94 ± 0.5		DSC			[20]
	341.95 ± 0.5	14.057 ± 0.46	DSC	>98%		[21]
	340.1 ± 2		Visual			[22]
	330.1 ± 1		DSC			[23]
	314.1 ± 4		DSC			[24]
	342.95 ± 0.5	25.5 ± 2.5	DSC		0.1% mas	[25]
	341.8 ± 0.5	21.7 ± 0.6	DSC			[26]
	340.1 ± 2		Visual			[27]
	340.1 ± 2		Visual	99%		[28]
	340 ± 2		Visual			[29]
[C ₂ mim][Cl]	370.1 ± 0.2	15.1 ± 0.6	DSC	99.80%	Not stated	[30]
	361.75 ± 0.5	15.35 ± 0.53	DSC		0,2% mass	[25]
	334 ± 82		DSC		<20 ppm	[31]
	360.7 ± 0.5	15.5 ± 0.5	DSC			[26]
	360 ± 1		Visual			[32]
	350 ± 1		Visual			[32]
	358.1 ± 4		Visual	99%		[28]
	360.75 ± 0.2	15.16 ± 0.6		99.6%	not detected	[33]
[Amim][Cl]	307.53	0.524	DSC			[34]
	290,15					[35]
	324.95	-15.44 ± 0.06	DSC	>98%	1332 ppm	This work
[C ₂ OHmim][Cl]	333.95 ± 2			Not stated	Not stated	[36]
	367.95	-22.78 ± 0.12	DSC	99%	723 ppm	This work
[Cho][DHP]	392	-	DSC	Not stated	Not stated	[8]
	395.55		DSC			This work

3.2. Melting point depression

Table 7 shows the melting temperatures at vacuum and at different pressures of CO₂. It is observed that the melting points observed at vacuum are similar in most cases to the onset temperature provided by the DSC measurement listed in Table 5, as it is expected when dealing with a first melting point method. Measurement was taken when the first melting signs were observed on the surface of the ionic salt. Fig. 2 shows images from the measurement of [Amim][Cl] and [C₄mim][Cl] melting points at 40 bar and 100 bar respectively.

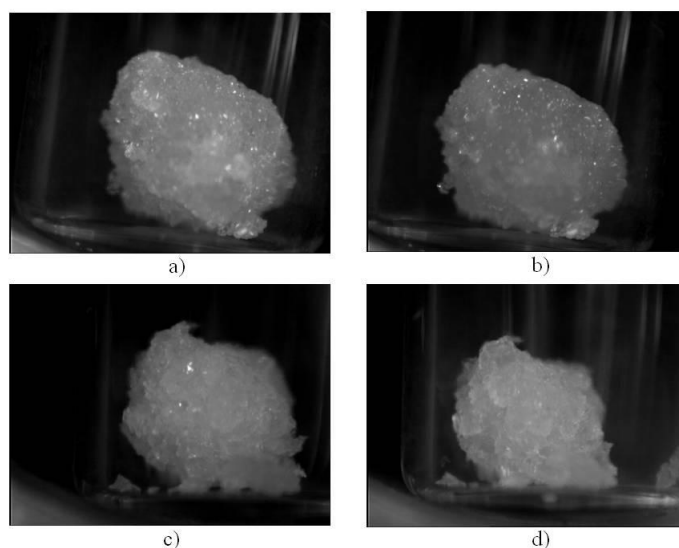


Fig. 2 Pictures from experimental melting point measurements with pressurized CO₂ in the high pressure view cell: a) [Amim][Cl] at room temperature and vacuum; b) [Amim][Cl] at 40 bar and 313 K (observe the melted surface); c) [C₄mim][Cl] at 100 bar and 316 K; d) [C₄mim][Cl] at 100 bar and 325 K (observe the beginning of the melted surface

Table 7 Experimental melting points at different pressures of CO₂

IL	P_{CO_2} (bar)	T_m (K)
[Amim][Cl]	vacuum	311.4 ± 1.3
	10.6 ± 0.5	311.2 ± 0.6
	20.3 ± 0.2	309.3 ± 0.1
	30.9 ± 0.2	306.6 ± 0.6
	41.9 ± 1.4	303.5 ± 0.6
[C ₂ mim][Cl]	Vacuum	341.1 ± 0.6
	12.3 ± 1	341.3 ± 0.2
	20.2 ± 0.3	340.6 ± 0.1
	31.5 ± 1.1	340.6 ± 0.3
	42.1 ± 2.4	339.9 ± 0.2
	50.9 ± 1.1	338.0 ± 1.0
100.7 ± 0.4	329.1 ± 0.5	
[C ₄ mim][Cl]	Vacuum	335.3 ± 2.0
	11.7 ± 0.7	335.2 ± 0.1
	21.7 ± 0.1	333.1 ± 0.1
	41.2 ± 1.1	334.5 ± 0.5
	51.2 ± 1	332.3 ± 0.1
	100.5 ± 0.4	325.3 ± 0.1
[C ₂ OHmim][Cl]	Vacuum	349.3 ± 0.4
	11.2 ± 1.3	349.5 ± 0.2
	20.7 ± 0.4	349.1 ± 0.5
	41 ± 0.4	348.5 ± 0.4
	52.3 ± 0.1	349.1 ± 1.7
	101.6 ± 1	343.5 ± 0.1
[Cho][DHP]	Vacuum	385.4 ± 0.3
	20.3 ± 0.3	361.9 ± 1.7
	31 ± 1.2	360.0 ± 1.2
	40.9 ± 0.5	354.1 ± 0.5
	50.1 ± 0.1	352.6 ± 1.0
	100.6 ± 0.2	352.2 ± 0.3

Much larger MPD was found with [Cho][DHP] than with imidazolium chloride ionic liquids. This is consistent with literature data that shown much larger CO₂ induced MPDs for ammonium based ILs than for imidazolium ones [15] 33 K vs. 10 K of imidazolium based ILs at 100 bar. The first melting point observed at vacuum was near

the onset temperature of the second DSC peak, considered the melting point in literature [8].

With regard to imidazolium chloride based ionic liquids at 40 bar, MPD is around 1 K, except for [Amim][Cl] for which is of 7.8 K, and more drastic MPD at pressures higher than 50 bar. At 100 bar MPD are much larger, of around 10 K in the following order: [C₂mim][Cl] > [C₄mim][Cl] > [C₂OHmim][Cl]. In literature it was also reported that for shorter alkyl chains in imidazolium based ILs, higher CO₂ induced MPD were observed [15]. The lowest one is observed in [C₂OHmim][Cl] which could be attributed to the lower affinity of hydroxyl group with CO₂ with respect to paraffine groups. This will be further discussed in the modeling section.

4. Thermodynamic modeling

The main objective of this section is to model the melting point decrease of the studied binary systems of CO₂ + alkylimidazolium chloride derivatives. Given the scarce information available of the ILs under investigation, we have adopted a group-contribution (GC) approach for the phase equilibrium modeling of these mixtures. The Group Contribution Equation of State (GC-EoS) originally developed by Skjold-Jørgensen [37] plus a mathematical expression for the solid fugacity has been applied to correlate and predict the melting temperature decrease of these mixtures. This model is based on Generalized van der Waals Theory with a local composition principle. In terms of the residual Helmholtz free energy, it can be expressed as a sum of free volume and attractive contributions:

$$\frac{A^R}{RT} = \frac{A^{fv}}{RT} + \frac{A^{att}}{RT} \quad (1)$$

There are two contributions to the residual Helmholtz energy in the GC-EoS model: free volume and attractive. The free volume term follows the expression developed by Mansoori and Leland [38]:

$$\frac{A^{fv}}{RT} = 3 \frac{\lambda_1 \lambda_2}{\lambda_1} (Y - 1) + \frac{\lambda_2^3}{\lambda_3} (Y^2 - Y - \ln Y) + n \ln Y \quad (2)$$

\tilde{q} with

$$Y = \left(1 - \frac{\pi \lambda_3}{6V} \right)^{-1} \quad (3)$$

$$\lambda_k = \sum_{i=1}^{NC} n_i d_i^k \quad (k = 1, 2, 3) \quad (4)$$

where n_i is the number of moles of component i , NC stands for the number of components, V represents the total volume, R stands for universal gas constant and T is temperature.

The following generalized expression is assumed for the hard sphere diameter temperature dependence:

$$d_i = 1.065655d_{ci} \left[1 - 0.12 \exp\left(\frac{-2T_{ci}}{3T}\right) \right] \quad (5)$$

where d_c is the value of the hard sphere diameter at the critical temperature, T_c , for the i -th component.

The attractive contribution to the residual Helmholtz energy, A^{att} , accounts for dispersive forces between functional groups. It is a van der Waals type contribution combined with a density-dependent, local-composition expression based on a group contribution version of the NRTL model [39]. Integrating van der Waals EoS, $A^{att}(T, V)$ is equal to $-a \cdot n \cdot \rho$ being a the energy parameter, n the number of moles and ρ the mole density. For a pure component a is computed as follows:

$$a = \frac{z}{2} q^2 g \quad (6)$$

where g is the characteristic attractive energy per segment and q is the surface segment area per mole as defined in the UNIFAC method [40]. The interactions are assumed to take place through the surface and the coordination number z is set equal 10 as usual. In GC-EoS the extension to mixtures is carried out using the two fluids model NRTL model, but using local surface fractions like in UNIQUAC [41] rather than local mole fractions. Therefore, the A^{att} for the mixture becomes

$$\frac{A^{att}}{RT} = -\frac{\frac{z}{2} \tilde{q}^2 g_{mix}}{RTV} \quad (7)$$

is the total number of surface segments and g_{mix} the mixture characteristic attractive energy per total segments and are calculated as follows:

$$g_{mix} = \sum_{i=1}^{NG} \theta_i \sum_{j=1}^{NG} \frac{\theta_j \tau_{ij} g_{ij}}{\sum_{k=1}^{NG} \theta_{ik} \tau_{ik}} \quad (8)$$

and

$$\tilde{q} = \sum_{i=1}^{NC} \sum_{j=1}^{NG} n_i v_{ij} q_j \quad (9)$$

where v_{ij} is the number of groups of type j in molecule i ; q_j stands for the number of surface segments assigned to group j ; θ_k represents the surface fraction of group k ;

$$\theta_k = \frac{1}{\tilde{q}} \sum_{i=1}^{NC} n_i v_{ik} q_k \quad (10)$$

$$\tau_{ij} = \exp\left(\alpha_{ij} \frac{\tilde{q} \Delta g_{ij}}{RTV}\right) \quad (11)$$

$$\Delta g_{ij} = g_{ij} - g_{jj} \quad (12)$$

g_{ij} stands for the attractive energy between groups i and j ; and α_{ij} is the non-randomness binary damping factor. The attractive energy between unlike groups is calculated from the corresponding interactions between like groups:

$$g_{ij} = k_{ij} \sqrt{g_{ii} g_{jj}} \quad (k_{ij} = k_{ji}) \quad (13)$$

with the following temperature dependence for the energy and interaction parameters:

$$g_{ii} = g_{ii}^* \left[1 + g'_{ii} \left(\frac{T}{T_i^*} - 1 \right) + g''_{ii} \ln \left(\frac{T}{T_i^*} \right) \right] \quad (14)$$

And

$$k_{ij} = k_{ij}^* \left[1 + k'_{ij} \ln \left(\frac{2T}{T_i^* + T_j^*} \right) \right] \quad (15)$$

where g_{ii}^* is the attractive energy and k_{ij}^* the interaction parameter at the reference temperature T_i^* and $\frac{T_i^* + T_j^*}{2}$, respectively.

4.1. Group contribution approach for methylimidazolium chloride based ionic liquids

In this work, the parameterization of a new group for methylimidazolium chloride based ILs ([-mim][Cl]) was performed. Fig. 3 illustrates the group decomposition for some ILs treated in this work. According previous to works [42,43], the corresponding IL molecule is divided in functional groups such as CH₃/CH₂ or CH₂OH, while the ionic contribution, i.e. cation + anion is kept as a single electroneutral group. Moreover, one methyl group attached to the imidazolium cation is kept within the whole ionic group in agreement with previous work for other imidazolium based ionic liquids [42,43].

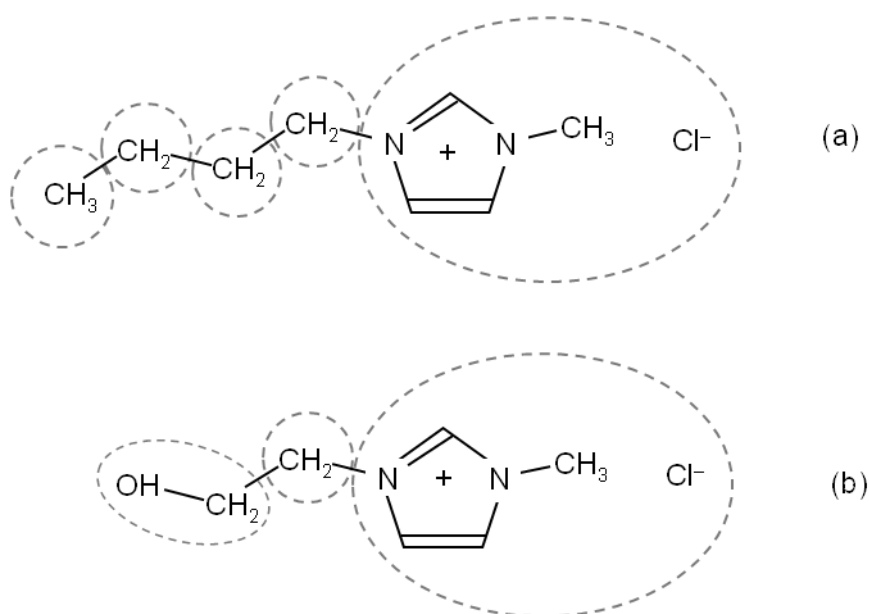


Fig. 3 Group decomposition of some methylimidazolium chloride based ionic liquids treated in this work. (a) [C₄mim][Cl]; (b) [C₂OHmim][Cl].

4.1.1. Parameterization of the free-volume term

The free-volume term of the residual Helmholtz energy contains only one characteristic parameter, that is, the critical hard sphere diameter (d_c). Values for d_c are normally calculated from critical properties or by fitting the equation to *one single* vapor pressure data point (generally the normal boiling point). Since the main characteristic of ionic liquids is their negligible vapor pressure, this type of information is not available. Espinosa et al. [44] developed a correlation between the critical diameter d_c and the normalized van der Waals molecular volume (R_i) of high molecular weight compounds (*n*-alkanes, *n*-alkenes, saturated and unsaturated triacylglycerides, and alkylesters).

This correlation was applied to calculate the critical diameter of ionic liquids from the estimated van der Waals volumes. Following a group-contribution approach, the normalized van der Waals volume of a compound, R_i can be calculated as the sum of the constituent group volume parameters r_j :

$$R_i = \sum_{j=1}^{NG} v_{ij} r_j \quad (16)$$

Where v_{ij} is the number of groups j in molecule i . Similarly, the number of surface segments, Q , of the i molecule can be obtained from its functional groups:

$$Q_i = \sum_{j=1}^{NG} v_{ij} q_j \quad (17)$$

Where q_j is the number of surface segments of group j . Although Eq. (16) and (17) are meant for molecules, they are also useful to calculate the reduced volume and surface of a larger group, as it is the case for the this new ionic group ([-mim][Cl]). Both r_j and q_j are defined as for the UNIFAC model [40] and Table 8 contains the values of r and q of the functional groups used in this work, all of which are calculated by means of the van der Waals volumes and surface areas given by Bondi [45]. The values of parameters R and Q for the [-mim][Cl] group have been calculated with its inner constituents shown in Fig. 4. The calculated normalized van der Waals volume and critical diameter of the ionic liquids studied in this work are reported in Table 9.

In order to evaluate the effective hard sphere diameter at a specified temperature, the GC-EoS requires an assigned value for the critical temperature, T_c , of the pure compound (see Eq. 5). In this work, the group contribution correlation of Valderrama and Rojas [46] has been applied to compute the values of the T_c of the ionic liquid studied in this work. All parameters referred to the free-volume term are listed also in Table 9.

Table 8 Normalized van der Waals segment volume and surface.

Group	r_j	q_j
CH ₃	0.9011	0.848
CH ₂	0.6744	0.540
CH=CH	1.1167	0.867
CH=CH ₂	1.3454	1.176
CH ₃ -N	1.1865	0.940
CH=N	0.7329	0.324
Cl	0.7910	0.724
CH ₂ OH	1.2044	1.124
[-mim][Cl]	3.8271	2.855

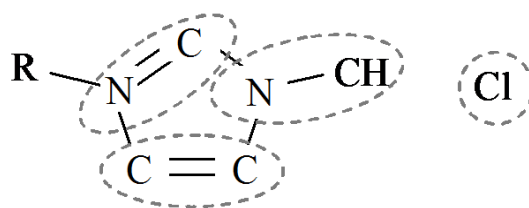


Fig. 4 Groups contained within the [-mim][Cl] group for evaluating parameters $r[-mim][Cl]$ and $q[-mim][Cl]$.

Table 9 Pure component properties required for the GC-EoS.

Ionic liquid	M	R_i	T_c^a (K)	d_c^b (cm ³ /mol ^{1/3})	$T_{fus}/T_{tr,i}$ (K)	$\Delta H_{fus}/\Delta H_{tr,i}$ (J/mol)	v_t^L (cm ³ /mol)	v_t^S (cm ³ /mol)
[C ₂ mim]Cl	146.6	5.4026	748.6	5.2194	361.75 ^c 353.15 ^d	15350 ^c -	137.03 ^a	123.6 ^g
[Amim][Cl]	158.6 ₃	5.8469	770.7	5.3925	312.9 ^d	15444 ^d	136.0 ^f	116.3 ^h
[C ₂ OHmim]Cl	162.6	5.7059	832.1	5.3925	349.7 ^d	22275 ^d	135.1 ^a	115.4 ^h
[C ₄ mim]Cl	174.7	6.7514	789.0	5.7223	342.95 ^c 341.95 ^e 335.48 ^d	25540 ^c 14050 ^e 20442 ^d	160.6 ^a	137.3 ^h
[C ₈ mim]Cl	230.8	9.4491	869.4	6.5742	-	-	-	-
[C ₁₀ mim]Cl	258.8 ₈	10.797	910.1	6.9464	311.17 ^e	30932 ^e	259.3 ^a	221.6 ^h
[C ₁₂ mim]Cl	286.9 ₆	12.146	951.5	7.2923	369.78/324. 13/283.21 ^e	604/23580 /1157 ^e	374.8 ^a	320.4 ^h

^a Obtained using Valderrama and Rojas [46] group contribution method. ^b Calculated with Espinosa et al. [44] correlation. ^c Kick et al. [25]. ^d This work. ^e Domańska et al. [21]. ^f Wu et al. [47]. ^g Bolkan et al. [48]. ^h Goodman et al. [49].

4.1.2. Parameterization of the attractive term

For the parameterization of the attractive contribution, self and binary interaction parameters of the [-mim][Cl] must be set. Group interaction parameters for alkanes, alkene, alcohol and CO₂ groups have been taken from previous works [37,50,51]. The procedure to correlate pure and binary [-mim][Cl] parameters follows the method described by Breure et al. [42] which require activity coefficients at infinite dilution with normal alkanes. Up to our knowledge, this information is only available for some *n*-alkanes in 1-octyl-3-methylimidazolium chloride ([C₈mim][Cl]) [52]. To add robustness in the parameterization procedure, the mutual solubility of [C₈mim][Cl] with *n*-heptane and *n*-dodecane at 298 K reported by Letcher et al. [53] was added to the objective function reported by Breure et al. Thus, the objective function defined in this work is:

$$O.F. = w_{\gamma}^2 \sum_{i=1}^{NGam} \left(\frac{\gamma_{clc,i}}{\gamma_{exp,i}} - 1 \right)^2 + w_x^2 \sum_{i=1}^{NEq} \left(\frac{x_{clc,i}}{x_{exp,i}} - 1 \right)^2 \quad (18)$$

Where NGam and NEq are the number of activity coefficient and binary phase composition data points, γ are the activity coefficients, x represent phase compositions and w_u represents weights assigned to different kind of experimental data. Both weights have been set to 1.

The correlation procedure is identical to the one described by Breure et al. [42] in order to keep the number of adjustable parameters as low as possible. A linear temperature dependence for $g[-mim][Cl]$ parameter was assumed ($g''[-mim][Cl] = 0$); initially, all binary interaction parameters are assumed to be temperature independent and the mixture is considered to behave as a regular solution ($k^*[-mim][Cl], i = 1; k'[-mim][Cl], i = 0; \alpha_{[-mim][Cl],i} = \alpha_{i,[-mim][Cl]} = 0$). This means that initially, the only adjustable parameters are self-interaction parameters: $g^*[-mim][Cl]$ and $g'[-mim][Cl]$. After this first correlation, self-interaction parameters are fixed and only binary interaction parameters $k^*[-mim][Cl], i$, $\alpha[-mim][Cl], i$ and $\alpha_{i,[-mim][Cl]}$ are used as adjustable parameters. Moreover, the non-randomness parameters are assumed to be the same within a family (for instance $\alpha_{[-mim][Cl],CH_3} = \alpha_{[-mim][Cl],CH_2}$, in accordance to previous works [37,42,43]). Last, a temperature dependence ($k'_{i,[-mim][Cl]}, i \neq 0$) for the binary interaction parameter, or distinction between groups *may be* then introduced if needed to improve correlation. On the other hand, the parameterization of the interaction parameters between [-mim][Cl] and the resting groups included also binary vapor-liquid (VLE) and solid-liquid equilibria (SLE).

4.2. Phase equilibrium equations

Binary and ternary phase equilibrium calculation were performed by solving the isofugacity of the system between phases α and β at fixed temperature, T , and pressure, P :

$$\hat{f}_i = x_{i,\alpha} \hat{\phi}_{i,\alpha} P = x_{i,\beta} \hat{\phi}_{i,\beta} P \quad i = 1, NC \quad (19)$$

where \hat{f}_i is the fugacity of component i at equilibrium, and $x_{i,j}$ and $\hat{\phi}_{i,j}$ represents the mole fraction and fugacity coefficient of component i in phase j . Fugacity coefficients of any component in the mixture are obtained by means of an equation of state. In this work, the GC-EoS model was applied to calculate the fugacity coefficients of all *fluid* phases. In case of solid-fluid equilibria, we follow the subcooled liquid reference state approach [54] assuming a pure solid phase for the heavy compound ($x_{iL,s} = 1$). For ILs treated in this work, many of the melting information to precisely evaluate the solid fugacity are not available. Up to our knowledge, no data about the heat capacity is available in open literature. With respect to density, experimental data of liquid [Amim][Cl] and solid [C₂mim][Cl] has been reported [47,48]. We have decided to: a) deprecate the change in the heat capacity during melting, which should not harm the solid fugacity calculation because the temperature ranges studied in this work are narrow in general; and b) to consider the change in volume during melting as constant. Thus, the expression proposed by Firoozabadi [54] for the fugacity of the solid becomes

$$f_{iL}^S(T, P) = f_{iL}^L(T, P) \exp \left[-\frac{\Delta H_{fus}}{R} \left(\frac{1}{T} - \frac{1}{T_{fus}} \right) - \frac{\Delta v_{fus} (P - P_{fus})}{RT} \right] \quad (20)$$

Where f_{iL}^S and f_{iL}^L are the pure IL fugacity as a solid and liquid, respectively; T_{fus} , ΔH_{fus} and Δv_{fus} are the pure fusion temperature, and change in the enthalpy and volume of the pure solid and liquid phases.

For the modeling of SLE of binary mixtures which are at atmospheric pressure, it is possible to neglect the Δv_{fus} , since its contribution is minor at this condition. However, Δv_{fus} cannot be neglected for the calculation of the CO₂-induced MPD because pressure arises up to 100 bars in our experimental data (see Table 7). To overcome this limitation, we propose the following approach. First, estimate the liquid molar volume at 298 K of [C₂mim][Cl], [C₄mim][Cl] and [C₂OHmim][Cl] using the correlation of Valderrama and Rojas [46]. Although these ILs are solid at 298 K, we intend to obtain an approximation of the liquid density at melting point. Secondly, for the solid density of [Amim][Cl], [C₄mim][Cl] and [C₂OHmim][Cl], we propose to use the correlation of Goodman et al. [49]. These authors developed a correlation to estimate the saturated solid density (ρ_t^S) from the liquid density at the triple point (ρ_t^L). They proposed the relation shown in eq. 21.

$$\rho_t^S = 1.17\rho_t^L \quad (21)$$

From eq. 21 it is possible to estimate the Δv_{fus} using the liquid or solid density information available. Values estimated using Eq. (21) are listed in Table 9, for the ILs studied in this work.

In principle, Eq. (20), together with the melting properties from Table 9 are enough for estimating the pure solid fugacity of the ILs in all binary mixtures with CO₂ studied in this work. Notwithstanding, Tables 7 and 9 highlights the existing dispersion regarding melting enthalpies of some imidazolium based ILs. Moreover, Eq. (21) provides only a rough estimation of the melting volume. Rodríguez Reartes et al. [55] faced a similar problem when dealing with the calculation of the solid-fluid equilibria of CO₂ with heavy compounds. These authors also state that errors in the constants ΔH_{fus} and Δv_{fus} will propagate to the calculated pure solid fugacity of the heavy compound, which also depends on the limitations of the selected EoS to calculate the liquid fugacity. In summary, Rodríguez Reartes et al. proposed an alternative parameterization approach, keeping constant the prediction of the pure melting line. In such condition, liquid and solid fugacities are equal, which leads to the following expression from Eq. (20):

$$P = P_{fus} - \frac{\Delta H_{fus}}{\Delta v_{fus}} \left(1 - \frac{T}{T_{fus}}\right) = P_{fus} + C_1 \left(1 - \frac{T}{T_{fus}}\right) \quad (22)$$

From Eq. (22) it is clear that if the relation $\frac{\Delta H_{fus}}{\Delta v_{fus}}$ (i.e. C_1) remains constant, the melting line of the pure compound is invariant. The pure solid fugacity may be then rewritten in terms of Δv_{fus} and C_1 :

$$f_{IL}^S(T, P) = f_{IL}^L(T, P) \exp \left[-\frac{\Delta v_{fus}}{RT_{fus}} \left[C_1 \left(1 - \frac{T}{T_{fus}}\right) - \frac{T_{fus}}{T} (P - P_{fus}) \right] \right] \quad (23)$$

Rodríguez Reartes et al. [55] then proposed a parameterization strategy keeping constant C_1 , (i.e., invariant pure melting line) while employing Δv_{fus} as an adjustable parameter. They show that perturbation in Δv_{fus} produces large and non-linear changes in the solid fugacity. Thus, using a custom value while keeping constant the pure heavy compound melting line is a reasonable choice.

Last, it is worth to mention that given the dispersion found in T_{fus} and ΔH_{fus} , we decided to model each binary SLE data set with its specific values of T_{fus} and ΔH_{fus} . As an example, consider the binary systems involving [C₄mim][Cl] studied in this work. The data modeled in Fig. 8, measured by Domańska et al. [20], considered T_{fus} and ΔH_{fus} obtained by the same authors (see Table 9). On the other hand, MPD of [C₄mim][Cl] listed in Table 7, depicted in Fig. 10.b were modeled using melting properties obtained in this work (see Table 9).

The solution procedure applied in this work to solve the system of Eq. (19) is the *TP* flash with stability analysis as described by Michelsen [56,57]. On the other hand, the calculation of the solid-liquid-vapor lines required for the prediction of the melting depression follows the work of Rodríguez Reartes et al. [55]. They published a detailed algorithm for the calculation of binary solid-fluid-fluid equilibrium lines of asymmetric mixtures, like the ones treated in this work.

4.3. Modeling results and discussion

4.3.1. Mixtures of alkyimidazolium chloride ILs + hydrocarbons

The parameters obtained through correlation of experimental data are listed in Table 10. Table 11 reports the deviation between the GC-EoS model and experimental data, together with temperature and pressure ranges, references and number of experimental data points. As can be seen, binary interaction parameters $k^*[-mim][Cl], i$ have been differentiated for $i = CH_3$ or CH_2 to improve correlation and prediction of experimental data, though no temperature dependence was introduced. On the other hand, the encountered binary dumping factors found to represent experimental data are asymmetric ($\alpha_{[-mim][Cl],i} \neq \alpha_{i,[-mim][Cl]}$) but not differentiation has been introduced between CH_3 and CH_2 groups. For $i = CH=CH_2$ and $i = ACCH_3$, only one single interaction parameter was correlated because the only experimental data available are the activity coefficients reported by David et al. [52]. Deviations from experimental data listed in Table 11 show that the model presents activity coefficients at infinite dilution and mutual solubility of $[C_8mim][Cl] + n$ -alkanes within the experimental error reported by the authors (3% for activity coefficients [52] and 0.006 for molar fractions [53]). The exceptions are the solubility of n -dodecane and n -hexadecane in $[C_8mim][Cl]$, for which deviation obtained with the GC-EoS doubles the reported error. Fig. 5 depicts graphical results of this correlation for activity coefficients. Fig. 6 shows the predictions of the ternary phase equilibria of $[C_8mim][Cl] + benzene + a n$ -alkane. The GC-EoS follows qualitatively the experimental tie-lines for intermediate compositions, founding little better results for n -dodecane than for n -heptane.

Table 10 New GC-EoS parameters for the [-mim][Cl] group.

Pure group parameter						
Group	q	$T^*(K)$	$g^*(\text{atm cm}^6/\text{mol}^2)$	g'	g''	Source
[-mim][Cl]	2.855	600.0	1844397	-0.1552	0	LLE of nC_7 or nC_{12} at 298 K + γ_∞ of nC_5 & nC_8 + [C ₈ mim][Cl]
Binary interaction parameters						
Group		k_{ij}^*	k_{ij}	α_{ij}	α_{ji}	Source
i	j					
[-mim][Cl]	CH ₃	0.8215	0	-0.7577	-0.2539	LLE of nC_7 or nC_{12} at 298 K + γ_∞ of nC_5 - nC_8 + [C ₈ mim][Cl]
	CH ₂	1.0838	0	-0.7577	-0.2539	
	CH=CH ₂	0.7850	0	0	0	γ_∞ of 1-heptene + [C ₈ mim][Cl]
	CO ₂	1.0409	0.1509	-1.4439	0.4677	Bubble pressures of CO ₂ + [C ₄ mim][Cl]
	ACH	0.8620	0.0271	0.6717	1.4377	LLE at 298K + γ_∞ of benzene + [C ₈ mim][Cl]
	ACCH ₃	0.9310	0	0	0	γ_∞ of toluene + [C ₈ mim][Cl]
	CH ₂ OH	1.0260	0	0.4148	-4.4988	SLE of C ₂ OH & C ₁₂ OH + [C ₄ mim][Cl].

Table 11 Model deviations of experimental data of correlated and predicted data points.

Compound		T (K)	P (bar)	ARD%(γ)		No exp points	Source
(1)	(2)						
<i>Activity coefficient</i>							
[C ₈ mim][Cl]	<i>n</i> -Pentane	298, 308, 318	1.01	3.0*		3	[52]
	<i>n</i> -Hexane	298, 308, 318	1.01	2.5		3	[52]
	<i>n</i> -Heptane	298, 308, 318	1.01	4.9		3	[52]
	<i>n</i> -Octane	298, 308, 318	1.01	2.6*		3	[52]
	1-Hexene	298, 308, 318	1.01	1.1		3	[52]
	1-Heptene	298, 308, 318	1.01	2.0*		3	[52]
	1-Octene	298, 308, 318	1.01	1.7		3	[52]
	Benzene	298, 308, 318	1.01	3.6*		3	[52]
	Toluene	298, 308, 318	1.01	2.8*		3	[52]
<i>Binary liquid-liquid & SC fluid-liquid equilibria</i>							
				AAD (ARD%) of x_{ij}			
				(1) in (2)	(2) in (1)		
[C ₈ mim][Cl]	<i>n</i> -Heptane	298	1.01	1.4E-3 (20)*	7.7E-3 (12)*	1	[53]
	<i>n</i> -Dodecane	298	1.01	6.2E-3 (65)*	1.2E-2 (49)*	1	[53]
	<i>n</i> -Hexadecane	298	1.01	5.9E-3 (62)	1.6E-2 (87)	1	[53]
	Benzene	298	1.01	1.5E-4 (2.1)*	1.6E-2 (2.3)*	1	[53]
[C ₄ mim][Cl]	CO ₂	353, 373	24-360	-	2.0E-2 (7.7)*	19	[17]
		358,363,368	26-340	-	2.0E-2 (7.6)	27	[17]
<i>Solid-liquid equilibria</i>							
[C ₂ mim][Cl]	[C ₄ mim][Cl]	318-360	1.01	2.8E-2 (4.0)	3.5E-2 (4.8)	18	[25]
[C ₄ mim][Cl]	Etanol	298-342	1.01	2.4E-2 (3.5)*	-	29	[20]

	1-Butanol	273-342	1.01	0.17 (25)	-	12	[20]
	1-Hexanol	285-342	1.01	7.6E-2 (15)	-	32	[20]
	1-Octanol	273-342	1.01	8.1E-2 (8.1)	-	15	[20]
	1-Decanol	279-342	1.01	0.13 (130)	1.4E-2 (1.4)	23 / 3	[20]
	1-Dodecanol	286-342	1.01	2.6E-2 (2.6)*	2.3E-2 (2.6)	26/5	[20]
[C ₁₀ mim][Cl]	Etanol	276-311	1.01	6.9E-2 (12)	-	13	[58]
	1-Butanol	275-311	1.01	9.6E-2 (20)	-	22	[58]
	1-Hexanol	277-311	1.01	0.16 (41)	-	17	[58]
	1-Octanol	292-311	1.01	0.22 (57)	-	15	[58]
	1-Decanol	277-311	1.01	0.28 (144)	-	17	[58]
	1-Dodecanol	297-311	1.01	0.39 (183)	-	19	[58]
[C ₁₂ mim][Cl]	<i>n</i> -Octane	322-370	1.01	0.28 (74)	-	29	[59]
	<i>n</i> -Decane	323-370	1.01	0.25 (49)	-	25	[59]
	<i>n</i> -Dodecane	324-370	1.01	0.36 (124)	-	20	[59]
	Benzene	291-370	1.01	0.12 (23)	-	17	[59]
	Etanol	274-370	1.01	6.2E-2 (9.2)	-	26	[60]
	1-Butanol	276-370	1.01	7.9E-2 (12)	-	26	[60]
	1-Hexanol	273-370	1.01	0.17 (14)	-	34	[60]
	1-Octanol	273-370	1.01	9.4E-2 (22)	-	37	[60]
	1-Decanol	279-370	1.01	0.24 (157)	1.1E-2 (1.1)	38/4	[60]
	1-Dodecanol	296-370	1.01	0.37 (545)	1.3E-2 (1.3)	50/3	[60]

* Data included in parameterization procedure.

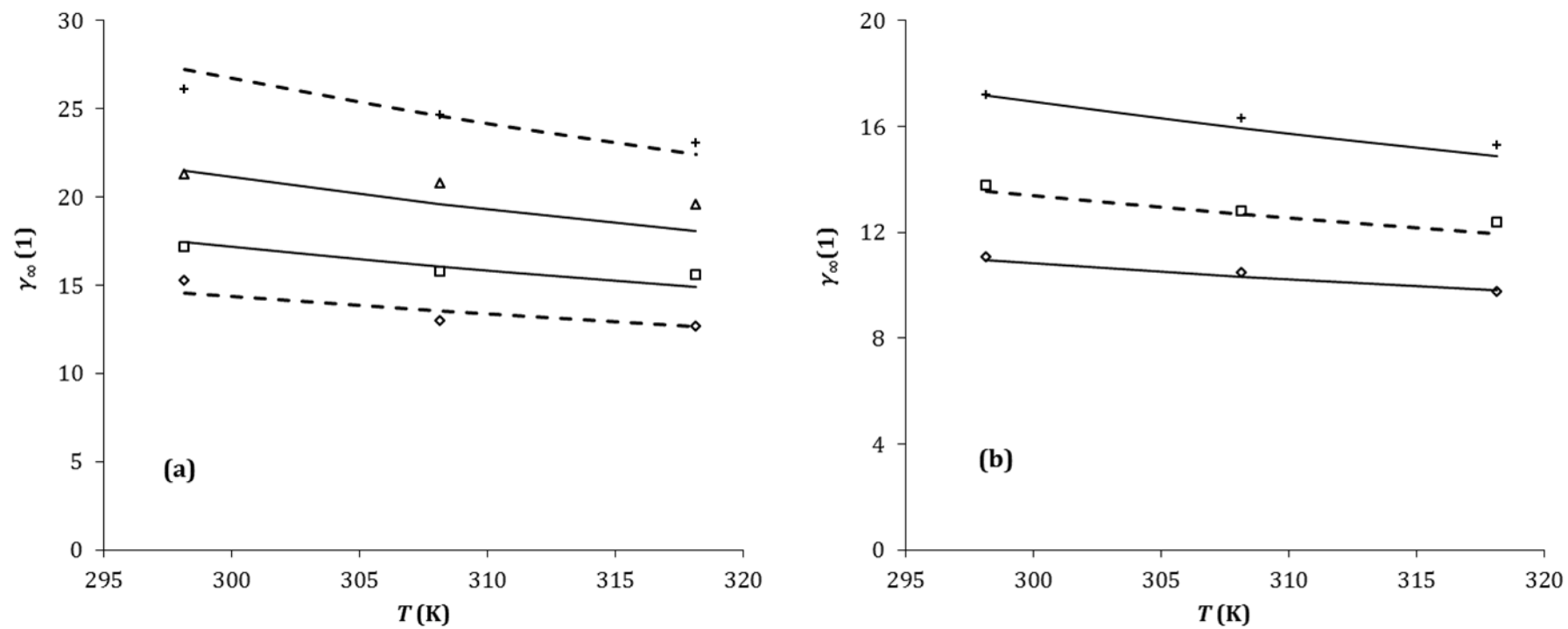


Fig. 5 Activity coefficients at infinite dilution of hydrocarbons (1) in $[C_8mim][Cl]$ (2) [52]. (a) (\diamond) n -Pentane, (\square) n -hexane, (\triangle) n -heptane and ($+$) n -octane. (b) (\diamond) 1-Hexene, (\square) 1-heptene and (\triangle) 1-octene. Dashed and solid lines: correlation and prediction using GC-EoS model, respectively, with parameters of Tables 9 and 10.

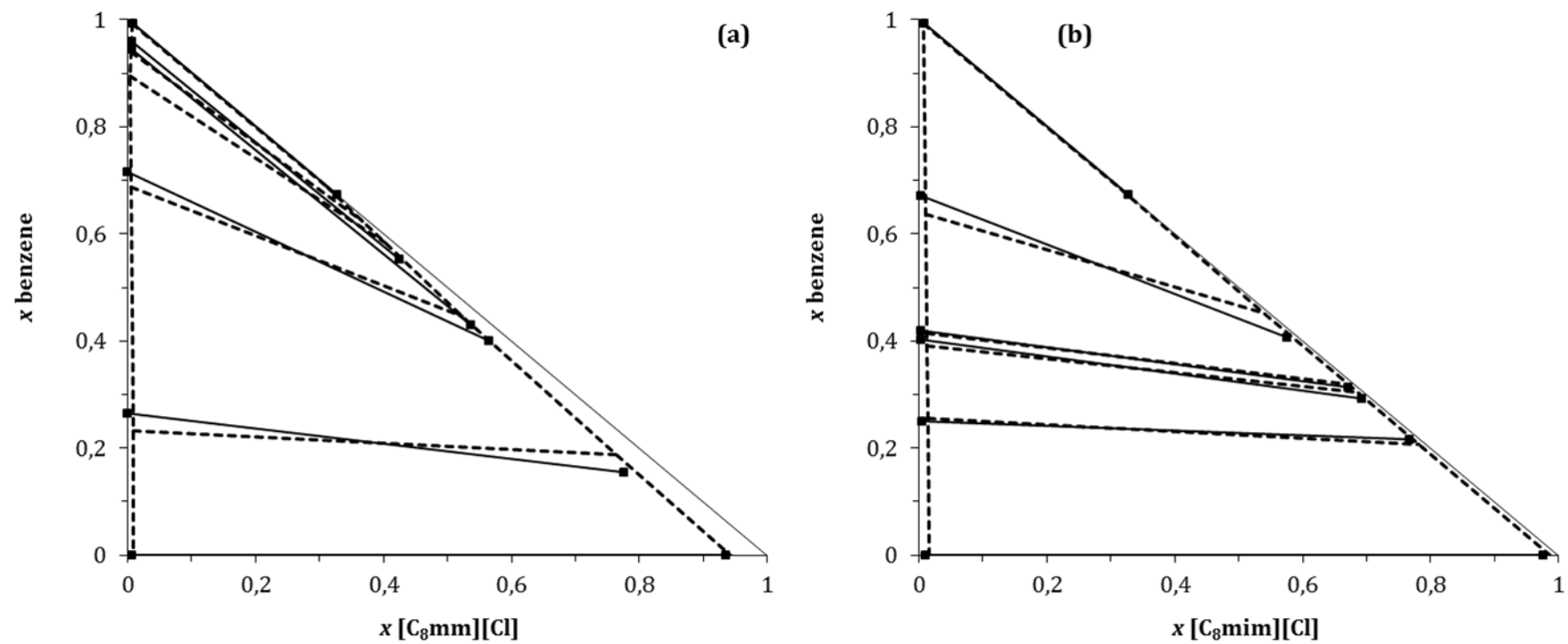


Fig. 6 Prediction of the liquid-liquid equilibria of the ternary system $[C_8mim][Cl]$ + benzene + n -alkane at 298 K. (a) n -Heptane; (b) n -dodecane. Symbols and solid lines represent experimental tie-lines [53], while the dashed lines are GC-EoS predictions.

Solid-liquid equilibria of [C₁₂mim][Cl] with alkanes deserves a special mention. This data type is an interesting challenge, since all interaction parameters are now fixed. Moreover, the phase equilibria of [C₁₂mim][Cl] presents polymorphism, showing pure solid-solid (SS) phase transitions. This is an important implication in the pure and mixture phase behavior, since the change in enthalpy of the first SS transition, $\Delta H_{tr,1}$, is much greater than ΔH_{fus} (see Table 9). Thus, specifically for the binary SLE data involving this compound, the following expression has been employed to model the fugacity of the solid phase:

$$f_{IL}^S(T, P) = f_{IL}^L(T, P) \exp \left[-\frac{\Delta H_{fus}}{R} \left(\frac{1}{T} - \frac{1}{T_{fus}} \right) - \sum_{i=1}^{NT} \frac{\Delta H_{tr,i}}{R} \left(\frac{1}{T} - \frac{1}{T_{tr,i}} \right) \right] \quad (24)$$

where $NT(T)$ is the number of SS transitions present between T and T_{fus} , and $T_{tr,i}$ and $\Delta H_{tr,i}$ are the temperature and enthalpy of the SS transition. Eq. (24) is basically the same as presented by Domańska et al. [60], but deprecating the specific heat change. Fig. 7 shows the prediction of the SLE of [C₁₂mim][Cl] + *n*-octane and *n*-dodecane, using Eq. (24) for the pure [C₁₂mim][Cl] solid fugacity. The model predictions depicted by lines follow qualitatively the experimental data presented by Domańska et al. [59]. These authors reported the occurrence of a liquid-liquid split in a narrow composition region for the [C₁₂mim][Cl] + *n*-dodecane binary system. On the other hand, the GC-EoS predicts a wide liquid-liquid split for the three binary systems studied by Domańska et al. [59]. However, the experimental data follows an extremely flat tendency with an almost constant phase transition temperature, which may indicate a phase split not found because of the presence of SLE.

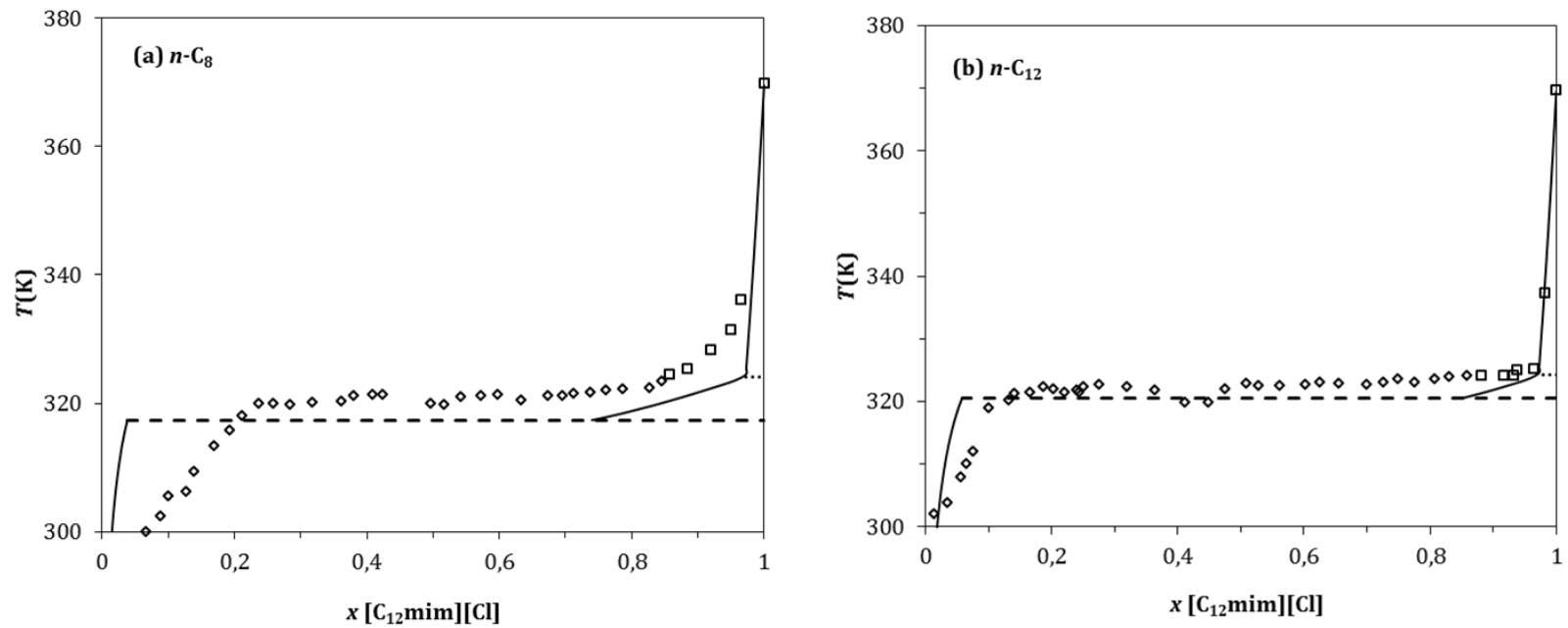


Fig. 7 Solid-liquid equilibria of the system $[C_{12}mim][Cl]$ + (a) n -octane and (b) n -dodecane. Experimental SLE data at atmospheric pressure taken from Domańska et al. [59]. Symbols represent experimental data of liquid + solid α (\square) or solid β (\diamond). Lines represent GC-EoS prediction of SLE (solid), SSLE (dotted) and SLLE (dashed). Notice that the $[C_{12}mim][Cl]$ fugacity as a pure solid was calculated by means of Eq. (24)

4.3.2. Mixtures of alkylimidazolium chloride ILs + alcohols

Experimental binary SLE data of alcohols with alkylimidazolium chloride based ILs is vast. The group of Domańska et al. have published an extensive study of SLE of the homologue series of *n*-alcohols with [C₄mim][Cl] [20], [C₁₀mim][Cl] [58] and [C₁₂mim][Cl] [60]. Moreover, Domańska et al. [21] measured the mutual solubility of 1-octanol + [C₈mim][Cl]. Table 11 lists all deviations of our modeling results from experimental data, which includes all SLE found, while Fig. 8 exemplify the correlation and predictions of the SLE of selected alcohols + ILs. LLE experimental data of 1-octanol + [C₈mim][Cl] were excluded from Table 11 because the model predicts one single phase for this system at experimental conditions studied in [20,21,58,60]. The experimental data reported shown a complex behavior, which is a challenge to any group-contribution thermodynamic model. For example, according to measured data, 1-octanol + [C₄mim][Cl] and [C₁₂mim][Cl] show complete miscibility in the liquid phase. However, as previously mentioned, the experimental data of the binary system 1-octanol + [C₈mim][Cl] present a phase split at the same temperature regions [21]. Moreover, the SLE of the binary 1-octanol + [C₁₀mim][Cl] reported by Domańska et al. [58] presents a flatness in temperature, typical of liquid phase splits (see Fig. 8.b). This non-linear transition of the mixture behavior when changing the length of the alkyl chain in the IL is not possible to be represented with a model such as the GC-EoS. The only difference between these compounds within the GC-EoS framework is the number of CH₂ in the IL and thus, the prediction of the phase behavior of mixtures of homologue series tends in general to be monotonic. A better approach could be to employ an association contribution to the Helmholtz free energy in Eq. (1) as it is done in the GCA-EoS model of Gros et al. [61], however, this is beyond the scope of this work. Given the limitations of the model to properly represent all analyzed experimental, the following approach as been proposed: selected binary systems were employed for the correlation of the experimental data, generating different sets of parameters. Then, the final set of parameters was selected between the different predictions achieved of the MPD of [C₂OHmim][Cl] in compressed CO₂. Nevertheless, this information was not included in the objective function defined in Eq. (18). The selected set of parameters were the result of the correlation of the SLE of [C₄mim][Cl] + ethanol and [C₄mim][Cl] + 1-dodecanol. Notice that groups [-mim][Cl] and CH₂OH are more concentrated in the mixture when the shorter the alkyl chain is (i.e., [C₄mim][Cl] + ethanol binary system), where less *noise* from other groups is present.

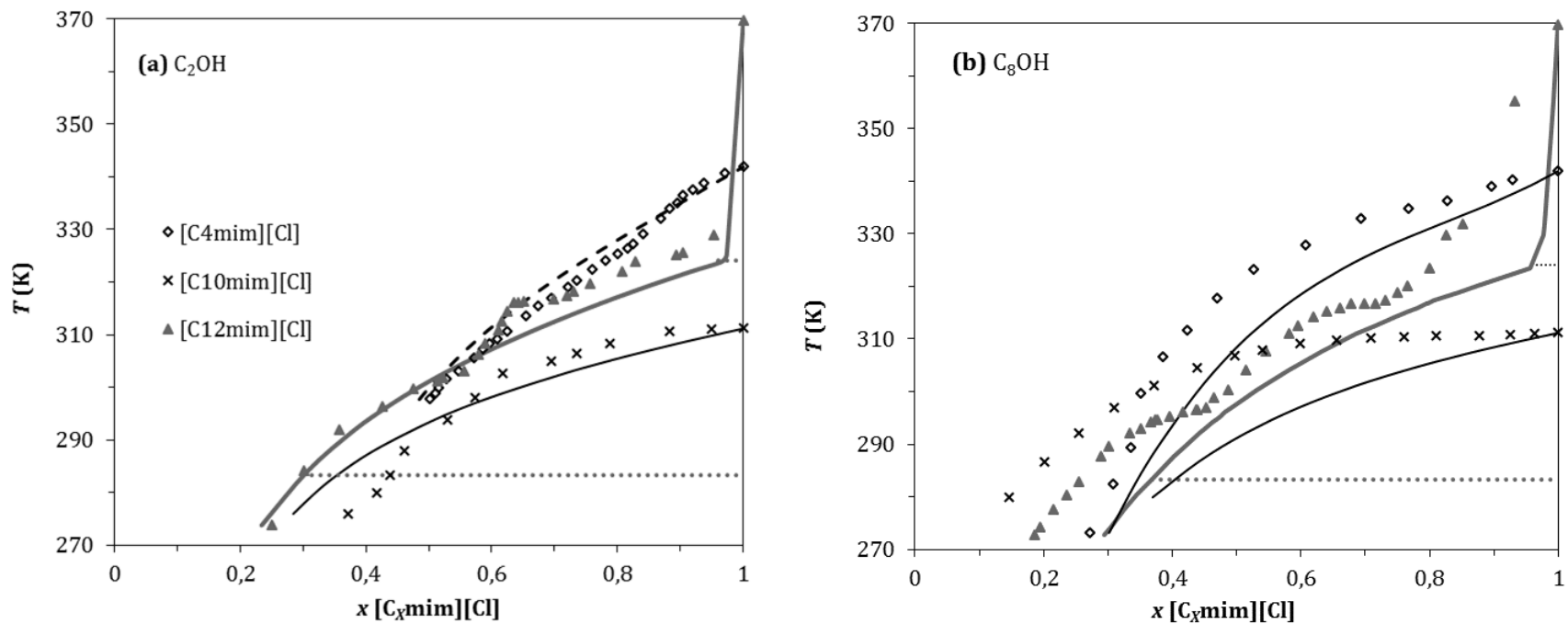


Fig. 8 Correlation (dashed line) and prediction (continuous lines) of the solubility of some the alkylmethylimidazolium chloride based ionic liquids in (a) ethanol and (b) 1-octanol. Symbols correspond to SLE experimental data of (\diamond) $[C_4mim][Cl]$, (\times) $[C_{10}mim][Cl]$ and (\blacktriangle) $[C_{12}mim][Cl]$ taken from Domańska et al. [20,58,60] at atmospheric pressure. The melting enthalpy used for $[C_4mim][Cl]$ has been taken from these authors. Dotted lines corresponds to the SSLE transition for systems $[C_{12}mim][Cl]$ + C_2OH and C_8OH , as reported by Domańska et al. [59]. Notice that the $[C_{12}mim][Cl]$ fugacity as a pure solid was calculated by means of Eq. (24).

4.3.3. Representation of the melting point depression of methylimidazolium based ILs with compressed CO₂

Phase equilibria of alkylimidazolium chloride based ILs + CO₂ is not plentiful. Up to our knowledge, only data of [C₄mim][Cl] at five temperatures have been reported by Jang et al [17], from which two of them were used in this work for correlation. Results of correlation and prediction of this data are shown in Table 11 and Fig. 9. From Fig. 9 it seems that the model represents well the solubility under 200 bar, but tends to deviate at higher pressures.

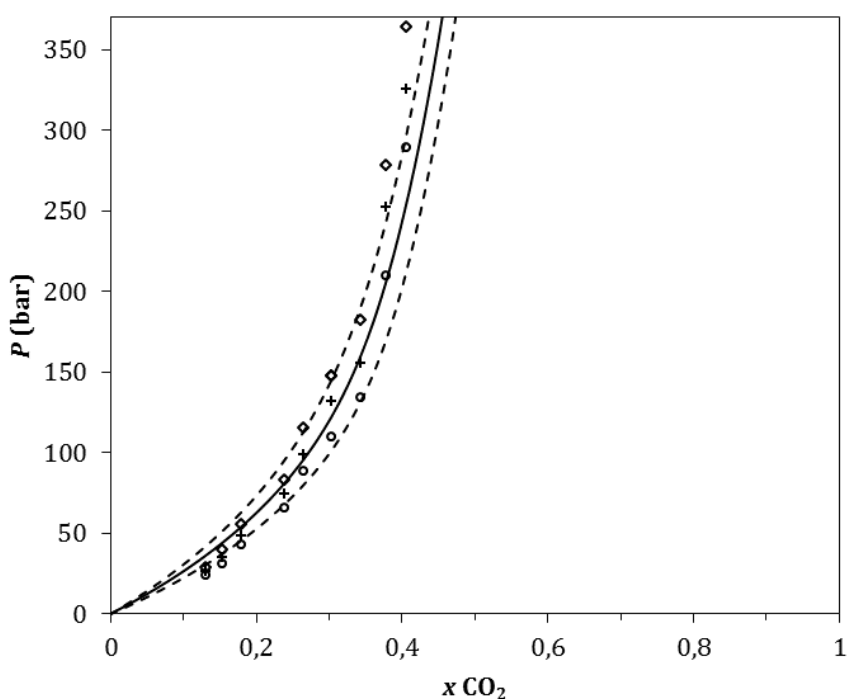


Fig. 9 Correlation (dashed lines) and prediction (solid line) of the CO₂ solubility in [C₄mim][Cl] at (○) 353 K, (+) 363 K and (◇) 373 K. Experimental data has been taken from the work of Jang et al. [17].

Table 12 Comparison between predicted and correlated melting points using Δv_{fus} calculated from Table 9 and correlated, respectively.

	C_1^a	Δv_{fus}^a (cm ³ /mol)	AAD (ARD%) in T_m (K)	Max. deviation in K (%)	Δv_{fus} correlated (cm ³ /mol)	AAD (ARD%) in T_m (K)	Max. deviation in K (%)
[C ₂ mim][Cl]	-11438	13.4	11 (3.3)	20 (6.1)	31	2.6 (0.8)	4.3 (1.3)
[Amim][Cl]	-7832	19.7	6.6 (2.1)	11 (3.8)	40	1.0 (0.3)	1.8 (0.5)
[C ₂ OHmim][Cl]	-11330	19.7	2.9 (0.8)	5.7 (1.7)	30	1.3 (0.4)	2.8 (0.8)
[C ₄ mim][Cl]	-8758	23.3	7.9 (2.4)	14 (4.4)	50	1.6 (0.3)	3.6 (1.1)
Total average			7.0 (2.1)	20 (6.1)		1.7 (0.5)	4.3 (1.3)

^a Calculated from values listed in Table 9. See text for details

Once all interaction parameters has been set, together to the pure compound melting parameters obtained in this work listed in Table 9, it is possible to predict the MPD of the methylimidazolium based ILs studied. It seems that the predictions obtained without correlation of Δv_{fus} systematically leads to higher MPDs than the experimentally observed. This is shown in Fig. 10 for the four ILs treated in this section, where the prediction is depicted with a solid line. There are two options to improve the prediction of this kind of data: include at least one binary data set of Table 7 together with the solubility information in the correlation, or use the approach of Rodríguez Reartes et al. [55] described in section 4.2. We have chosen the second approach, given the uncertainty in Δv_{fus} and the absence of the liquid composition values for the melting points. The results of the correlation of Δv_{fus} are also shown in Fig. 10 as dashed lines. Furthermore, Table 12 compares the predicted and correlated values of Δv_{fus} and deviations from experimental MPDs measured in this work with the predictions of the GC-EoS. After the correlation of the melting points, the average deviation diminishes from 7 K (2.1%) to ~2 K (0.5%), though the model seems to follow only a qualitative description. Notice that Fig. 10 also depicts the predicted pure melting line (thin dotted) computed with Eq. (23), which remains invariant after Δv_{fus} correlation.

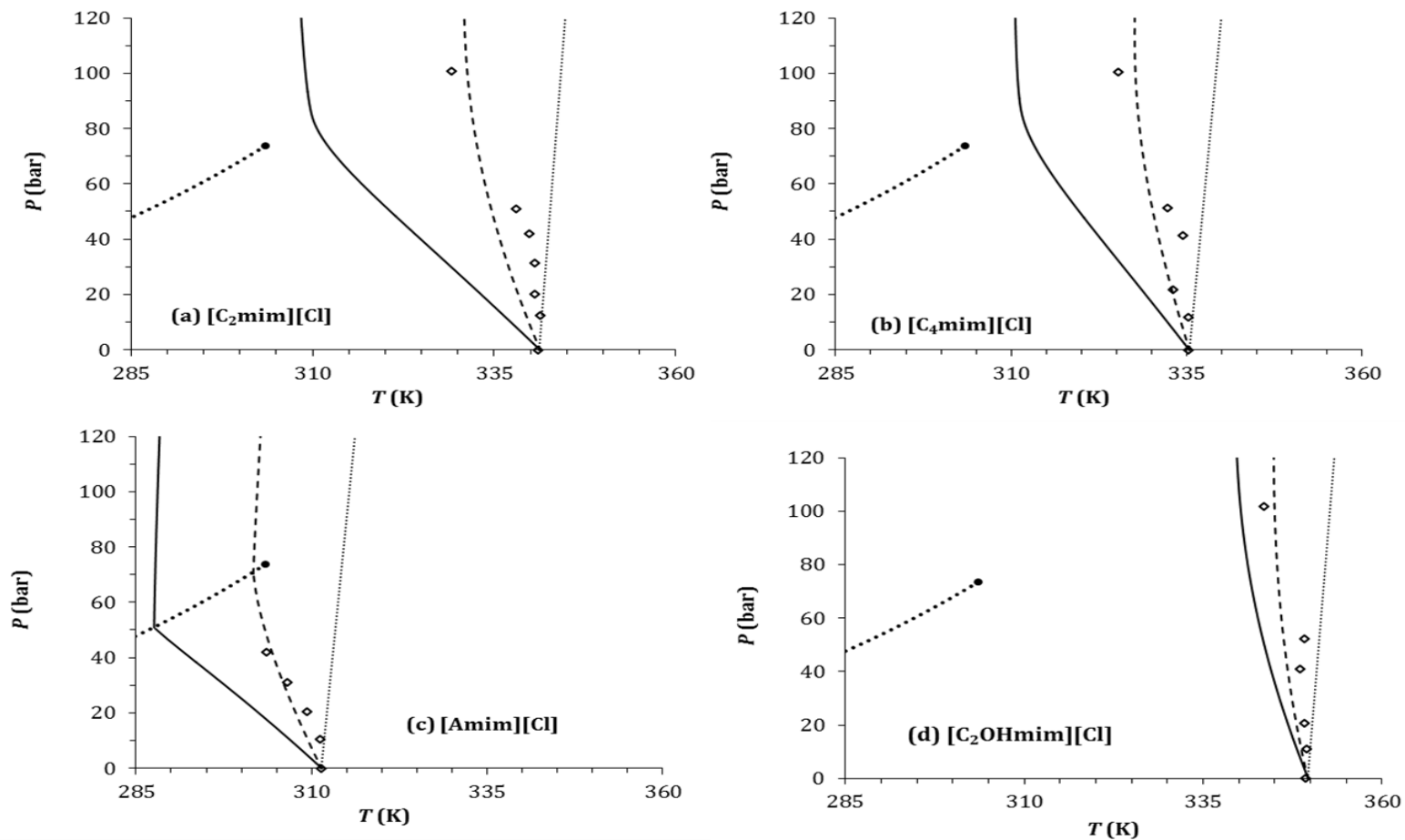


Fig. 10 Melting point depression of the imidazolium chloride based ILs treated in this work: (a) [C₂mim][Cl], (b) [C₄mim][Cl], (c) [Amim][Cl] and (d) [C₂OHmim][Cl]. Empty diamonds (◇) are experimental data presented in Table 7. Solid lines are model predictions using melting parameters defined in Table 9 from this work; the dashed lines are results of a melting point correlation using Δv_{fus} as adjustable parameter (see text for details), which are listed in Table 12. The thin dotted line represents the pure IL melting line, and the thick dotted and solid circle (●) correspond the pure CO₂ vapor pressure and critical point, respectively.

Fig. 11 compares the prediction of the solubility of CO₂ in other imidazolium chloride based ILs treated in this work evaluated at the melting temperature of each IL. The model predicts the larger solubility for CO₂ in [Amim][Cl], and at the same time, this is the system that shows the larger MPD (see Table 7 and Fig. 10). The opposite situation is found for [C₂OHmim]Cl, in which CO₂ is less soluble, and the melting point is less affected. [C₂mim][Cl] and [C₄mim]Cl are in an intermediate situation, being CO₂ more soluble in the last, though both binary systems present approximately the same MPD. Three reasons may be responsible for this behavior: the magnitude of the melting temperature of the IL (more temperature implies in general, less gas solubility), the slope of the pure melting line of the IL (which in this case, all are barely the same); and last, the CO₂ affinity with the substituent in the imidazolium ring.

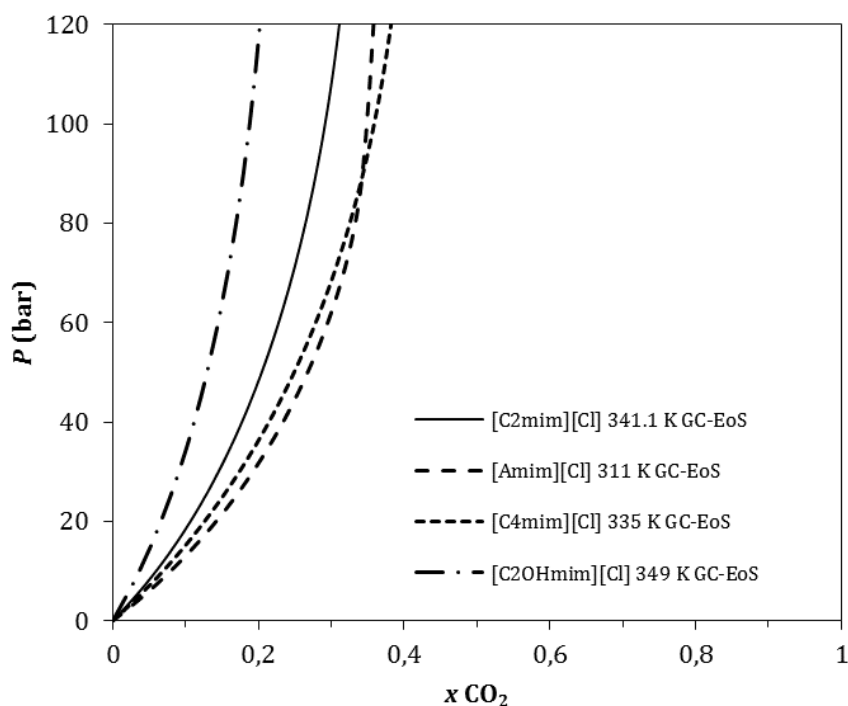


Fig. 11 Comparison of the predicted solubility of CO₂ in the alkylmethylimidazolium chloride based ILs used in this work at the vacuum melting point stated in Table 7. [C₂mim][Cl] (solid line), [Amim][Cl] (dashed line), [C₄mim][Cl] (dotted line) and [C₂OHmim][Cl] (dashed dotted line).

5. Conclusions

Carbon dioxide induced MPD in ILs has been experimentally determined in a high pressure cell at vacuum and at CO₂ pressures up to 100 bar using the first melting point method. The first melting points observed at vacuum were similar to the onset temperatures observed in DSC. Much higher MPDs were observed for ammonium based IL than for imidazolium based ones. Among the imidazolium based ones the highest MPD was observed for [Amim][Cl].

The GC-EoS was applied to model the experimental data of the imidazolium chloride ILs measured in this work. A new group, [-mim][Cl], exclusive for this family of compounds has been defined. Self and binary interaction parameters with groups CH₃/CH₂, CH=CH₂, ACH, ACC₃, CH₂OH and CO₂ were adjusted. After the correlation of experimental data the model is able to follow qualitatively the MPDs obtained in this work. Better results are achieved after the correlation of the change in the pure IL volume during melting, a procedure previously described by Rodríguez Reartes et al. [55]. The differences in the MPDs could be ascribed to by the affinity of CO₂ to the substituent in the imidazolium ring, and to the magnitude of the pure melting temperature of the IL.

List of symbols

A	Helmholtz free energy.
$AAD(Z)$	Average absolute deviation in variable Z : $\frac{1}{N} \sum_i^N Z_{exp\ i} - Z_{cal\ ci} $
$ARD(Z)\%$	Average relative deviation in variable Z : $\frac{1}{100} \sum_i^N \left 1 - \frac{Z_{cal\ ci}}{Z_{exp\ i}} \right $
DSC	Differential scanning calorimetry
d_i	Effective hard sphere diameter of component i .
f_i	Fugacity of pure i .
\hat{f}_i	Fugacity of i -th component of the mixture
g_j	Self-interaction parameter of group j .
H	Molar enthalpy
HC	Hydrocarbon
k_{ij}	GC-EoS binary interaction parameter between group i and j .
LLE	Liquid-liquid equilibria.
NC	Number of components in the mixture.
NG	Number of attractive groups in the mixture.
$NT(T)$	Number of solid-solid transitions at T .
NGam	Number of experimental activity coefficients at infinite dilution included in

	objective function.
NEq	Number of experimental mutual solubility included in objective function.
P	Pressure.
Q_i	Reduce van der Waals surface of component i .
q_j	Reduce van der Waals surface of group j .
R	Universal gas constant.
R_i	Reduce van der Waals volume of component i .
r_j	Reduce van der Waals volume of group j .
SLE	Solid-liquid equilibria.
SLLE	Solid-liquid-liquid equilibria.
SSLE	Solid-solid-liquid equilibria.
SLVE	Solid-liquid-vapor equilibria.
T	Temperature.
V	Total volume.
VLE	Vapor-liquid equilibria.
v	Molar volume.
w_i	Objective function weight parameter.
x_i	Molar composition in of component i .
Z	Dummy variable.
z	Coordination number.

Greek symbols

α_{ij}	Non-randomness parameter between groups i and j .
γ_∞	Activity coefficient at infinite dilution.
ΔZ	Change in the variable Z .
ν_{ij}	Number of groups j in compound i .
ρ	Mole density.

$\hat{\phi}_i$ Fugacity coefficient of compound i in the mixture.

Subscripts and superscripts

c Critical property.

fus Property of a pure compound at melting point.

m Property at melting point in a mixture.

L Liquid phase.

S Solid phase.

tr Solid-solid transition property.

V Vapor phase.

Acknowledgments

Authors thank the Marie Curie Program for the Project DoHip “Training program for the design of resource and energy efficient products for high pressure process”, the Junta de Castilla y León for funding through the project VA295U14 and and Competitiveness Ministry for funding through the project CTQ 2011 - 14825 - E (Program Explora). MDB and AM thank the Spanish Ministry of Economy and Competitiveness for the Ramón y Cajal research fellowships. FAS acknowledge the financial support granted by the Consejo Nacional de Investigaciones Científicas y Técnicas (CONICET) and the Agencia Nacional de Promoción Científica y Tecnológica (ANPCyT).

References

- 1 K.R. Seddon, Ionic liquids for clean technology, *Journal of Chemical Technology and Biotechnology*. 68 (1997) 351–356.
- 2 J.F. Brennecke, E.J. Maginn, Ionic liquids: Innovative fluids for chemical processing, *AIChE Journal*. 47 (2001) 2384–2389. doi:10.1002/aic.690471102.
- 3 R.P. Swatloski, S.K. Spear, J.D. Holbrey, R.D. Rogers, Dissolution of cellulose with ionic liquids, *Journal of the American Chemical Society*. 124 (2002) 4974–4975. doi:10.1021/ja025790m.
- 4 A. Pinkert, K.N. Marsh, S. Pang, M.P. Staiger, Ionic liquids and their interaction with cellulose, *Chemical Reviews* 109 (2009) 6712–6728. doi:10.1021/cr9001947.

- 5 S. Morales-delaRosa, J.M. Campos-Martin, J.L.G. Fierro, High glucose yields from the hydrolysis of cellulose dissolved in ionic liquids, *Chemical Engineering Journal*. 181-182 (2012) 538–541. doi:10.1016/j.cej.2011.11.061.
- 6 F.M. Gaciño, T. Regueira, L. Lugo, M.J.P. Comuñas, J. Fernández, Influence of Molecular Structure on Densities and Viscosities of Several Ionic Liquids, *Journal of Chemical & Engineering Data*. 56 (2011) 4984–4999. doi:10.1021/je200883w.
- 7 H. Olivier-Bourbigou, L. Magna, D. Morvan, Ionic liquids and catalysis: Recent progress from knowledge to applications, *Applied Catalysis A: General*. 373 (2010) 1–56. doi:10.1016/j.apcata.2009.10.008.
- 8 K. Fujita, D.R. MacFarlane, K. Noguchi, H. Ohno, Choline dihydrogen phosphate, *Acta Crystallographica Section E: Structure Reports Online*. 65 (2009) o709. doi:10.1107/S1600536809007259.
- 9 K.R. Seddon, A. Stark, M.-J. Torres, Influence of chloride, water, and organic solvents on the physical properties of ionic liquids, *Pure and Applied Chemistry*. 72 (2000) 2275–2287. doi:10.1351/pac200072122275.
- 10 L.A. Blanchard, D. Hancu, E.J. Beckman, J.F. Brennecke, scientific correspondence A stimulatory phalloid organ in a weaver bird Green processing using ionic liquids and CO₂, *Nature*. 399 (1999) 28–29. doi:10.1038/19887.
- 11 S. Raeissi, C.J. Peters, Carbon dioxide solubility in the homologous 1-alkyl-3-methylimidazolium bis(trifluoromethylsulfonyl)imide family, *Journal of Chemical & Engineering Data*. 54 (2009) 382–386. doi:10.1021/je800433r.
- 12 S.G. Kazarian, N. Sakellarios, C.M. Gordon, High-pressure CO₂-induced reduction of the melting temperature of ionic liquids, *Chemical Communications*. (2002) 1314–1315. doi:10.1039/b202759c.
- 13 A.M. Scurto, W. Leitner, Expanding the useful range of ionic liquids: melting point depression of organic salts with carbon dioxide for biphasic catalytic reactions., *Chemical Communications*. (2006) 3681–3683. doi:10.1039/b606130c.
- 14 A.M. Scurto, E. Newton, R.R. Weikel, L. Draucker, J. Hallett, C.L. Liotta, et al., Melting point depression of ionic liquids with CO₂: Phase equilibria, *Industrial & Engineering Chemistry Research*. 47 (2008) 493–501. doi:10.1021/ie070312b.
- 15 A. Serbanovic, Ž. Petrovski, M. Manic, C.S. Marques, L.C. Carrera, Gonçalo V.S.M. Branco, C.A.M. Afonso, et al., Melting behaviour of ionic salts in the presence of high pressure CO₂, *Fluid Phase Equilibria*. 294 (2010) 121–130. doi:10.1016/j.fluid.2010.03.015.

- 16 M.E. Zakrzewska, A.A. Rosatella, S.P. Simeonov, C.A.M. Afonso, V. Najdanovic-Visak, M. Nunes da Ponte, Solubility of carbon dioxide in ammonium based CO₂-induced ionic liquids, *Fluid Phase Equilibria*. 354 (2013) 19–23. doi:10.1016/j.fluid.2013.06.011.
- 17 S. Jang, D.-W. Cho, T. Im, H. Kim, High-pressure phase behavior of CO₂+1-butyl-3-methylimidazolium chloride system, *Fluid Phase Equilibria*. 299 (2010) 216–221. doi:10.1016/j.fluid.2010.09.039.
- 18 E. de Paz, Á. Martín, S. Rodríguez-Rojo, J. Herreras, M.J. Cocero, Determination of phase equilibrium (solid-liquid-gas) in poly-(ϵ -caprolactone)-carbon dioxide systems, *Journal of Chemical & Engineering Data*. 55 (2010) 2781–2785. doi:10.1021/jc900997t.
- 19 M.B. Alves, A.P. Umpierre, V.O. Santos, V.C.D. Soares, J. Dupont, J.C. Rubim, et al., The use of Differential Scanning Calorimetry (DSC) to characterize phase diagrams of ionic mixtures of 1-*n*-butyl-3-methylimidazolium chloride and niobium chloride or zinc chloride, *Thermochimica Acta*. 502 (2010) 20–23. doi:10.1016/j.tca.2010.01.023.
- 20 U. Domańska, E. Bogel-Łukasik, Solid–liquid equilibria for systems containing 1-butyl-3-methylimidazolium chloride, *Fluid Phase Equilibria*. 218 (2004) 123–129. doi:10.1016/j.fluid.2003.11.011.
- 21 U. Domańska, E. Bogel-Łukasik, R. Bogel-Łukasik, 1-Octanol/Water Partition Coefficients of 1-Alkyl-3-methylimidazolium Chloride, *Chemistry - A European Journal* 9 (2003) 3033–3041. doi:10.1002/chem.200204516.
- 22 W. Guan, J.-Z. Yang, L. Li, H. Wang, Q.-G. Zhang, Thermo-chemical properties of aqueous solution containing ionic liquids, *Fluid Phase Equilibria*. 239 (2006) 161–165. doi:10.1016/j.fluid.2005.11.015.
- 23 H.-C. Hu, A.N. Soriano, R.B. Leron, M.-H. Li, Molar heat capacity of four aqueous ionic liquid mixtures, *Thermochimica Acta*. 519 (2011) 44–49. doi:10.1016/j.tca.2011.02.027.
- 24 J.G. Huddleston, A.E. Visser, W.M. Reichert, H.D. Willauer, G.A. Broker, R.D. Rogers, Characterization and comparison of hydrophilic and hydrophobic room temperature ionic liquids incorporating the imidazolium cation, *Green Chemistry*. 3 (2001) 156–164. doi:10.1039/b103275p.
- 25 M. Kick, P. Keil, A. König, Solid–liquid phase diagram of the two Ionic Liquids EMIMCl and BMIMCl, *Fluid Phase Equilibria*. 338 (2013) 172–178. doi:10.1016/j.fluid.2012.11.007.
- 26 S.P. Verevkin, D.H. Zaitsau, V.N. Emel'Yanenko, R. V. Ralys, A. V. Yermalayeu, C. Schick, Does alkyl chain length really matter? Structure-property relationships in thermochemistry of ionic liquids, *Thermochimica Acta*. 562 (2013) 84–95. doi:10.1016/j.tca.2013.04.003.

- 27 Y. Wei, Q.G. Zhang, Y. Liu, X. Li, S. Lian, Z. Kang, Physicochemical property estimation of an ionic liquid based on glutamic acid-BMIGlu, *Journal of Chemical & Engineering Data*. 55 (2010) 2616–2619. doi:10.1021/jc900865y.
- 28 J.S. Wilkes, J.A. Levisky, R.A. Wilson, C.L. Hussey, Dialkylimidazolium chloroaluminate melts: a new class of room-temperature ionic liquids for electrochemistry, spectroscopy and synthesis, *Inorganic Chemistry*. 21 (1982) 1263–1264. doi:10.1021/ic00133a078.
- 29 Q.G. Zhang, F. Xue, J. Tong, W. Guan, B. Wang, Studies on volumetric properties of concentrated aqueous solutions of the ionic liquid BMIBF₄, *J. Solution Chem.* 35 (2006) 297–309. doi:10.1007/s10953-005-9004-y.
- 30 P. Keil, A. König, Enthalpies of solution of 1-ethyl-3-methyl-imidazolium chloride and aluminum chloride in molten chloroaluminate ionic liquids, *Thermochimica Acta*. 524 (2011) 202–204. doi:10.1016/j.tca.2011.07.006.
- 31 H.L. Ngo, K. LeCompte, L. Hargens, A.B. McEwen, Thermal properties of imidazolium ionic liquids, in: *Thermochimica Acta*, 2000: pp. 97–102. doi:10.1016/S0040-6031(00)00373-7.
- 32 J. Vila, B. Fernández-Castro, E. Rilo, J. Carrete, M. Domínguez-Pérez, J.R. Rodríguez, et al., Liquid-solid-liquid phase transition hysteresis loops in the ionic conductivity of ten imidazolium-based ionic liquids, *Fluid Phase Equilibria*. 320 (2012) 1–10. doi:10.1016/j.fluid.2012.02.006.
- 33 J.L. Solà Cervera, P. Keil, A. König, Determination of distribution coefficients in 1-ethyl-3-methyl imidazolium chloride-methylimidazole mixtures by zone melting, *Chemical Engineering & Technology* 33 (2010) 821–826. doi:10.1002/ceat.200900555.
- 34 C.I. Melo, A.I. Rodrigues, R. Bogel-Lukasik, E. Bogel-Lukasik, Outlook on the phase equilibria of the innovative system of “protected glycerol”: 1,4-dioxaspiro[4.5]decane-2-methanol and alternative solvents, *The Journal of Physical Chemistry A* 116 (2012) 1765–1773. doi:10.1021/jp2107796.
- 35 H. Zhang, J. Wu, J. Zhang, J. He, 1-allyl-3-methylimidazolium chloride room temperature ionic liquid: A new and powerful nonderivatizing solvent for cellulose, *Macromolecules*. 38 (2005) 8272–8277. doi:10.1021/ma0505676.
- 36 S.H. Yeon, K.S. Kim, S. Choi, H. Lee, H.S. Kim, H. Kim, Physical and electrochemical properties of 1-(2-hydroxyethyl)-3-methyl imidazolium and N-(2-hydroxyethyl)-N-methyl morpholinium ionic liquids, *Electrochimica Acta*. 50 (2005) 5399–5407. doi:10.1016/j.electacta.2005.03.020.
- 37 S. Skjold-Jørgensen, Group contribution equation of state (GC-EOS): A predictive method for phase equilibrium computations over wide ranges of temperature and pressures up to 30 MPa, *Industrial & Engineering Chemistry Research*. 27 (1988) 110–118.

- 38 G.A. Mansoori, N.F. Carnahan, K.E. Starling, T.W. Leland Jr., Equilibrium Thermodynamic Properties of the Mixture of Hard Spheres, *J. Chem. Phys.* 54 (1971) 1523–1525. doi:10.1063/1.1675048.
- 39 H. Renon, J.M. Prausnitz, Local compositions in thermodynamic excess functions for liquid mixtures, *AIChE Journal*. 14 (1968) 135–144. doi:10.1002/aic.690140124.
- 40 A. Fredenslund, R.L. Jones, J.M. Prausnitz, Group-contribution estimation of activity coefficients in nonideal liquid mixtures, *AIChE Journal*. 21 (1975) 1086–1099. doi:10.1002/aic.690210607.
- 41 D.S. Abrams, J.M. Prausnitz, Statistical thermodynamics of liquid mixtures: A new expression for the excess Gibbs energy of partly or completely miscible systems, *AIChE Journal*. 21 (1975) 116–128. doi:10.1002/aic.690210115.
- 42 B. Breure, S.B. Bottini, G. Witkamp, C.J. Peters, Thermodynamic Modeling of the Phase Behavior of Binary Systems of Ionic Liquids and Carbon Dioxide with the Group Contribution Equation of State, *The Journal of Physical Chemistry B*. 111 (2007) 14265–14270.
- 43 M.D. Bermejo, T.M. Fieback, Á. Martín, Solubility of gases in 1-alkyl-3-methylimidazolium alkyl sulfate ionic liquids: Experimental determination and modeling, *The Journal of Chemical Thermodynamics*. 58 (2013) 237–244. doi:10.1016/j.jct.2012.11.018.
- 44 S. Espinosa, T. Fornari, S.B. Bottini, E.A. Brignole, Phase equilibria in mixtures of fatty oils and derivatives with near critical fluids using the GC-EOS model, *The Journal of Supercritical Fluids*. 23 (2002) 91–102. doi:10.1016/S0896-8446(02)00025-6.
- 45 A. Bondi, van der Waals Volumes and Radii, *J. Phys. Chem.* 68 (1964) 441–451. doi:10.1021/j100785a001.
- 46 J.O. Valderrama, R.E. Rojas, Critical Properties of Ionic Liquids. Revisited, *Industrial & Engineering Chemistry Research*. 48 (2009) 6890–6900. doi:10.1021/ie900250g.
- 47 D. Wu, B. Wu, Y.M. Zhang, H.P. Wang, Density, Viscosity, Refractive Index and Conductivity of 1-Allyl-3-methylimidazolium Chloride + Water Mixture, *Journal of Chemical & Engineering Data*. 55 (2010) 621–624. doi:10.1021/je900545v.
- 48 S.A. Bolkan, J.T. Yoke, Room temperature fused salts based on copper(I) chloride-1-methyl-3-ethylimidazolium chloride mixtures. 1. Physical properties, *Journal of Chemical & Engineering Data*. 31 (1986) 194–197. doi:10.1021/je00044a019.
- 49 B.T. Goodman, W.V. Wilding, J.L. Oscarson, R.L. Rowley, A Note on the Relationship between Organic Solid Density and Liquid Density at the Triple Point, *Journal of Chemical & Engineering Data*. 49 (2004) 1512–1514. doi:10.1021/je034220e.
- 50 J. Pusch, J. Schmelzer, Extension of the Group-Contribution Equation of State Parameter Matrix for the Prediction of Phase Equilibria Containing Argon, Ammonia,

- Propene and Other Alkenes, *Berichte der Bunsengesellschaft für physikalische Chemie*. 97 (1993) 597–603.
- 51 T. Fornari, Revision and summary of the group contribution equation of state parameter table: Application to edible oil constituents, *Fluid Phase Equilibria*. 262 (2007) 187–209. doi:10.1016/j.fluid.2007.09.007.
- 52 W. David, T.M. Letcher, D. Ramjugernath, J. David Raal, Activity coefficients of hydrocarbon solutes at infinite dilution in the ionic liquid, 1-methyl-3-octyl-imidazolium chloride from gas–liquid chromatography, *The Journal of Chemical Thermodynamics*. 35 (2003) 1335–1341. doi:10.1016/S0021-9614(03)00091-0.
- 53 T.M. Letcher, N. Deenadayalu, Ternary liquid–liquid equilibria for mixtures of 1-methyl-3-octyl-imidazolium chloride+benzene+an alkane at $T = 298.2\text{K}$ and 1atm, *The Journal of Chemical Thermodynamics*. 35 (2003) 67–76. doi:10.1016/S0021-9614(02)00300-2.
- 54 A. Firoozabadi, *Thermodynamics of Hydrocarbon Reservoirs*, 1st ed., McGraw Hill, USA, 1999.
- 55 S.B. Rodriguez-Reartes, M. Cismondi Duarte, M.S. Zabaloy, Computation of solid–fluid–fluid equilibria for binary asymmetric mixtures in wide ranges of conditions, *The Journal of Supercritical Fluids*. 57 (2011) 9–24. doi:10.1016/j.supflu.2011.02.004.
- 56 M.L. Michelsen, The isothermal flash problem. Part I. Stability, *Fluid Phase Equilibria*. 9 (1982) 1–19. doi:10.1016/0378-3812(82)85001-2.
- 57 M.L. Michelsen, The isothermal flash problem. Part II. Phase-split calculation, *Fluid Phase Equilibria*. 9 (1982) 21–40. doi:10.1016/0378-3812(82)85002-4.
- 58 U. Domańska, E. Bogel-Łukasik, U. Doman, Measurements and Correlation of the (Solid + Liquid) Equilibria of [1-Decyl-3-methylimidazolium Chloride + Alcohols ($\text{C}_2 - \text{C}_{12}$)], *Industrial & Engineering Chemistry Research*. 42 (2003) 6986–6992. doi:10.1021/ie030464g.
- 59 U. Domańska, L. Mazurowska, Solubility of 1,3-dialkylimidazolium chloride or hexafluorophosphate or methylsulfonate in organic solvents: effect of the anions on solubility, *Fluid Phase Equilibria*. 221 (2004) 73–82. doi:10.1016/j.fluid.2004.03.006.
- 60 U. Domańska, E. Bogel-Łukasik, R. Bogel-Łukasik, Solubility of 1-Dodecyl-3-methylimidazolium Chloride in Alcohols ($\text{C}_2 - \text{C}_{12}$), *The Journal of Physical Chemistry B*. 107 (2003) 1858–1863. doi:10.1021/jp021332o.
- 61 H.P. Gros, S.B. Bottini, E.A. Brignole, A group contribution equation of state for associating mixtures, *Fluid Phase Equilibria*. 116 (1996) 537–544. doi:10.1016/0378-3812(95)02928-1.

Chapter 3. Experimental determination of viscosities and densities of mixtures carbon dioxide + 1-allyl-3-methylimidazolium chloride

Abstract

The effect of viscosity reduction caused by the solubilization of CO₂ is studied in order to improve the biomass processing in ionic liquids. To do so, densities and viscosities of the pure ionic liquid 1-allyl-3-methylimidazolium chloride and its mixtures with CO₂ up molar fractions of 0.25 and temperatures between 333 and 372 K have been experimentally determined. Viscosities were correlated as a function of temperature and CO₂ molar fractions with an average relative error of 2.5%. The viscosities of other mixtures CO₂ + ionic liquids were also correlated for other ionic liquids with an average relative error between 4.4 and 13%. In general these ionic liquids present a linear decrease of viscosity with CO₂ molar fractions up to around 0.5 that is more pronounced at lower temperatures and depends of each ionic liquid, and can reach between 60-100% viscosity reduction with respect the viscosity of the pure ionic liquid, making the CO₂ a promising co-solvent for viscosity reduction in process with ionic liquids.

1. Introduction

There is an increasing interest in the use of ionic liquids (ILs) for processing cellulose and other biopolymers [1]. However, the high viscosity of ILs, which is greatly increased when they dissolve cellulose, is the main limitation for their use in these processes [2]. Imidazolium chlorides, acetates and alkylphosphates can dissolve high amounts of cellulose and other biopolymers, but recently acetates and alkylphosphates has been preferred due to their lower viscosities and melting points [1], while the imidazolium chlorides present higher viscosities. For these reasons, these ILs are sometimes set aside in cellulose processing, even though they are cheaper and more effective than others in cellulose reactions such as hydrolysis [3].

It is known that mixing an IL with molecular solvents allows decreasing its viscosity [4]. This is also possible when using carbon dioxide (CO₂) as a co-solvent, which has the advantages of being non-toxic, cheap, and can be easily separated of the IL by depressurization. ILs and CO₂ are considered to be a promising media for the development of "green" technology [5]. In biphasic mixtures IL-CO₂ at moderate or high pressure, CO₂ can dissolve significantly into the IL-rich liquid phase, up to concentrations as high as 75% in mol, but no ionic liquid dissolves in the gas phase [5],[6]. Nevertheless in the case of imidazolium chloride ionic liquids CO₂ solubility is reduced to values round 30-40% in mol [7].

So far, only a few viscosity data of mixtures carbon dioxide + IL can be found in literature: Tomida and coworkers determined the viscosities of CO₂ + 1-butyl-3-methylimidazolium tetrafluoroborate ([Bmim][BF₄]) [8]; CO₂ + 1-butyl-3-methylimidazolium hexafluorophosphate ([Bmim][PF₆]) [9]; CO₂ + 1-hexyl-3-methylimidazolium hexafluorophosphate ([Hmim][PF₆]) and CO₂ + 1-octyl-3-methylimidazolium hexafluorophosphate ([Omim][PF₆]) + CO₂ [10]; Liu et al determined the viscosities of CO₂ + 1-butyl-3-methylimidazolium tetrafluoroborate ([Bmim][BF₄]) [11] and Ahosseini et al. [12] measured the viscosity of mixtures of several ionic liquids of the n-alkyl-3-methylimidazolium bis(trifluoromethylsulfonyl)imide family [-mimTf₂N] with CO₂. In general, the decrease in viscosity is between 85 and 45 % for BF₄ ILs with CO₂ solubilities between 45 and 35% CO₂ in mol [8]. For PF₆ ILs with 40-45% in mol CO₂ the decrease lies between 80 and 45% of the density of the pure IL [9,10]. For the Tf₂N ILs which present solubilities of CO₂ sometimes as high as 90% the decrease in viscosity can reach 100% [12] at moderate pressures of 10-12 MPa, but with molar fractions as low as 10% of CO₂ decrease of 30-40% of the pure IL viscosity is already observed. In all cases the effect in viscosity reduction with CO₂ is more remarkable at lower temperatures.

There are much more data of densities of mixtures CO₂ + ILs, including the systems: CO₂ + methylimidazolium hexafluorophosphates ionic liquids [9], [10]; CO₂ + 1-ethyl-3-methylimidazolium ethylsulphate [13]; CO₂ + imidazolium bis[(trifluoromethyl)sulfonyl]imide and triflate ILs [14]; CO₂ + 1-ethyl-3-methylimidazolium diethyl phosphate, CO₂ + 1-ethyl-3-methylimidazolium hydrogen sulfate [15], to mention only a few of them. In general densities present little change with increasing CO₂ concentration in the ionic liquid, meaning that these systems present considerable lower volume expansions than those of common organic solvents [13], [14], [16]. This has been interpreted as a consequence of the CO₂ is dissolving in the ionic

liquid by occupying the bulk free space in the molecule, as confirmed by atomistic simulation [17], [18] and through Raman spectroscopy [19]. As a consequence, large negative molecular volumes are found, due to the lack of expansion of the ionic liquids and the big difference in molecular mass between the ILs and the CO₂ [13].

In this work the viscosities and densities of pure 1-Allyl-3-methylimidazolium chloride ([Amim][Cl]) and several CO₂ + [Amim][Cl] mixtures were experimentally determined at temperatures between 333 and 372 K and pressures between 1 and 7 MPa, comprising CO₂ concentrations between 5 and 25% in mol. Using density data, excess molar volumes were calculated. Viscosity data were correlated and, in order to test the correlation, viscosity data of other CO₂ + ILs mixtures from literature were correlated showing average deviations from 2 to 13%.

2. Experimental Section

2.1. Materials

The ionic liquid used in this work was 1-allyl-3-methylimidazolium chloride, [Amim][Cl], purchased from Iolitec (Germany), with a purity higher than 98%. The water contents were determined by Karl-Fischer volumetric titration (Metrohm 870 KF Titrino Plus) obtaining 0.59% ww in water. Carbon dioxide (99.9% purity) was supplied by Yara and was used without further purification.

2.2 Apparatus

To determine the densities and viscosities a tuning fork vibration viscosimeter was used (Solartron Viscosimeter 7827). In the ranges of viscosities determined the precision was ± 1 mPa·s in the range 1-100 mPa·s and of ± 10 mPa·s in the range 100-1000 mPa·s. Density was determined with a precision of ± 1 kg·m⁻³. The viscosimeter worked inside of a 1.7 L pressure vessel able to stand 200°C and 20 MPa. Temperature in the gas phase was determined with a thermocouple type K and in the liquid phase (where the tuning fork was situated) with a Pt100. A signal converter Solartron 7946 able to work in the T range (-200-200°C) was used with a resolution of 0.1°C and a maximum error of ± 0.3 °C. Temperature was kept constant by using a circulating bath Lauda Proline P5. Pressure was determined with WIKA type S-11 pressure transmitter with an accuracy of 1 bar (0.25% of the span (0-400 bar)).

2.3 Experimental procedure

The ionic liquid was charged in the pressure vessel and kept at 90°C at vacuum in order to reduce the water content for 8 h. In these conditions the density and viscosities of the pure ionic liquids were determined. After that CO₂ was charged in the pressure vessel and the system was equilibrated before determining the viscosity and density. Then the temperature and pressure

were changed in order to determine new experimental points. After finishing all the measurements the water content was determined by Karl Fischer titration.

3. Results and Discussion

3.1 Density and viscosity of the pure ionic liquid

Densities and viscosities of the pure ionic liquid as a function of temperature are listed in Table 1. In Fig. 1 data were plotted together with literature data [20], [21], [22]. It is observed that both, density and viscosity decrease with increasing temperature and that the data determined in this work were consistent with literature data.

Table 1 Densities and viscosities of 1-allyl-3methylimidazolium chloride determined under vacuum

T/K	Viscosity/mPa·s	Density/kgm ⁻³
307.0	790	1141
311.7	530	1138
319.9	280	1133
330.0	150	1127
337.1	100	1123
347.3	61	1118
361.1	35	1110
373.2	24	

Viscosity precision ± 1 mPa·s in the range 1-100 mPa·s and ± 10 mPa·s in the range 100-1000 mPa·s. Density was determined with a precision of ± 1 kg·m⁻³. Temperature maximum error of $\pm 0.3^\circ\text{C}$. Water molar fraction of AmimCl ($x_{\text{H}_2\text{O}}=0.497$)

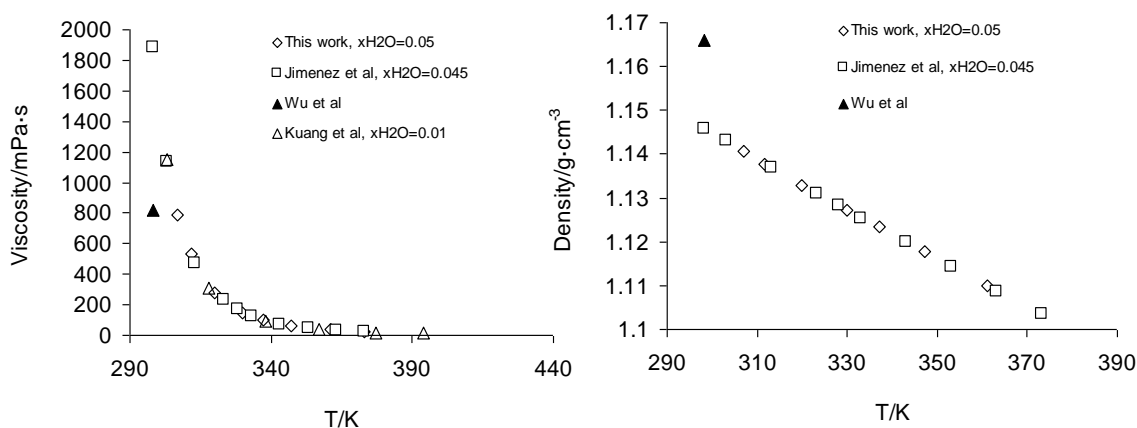


Fig. 1 Comparison of viscosity and density measurement of pure 1-allyl-3-methylimidazolium chloride measured in this work and literature data [20], [21], [22]

3.2 Density and viscosity of the mixtures CO₂ + AmimCl

Experimental densities and viscosities and calculated molar values of the mixtures CO₂ + AmimCl were listed in Table 2. The CO₂ molar fractions were calculated with Group Contribution Equation of State developed by Skold-Jorgensen (GC-EoS) using the parameters fitted in a previous work for mixtures of CO₂ + AmimCl [23]. Densities of CO₂ at the given temperature and pressure were calculated from NIST data [24].

Table 2 Densities and viscosities of saturated mixtures CO₂ + 1-allyl-3-methylimidazolium chloride at different pressures and temperatures

T/K	P/MPa	x_{CO_2}	Viscosity/mPa·s	Density/kg·m ⁻³	$V^{\text{Ex}}/\text{cm}^3 \text{mol}^{-1}$
334.7	1.0	0.054	100	1125	-143
356.6	1.0	0.039	39	1113	-111
371.5	1.0	0.032	24	1104	-95.8
368.9	4.0	0.113	24	1106	-74.0
345.3	4.0	0.148	53	1119	-87.9
368.7	5.8	0.152	22	1106	-61.8
337.3	5.0	0.194	72	1124	-80.8
349.3	4.3	0.150	44	1106	-80.7
333.6	7.2	0.251	68	1126	-58.7

Viscosity precision ± 1 mPa·s in the range 1-100 mPa·s and ± 10 mPa·s in the range 100-1000 mPa·s. Density was determined with a precision of ± 1 kg·m⁻³. Temperature maximum error of $\pm 0.3^\circ\text{C}$. Water molar fraction of AmimCl ($x_{\text{H}_2\text{O}}=0.497$). Pressure was determined with an accuracy of ± 0.1 MPa. CO₂ molar fractions calculated using GC-EoS.

It is observed that excess molar volumes present highly negative values, two orders of magnitude more negative than in the case of water + AmimCl mixtures 20]. This negative molar volumes are consistent with observed by other authors 13] in different ionic liquids indicate that the CO₂ + AmimCl mixtures present a highly packed structure, as the mixture has a molar volume much lower than this expected for an ideal mixture. This can confirm the theory that CO₂ is dissolved in the free spaces of ionic liquids and that the expansion of the ionic liquid induced by the presence of CO₂ is very small 13],17], 18],19].

3.3 Correlation of viscosity data

Viscosity data were correlated with an equation derived from the one used by Seddon et al. [5], and that was used by Jimenez et al for correlating viscosity data of aqueous mixtures with several imidazolium chloride mixtures 20]. Even when the initial water content of the IL was low, it can strongly affect viscosity, thus, this concentration was taken into account when making the parameterization, introducing a correction of the molar concentration of both CO₂ and water, as shown in eq. 1.

$$\mu / mPa \cdot s = \exp\left(\frac{E}{(T/K)^2} + \frac{A}{T/K} + B\right) \cdot \exp\left(\frac{x_{H_2O}}{C + D \cdot T/K}\right) \cdot \exp\left(\frac{x_{CO_2}}{F + G \cdot T/K}\right) \quad (1)$$

Where μ is the viscosity in mPa·s, T is temperature in K, x_{H_2O} and x_{CO_2} are water and CO₂ molar fraction are expressed with relation to the ionic liquid, respectively in CO₂ and water free basis. A, B, C, D, E, F, G are empirically obtained parameters. The parameters used for the pure IL (A, B and E) and for the influence of water concentration (C and D) are the same used by Jimenez et al 20], and the parameters E and F adjusted to correct viscosity with CO₂ concentration were adjusted in this work. Parameterization was performed by minimizing the average relative deviation (ARD %) defined as shown in eq. 2.

$$ARD\% = \sum \left(\frac{|\mu_{exp} - \mu_{calc}|}{\mu_{exp}} \right) \quad (2)$$

Adjusted parameters are shown in Table 3. The ARD% of the equation is of 2.5% while the maximum deviation with respect to experimental data is 5.7%.

Table 3 Parameters fitted to the correlations for calculating the viscosities mixtures CO₂ + H₂O+ 1-allyl-3-methylimidazolium chloride at different . Deviations referred to viscosity.

$$\mu / mPa \cdot s = \exp\left(\frac{E}{(T/K)^2} + \frac{A}{T/K} + B\right) \cdot \exp\left(\frac{x_{H_2O}}{C + D \cdot T/K}\right) \cdot \exp\left(\frac{x_{CO_2}}{F + G \cdot T/K}\right)$$

A	-15113	Jimenez et al [20]
B	17.64	Jimenez et al [20]
C	0.784	Jimenez et al [20]
D	-3.10·10 ⁻³	Jimenez et al [20]
E	3636000	Jimenez et al [20]
F	3.731 ± 0.015	This work
G	-1.255·10 ⁻²	This work
ARD%	2.5%	
Max. Dev.	5.7%	

The predicted viscosities of several CO₂+AmimCl mixture with low water concentration and water free predicted by the correlation are plotted in Fig. 2 as a function of pressure and of CO₂ molar fraction. Please note that the molar fractions in the ionic liquid corresponding to a given P,T data were calculated with the GC-EoS [23]. It is observed that CO₂ can reduce the viscosity of the AmimCl up to 43% at 60°C and 7.5 MPa and molar fractions of 0.25 of CO₂ with respect to the ionic liquid. At higher temperatures the effect of CO₂ in viscosity is lower i.e. at 95°C, the pressure necessary to have a molar fraction of 0.25 in the ionic liquid is of 13 MPa, and the viscosity is reduced only a 25% with respect the viscosity of the pure ionic liquid.

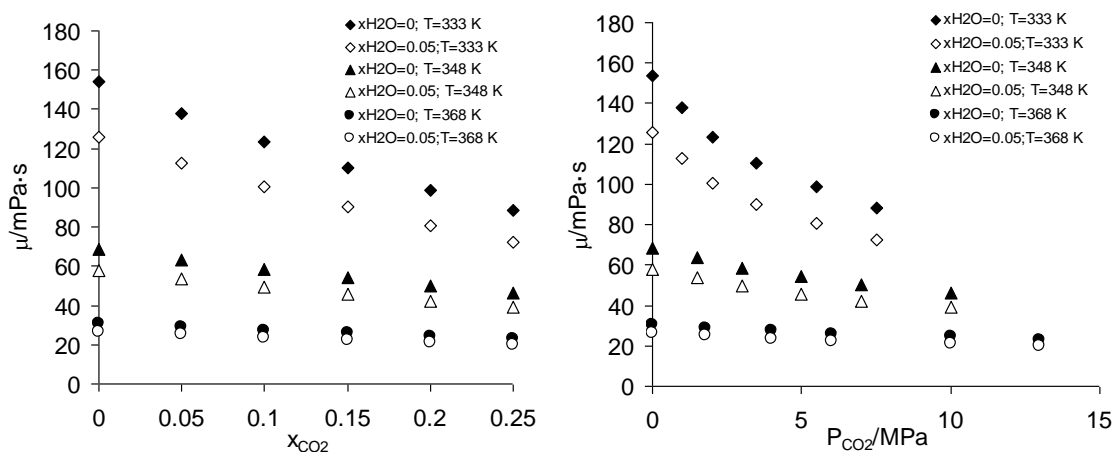


Fig. 2. Viscosity predicted by the correlation as a function of CO₂ molar fraction and CO₂ pressure for different temperatures and initial water concentrations of the ionic liquid AmimCl

To test the validity of this correlation with other CO₂ + IL mixtures, literature viscosity data were correlated for several CO₂ + ionic liquids mixtures using literature data: 1-butyl-3-methylimidazolium tetrafluoroborate (bmimBF₄) [8]; 1-butyl-3-methylimidazolium hexafluorophosphate (bmimPF₆) [9]; 1-hexyl-3-methylimidazolium hexafluorophosphate (hmimPF₆) [10], [25], [26]; 1-octyl-3-methylimidazolium hexafluorophosphate (omimPF₆) [10], [26], [27]; 1-ethyl-3-methylimidazolium trifluoromethylsulfonylimide (emimTf₂N) [12], [28]; 1-hexyl-3-methylimidazolium trifluoromethylsulfonylimide (hmimTf₂N) [12], [29] and 1-decyl-3-methylimidazolium trifluoromethylsulfonylimide (dmimTf₂N) [12], [30]. Parameters adjusted, ARDs and maximum deviations from experimental data are presented in Table 4. Viscosities can be predicted with average deviations from 4 to 13% and maximum deviations from 15 to 46%.

Table 4. Parameters fitted to the correlations for calculating the viscosities mixtures CO₂ + IL for the ILs: bmimBF₄ [8]; bmimPF₆ [9]; hmimPF₆ [10],[25], [26] ; omimPF₆ [10], [26], [27]; emimTf₂N [12], [28]; hmimTf₂N [12], [29] and dmimTf₂N [12], [30]

$$\mu / mPa \cdot s = \exp\left(\frac{E}{(T/K)^2} + \frac{A}{T/K} + B\right) \cdot \exp\left(\frac{x_{CO_2}}{F + G \cdot T/K}\right)$$

Parameters	bmimBF ₄	bmimPF ₆	hmimPF ₆	omimPF ₆	emimTf ₂ N	hmimTf ₂ N	dmimTf ₂ N
A	-4260	-4690	-6950	-6320	-3980	-2300	-4700
B	4.03	4.59	7.62	6.39	4.68	1.44	4.90
E	1330950	1508250	1945200	1902000	1079740	936800	1390300
F	1.17	0.698	0.7337	0.621	1.632	0.968	1.006
G	-4.74·10 ⁻³	-3.02·10 ⁻³	-3.20·10 ⁻³	-3.02·10 ⁻³	-6.65·10 ⁻³	-4.30·10 ⁻³	-4.26·10 ⁻³
ARD %	4.6%	4.5%	4.4%	8.3%	6.4%	13%	6.2%
Max Dev	16%	15%	26%	29%	27%	46%	35%
Ref.	[8]	[9]	[10],[25], [26]	[10],[26],[27]	[12], [28]	[12], [29]	[12], [30]

In Fig. 3 predicted viscosity of mixtures CO₂ + IL are compared to experimental data is shown. A good reproducibility of the experimental data is observed.

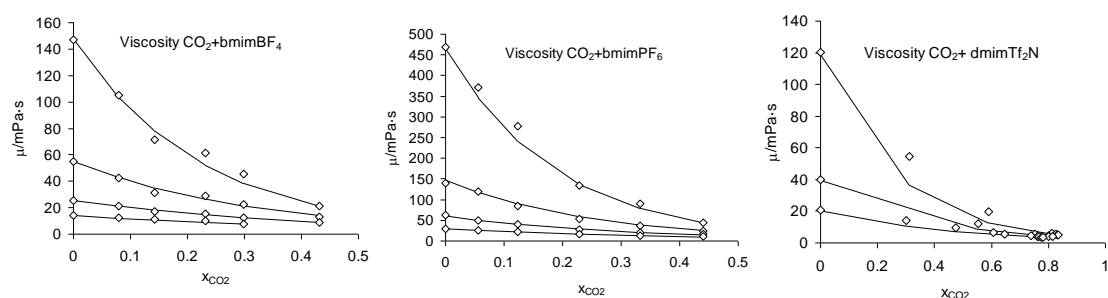


Fig. 3. Comparison of the viscosity predicted by the model and the experimental data for the mixtures CO₂ +IL: bmimBF₄ [8]; ; bmimPF₆ [9]; and dmimTf₂N [12], [30]. Symbols represent the experimental data and lines represent the predictions of the model.

In Fig. 4 the percentage of viscosity reduction vs molar fraction of CO₂ with respect to the viscosity of the pure IL at the same temperature is plotted for some ionic liquids of the different families considered in this work, at 333 and at 293 K. It is observed that viscosity reduced linearly with CO₂ molar fraction until reached a certain concentration of CO₂ beyond which the reduction of CO₂ is lower. The viscosity reduction can reach between 60-90% depending on the ionic liquid and it is more pronounced at lower temperatures.

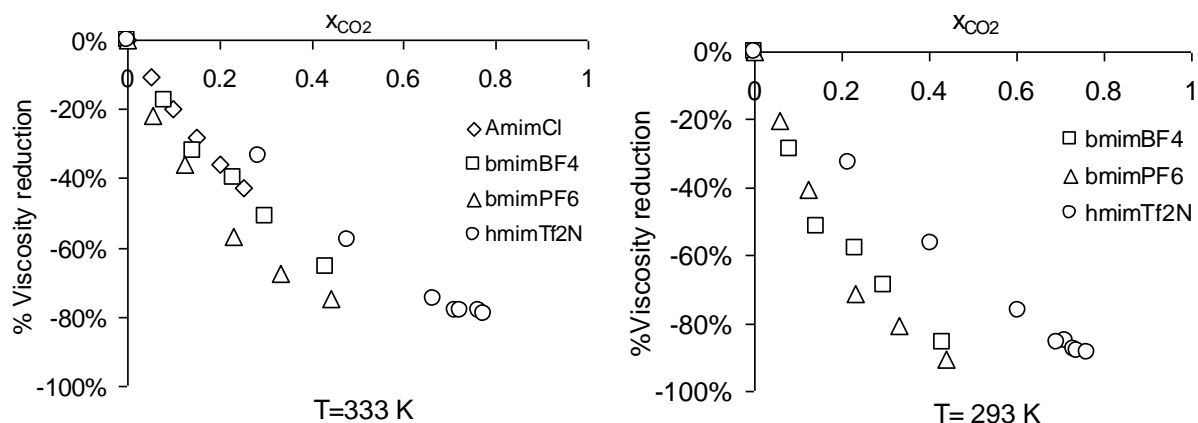


Fig. 4. Percentage of viscosity reduction with CO₂ molar fraction for the ionic liquids bmimBF₄ [9], bmimPF₆ [10], hmimTf₂N [12] and AmimCl at 333 and 293 K.

4. Conclusions

The viscosities and densities of the pure ionic liquids 1-allyl-3-methylimidazolium chloride (AmimCl) have been experimentally determined as well as for mixtures CO₂ + AmimCl with molar fractions up to 0.25 and temperatures in the range 333-372 K.

Densities were used to calculate excess molar values that resulted strongly negative with values -60 and -140 cm³/mol, being less negative at higher temperatures and CO₂ molar fractions. This indicates that the CO₂ + AmimCl mixtures present a highly packed structure and can confirm the generally accepted theory that CO₂ is dissolved in the free spaces of ionic liquids and that the expansion of the ionic liquid induced by the presence of CO₂ is very small.

Viscosities were correlated as a function of temperature and carbon dioxide molar fractions with an average relative error of 2.5%. The viscosities of other mixtures CO₂ + ionic liquids were also correlated for ionic liquids of the families imidazolium tetrafluoroborate, imidazolium hexafluorophosphate and imidazolium trifluoromethylsulfonylimide with an average error between 4.4 and 13%.

In general [Amim][Cl] and the other ionic liquids present a linear decrease of viscosity with CO₂ molar fractions up to around 0.5 mol that more pronounced at lower temperatures and depends of each ionic liquid, and can reach between 60-100% viscosity reduction with respect the viscosity of the pure ionic liquid, making the CO₂ a promising co-solvent for viscosity reduction in process with ionic liquids.

Acknowledgments

Authors thank the Marie Curie Program for the Project DoHip “Training program for the design of resource and energy efficient products for high pressure process”, the Junta de Castilla y León for funding through the project VA295U14 . MDB and AM thank the Spanish Ministry of Economy and Competitiveness for the Ramón y Cajal research fellowships.

References

- 1 A. Pinkert, K.N. Marsh, S. Pang, M.P. Staiger, Ionic liquids and their interaction with cellulose, *Chemical Reviews* 109 (2009) 6712–6728. doi:10.1021/cr9001947.
- 2 H. Cruz, M. Faselow, J.D. Holbrey, K.R. Seddon KR, Determining relative rates of cellulose dissolution in ionic liquids through in situ viscosity measurement, *Chemical Communications* 48 (2012) 5620–5622. doi:10.1039/C2CC31487H
- 3 S. Morales de la Rosa, J.M. Campos-Martin, J.L.G. Fierro, High glucose yields from the hydrolysis of cellulose dissolved in ionic liquids, *Chemical Engineering J.* 181-182 (2012) 538–541. doi:10.1016/j.cej.2011.11.061.
- 4 K.R. Seddon, A. Stark, M.J. Torres, Influence of chloride, water, and organic solvents on the physical properties of ionic liquids, *Pure and Applied Chemistry* 72 (2000) 2275–2287. doi:10.1351/pac200072122275.
- 5 L.A. Blanchard, D. Hancu, E.J. Beckman, J.F. Brennecke, Green processing using ionic liquids and CO₂, *Nature*. 399 (1999) 28–29. doi:10.1038/19887.
- 6 S. Raeissi, C.J. Peters, Carbon dioxide solubility in the homologous 1-alkyl-3-methylimidazolium bis(trifluoromethylsulfonyl)imide family, *J. of Chemical & Engineering Data* 54 (2009) 382–386. doi:10.1021/jc800433r.
- 7 S. Jang, D. W. Cho, T. Im, H. Kim, High-pressure phase behavior of CO₂+1-butyl-3-methylimidazolium chloride system, *Fluid Phase Equilibria* 299 (2010) 216–221. doi:10.1016/j.fluid.2010.09.039.
- 8 D. Tomida, A. Kumagai, K. Qiao, C. Yokoyama, Viscosity of 1-butyl-3-methylimidazolium tetrafluoroborate + CO₂ mixture, *High Temp. (Engl. Transl.)* 37 (2008) 81-89.

- 9 D. Tomida, A. Kumagai, K. Qiao, C. Yokoyama, C. , Viscosity of 1-Butyl-3-methylimidazolium Hexafluorophosphate + CO₂ Mixture J. Chem. Eng. Data 52 (2007) 1638-1640.
- 10 D. Tomida, S. Kenmochi, K. Qiao, Q. Bao, C. Yokoyama, C. Viscosity of ionic liquid mixtures of 1-alkyl-3-methylimidazolium hexafluorophosphate + CO₂, Fluid Phase Equilibria 307(2011) 185-189
- 11 Z. Liu, W. Wu, B. Han, Z. Dong, G. Zhao, J. Wang, T. Jiang, G. Yang, (2003) Study on the Phase Behaviors, Viscosities, and Thermodynamic Properties of CO₂/[C₄mim][PF₆]/methanol system at Elevated Pressures, Chemistry -A European J. 9 (2003) 3897-3903.
- 12 A. Aghosseini, E. Ortega, B. Sensenich, A.M. Scurto, Viscosity of n-alkyl-3-methylimidazolium bis(trifluoromethylsulfonyl)amide ionic liquids saturated with compressed CO₂, Fluid Phase Equilib. 286 (2009) 72 -78
- 13 P.J. Carvalho, T. Regueira, J. Fernandez, L. Lugo, J. Safarov, E. Hassel, J.A.P. Coutinho, High pressure density and solubility for the CO₂+ 1-ethyl-3-methylimidazolium ethylsulfate system J. Supercritical Fluids 88 (2014) 46-55.
- 14 S. N. V. K. Aki, B.R. Mellein, E. Saurer, J.F. Brennecke, High-Pressure Phase Behavior of Carbon Dioxide with Imidazolium-Based Ionic Liquids J. Physical Chemistry B 108 (2004) 20355-20365
- 15 I. Mejia, K. Stanley, R. Canales, J. Brennecke, On the High-Pressure Solubilities of Carbon Dioxide in Several Ionic Liquids, J. Chem. Eng. Data 58 (2013), 2642-2653
- 16 D. Kodama, M. Kanakubo , M. Kokuboa, T. Onoa, H. Kawanamib, T. Yokoyama, H. Nanjo, M. Kato, CO₂ absorption properties of Brønsted acid–base ionic liquid composed of N,N-dimethylformamide and bis(trifluoromethanesulfonyl)amide, J. Supercritical Fluids, 52 (2010) 189–192
- 17 W. Shi, E.J. Maginn, Atomistic simulation of the absorption of carbon dioxide and water in the ionic liquid 1-n-hexyl-3-methylimidazolium bis(trifluoromethylsulfonyl)imide ([hmim][Tf₂N]), J. Physical Chemistry B 112 (2008) 2045–2055.
- 18 X. Huang, C.J. Margulis, Y. Li, B.J. Berne, Why is the partial molar volume of CO₂ so small when dissolved in a room temperature ionic liquid? Structure and dynamics of CO₂ dissolved in [Bmim⁺][PF₆⁻], J. American Chemical Society 127 (2005) 17842–17851
- 19 M.I. Cabac , M. Besnard, Y. Danten, J.A.P. Coutinho, Solubility of CO₂ in 1-butyl-3-methyl-imidazolium-trifluoro acetate ionic liquid studied by Raman spectroscopy and DFT investigations, J. Physical Chemistry B 115 (2011) 3538–3550. 20 C. Jiménez de la Parra, J. R. Zambrano, M. D. Bermejo, Á. Martín, J. J. Segovia, M. J. Cocero, Influence of water concentration in the viscosities and densities of cellulose dissolving ionic liquids. J Chemical Thermodynamics 91 (2015) 8-16

- 21 Q. Kuang, J. Zhang, Z. Wang, Revealing Long-Range Density Fluctuations in Dialkylimidazolium Chloride Ionic Liquids by Dynamic Light Scattering, *J. Physical Chemistry B* 111(2007) 9858-9863
- 22 D. Wu, B. Wu, Y. M. Zhang, H. P. Wang, Density, Viscosity, Refractive Index and Conductivity of 1-Allyl-3-methylimidazolium Chloride + Water Mixture, *J. Chemical Engineering Data*, 55 (2010) 621–624
- 23 J. M. Lopes, F. A. Sánchez, S. B. Rodríguez Reartes, M. D. Bermejo, Á. Martín, M. J. Cocero, Melting point depression effect with CO₂ in high melting temperature cellulose dissolving ionic liquids. Modeling with group contribution equation of state, *J. Supercritical Fluids* (In Press) 2015
- 24 <http://webbook.nist.gov/chemistry/> (last accessed 9th October 2015)
- 25 K.R. Harris, M. Kanakubo, L. A. Woolf, Temperature and Pressure Dependence of the Viscosity of the Ionic Liquids 1-Hexyl-3-methylimidazolium Hexafluorophosphate and 1-Butyl-3-methylimidazolium Bis(trifluoromethylsulfonyl)imide, *J. Chemical Engineering Data* 52 (2007) 1080-1085
- 26 D. Tomida, A. Kumagai, S. Kenmochi, K. Qiao, C. Yokoyama, Viscosity of 1-Hexyl-3-methylimidazolium Hexafluorophosphate and 1-Octyl-3-methylimidazolium Hexafluorophosphate at High Pressure *J. Chemical Engineering Data* 52 (2007) 577-579
- 27 K.R. Harris, M. Kanakubo, L.A. Woolf, Temperature and Pressure Dependence of the Viscosity of the Ionic Liquids 1-Methyl-3-octylimidazolium Hexafluorophosphate and 1-Methyl-3-octylimidazolium Tetrafluoroborate, *J. Chemical Engineering Data* 51 (2006) 1161-1167
- 28 C. Schreiner, S. Zugmann, R. Hartl, H.J. Gores, Fractional Walden Rule for Ionic Liquids: Examples from Recent Measurements and a Critique of the So-Called Ideal KCl Line for the Walden Plot, *J. Chemical Engineering Data* 55 (2010) 1784-1788
- 29 M.E. Kandil, K.N. Marsh, A.R.H. Goodwin, Measurement of the Viscosity, Density, and Electrical Conductivity of 1-Hexyl-3-methylimidazolium Bis(trifluorosulfonyl)imide at Temperatures between (288 and 433) K and Pressures below 50 MPa, *J. Chemical Engineering Data* 52 (2007) 2382-2387
- 30 M. Tariq, P. Carvalho, J.A.P. Coutinho, I.M. Marrucho, J.N.C. Lopes, L.P.N. Rebelo, Viscosity of (C2-C14) 1-alkyl-3-methylimidazolium bis(trifluoromethylsulfonyl)amide ionic liquids in an extended temperature range, *Fluid Phase Equilibria* 301 (2011) 22-3

Part III. Influence of CO₂ as reaction media in dissolution and acetylation of cellulose

Chapter 4. Analysis of the synthesis of cellulose acetate in ionic liquids. Experimental study, modeling and use of additives and co-solvents

Abstract

The capacity of the ionic liquids of dissolving high concentrations of cellulose and at relatively low temperatures makes them promising solvents for the so called biorefinery process, especially production of esters of cellulose. In this work, the well known process of cellulose acetate synthesis in alkylimidazolium chloride ionic liquids is analyzed. In the first place, it is investigated if the presence of CO₂ is able to increase the rate of cellulose dissolution in different ionic liquids. Secondly, a reaction kinetic model able to describe the reaction is proposed and kinetics parameters are adjusted. New experiments of cellulose acetylation are performed using as a solvent the ionic liquid [Amim][Cl], at temperatures of 80, 60 and 40°C (lower temperature than those used in literature with alkylimidazolium ionic liquids) and these data are used to extend the model to lower temperatures. In addition, the effect of scandium III triflate as a catalyst was investigated resulting in very low increasing of the degree of substitution. The use of CO₂ as a co-solvent was investigated in order to decrease the viscosity of the reaction media. Nevertheless, analysis suggests that carbon dioxide can be unexpectedly incorporating to the polymer structure.

1. Introduction

Cellulose esters are applied in a wide range of products including: coatings for food and pharmaceutical products, plastics, composite materials, optical films, membranes and others [1]. The most prominent example of a commercial cellulose ester is cellulose acetate (CA). The fibres have been used in the textile industry due to its softness and the ability to manufacture breathable fabrics. Other applications include: lacquers, plastics, coatings, membranes, cigarette filters and LCD screens [2]. The raw material of this compound is cellulose. Cellulose is the most abundant natural polymer and is considered a renewable resource. The structure is based on the monomer cellobiose which consists of two glucose molecules linked via β -1,4-O-glycosidic. Cellulose processing has attracted increasing attention because of the consumption and over-exploitation of non-renewable resources, such as coal and oil. Wood pulp is the most important raw material source for cellulose processing. Most of it is used for the production of paper after partial removal of the non-cellulosic constituents from its original fibre form [3]. The conventional process of CA production is performed in two stages. In the first one the cellulose is activated with acetic or sulphuric acid. Then, the acetylation takes place with a mixture containing acetic anhydride, acetic acid and sulfuric acid. Thus, it is obtained cellulose acetate or triacetate which is submitted to a treatment that depends on the desired degree of substitution [4].

The research of cellulose processing in ionic liquids (ILs) has been increasing over the last years. ILs are substances composed exclusively by ions, which can be fluid at room temperature. This is due to the asymmetry between the cation and the anion, which prevents the formation of a solid network. ILs unique properties lead to their application in a variety of fields. ILs have low vapour pressure which makes them to be considered “green” solvents because they do not evaporate like the organic solvents. Furthermore, they present high thermal stability, non-flammability, wide electrochemical window, high solvation ability to dissolve various organic and inorganic substances and wide liquid range which provides a great kinetic control of reactions [5]. In 2002 Swatoski et al. found that alkylimidazolium-based ILs could dissolve up to 25% of cellulose and increase the rate applying microwaves [6]. The dissolution mechanism implies the formation of hydrogen bonds between the IL and the hydroxyl groups of the cellulose. Consequently, the cellulose solubility decreases in ILs with solvent addition to the mixture [7].

One of the applications with special interest is the functionalization of dissolved cellulose. ILs are able to dissolve cellulose without decomposing it. The process of biopolymers modification in ILs was patented in 2007 [8] including cellulose modification and cellulose esters with sulfate or sulfonate groups. Other authors have functionalized cellulose producing different cellulose derivatives: cellulose acetate synthesized in 1-ethyl-3-methylimidazolium cation, [Emim]⁺ and chloride anion, Cl⁻ [9] and in 1-allyl-3-methylimidazolium chloride, ([Amim][Cl]) without catalyst [10], cellulose succinate and phthalate [11, 12] at temperatures between 60 and 120°C, residence times between 30 minutes and 12 h and higher degree of substitution with increasing excess of reagents and residence times. The application of microwaves can reduce the

dissolution time from several hours to 10 min and complete functionalization of cellulose can be reduced from residence times of 24 h to 8 h [13].

There are an extensive number of data published of synthesis cellulose acetate by different authors and different alkylimidazolium chloride ionic liquids, and significantly different results are obtained as shown in Table 1. From the complete conversion obtained residence times of 2 h obtained by Heinze and co-workers in ionic liquids such as [Emim][Cl] or [Bmim][Cl] [14] at 80°C to the necessary residence time of 5, 8 or even 24 h of other authors [15-17] alkyl imidazolium ILs containing the allyl group.

Table 1 Experimental data of cellulose acetylation in different ionic liquids from the literature

Ionic liquid	Biomass, w/w ^a	Reagent ^b	Molar ratio ^c	t(h)	T(°C)	Heating ^d	DS ^e	Ref.
ABimCl	MCC, 5 %	Ac ₂ O	3	24	80	Conv	2	[18]
ABimCl	MCC, 5 %	Ac ₂ O	3	24	80	Conv	2	[18]
ABimCl	MCC, 5 %	Ac ₂ O	4.5	8	80	Conv	2.2	[18]
ABimCl	MCC, 5 %	Ac ₂ O	4.5	24	80	Conv	2.9	[18]
ABimCl	MCC, 5 %	Ac ₂ O	2.7	24	80	Conv	1.7	[18]
ABimCl	MCC, 5 %	Ac ₂ O	3	24	80	Conv	2	[18]
ABimCl	MCC, 5 %	Ac ₂ O	3.6	24	80	Conv	2.4	[18]
ABimCl	MCC, 5 %	Ac ₂ O	3	2	60	MW	1.5	[13]
ABimCl	MCC, 5 %	Ac ₂ O	3	3	60	MW	1.6	[13]
ABimCl	MCC, 5 %	Ac ₂ O	3	2	60	MW	1.7	[13]
ABimCl	MCC, 5 %	Ac ₂ O	4.5	5	80	MW	2.5	[13]
ABimCl	MCC, 5 %	Ac ₂ O	4.5	8	80	MW	2.8	[13]
ABimCl	MCC, 5 %	Ac ₂ O	2.4	8	80	MW	1.5	[13]
ABimCl	MCC, 5 %	Ac ₂ O	3	8	80	MW	2	[13]
ABimCl	MCC, 5 %	Ac ₂ O	3.6	8	80	MW	2.3	[13]
ABimCl	MCC, 5 %	Ac ₂ O	4.5	8	80	MW	2.2	[13]
AmimCl	Cornhusk cellulose, 4 %	Ac ₂ O	5	1	100	Conv	2.16	[10]
AmimCl	Cornhusk	Ac ₂ O	5	2	100	Conv	2.24	[10]

	cellulose, 4 %								
AmimCl	Cornhusk cellulose, 4 %	Ac ₂ O	5	3	100	Conv	2.46	[10]	
AmimCl	Cornhusk cellulose, 4 %	Ac ₂ O	5	4	100	Conv	2.49	[10]	
AmimCl	Cornhusk cellulose, 4 %	Ac ₂ O	5	5	100	Conv	2.51	[10]	
AmimCl	Cornhusk cellulose, 4 %	Ac ₂ O	5	6	100	Conv	2.55	[10]	
AmimCl	Cornhusk cellulose, 4 %	Ac ₂ O	5	7	100	Conv	2.58	[10]	
AmimCl	Cornhusk cellulose, 4 %	Ac ₂ O	5	8	100	Conv	2.63	[10]	
AmimCl	Pulp, 4 %	Ac ₂ O	5	0.25	80	Conv., N ₂	0.94	[19]	
AmimCl	Pulp, 4 %	Ac ₂ O	5	0.5	80	Conv., N ₂	1.39	[19]	
AmimCl	Pulp, 4 %	Ac ₂ O	5	1	80	Conv., N ₂	1.61	[19]	
AmimCl	Pulp, 4 %	Ac ₂ O	5	2	80	Conv., N ₂	1.80	[19]	
AmimCl	Pulp, 4 %	Ac ₂ O	5	3	80	Conv., N ₂	1.86	[19]	
AmimCl	Pulp, 4 %	Ac ₂ O	5	4	80	Conv., N ₂	2.21	[19]	
AmimCl	Pulp, 4 %	Ac ₂ O	5	8	80	Conv., N ₂	2.49	[19]	
AmimCl	Pulp, 4 %	Ac ₂ O	5	23	80	Conv., N ₂	2.74	[19]	
AmimCl	Pulp, 4 %	Ac ₂ O	4	4	80	Conv., N ₂	2.15	[19]	
AmimCl	Pulp, 4 %	Ac ₂ O	6.5	4	80	Conv., N ₂	2.43	[19]	
AmimCl	Pulp, 4 %	Ac ₂ O	8	4	80	Conv., N ₂	2.38	[19]	
AmimCl	Pulp, 4 %	Ac ₂ O	3	3	100	Conv., N ₂	1.99	[19]	
AmimCl	Pulp, 4 %	Ac ₂ O	4	3	100	Conv., N ₂	2.09	[19]	
AmimCl	Pulp, 4 %	Ac ₂ O	5	3	100	Conv., N ₂	2.30	[19]	
AmimCl	Wood pulp, 8 – 12 %	Ac ₂ O	5	0.5	110	Conv	2.0±0.1	[20]	
AmimCl	Wood pulp, 8 – 12 %	Ac ₂ O	5	1	110	Conv	2.3±0.1	[20]	

AmimCl	Wood pulp, 8 – 12 %	Ac ₂ O	5	2	110	Conv	2.5±0.1	[20]
AmimCl	Wood pulp, 8 – 12 %	Ac ₂ O	5	3	110	Conv	2.7±0.1	[20]
AmimCl	Wood pulp, 8 – 12 %	Ac ₂ O	5	5	110	Conv	2.9±0.1	[20]
AmimCl	Wood pulp, 8 – 12 %	Ac ₂ O	5	3	50	Conv	1.2±0.1	[20]
AmimCl	Wood pulp, 8 – 12 %	Ac ₂ O	5	3	70	Conv	2.1±0.1	[20]
AmimCl	Wood pulp, 8 – 12 %	Ac ₂ O	5	3	90	Conv	2.4±0.1	[20]
AmimCl	Wood pulp, 8 – 12 %	Ac ₂ O	5	3	110	Conv	2.7±0.1	[20]
AmimCl	Wood pulp, 8 – 12 %	Ac ₂ O	5	3	130	Conv	2.9±0.1	[20]
AmimCl	Wood pulp, 8 – 12 %	Ac ₂ O	1	3	110	Conv	0.5±0.1	[20]
AmimCl	Wood pulp, 8 – 12 %	Ac ₂ O	2	3	110	Conv	1.5±0.1	[20]
AmimCl	Wood pulp, 8 – 12 %	Ac ₂ O	3	3	110	Conv	2.4±0.1	[20]
AmimCl	Wood pulp, 8 – 12 %	Ac ₂ O	5	3	110	Conv	2.7±0.1	[20]
AmimCl	Wood pulp, 8 – 12 %	Ac ₂ O	7	3	110	Conv	2.9±0.1	[20]
BmimCl	Avicel, 10 %	Ac ₂ O	5	2	80	Conv	2.72	[16]
BmimCl	Avicel, 10 %	Ac ₂ O	3	2	80	Conv	2.56	[16]
BmimCl	Avicel, 10 %	Ac ₂ O	5	2	80	Conv	2.94	[16]
BmimCl	Avicel, 10 %	Ac ₂ O	10	2	80	Conv	3	[16]
BmimCl	Avicel, 10 %	AcCl	5	2	80	Conv	2.93	[16]
BmimCl	Avicel, 10 %	AcCl	3	2	80	Conv	2.81	[16]
BmimCl	Avicel, 10 %	AcCl	5	2	80	Conv	3	[16]

BmimCl	Avicel, 10 %	AcCl	10	2	80	Conv	3	[16]
BmimCl	Avicel, 10 %	AcCl	5	0.25	80	Conv	2.93	[16]
BmimCl	Avicel, 10 %	AcCl	5	0.5	80	Conv	3	[16]
BmimCl	Avicel, 10 %	AcCl	3	2	80	Conv	3	[16]
BmimCl	Sulfite spruce pulp, 10 %	AcCl	5	2	80	Conv	3	[16]
BmimCl	Sulfite spruce pulp, 10 %	AcCl	3	2	80	Conv	2.85	[16]
BmimCl	Cotton, 10 %	AcCl	5	2	80	Conv	3	[16]
BmimCl	Eucalyptus pulp, 12.2 %	Ac ₂ O	0.25	2	75	Conv	0.06	[21]
BmimCl	Eucalyptus pulp, 12.5 %	Ac ₂ O	1	2	75	Conv	0.5	[21]
BmimCl	Eucalyptus pulp, 13 %	Ac ₂ O	1.6	2	75	Conv	1	[21]
BmimCl	Eucalyptus pulp, 13.5 %	Ac ₂ O	2	2	75	Conv	1.2	[21]
BmimCl	Eucalyptus pulp, 13.5 %	Ac ₂ O	3	2	75	Conv	1.4	[21]
BmimCl	Eucalyptus pulp, 14.4 %	Ac ₂ O	5	2	75	Conv	2.38	[21]
BmimCl	Avicel, 10 %	Ac ₂ O	3	2	80	Conv	1.87	[15]
BmimCl	Avicel, 10 %	Ac ₂ O	5	2	80	Conv	2.72	[15]
BmimCl	Avicel, 10 %	Ac ₂ O	3 ^c	2	80	Conv	2.56	[15]
BmimCl	Avicel, 10 %	Ac ₂ O	5 ^c	2	80	Conv	2.94	[15]
BmimCl	Avicel, 10 %	Ac ₂ O	10 ^c	2	80	Conv	3	[15]
BmimCl	Avicel, 10 %	AcCl	5 ^c	2	80	Conv	2.93	[15]
BmimCl	Avicel, 10 %	AcCl	3	2	80	Conv	2.81	[15]
BmimCl	Avicel, 10 %	AcCl	5	0.25	80	Conv	2.93	[15]
BmimCl	Avicel, 10 %	AcCl	5	0.5	80	Conv	3	[15]
BmimCl	Avicel, 10 %	AcCl	5	2	80	Conv	3	[15]

EmimCl	Avicel, 10 %	Ac ₂ O	3	2	80	Conv	3	[15]
BdmimCl	Avicel, 10 %	Ac ₂ O	3	2	80	Conv	2.92	[15]
AdmimBr	Avicel, 10 %	Ac ₂ O	3	2	80	Conv	2.67	[15]

^a Concentration of cellulose in ionic liquid in percentage of weight

^b Ac₂O = acetic anhydride; AcCl = acetyl chloride

^c mol of reagent per mol of anhydroglucose unit (AGU)

^d Heating methods: conv (conventional heating) and MW (microwaves heating)

^e Additionally, 2.5 mol of pyridine per mol of AGU

In general it is observed that the substitution is increased with residence time and it is improved at higher temperatures and with acylation reagent excess. Acylation agents as acetic anhydride or acetyl chloride are tested, obtaining somewhat better results with the last one. Pyridine was used as additive obtaining only slightly better results compared to those with other additives [16].

It is known that some authors has used scandium III triflate as catalyst in acetylation reagents of starch [22] in IL media, but to the best of our knowledge it has not been tested in the acylation of cellulose in ILs so far.

One of the major factors limiting the speed reaction of homogeneous acetylation of cellulose is the high viscosity of the cellulose solution, which hinders de diffusion of reagents [13]. In the case of ILs this is a great challenge due to the high viscosity at their pure state and non-Newtonian behaviour when mixed with cellulose. Increase the reaction temperature above 80°C and increase the stirring is common to overcome the viscosity problem.

Supercritical CO₂ is considered to be a sustainable solvent because is not flammable, is cheap, is available and is not toxic. Additionally, the gas properties can be tuned adjusting the pressure and temperature. There are many advantages when ILs are combined with CO₂ [23]. The viscosity of ILs decrease when these are mixed with molecular solvents [24]. This also happens when ILs are mixed with supercritical CO₂ [25], which is also able to decrease the melting point [26]. The CO₂ is quite soluble in ILs and the solubility can be controlled adjusting the pressure.

The objective of this chapter is analyzing the synthesis of cellulose acetate in ILs. To do so literature data are thoroughly analyzed. A mathematical model was developed and kinetics parameters are adjusted. Following, additional reactions were performed at lower temperature than those studied in literature in the IL [Amim][Cl] and the influence of additive of scandium III triflate and CO₂ was investigated. The influence of the water content is also analyzed.

2. Material and methods

2.1. Materials

The cellulose used was microcrystalline cellulose from Alfa Aesar with a degree of polymerization < 350 and a particle size of <1% + 60 mesh (250 μm) and <30% +200 mesh (75 μm). The cellulose was dried at 60°C in a vacuum oven for 3-6 h prior to use. The ionic liquids were purchased from Iolitec (Germany) and the respective names, abbreviation, purity and water content are presented in Table 2. Two different lots of [Amim][Cl] have been used. K00219.1.2 was used in dissolution and reactions experiments and M00363.1 only for reaction experiments. The water content of [Amim][Cl] was reduced from 0.247 wt% till 0.06 wt% by application of vacuum at 90°C with stirring for 3 days and determined by Karl-Fischer coulometric titration (Mettler Toledo C20 coulometric KF titrator). Acetic anhydride, Ac_2O ($\geq 99\%$ purity) and scandium III triflate, $\text{sc}(\text{OTf})_3$ (99% purity) were purchased from Sigma Aldrich. Carbon dioxide (99.55% purity) was supplied by Carbueros Metalicos (Spain) and was used without purification. All samples were prepared under N_2 inside a glove box to prevent water absorption.

Table 2 Ionic liquids used in this work

Lot./Product No.	Ionic liquid	Abbreviation	Purity (%)	water (wt%)
K00219.1.2	1-allyl-3-methylimidazolium chloride	[Amim][Cl]	>98	0.519
M00363.1	1-allyl-3-methylimidazolium chloride	[Amim][Cl]	>98	0.247
K00715.3.1	1-butyl-3-methylimidazolium chloride	[Bmim][Cl]	>99	0.353
J00420.4	1-ethyl-3-methylimidazolium acetate	[Emim][Ac]	>95	0.385
K00120.1	1-ethyl-3-methylimidazolium dimethylphosphate	[Emim][DMP]	98	0.004

2.2. Acetylation reactions

The apparatus includes a stainless steel 40 ml cylindrical high pressure cell with a threaded closing. The maximum operating temperature is 200°C and pressure is 150 bar. The internal temperature of the cell was controlled by a PID temperature controller (Desin Instruments BS-2100) acting over two electrical jackets. The temperature was measured with a K type thermocouple with accuracy of 1°C. The pressure was measured with a membrane relative pressure meter (Gems Sensors & Controls), range 0 – 160 bar.

2.2.1. Dissolution of microcrystalline cellulose in [Amim][Cl]

The cellulose was dispersed into [Amim][Cl] in a N₂ glove box to avoid moisture absorption. The mixture was heated at 80°C for 4h under mechanical stirring (600 rpm). A clear yellow viscous cellulose solution was obtained.

2.2.2. Acetylation of microcrystalline cellulose in acetic anhydride

After dissolution step the mixture cellulose/[Amim][Cl] was cooled down to room temperature. Acetic anhydride and/or scandium III triflate was added under N₂ to the solution. The solution was stirred at desired temperature and time. Then the cellulose acetate solution was precipitated by adding approximately 5-fold IL-cellulose volume of ultrapure water (MilliQ-Millipore System) or isopropanol (Cofarcas, S. A. 99% purity). The resulting suspension was vigorously stirred for 15 min. The precipitate was recovered by filtration through a glass fibre prefilter (Merck Millipore Ltd.), while the liquid fraction was collected and stored for further analysis and IL recovery. The solid was washed 3 times with anti-solvent at room temperature, and oven dried overnight at 105°C.

2.3. Characterization

The FTIR spectra of cellulose, ionic liquid and cellulose esters were recorded on a Fourier Transform infrared instrument (Bruker Platinum-ATR) equipped with software of OPUS Optik GmbH in the range from 400 to 4400 cm⁻¹ of wavelength. The FTIR spectra were used to determine the degree of substitution (DS) of the samples. The cellulose acetylation conversion in [Amim][Cl] was calculated by integration of the area under the curve around peak 1750 cm⁻¹ in the solid sample, dissolved cellulose and in the cellulose acetate dissolved and regenerated. The FTIR spectra were used to determine the degree of substitution (DS) of the samples where the integration of the areas with respect to the absorbance (Fig. 1) values of the C=O stretching (1750 cm⁻¹), is related to the DS of commercial cellulose acetate (39.7% wt acetyl (DS=2.46), provided by Sigma Aldrich) (Fig. 1), as described in eq.1:

$$DS = 3 \times X = \frac{A_{\text{sample}} - A_{\text{cellulose}}}{A_{\text{CA}} - A_{\text{cellulose}}} \times \frac{2.46}{3} \quad (1)$$

Where DS is the degree of substitution, X is the conversion, A_{sample}, A_{cellulose} and A_{CA} are the areas under the curve around peak (1750 cm⁻¹) for the solid sample, the cellulose and the commercial cellulose acetate.

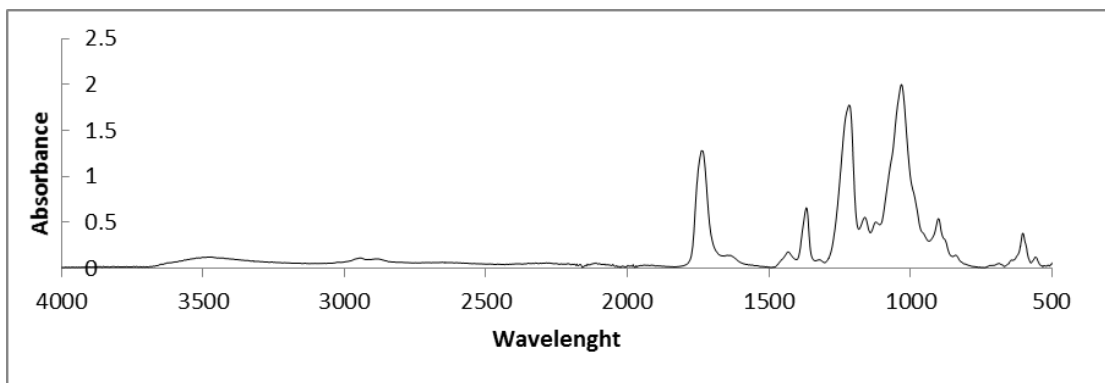


Fig. 1 FTIR of cellulose acetate used as standard in cellulose esters infrared characterization

^1H NMR spectra were recorded with 500 Agilent technologies.500 MHz spectrometer. The determination of acetyl content of cellulose acetate was carried out as follows: The ester was dissolved in DMSO-d_6 (17 mg mL^{-1}); the ^1H NMR spectrum was recorded at 80°C . The quantification was based on the calculation of areas of the methyl proton signals ($1.8 - 2.2 \text{ ppm}$) of the acetyl groups and those of the anhydroglucose units (AGU) ($3.3 - 5.8 \text{ ppm}$) as described in [27]. Each acetyl group has three protons and each AGU has seven protons excluding the OH-protons (Fig. 2).

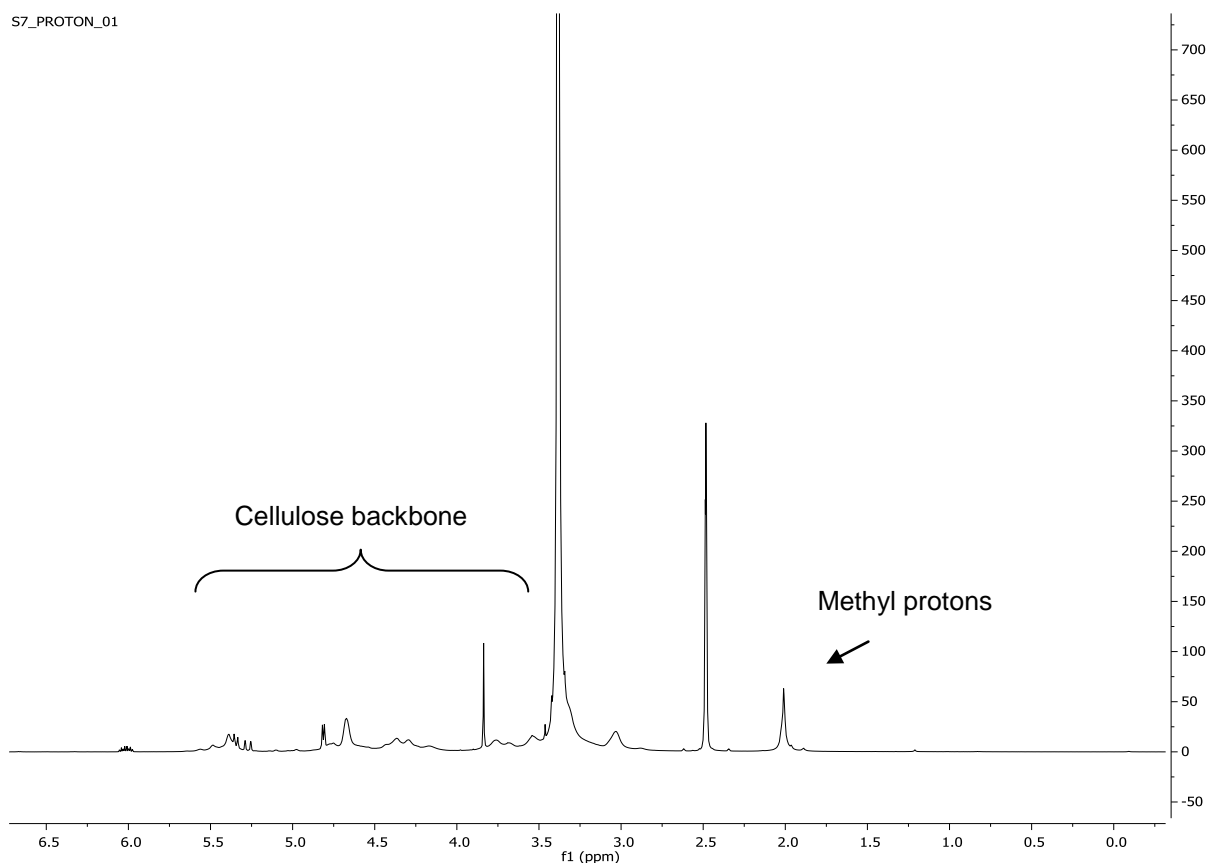


Fig. 2 NMR spectra of cellulose acetylated at 40C for 24h

The degree of substitution determined by ^1H NMR and FTIR is compared in Table 3 for different conditions of reaction. The values of DS determined by ^1H NMR are slightly lower and calculated as follows in equation (2).

$$DS = \frac{7 \times \text{methyl_protons}}{3 \times \text{AGU_protons}} \quad (2)$$

Table 3 Comparison of degree of substitution determined by H^1 NMR and FTIR

mol reagent/molAGU	t (h)	T ($^{\circ}\text{C}$)	DS (NMR)	DS (FTIR)
10	1	80	2.22	2.4
5	6	60	1.98	2.0
5	24	40	1.16	1.4

2.4. Dissolution of cellulose in [Amim][Cl] with low pressure of CO_2

In a typical experiment, the IL is weighted before the cellulose, which is placed on top of the ionic liquid, without stirring in a 15 ml vial. The mixture containing 5 wt% of cellulose in ionic liquid is placed into a 70 ml stainless steel high pressure cell and the air inside is extracted with a vacuum pump to avoid water in the sample. The measurements were performed at temperatures of 50°C and 80°C with stirring. After the vessel reached the set temperature, CO_2 was pressurized by continuous bubbling at 7 bar in processing times of 30 minutes. Control measurements were also done in absence of CO_2 . The remained undissolved cellulose was washed in water to remove ionic liquid, dried at 60°C in vacuum for 12 h and weighted. This method presented some difficulties regarding the separation of cellulose from the ILs particularly from [Bmim][Cl] due to its high viscosity. Each measurement was repeated at least five times due to the high dispersion of the data which led to a few high standard errors. The dissolved cellulose was precipitated with water Milli-Q and analyzed with FTIR.

3 Reaction modeling

A kinetic model of the acetylation reaction of cellulose in the IL [Amim][Cl] is developed using acetic anhydride as acetylation agent is proposed. Each AGU conforming the cellulose has three -OH groups that can be substituted by an acetyl group. These -OH groups are situated in the carbon 2, 3 and 6 of cellulose. Experimental results obtained by NMR analysis show that acetylation is produced faster in the Carbon 6 of the AGU, followed by C3 and the acetylation in C2 is taking a much longer time. Due to the characteristics of the NMR techniques the degree of acetylation of each Carbon cannot be accurately determined, but a qualitative result obtained by [19] is showed in Table 4.

Table 4 Degree of substitution of carbon 6, 3 and 2 and the total from [19]

DS				
C6	C3	C2	DS total	t (h)
0	0	0	0	0
0,7	0,15	0	0,85	1
0,9	0,55	0,3	1,75	1,75
1	1	0,8	2,8	2,75

If experimental acetylation data of total Degree of Substitution (DS) of different authors at different reactions temperatures are shown it can be appreciated that the DS is increasing very fast at reactions time obtaining DS higher than 1 in reactions times of about an hour, followed by an step in which DS is increasing more slowly until reaching values of around 2-2.2 and the last step until reaching DS of 3 is very slow. Thus, it is reasonable to propose that the first step is corresponding mostly with the acetylation of C6, the second with the acetylation of C3 and the third one with the acetylation of C2.

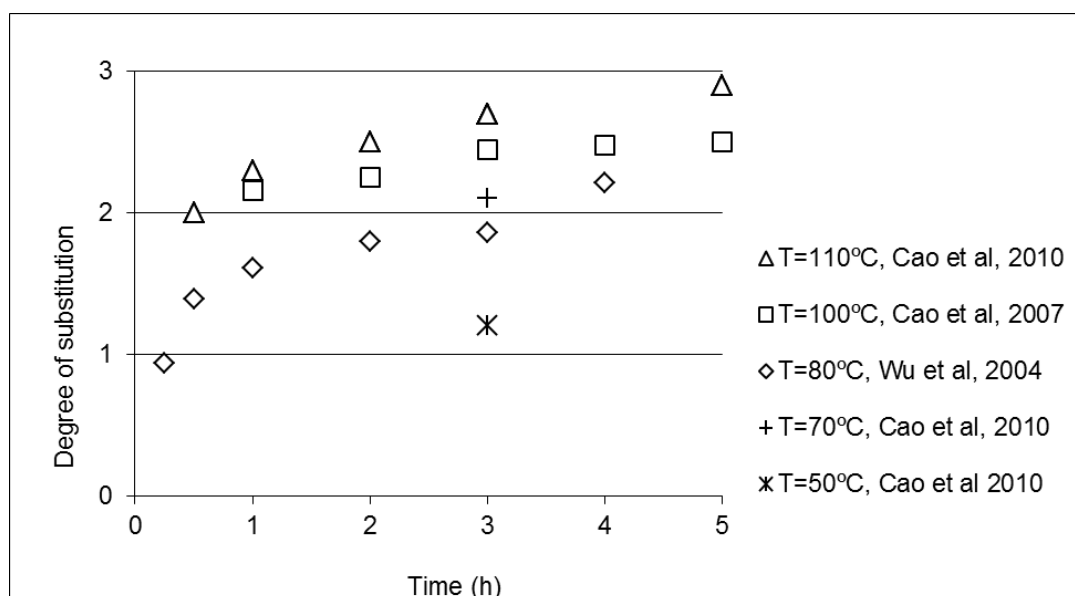


Fig. 3 Experimental data from the literature [10], [19, 20] of the degree of substitution as a function of time (h) of reactions at 50, 70, 80, 100 and 110°C with 5 mol of acetic anhydride per mol of AGU

At the same time it is observed that while cellulose concentration does not seem to greatly affect the reaction rate [20] the excess of acetic anhydride affects strongly to the reaction.

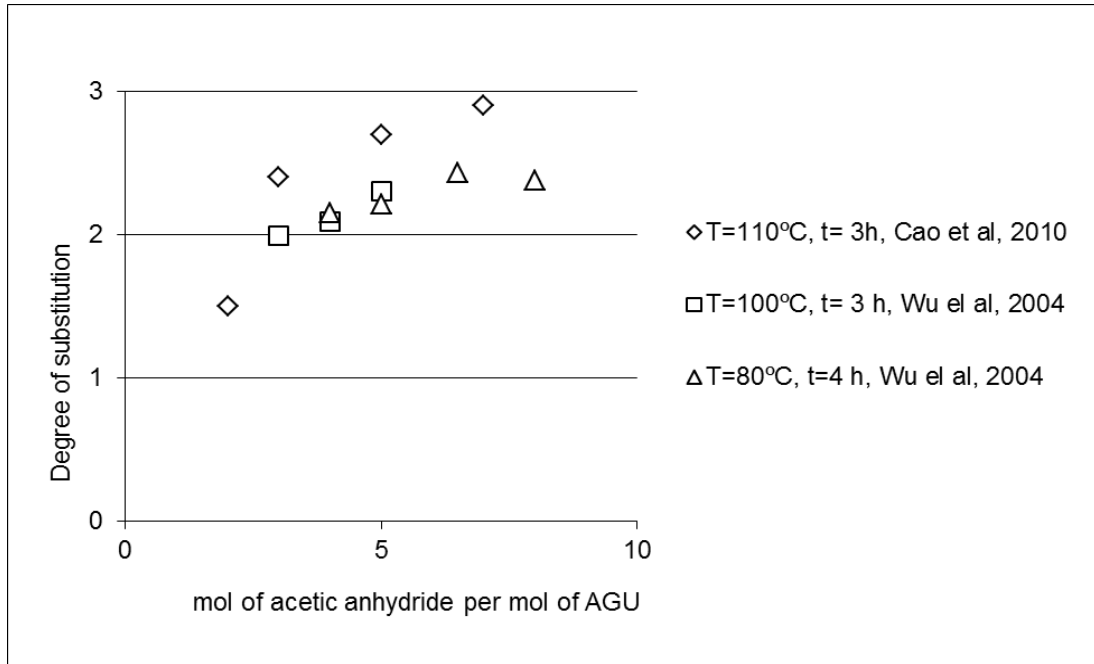


Fig. 4 Experimental data from the literature [19, 20] of the degree of substitution as a function of the mol of acetic anhydride per mol of AGU

As both the cellulose and acetic anhydride are dissolved in the IL forming a homogeneous phase a homogeneous kinetic model is considered

$$\frac{dDS_6}{dt} = A_6 \cdot e^{-\frac{E_{a6}}{RT}} \cdot C_o \cdot (1 - DS_6) \cdot (Ex - DS_6 - DS_3 - DS_2) \quad (3)$$

$$\frac{dDS_3}{dt} = A_3 \cdot e^{-\frac{E_{a3}}{RT}} \cdot C_o \cdot (1 - DS_3) \cdot (Ex - DS_6 - DS_3 - DS_2) \quad (4)$$

$$\frac{dDS_2}{dt} = A_2 \cdot e^{-\frac{E_{a2}}{RT}} \cdot C_o \cdot (1 - DS_2) \cdot (Ex - DS_6 - DS_3 - DS_2) \quad (5)$$

$$DS_7 = DS_6 + DS_3 + DS_2 \quad (6)$$

Where,

DS_6 , DS_3 and DS_2 are the degree of substitution of the acetyl group in the carbons 6, 3 and 2 of each AGU (each monomer of cellulose). Each one can have values of between 0 and 1. Zero means that none of the considered carbons of the AGU units is substituted with an acetyl group and 1 means that all the C_i carbons from AGUs are substituted with an acetyl group.

DS_T is the total substitution of acetyl group. As three carbons can be substituted DS can reach a maximum value of 3.

A_i and E_{ai} are the pre-exponential factor and the energy of activation of the substitution reaction of the carbons 6, 3 and 2 respectively. In order to simplify the model, it is assumed that the temperature dependence is the same for the three reactions and the energy of activation is the same for the three reactions $E_{a6}=E_{a3}=E_{a2}$. E_x are the mol of acetic anhydride per mol of AGU and C_o is the initial concentration of AGUs in mol/L.

4 Results and Discussion

4.1. Influence of reaction conditions on cellulose acetylation

Temperature, reaction time, reagent excess, addition of catalyst and addition of pressurized CO₂ were investigated and are summarized in Table 5.

The DS in Table 5 was calculated by FTIR and the Recovery Yield was determined by equation (7):

$$Y = \frac{R \times M}{\overline{M}} \quad (7)$$

$$\overline{M} = M \times (1 - X) \times M_m \times X \quad (8)$$

where, Y is the yield (%), R(%) is the percentage of dried solid that has been recovered, M is the molar weight of anhydroglucose unit, \overline{M} is the mass average, X is the reaction conversion and M_m is the mass of the monomer of cellulose triacetate.

Table 5 Summary of results on acetylation of 5 wt% cellulose in [Amim][Cl] with acetic anhydride at 40, 60 and 80°C

H ₂ O (wt%)	mol/mol AGU	CO ₂ ^a	Catalyst ^b	T (°C)	t (h)	Recovery (%)	DS ^c
0.58	1.5	-	-	80	1	41.32±2.01	1.30±0.01
0.58	1.5	-	-	80	3	60.52±5.68	1.19±0.22
0.58	1.5	-	-	80	6	65.41±19.00	0.55±0.06
0.58	1.5	-	-	60	3	56.05±16.74	0.87±0.01
0.25	4.5	-	-	80	1	55.19	2.11
0.06	4.5	-	-	80	6	74.76	2.00
0.58	4.5	-	-	80	24	78.05	2.88

0.58	4.5	-	-	60	1	72.99±2.38	1.33±0.04
0.58	4.5	-	-	60	6	70.59±13.23	1.75±0.30
0.58	4.5	-	-	60	24	65.06	2.40
0.58	4.5	-	-	40	1	71.83±4.67	0.88±0.03
0.58	4.5	-	-	40	6	75.59±19.94	1.24±0.66
0.58	4.5	-	-	40	24	82.04	1.40
0.58	4.5	-	+	80	1	62.97	2.23
0.58	4.5	-	+	60	1	53.54	2.20
0.58	4.5	-	+	40	1	89.77	0.62
0.25	4.5	+	-	80	1	62.39	3.59
0.58	4.5	+	-	60	1	44.63	2.78
0.58	4.5	+	-	40	1	69.86	1.16
0.06	4.5	+	-	80	6	50.96	4.16
0.58	4.5	+	-	60	6	38.21	6.47
0.58	4.5	+	-	60	24	45.61	4.54
0.58	4.5	+	-	40	24	50.04	3.18
0.58	4.5	+	+	60	1	82.37±1.71	1.73±0.00
0.58	4.5	+	+	40	1	77.95±7.04	0.80±0.28

^a80 bar of CO₂ added to the reaction mixture

^b1 mol% of scandium III triflate added to the reaction mixture

^cDegree of substitution (DS) determined by Fourier Transform infrared (FTIR)

Temperature and reaction time influence on cellulose acetylation in the presence and absence of CO₂ in the reaction mixture was investigated. From Fig. 5 to 7 is clear that the reaction conversion increases with temperature (40, 60 and 80°C), time (1, 6 and 24 h) and with addition of supercritical CO₂ (80 bar).

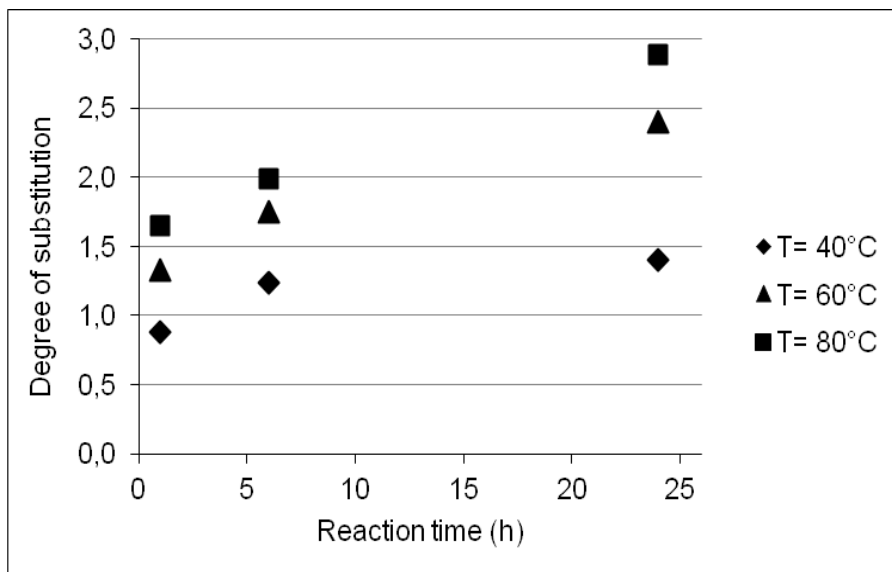


Fig. 5 Degree of substitution plotted as a function of the reaction time

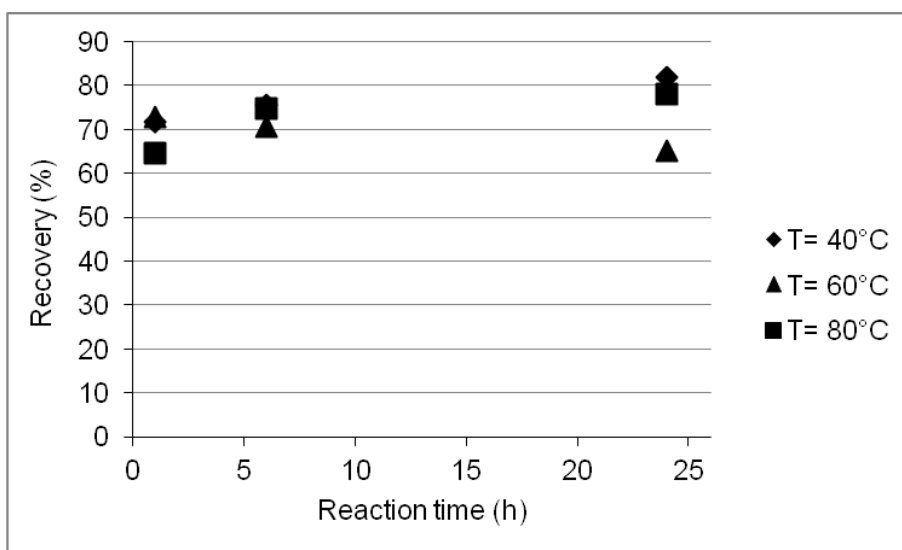


Fig. 6 Recovery yields plotted as a function of the reaction time for control reactions

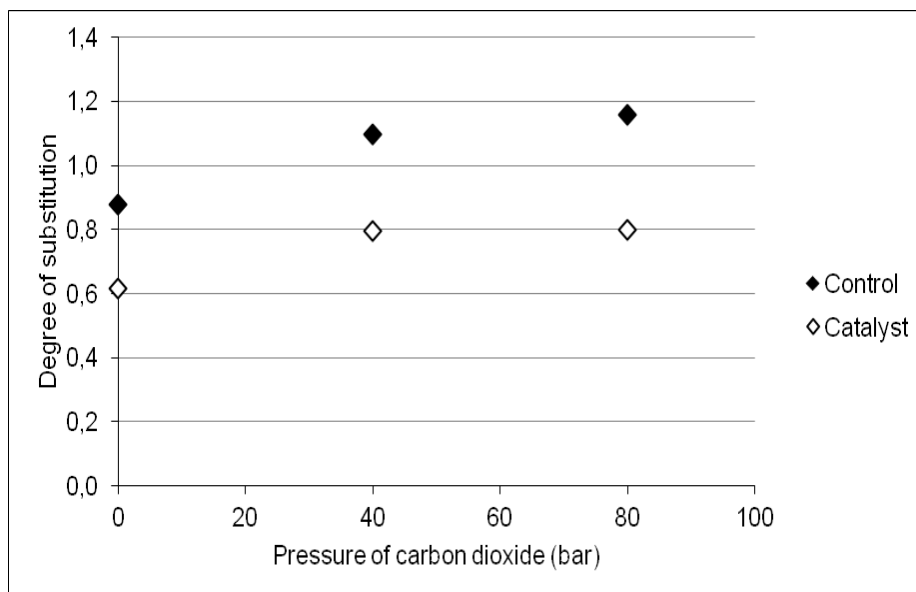


Fig. 7 Degree of substitution as a function of the pressure of carbon dioxide of the reaction at 40°C for 1h with and without scandium III triflate

Nevertheless, the addition of supercritical CO₂ to the reaction mixture is causing a great increase in the degree of substitution exceeding 3 as shown in the FTIR spectra (Fig. 8). The highest DS obtained with pressurized CO₂ is 6.47 from the reaction at 60°C for 6h followed by 4.54 with 24h. This can be due to that the method for DS calculation from FTIR is based in the detection the peak at 1750 cm⁻¹ corresponding to the group C=O, also present in CO₂. Additionally to the increase in peak at 1750 cm⁻¹, a peak at 2200 cm⁻¹ appears in samples where CO₂ was present: it is stronger at 60°C and 6h decreasing with time and temperature as shown which suggests that CO₂ could be being captured together with acetyl group by cellulose and making the apparent increasing on DS. However, water in [Amim][Cl] could be affecting the DS in the presence of CO₂. For instance at 80°C a DS of 3.59 has been achieved with a water concentration in [Amim][Cl] of 0.06 wt% which could be decreasing the CO₂ effect on acetylation in comparison with the experiment at 60°C which presented a 0.58 wt% water concentration in [Amim][Cl].

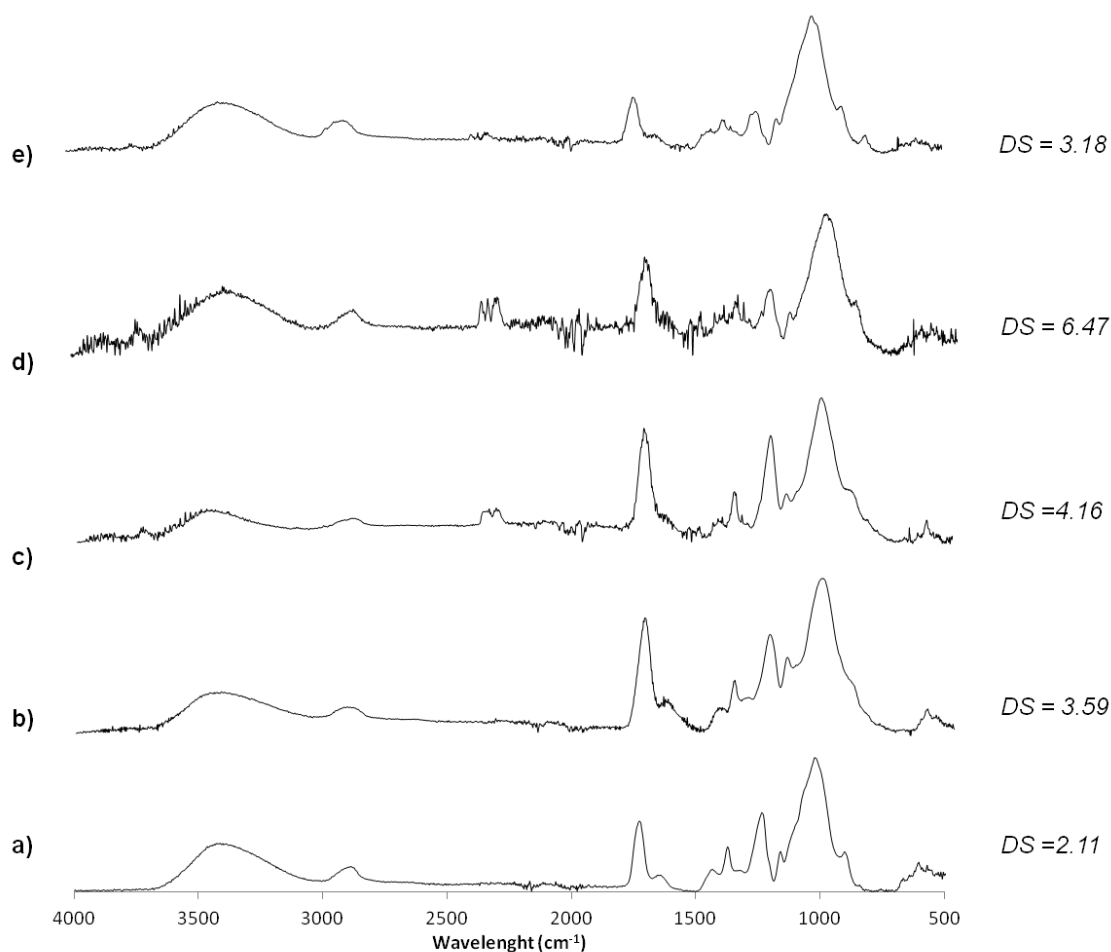


Fig. 8 FTIR spectra of acetylated cellulose in different reaction conditions: a) at 80°C for 1h without CO₂ (control) ; b) at 80°C for 1h with 80 bar of CO₂; c) at 80°C for 6h with 80 bar of CO₂; d) at 60°C for 6h with 80 bar of CO₂; e) at 40°C for 24h with 80 bar of CO₂

The experimental reaction has been also performed using a catalyst (scandium III triflate). It was not found a significant increase in the DS for higher temperature. Moreover, the DS decreased with the addition of pressurized CO₂ (80 bar) and catalyst (1% mol) to the reaction mixture. In general the yields are higher for acetylation in absence of CO₂ or in the presence of CO₂+catalyst even at lower temperature. In fact the DS of the reaction at 40 and 60°C for 1h showed high yields in CO₂+catalyst media (77.95 and 82.37% respectively).

The recovery yields of cellulose range from 45 to 90%. Literature values from [15] are from 63 to 98.9%. It is well known that imidazolium ionic liquids present some tendency to degrade cellulose [28, 29] especially at high temperatures. The recovery yields do not follow a constant pattern, but seems to be lower in reactions in which CO₂ is introduced in the reaction.

4.2. Influence of CO₂ on cellulose dissolution

Microcrystalline cellulose was mixed with ionic liquid inside a high pressure cell and bubbled with 7 bar of CO₂ for 30 min. The experiments were performed at 50 and 80°C due to the range of melting points of the ionic liquids used in this work. The dissolution at 50°C was tested with [Amim][Cl], [Emim][Ac] and [Emim][DMP] and at 80°C those and [Bmim][Cl]. The samples were prepared under a N₂ atmosphere and previous to the addition of CO₂, vacuum was applied to eliminate humidity inside the vessel that could be in contact with the mixture.

In general CO₂ accelerated the dissolution of cellulose in the ionic liquid. A slight increase in the rate of cellulose dissolution in the different ionic liquids is higher at lower temperature of 50°C.

Cellulose dissolution experiments at 50°C (Fig. 9) were obtained with an average deviation ±0,05 %gcel/gIL and a maximum deviation: ±0.08 %gcel/gIL. The amount of dissolved cellulose was higher for dimethylphosphate (DMP⁻) up to 0.27 gcel/gIL in the presence of CO₂. In this case it is expected that [Emim][DMP] dissolves more cellulose due to its low melting point (21°C). The two ionic liquids which showed the same dissolution rate (0.18 gcel/gIL) at 50°C are [Emim][Ac] and [Amim][Cl] although their melting points are quiet apart, <30°C and 55°C respectively.

The effect of temperature on the dissolution is shown by comparison of Fig. 9 and 10. In general at higher temperature the dissolution accelerates with an exception. In the case of [Emim][DMP] at 80°C no changes regarding the 50°C experiments were observed. However, for [Emim][Ac] and for [Bmim][Cl] is clear that at 80°C the viscosity of the mixture is lower thus more cellulose was dissolved. Adding CO₂ to cellulose/[Emim][Ac] increased the amount of dissolved cellulose to 1.06 gcel/gIL.

Chloride anion showed better results with [Amim]⁺ cation at lower temperature (50°C). [Amim][Cl] is highly hygroscopic thereby the decrease of the cellulose dissolution could be due to moisture that has been absorbed by the ionic liquid. Moreover, it is expected that at 80°C the effect of CO₂ on cellulose dissolution is not significant for low viscosity ionic liquids as observed for [Emim][DMP].

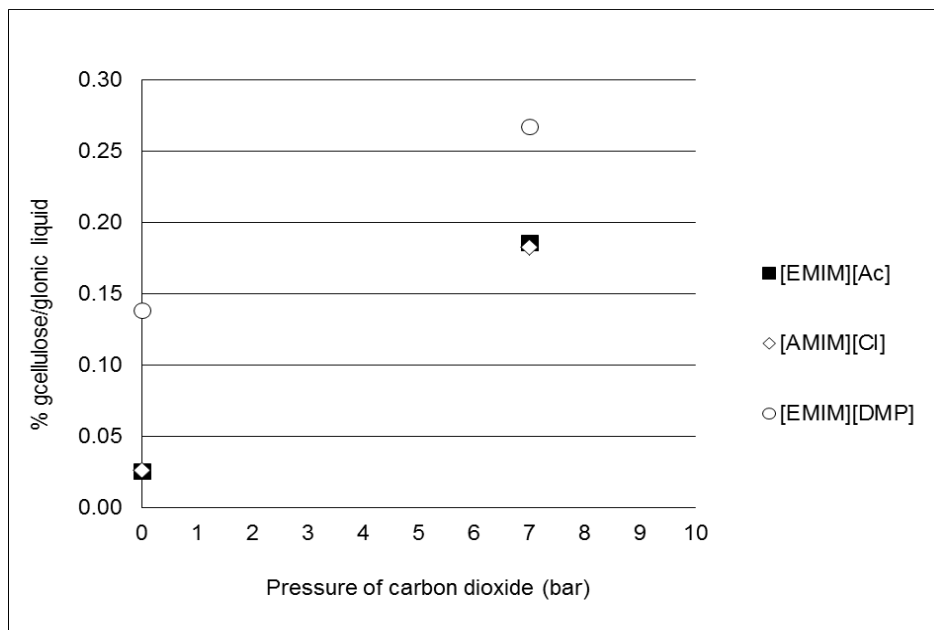


Fig. 9 Mass of dissolved cellulose per mass of ionic liquid in the presence of CO₂ at 50°C

Cellulose dissolution experiments at 80°C were obtained with an average deviation of $\pm 0,05$ %gcel/gLI and maximum deviation of $\pm 0,19$ %gcel/gLI

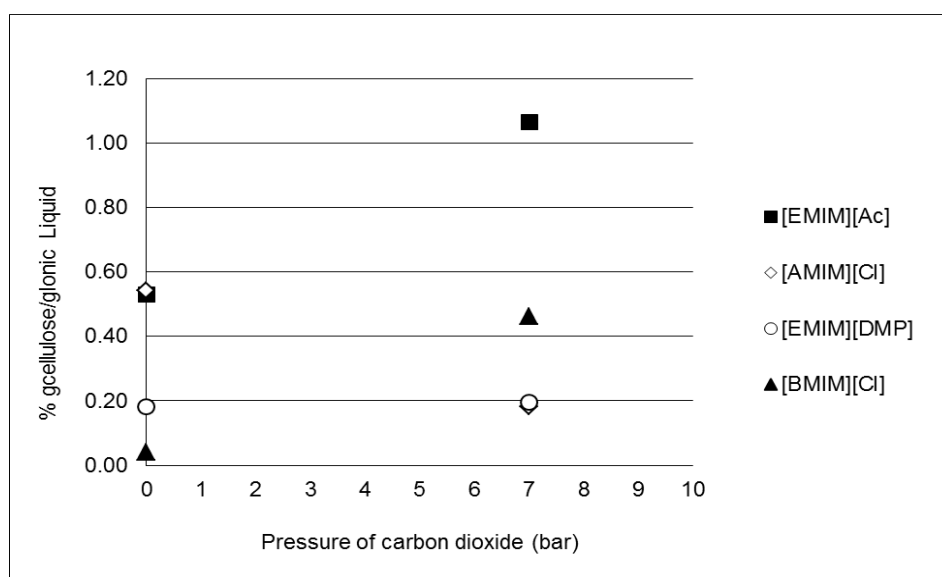


Fig. 10 Mass of cellulose dissolved per mass of ionic liquid in the presence of CO₂ at 80°C

4.3. Modeling

Parameters have been fitted using the function `fminsearch` of Matlab and the following constant are obtained. These parameters are fitted in Table 6. 101 kinetic data of different authors, included those obtained in this work, were used to fit the kinetics and the average deviation with respect to the experimental data was of 14.51%.

Table 6 Parameters fitted with using experimental data from this work and literature

A_6 (L·mol ⁻¹ h ⁻¹)	$3.006 \cdot 10^9$
A_3 (L·mol ⁻¹ h ⁻¹)	$3.324 \cdot 10^8$
A_2 (L·mol ⁻¹ h ⁻¹)	$3.897 \cdot 10^7$
E_a (J mol ⁻¹)	$6.001 \cdot 10^4$

The constant calculated at different temperatures are listed in Table 7.

Table 7 Constant calculated at different temperatures

T (°C)	k_2 (Lmol ⁻¹ h ⁻¹)	k_3 (Lmol ⁻¹ h ⁻¹)	k_6 (Lmol ⁻¹ h ⁻¹)
50	0.01	0.07	0.60
60	0.02	0.13	1.17
70	0.03	0.24	2.20
80	0.05	0.44	4.00
90	0.09	0.78	7.02
100	0.16	1.32	11.96
110	0.26	2.19	19.81
120	0.41	3.54	31.99
130	0.65	5.58	50.45

In the Fig. 11-14 some examples of the reaction evolution predicted by the model and compared to experimental data from other authors are shown. In Fig. 15-18 are shown

predictions of the reaction evolution for 40, 60 and 80°C and for 1.5 and 4.5 mol of reagent per mol of AGU.

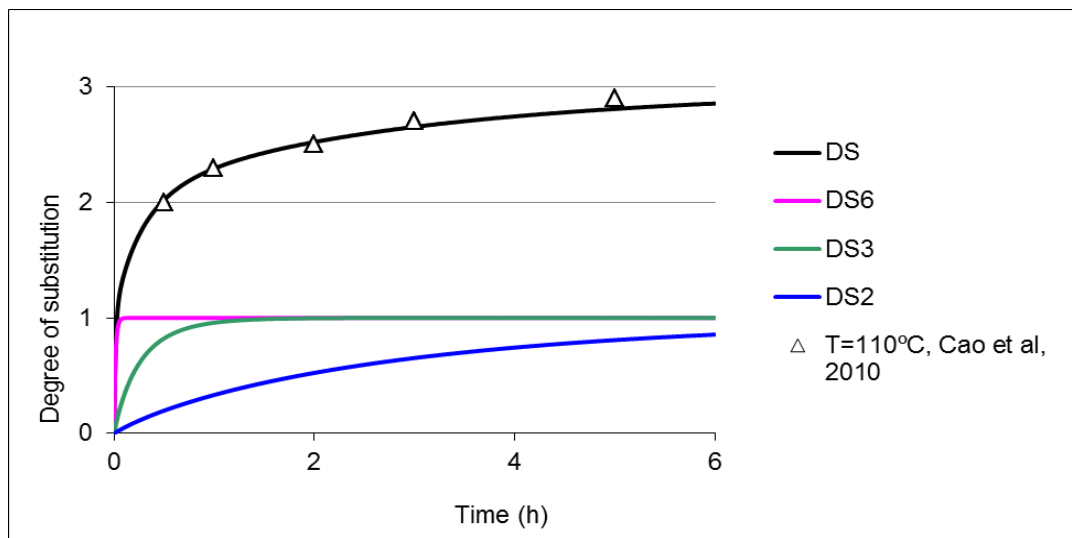


Fig. 11 Comparison of DS predicted by the model to experimental data from literature [20], at 110°C, 8 wt% cellulose concentration in [Amim][Cl] with 5 mol excess of acetic anhydride

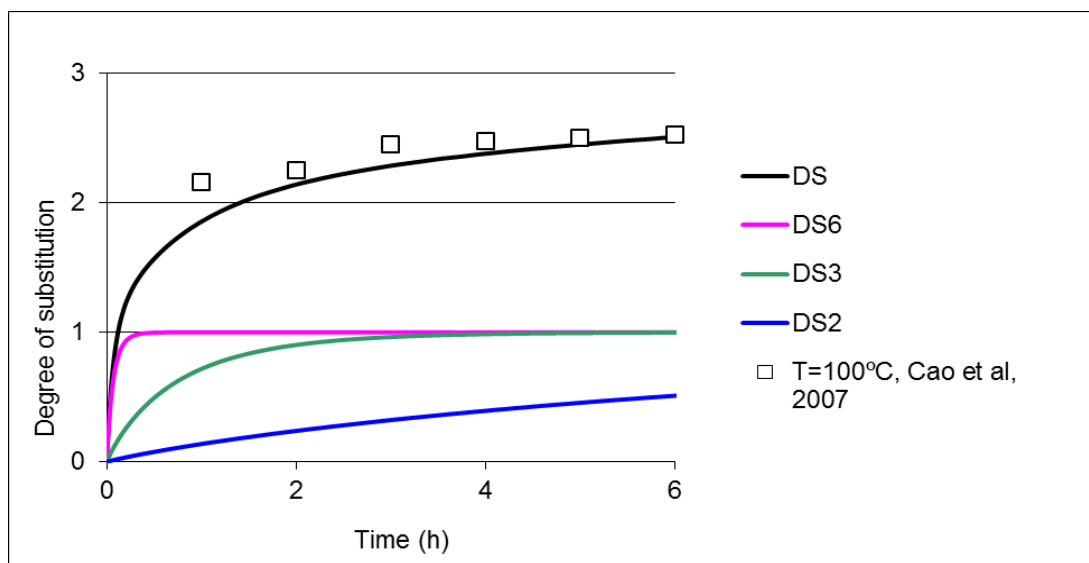


Fig. 12 Comparison of DS prediction by the model and experimental data from literature [10], at 100°C, 4 wt% cellulose concentration in [Amim][Cl] with 5 mol excess of acetic anhydride

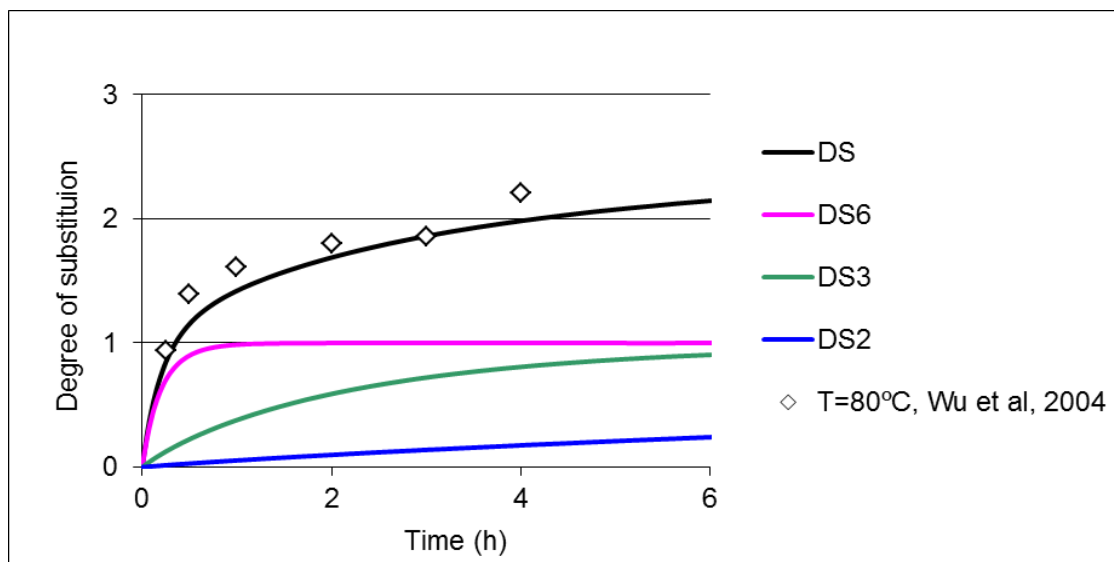


Fig. 13 Comparison of DS predicted by the model to experimental data from literature [19], at 80°C, 4 wt% cellulose concentration in [Amim][Cl] with 5 mol excess of acetic anhydride

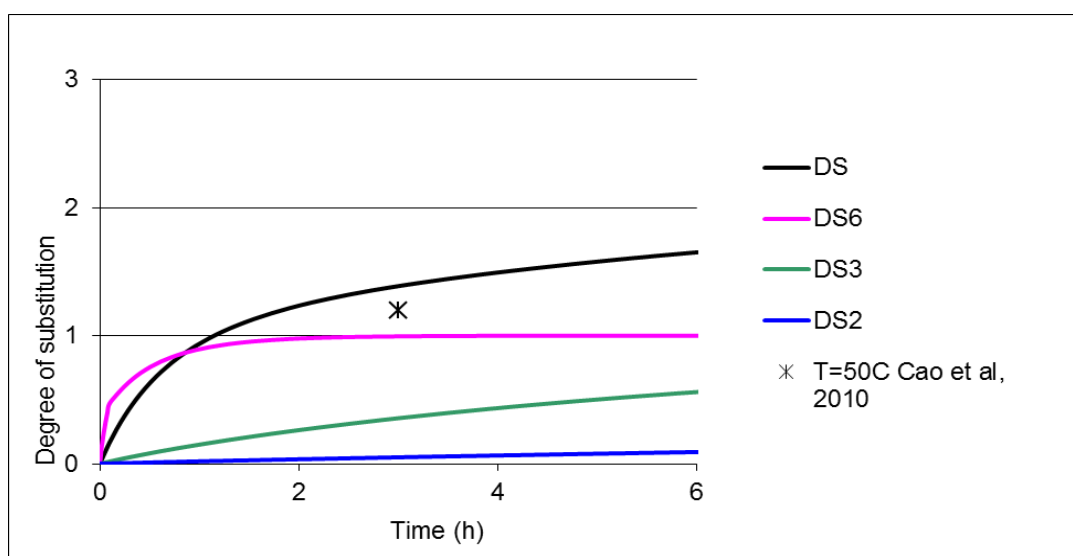


Fig. 14 Comparison of DS prediction by the model and experimental data from literature [20] at 50°C, 8 wt% cellulose concentration in [Amim][Cl] with 5 mol excess of acetic anhydride

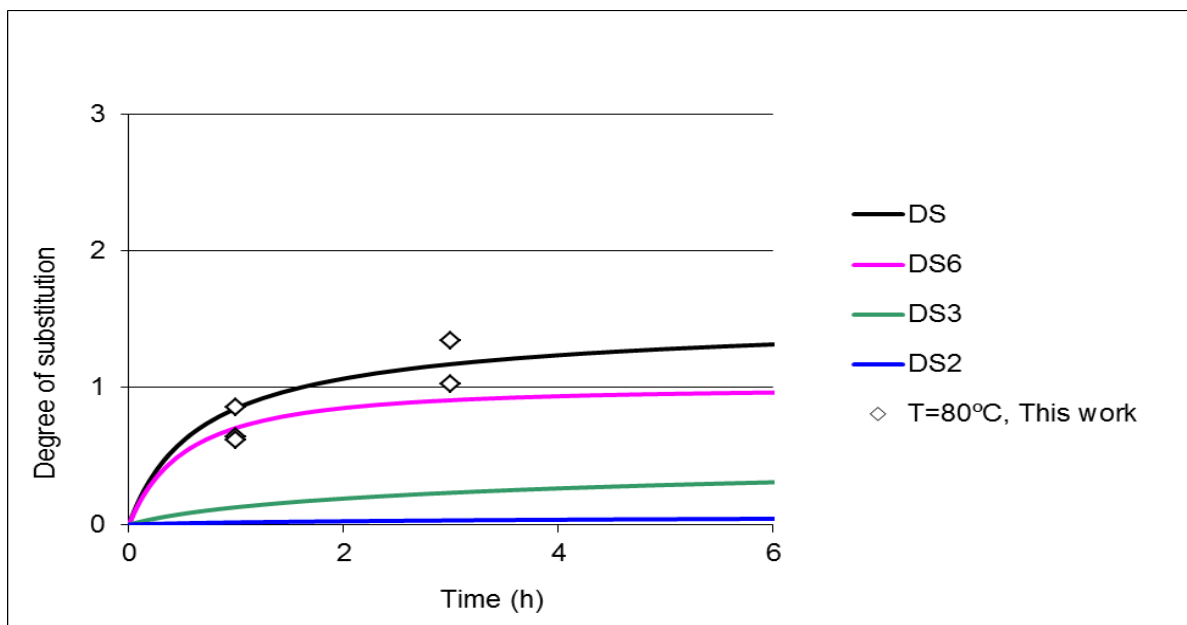


Fig. 15 Comparison of DS predicted by the model to experimental data from this work of the reaction at 80°C, 5 wt% cellulose concentration in [Amim][Cl] with 1.5 mol of acetic anhydride per mol of AGU

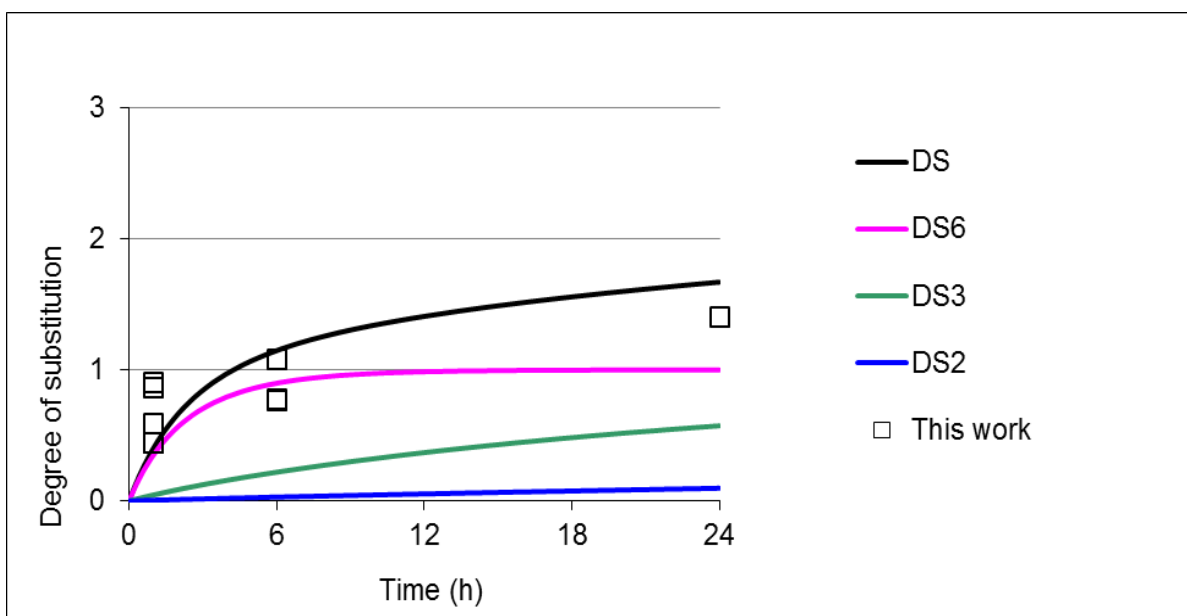


Fig. 16 Comparison of DS predicted by the model to experimental data from this work of the reaction at 40°C, 5 wt % cellulose concentration in [Amim][Cl] with 4.5 mol of acetic anhydride per mol of AGU

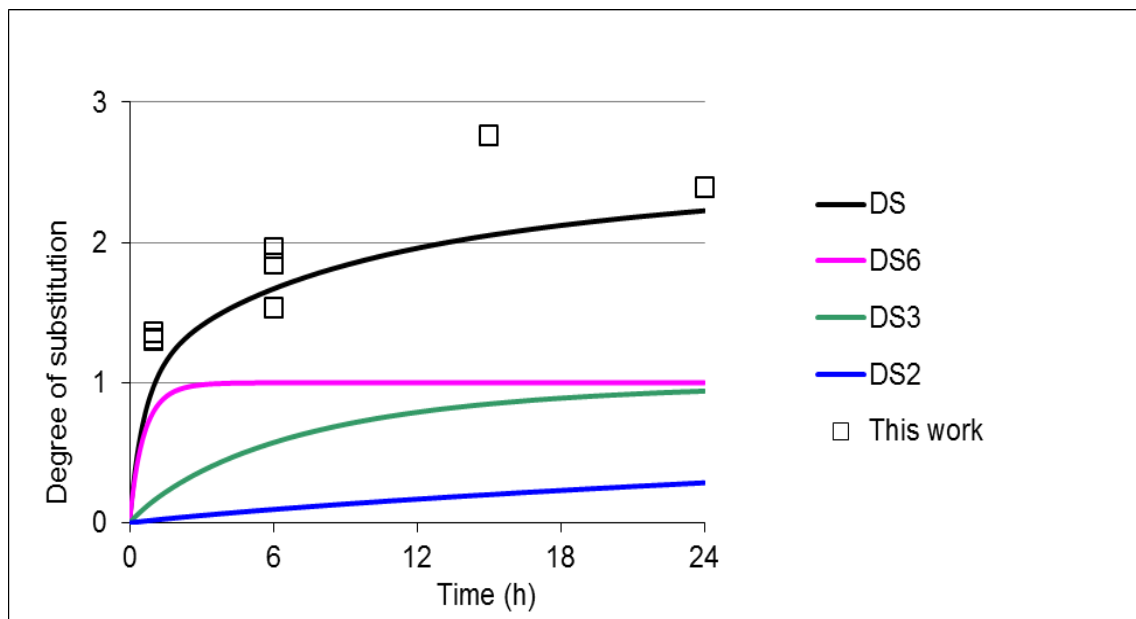


Fig. 17 Comparison of DS predicted by the model to experimental data from this work of the reaction at 60°C, 5 wt% cellulose concentration in [Amim][Cl] with 4.5 mol of acetic anhydride per mol of AGU

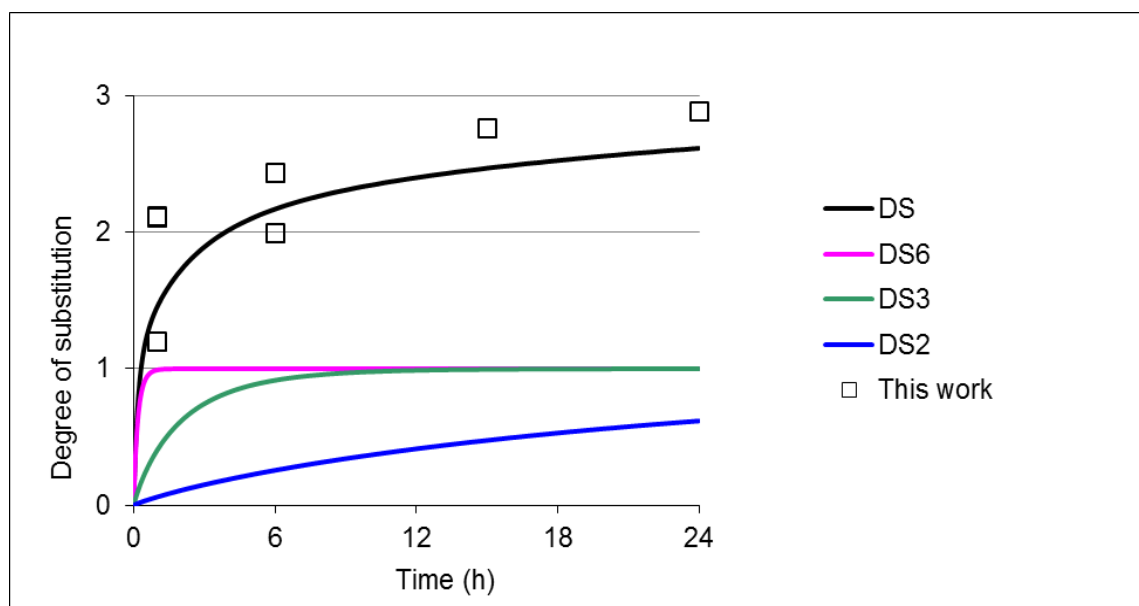


Fig. 18 Comparison of DS predicted by the model to experimental data from this work of the reaction at 80°C, 5 wt% cellulose concentration in [Amim][Cl] with 4.5 mol of acetic anhydride per mol of AGU

In Fig. 19 the influence of the relation acetic anhydride/AGU according to the model is shown and compared to different experimental data

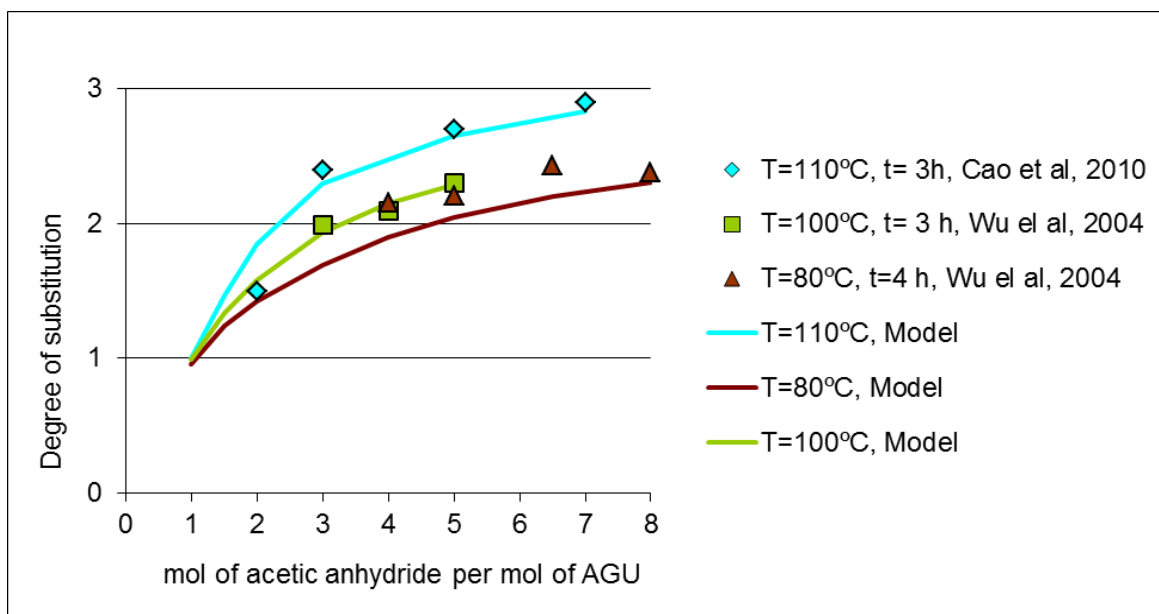


Fig. 19 Comparison of experimental data from the literature to the model prediction of the degree of substitution as a function of mol of reagent per mol of AGU for reactions at 80, 100 and 110°C

In order to check if the present kinetic model adjusted for acetylation reaction in [Amim][Cl] is valid for other ILs reaction data from [Bmim][Cl] are compared to the results of the model, as shown in Table 8. Relative deviations of 27% have been found in the DS predicted by the model. Unfortunately, another model of the kinetic reaction in [Bmim][Cl] cannot be adjusted due to the lack of experimental data at different reaction times.

Table 8 Comparison of data from works with [Bmim][Cl] and the model predictions

Ionic liquid	Cellulose (% ww)	(mol Ac ₂ O /mol AGU) ^a	t (h)	T(°C)	DS Exp	DS _{Model}	Deviation	Ref.
[Bmim][Cl]	12.2%	0.25	2	75	0.06	0.25	317%	[21]
[Bmim][Cl]	12.5%	1	2	75	0.5	0.97	93%	[21]
[Bmim][Cl]	13%	1.6	2	75	1	1.31	31%	[21]
[Bmim][Cl]	13.5%	2	2	75	1.2	1.47	23%	[21]
[Bmim][Cl]	13.5%	3	2	75	1.4	1.78	27%	[21]
[Bmim][Cl]	10.%	3	2	80	1.87	1.76	-6%	[15]
[Bmim][Cl]	10%	5	2	80	2.72	2.1	-22%	[16]
[Bmim][Cl]	14.4%	5	2	75	2.38	2.16	-9%	[21]
[Bmim][Cl]	10%	5	2	80	2.72	2.11	-22%	[15]
[Bmim][Cl]	10%	10	2	80	3	2.47	-18%	[16]

^amol Ac₂O/mol AGU means mol of acetic anhydride per mol of anhydroglucose unit

For the ionic liquid 1-Allyl-3-butylmethylimidazolium chloride ([ABmim][Cl]) the model has been used to calculate the conversion for both experimental conditions, that is using conventional and MW heating. In general the model presents a deviation of 8% in DS of data with conventional heating and 15% with data with MW heating. This comparison is shown in Table 9.

Table 9 Predictions of degree of substitution with experimental data found in literature

Ionic liquid	Cellulose (% ww)	mol Ac ₂ O /molAGU ^a	t (h)	T (°C)	DS	DS	Deviation	Heating	Ref.
					Exp	Model			
[ABim][Cl]	5%	3	24	80	2	2.3	5%	Conventional	[18]
[ABim][Cl]	5%	4.5	8	80	2.2	2.7	-8%	Conventional	[18]
[ABim][Cl]	5%	4.5	24	80	2.9	2.4	18%	Conventional	[18]
[ABim][Cl]	5%	3	24	80	2	2.5	4%	Conventional	[18]
[ABim][Cl]	5%	3.6	24	80	2.4	2.3	5%	Conventional	[18]
[ABim][Cl]	5%	4.5	8	80	2.2	1.2	-19%	Conventional	[13]
[ABim][Cl]	5%	3	2	60	1.5	1.3	-17%	MW	[13]
[ABim][Cl]	5%	3	3	60	1.6	2.1	-15%	MW	[13]
[ABim][Cl]	5%	4.5	5	80	2.5	2.3	-18%	MW	[13]
[ABim][Cl]	5%	4.5	8	80	2.8	1.8	21%	MW	[13]
[ABim][Cl]	5%	2.4	8	80	1.5	2.0	1%	MW	[13]
[ABim][Cl]	5%	3	8	80	2	2.2	5%	MW	[13]

^amol of acetic anhydride per mol of anhydroglucose unit

Using [Bmim][Cl] as solvent and Acetyl Chloride as a acylation reagent the model underpredicts the DS with an average of 36%, as shown in Table 10.

Table 10 Prediction of DS by the reaction model using [Bmim][Cl] and acetyl chloride.

Ionic liquid	Reagent	Cellulose (% ww)	molAc ₂ O /molAGU	t (h)	T (°C)	DS Exp	DS Model	Deviation	Ref.
[Bmim][Cl]	Acetyl Cl	10%	5	2	80	2.93	2.1	-28%	[16]
[Bmim][Cl]	Acetyl Cl	10%	3	2	80	2.81	1.8	-38%	[16]
[Bmim][Cl]	Acetyl Cl	10%	5	2	80	3	2.1	-30%	[16]
[Bmim][Cl]	Acetyl Cl	10%	10	2	80	3	2.5	-18%	[16]
[Bmim][Cl]	Acetyl Cl	10%	5	0.25	80	2.93	1.35	-55%	[16]
[Bmim][Cl]	Acetyl Cl	10%	5	0.5	80	3	1.55	-49%	[16]
[Bmim][Cl]	Acetyl Cl	10%	3	2	80	3	8	-41%	[16]
[Bmim][Cl]	Acetyl Cl	10%	5	2	80	3	2.1	-30%	[16]
[Bmim][Cl]	Acetyl Cl	10%	3	2	80	2.85	1.8	-38%	[16]
[Bmim][Cl]	Acetyl Cl	10%	5	2	80	3	2.114	-30%	[16]
[Bmim][Cl]	Acetyl Cl	10%	5	2	80	2.93	2.114	-28%	[15]
[Bmim][Cl]	Acetyl Cl	10%	3	2	80	2.81	1.7562	-38%	[15]
[Bmim][Cl]	Acetyl Cl	10%	5	0.25	80	2.93	1.3081	-55%	[15]
[Bmim][Cl]	Acetyl Cl	10%	5	0.5	80	3	1.5302	-49%	[15]
[Bmim][Cl]	Acetyl Cl	10%	5	2	80	3	2.114	-30%	[15]
[Bmim][Cl]	Acetyl Cl	10%	3	2	80	3	1.7562	-41%	[15]
[Bmim][Cl]	Acetyl Cl	10%	5	2	80	3	2.114	-30%	[15]
[Bmim][Cl]	Acetyl Cl	10%	3	2	80	2.85	1.7562	-38%	[15]
[Bmim][Cl]	Acetyl Cl	10%	5	2	80	3	2.114	-30%	[15]

Using some data of other different ionic liquids found in literature the predictions of the model can be compared in Table 11. All these results suggest that the specific ionic liquid used is affecting the reaction kinetic and it is not acting exclusively as a solvent.

Table 11 Comparison of experimental DS found in the literature with different ionic liquids to the predicted DS by the model

Ionic liquid	Cellulose (% ww)	mol Ac ₂ O/AGU	t (h)	T (°C)	DS Exp	DS Model	Deviation	Ref.
[Emim][Cl]	10%	3	2	80	3	1.76	-41%	[15]
[Bdmim][Cl]	10%	3	2	80	2.92	1.76	-40%	[15]
[Admim][Br]	10%	3	2	80	2.67	1.76	-34%	[15]

The kinetic constant of the reactions of the different ILs/reagent and temperature have been adjusted and compared in Table 12.

Table 12 Comparison of the adjusted kinetic constants

Ionic liquid	Reagent	Heating	T(°C)	k ₂	k ₃	k ₆	Dev	Viscosity (mPa·s)
[ABIm][Cl]	Ac ₂ O	Conventional	80	0.0908	1.979	1.9954	7.27%	42
[ABIm][Cl]	Ac ₂ O	MW	60	0.07	0.40	8.74	10.54%	200
[ABIm][Cl]	Ac ₂ O	MW	80	0.19	1.07	23.10	10.54%	42
[Bmim][Cl]	Ac Cl	Conventional	80	2.7087	9.8718	96.5869	1.18%	180
[Amim][Cl]	Ac ₂ O	Conventional	50	0.01	0.07	0.60	14.51%	299
[Amim][Cl]	Ac ₂ O	Conventional	60	0.02	0.13	1.17	14.51%	155
[Amim][Cl]	Ac ₂ O	Conventional	70	0.03	0.24	2.20	14.51%	89
[Amim][Cl]	Ac ₂ O	Conventional	80	0.05	0.44	4.00	14.51%	55
[Amim][Cl]	Ac ₂ O	Conventional	90	0.09	0.78	7.02	14.51%	37
[Amim][Cl]	Ac ₂ O	Conventional	100	0.16	1.32	11.96	14.51%	26
[Amim][Cl]	Ac ₂ O	Conventional	110	0.26	2.19	19.81	14.51%	20
[Amim][Cl]	Ac ₂ O	Conventional	120	0.41	3.54	31.99	14.51%	15
[Amim][Cl]	Ac ₂ O	Conventional	130	0.65	5.58	50.45	14.51%	13

5. Conclusions

Cellulose esters containing acetyl were synthesized in [Amim][Cl] at temperatures of 80, 60 and 40°C, focussing on temperatures lower than normally used in this reaction when using alkylimidazolium chloride ionic liquid. Through lower temperatures recovery yields ranging from 40 to 90% were obtained.

Some experiments were performed in the presence of supercritical CO₂ and of catalyst scandium III triflate. Catalyst showed non significant increment in the degree of substitution. In experiments using CO₂ degrees of substitution significantly higher than the average were found, indicating that carbon dioxide can be incorporating to the structure of the polymer.

A kinetic model of the acetylation reaction of cellulose in [Amim][Cl] was developed using acetic anhydride as acetylation agent. The evolution of the reaction was predicted by the proposed model and a good adjustment was performed with experimental data from this work and from other authors. It is found that the model is not able to predict the reaction rate when using other ionic liquids, even when all the ionic liquids used are of the alkylimidazolium family, suggesting the selected ionic liquid has an important role in the reaction.

It has been observed that very low pressures of CO₂ increases slightly the cellulose dissolution rate. This effect is more pronounced at lower temperature.

References

1. Edgar, K.J., C.M. Buchanan, J.S. Debenham, P.A. Rundquist, B.D. Seiler, M.C. Shelton and D. Tindall, *Advances in cellulose ester performance and application*. Progress in Polymer Science, 2001. 26(9): p. 1605-1688.
2. Rustemeyer, P., 1. History of CA and evolution of the markets. *Macromolecular Symposia*, 2004. 208(1): p. 1-6.
3. Klemm, D., B. Heublein, H.-P. Fink and A. Bohn, *Cellulose: Fascinating Biopolymer and Sustainable Raw Material*. *Angewandte Chemie International Edition*, 2005. 44(22): p. 3358-3393.
4. Kuo, C.M. and R.T. Bogan, *Process for the manufacture of cellulose acetate*. 1997.
5. Marsh, K.N., J.A. Boxall and R. Lichtenthaler, Room temperature ionic liquids and their mixtures—a review. *Fluid Phase Equilibria*, 2004. 219(1): p. 93-98.

6. Swatloski, R.P., S.K. Spear, J.D. Holbrey and R.D. Rogers, Dissolution of Cellulose with Ionic Liquids. *Journal of the American Chemical Society*, 2002. 124(18): p. 4974-4975.
7. Pinkert, A., K.N. Marsh, S. Pang and M.P. Staiger, Ionic Liquids and Their Interaction with Cellulose. *Chemical Reviews*, 2009. 109(12): p. 6712-6728.
8. Scheibel, J.J., C.J. Kenneally, J.A. Menkaus, K.R. Seddon and P. Chwala, Methods for modifying cellulosic polymers in ionic liquids. 2007.
9. Köhler, S., T. Liebert, M. Schöbitz, J. Schaller, F. Meister, W. Günther and T. Heinze, Interactions of Ionic Liquids with Polysaccharides 1. Unexpected Acetylation of Cellulose with 1-Ethyl-3-methylimidazolium Acetate. *Macromolecular Rapid Communications*, 2007. 28(24): p. 2311-2317.
10. Cao, Y., J. Wu, T. Meng, J. Zhang, J. He, H. Li and Y. Zhang, Acetone-soluble cellulose acetates prepared by one-step homogeneous acetylation of cornhusk cellulose in an ionic liquid 1-allyl-3-methylimidazolium chloride (AmimCl). *Carbohydrate Polymers*, 2007. 69(4): p. 665-672.
11. Liu, C.F., R.C. Sun, A.P. Zhang, J.L. Ren and Z.C. Geng, Structural and thermal characterization of sugarcane bagasse cellulose succinates prepared in ionic liquid. *Polymer Degradation and Stability*, 2006. 91(12): p. 3040-3047.
12. Liu, C.F., R.C. Sun, A.P. Zhang and J.L. Ren, Preparation of sugarcane bagasse cellulosic phthalate using an ionic liquid as reaction medium. *Carbohydrate Polymers*, 2007. 68(1): p. 17-25.
13. Possidonio, S., L.C. Fidale and O.A. El Seoud, Microwave-assisted derivatization of cellulose in an ionic liquid: An efficient, expedient synthesis of simple and mixed carboxylic esters. *Journal of Polymer Science Part A: Polymer Chemistry*, 2010. 48(1): p. 134-143.
14. Heinze, T., S. Dorn, M. Schöbitz, T. Liebert, S. Köhler and F. Meister, Interactions of Ionic Liquids with Polysaccharides – 2: Cellulose. *Macromolecular Symposia*, 2008. 262(1): p. 8-22.
15. Barthel, S. and T. Heinze, Acylation and carbanilation of cellulose in ionic liquids. *Green Chemistry*, 2006. 8(3): p. 301-306.
16. Heinze, T., K. Schwikal and S. Barthel, Ionic Liquids as Reaction Medium in Cellulose Functionalization. *Macromolecular Bioscience*, 2005. 5(6): p. 520-525.
17. Huang, K., B. Wang, Y. Cao, H. Li, J. Wang, W. Lin, C. Mu and D. Liao, Homogeneous Preparation of Cellulose Acetate Propionate (CAP) and Cellulose Acetate Butyrate

- (CAB) from Sugarcane Bagasse Cellulose in Ionic Liquid. *Journal of Agricultural and Food Chemistry*, 2011. 59(10): p. 5376-5381.
18. Fidale, L.C., S. Possidonio and O.A. El Seoud, Application of 1-Allyl-3-(1-butyl)imidazolium Chloride in the Synthesis of Cellulose Esters: Properties of the Ionic Liquid, and Comparison with Other Solvents. *Macromolecular Bioscience*, 2009. 9(8): p. 813-821.
 19. Wu, J., J. Zhang, H. Zhang, J. He, Q. Ren and M. Guo, Homogeneous Acetylation of Cellulose in a New Ionic Liquid. *Biomacromolecules*, 2004. 5(2): p. 266-268.
 20. Cao, Y., J. Zhang, J. He, H. Li and Y. Zhang, Homogeneous Acetylation of Cellulose at Relatively High Concentrations in an Ionic Liquid. *Chinese Journal of Chemical Engineering*, 2010. 18(3): p. 515-522.
 21. Kosan, B., S. Dorn, F. Meister and T. Heinze, Preparation and Subsequent Shaping of Cellulose Acetates Using Ionic Liquids. *Macromolecular Materials and Engineering*, 2010. 295(7): p. 676-681.
 22. Shogren, R., Scandium triflate catalyzed acetylation of starch at low to moderate temperatures. *Carbohydrate Polymers*, 2008. 72(3): p. 439-443.
 23. Keskin, S., D. Kayrak-Talay, U. Akman and Ö. Hortaçsu, A review of ionic liquids towards supercritical fluid applications. *The Journal of Supercritical Fluids*, 2007. 43(1): p. 150-180.
 24. Seddon, K., A. Stark and M. Torres, Influence of chloride, water, and organic solvents on the physical properties of ionic liquids in 15th International Conference on Physical Organic Chemistry (ICPOC 15). 2000, Int Union Pure Applied Chemistry: Gothenburg, Sweden. p. 2275-2287.
 25. Ahosseini, A., E. Ortega, B. Sensenich and A.M. Scurto, Viscosity of n-alkyl-3-methylimidazolium bis(trifluoromethylsulfonyl)amide ionic liquids saturated with compressed CO₂. *Fluid Phase Equilibria*, 2009. 286(1): p. 72-78.
 26. Scurto, A.M. and W. Leitner, Expanding the useful range of ionic liquids: melting point depression of organic salts with carbon dioxide for biphasic catalytic reactions. *Chemical Communications*, 2006(35): p. 3681-3683.
 27. Elomaa, M., T. Asplund, P. Soininen, R. Laatikainen, S. Peltonen, S. Hyvärinen and A. Urtti, Determination of the degree of substitution of acetylated starch by hydrolysis, ¹H NMR and TGA/IR. *Carbohydrate Polymers*, 2004. 57(3): p. 261-267.

28. Chen, H.-Z., N. Wang and L.-Y. Liu, Regenerated cellulose membrane prepared with ionic liquid 1-butyl-3-methylimidazolium chloride as solvent using wheat straw. *Journal of Chemical Technology & Biotechnology*, 2012. 87(12): p. 1634-1640.
29. Tan, H.T. and K.T. Lee, Understanding the impact of ionic liquid pretreatment on biomass and enzymatic hydrolysis. *Chemical Engineering Journal*, 2012. 183: p. 448-458.

Part IV. Recovery of valuable products

Chapter 5. Cellulose aerogels regenerated from microcrystalline cellulose + ionic liquid solution: properties and drug loading capacity study

Abstract

Cellulose aerogels obtained from cellulose/ionic liquid solutions were prepared using five different alkylmethylimidazolium ionic liquids. The influence of the ionic liquid anion, dissolution temperature and composition of the coagulation bath on surface area, pore volume and pore size was investigated. Optimal cellulose concentrations are between 1-2 wt%. Aerogels prepared from chloride anion ionic liquids have high surface areas. Aerogels prepared from alkylphosphate anion ionic liquid at lower dissolution temperature (40°C) showed lower surface area (approx. 300 m² g⁻¹) and higher pore volume and pore size as a result of slower gelation. Using absolute ethanol instead of aqueous ethanol as coagulation solvent improved surface area, pore volume and pore size of aerogels, and at the same time simplified the preparation. Drug loading capacity of the cellulose aerogels was investigated by impregnating phytol as model compound into the aerogels, using SC-CO₂ at 100 bar and 40°C with 0.1 of cellulose/phytol mass ratio. The aerogel prepared from 2 wt% cellulose in [Emim][DEP] solution showed the highest loading capacity. The high amount of drug loaded (approx 50% w/w) in the cellulose aerogels prepared from ionic liquid solutions shows their potential uses in the pharmaceutical or medical industry.

1. Introduction

Natural polymers are promising materials for preparing polysaccharide-based aerogels with high surface area (70 – 680 m²/g) [1]. Cellulose is a natural polymer extensively used for the production of aerogels [2]. Aerogels have been described as materials of extremely low density in which the typical structure of the pore network of gels is maintained while the liquid filling the pores of the gel is replaced by air [3].

Different applications of cellulose aerogels have been proposed: as carriers of bioactive compounds [4], for protein adsorption [5], oil absorption [6], lightweight shielding material [7] or as food additives [8].

The production of cellulose-based aerogels starts by dissolving cellulose in non-derivatizing solvents such as lithium chloride/dimethylacetamide (LiCl/DMAc), N-methylmorpholine-N-oxide (NMMO) or ionic liquids (ILs), among other solvents. In particular, the preparation of gels using cellulose dissolved in ILs has been intensively studied due to the unique properties of ILs as solvents [9]. ILs are a group of salts that are liquid below or around 100°C. An important advantage of working with ionic liquids is their low vapor pressure: ILs do not evaporate like organic solvents. The most studied cations in cellulose processing are those derived from imidazolium. ILs with alkylmethylimidazolium-based cations combined with chloride, acetate and phosphate anions are known to be good solvents of cellulose [10-14].

The next step in the preparation of the aerogel is the coagulation of the gel. Cellulose gels are prepared directly from cellulose through physical cross-linking (molecular self-assembly through ionic or hydrogen bonds) without the need of adding a crosslinking reagent as happens with the gels of other substances. A cellulose hydrogel can be obtained by soaking homogeneous mixtures of cellulose with ionic liquid into water [15] to cause the coagulation of cellulose. If the solution is soaked into an alcohol (e.g. ethanol) the gel obtained is known as alcogel. The morphology of coagulated microcrystalline cellulose (MCC) in water is similar to the morphology in ethanol as showed by FTIR spectra of regenerated cellulose from 1-ethyl-3-methylimidazolium acetate ([Emim][Ac]) [16].

After the coagulation of the hydrogel or alcogel the last step is the removal of the coagulation solvent by drying. Different drying methods can be used, including air drying, oven drying, nitrogen freeze drying, regular freeze drying, reduced pressure and supercritical carbon dioxide (SC-CO₂) drying. Using different drying methods, different cellulose materials are obtained. To obtain cellulose as aerogels, freeze drying and SC-CO₂ drying have been used. As freezing or evaporation of water inside the gel pores can damage the aerogel's pore structure, water present in the coagulation solvent media has to be exchanged with an alcohol (usually ethanol) prior drying. To avoid damages to the gel, water replacement is usually performed stepwise using water-ethanol solutions of increasing ethanol concentration. Freeze drying and SC-CO₂ drying have been used to prepare cellulose aerogels for several applications, e.g. protein adsorption, oil absorption [6] or bioactive compounds release.

Properties of cellulose aerogels prepared from different biomass/IL solutions and with different conditions of supercritical drying are found in literature. MCC in particular is used to obtain lower density materials, although those can be more fragile due to the structure of the dissolved and regenerated cellulose [17]. Lignocellulose aerogels made from wood dissolved in [Bmim][Cl] have been reported to be much harder and exhibit more structural strength than cellulose aerogels [18]. The morphology and porosity of lignocellulose aerogels preparation from solution of wood in [Amim][Cl] can be tuned by adjusting freeze thawing, a treatment prior to supercritical drying [19]. Using exclusively supercritical drying, nanoporous cellulose aerogels have been prepared from cellulose soft pulp (DP=1283) dissolved in [Amim][Cl] [20] and aerocellulose from cellulose or cotton/[Emim][Ac] and [Bmim][Cl] [21]. Photoluminescent cellulose aerogels have been prepared from eucalyptus pulp dissolved in [Hmim][Cl] [22] and cellulose-silica aerogels have been prepared in [Emim][Ac] prior to forced flow impregnation with silica (20wt% of SiO₂ in ethanol) phase and polyethoxydisiloxane [23]. There are also a number of studies in which cellulose aerogels have been produced using ILs, some including the study of the different preparation parameters (biopolymer concentration, dissolution time, coagulation temperature) of the cellulose solution and coagulation process on the properties of these aerogels [18, 24].

In this work the influence of different operational parameters on the properties of cellulose aerogels produced using ILs is studied: various alkylmethylimidazolium-based ILs are employed, at low dissolution temperature, and with several cellulose concentrations and coagulation conditions. In the second part of this work, an impregnation study was performed to determine the loading capacity of the cellulose aerogels with a bioactive compound, using phytol as model natural compound.

2. Experimental section

2.1. Materials

Microcrystalline cellulose was supplied by Alfa Aesar and dried for 5h at 60°C under vacuum before the dissolution. Ionic liquids 1-butyl-3-methylimidazolium chloride ([Bmim][Cl]) with purity >99 % and moisture of 0.140 wt%, 1-(2-hydroxyethyl)-3-methylimidazolium chloride ([HOemim][Cl]) with purity of >99 % and moisture of 0.214 wt%, 1-ethyl-3-methylimidazolium acetate ([Emim][Ac]) with purity of >95% and moisture of 0.385 wt% and 1-ethyl-3-methylimidazolium diethyl phosphate ([Emim][DEP]) with purity of 98% and moisture of 0.067 wt%, were provided by Iolitec (Germany). 1-allyl-3-methylimidazolium chloride ([Amim][Cl]) was purchased from Alfa Aesar with purity of 98% and moisture content of 0.247 wt%. The water content was measured by Karl-Fischer titration (Mettler Toledo C20 Coulometric KF titrator).

2.2. Methods

The complete procedure for aerogels preparation is summarized in Fig. 1. Each step is described in following sections.

2.2.1. Preparation of cellulose alcogel

The cellulose solution was prepared by dissolving MCC in ionic liquid. Samples were handled under N₂ atmosphere to avoid water absorption. After heating and stirring a clear solution was obtained indicating the total dissolution of cellulose. Then the cellulose/IL solution was transferred to cylindrical moulds (1.5 cm of diameter and 0.3 cm of diameter) and washed with an aqueous solution of ethanol at room temperature to extract the ionic liquid. The volume of the solution employed was 10 times higher than the ionic liquid volume in order to ensure that the ionic liquid was completely washed out. As a sudden change of the solvent composition can damage the gel structure, the gels were successively soaked in solutions of increasing ethanol concentration: 10, 30, 50, 90 and 100%, in 2 h cycles.

2.2.2. Supercritical drying

Finally, the cellulose aerogels were collected after the SC-CO₂ drying at 120 ± 5 bar and 40°C. The procedure employed is similar to the method described elsewhere [25, 26] with slight modifications in the total drying time: drying was done in 3 cycles of CO₂ flow, each one lasting 2 h. At the end of each cycle, the extracted ethanol was collected and fresh CO₂ was introduced. After completing the total period of 6 h of SC drying, the system was depressurized at rate of 2 bar/min to avoid shrinkage of cellulose aerogels.

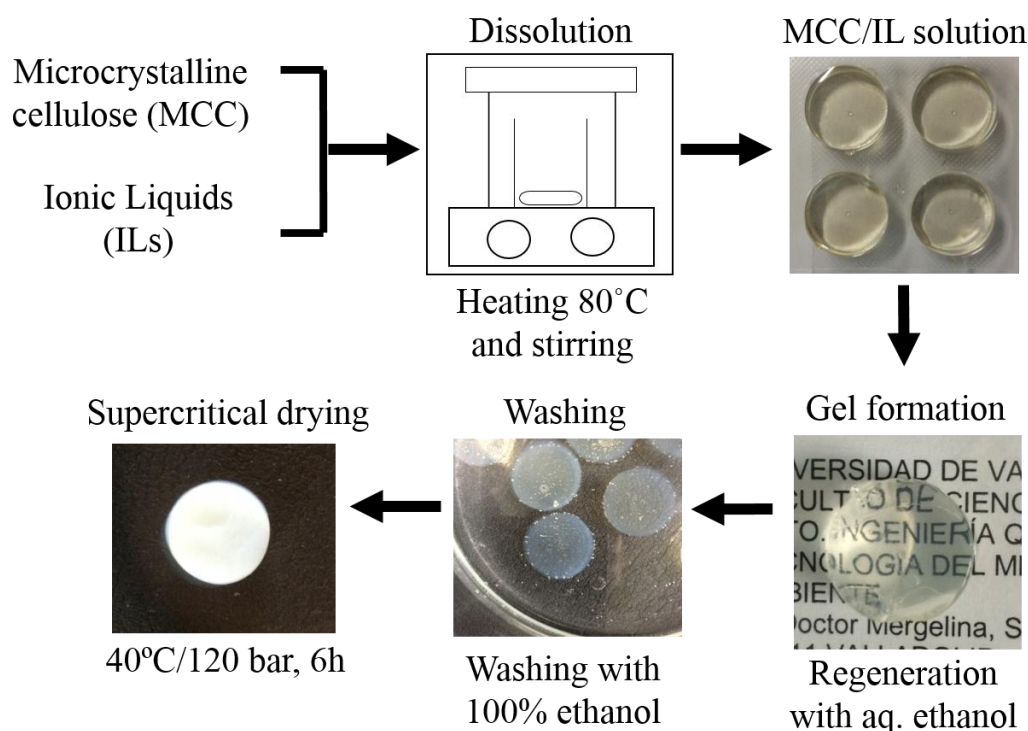


Fig. 1 Scheme of cellulose aerogel preparation in ionic liquid using supercritical CO₂ drying

2.2.3. Supercritical Impregnation (SCI)

The impregnation study was performed to determine the loading capacity of the cellulose aerogels with bioactive compounds. The impregnation process was carried out using the set up shown in Fig. 2. A 70 mL stainless steel high pressure autoclave with a maximum working pressure of 150 bar was used. A known mass of pure phytol was placed at the bottom of the autoclave. Meanwhile a known mass of dried cellulose aerogels was wrapped in metal filters and separated from the phytol by lifting them up from the bottom of the autoclave applying a cylindrical metal platform. The autoclave was heated to 40°C and pressurized with CO₂ to 100 bar at rate of 2 bar/min. The pressure was maintained for 24 h to ensure a maximum solubility of phytol in SC-CO₂. Magnetic stirrer was employed to additionally enhance the dissolution of phytol. After that time, the system was slowly depressurized at a rate of 2 bar/min to avoid aerogels shrinkage or collapse of the mesoporous structure of the aerogels. The impregnated aerogels were recovered from the autoclave and the loading of compounds was determined gravimetrically and calculated as indicated in eq. (1):

$$\frac{w_a (g) - w_b (g)}{w_a (g)} \times 100\% \quad (1)$$

Where W_a is the mass of cellulose aerogels after impregnation, W_b is the mass of cellulose aerogels before impregnation (g).

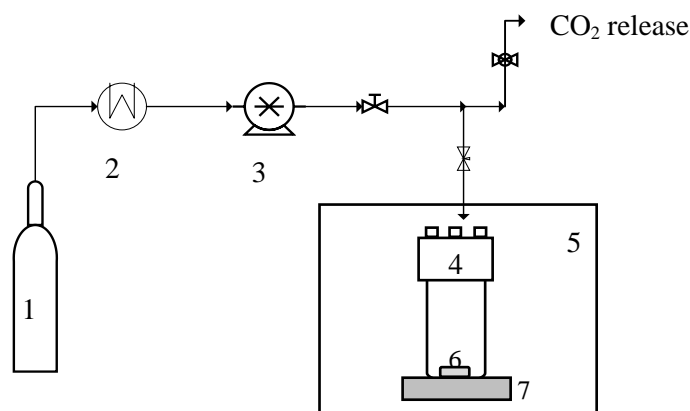


Fig. 2 Supercritical CO₂ impregnation Setup; 1) CO₂ tank, 2) pump, 3) cooler, 4) impregnation autoclave, 5) oven, 6) magnetic bar, 7) magnetic stirrer

2.3. Characterization

Textural properties (surface area, pore volume, pore size) of aerogels were determined by gas N₂ adsorption-desorption analysis. All experiments were carried out at -196°C and prior to the analysis the samples were degassed under vacuum at 70°C for 660 min. The samples from run 3, 4, 8 and 10 were analyzed using a Micrometrics ASAP 2020MP instrument and all the other samples with an ASAP 2420 V2.09 instrument. The method applied for measuring the textural properties of the aerogels was the same regardless the instrument used. The specific surface areas were calculated from the Brunauer-Emmet-Teller (BET) equation, and the average mesopore diameter distributions were determined from desorption isotherms by the Barret-Joyner-Halenda (BJH) method.

The melting point was measured with a differential scanning calorimetry (DSC) apparatus (DSC 822e Mettler Toledo SAE) equipped with a ceramic sensor FSR5, under a stream of N₂ at a flow rate of 50 cc min⁻¹. The analysis was carried out over a temperature range of 25 to 300°C, at a heating rate of 10°C min⁻¹.

The surface morphology of the cellulose aerogels was examined by scanning electron microscopy (SEM) using a SEM JEOL JSM 820 equipment. The samples were splattered-coated with gold layer prior to the scanning at voltage of 2-4kV.

The FTIR spectra was recorded on a Fourier Transform infrared instrument (Bruker Platinum-ATR) equipped with software of OPUS Optik GmbH in the range from 400 to 4400 cm⁻¹ of wavelength.

3. Results and discussion

3.1. Textural and morphological properties of cellulose aerogels

Cellulose aerogels were prepared from cellulose/IL solutions with MCC concentration between 0.2 and 4 wt% in five alkylmethylimidazolium-based ILs. The results of surface area, pore volume and pore size are presented in Table 11.

Table 11 Experimental data: surface area ($\text{m}^2 \text{g}^{-1}$), pore volume ($\text{cm}^3 \text{g}^{-1}$) and pore size (nm) of cellulose aerogels prepared from microcrystalline cellulose dissolved in ionic liquid at 80°C for 18h

Run	Ionic Liquid (IL)	wt% ^a	Surface area ($\text{m}^2 \text{g}^{-1}$)	Pore volume ($\text{cm}^3 \text{g}^{-1}$)	Pore size (nm)
1	[Amim][Cl]	0.2	-	-	-
2	[Amim][Cl]	0.5	-	-	-
3	[Amim][Cl]	1	434	0.7	8.7
4	[Amim][Cl]	2	426	0.8	9.4
5	[Amim][Cl]	4	278	2.4	34
6	[Bmim][Cl]	2	428	1.1	11.7
7	[Bmim][Cl]	1	-	-	-
8	[HOemim][Cl]	2	154	0.3	7.9
9	[HOemim][Cl]	1	-	-	-
10	[Emim][Ac]	2	282	1.9	26
11	[Emim][DEP]	2	326	1.4	18
12	[Emim][DEP] ^b	2	280	1.8	26
13	[Emim][DEP] ^c	2	290	3.4	47

^aConcentration of cellulose in ionic liquid by weight

^bDissolution at 40°C

^cDissolution at 40°C and coagulation in 100% ethanol

“-“ Not possible to dry these samples due to fragility of the gels

It is observed that aerogels with higher surface area are produced with [Amim][Cl] and [Bmim][Cl] ILs, being the first one easier to handle due to its lower viscosity and melting point [27, 28], [1]. The highest surface area (434 m² g⁻¹) was obtained using 1 wt% cellulose dissolved in [Amim][Cl]. This area is relatively high compared to literature results of cellulose aerogels prepared from ILs by SC drying: aerogels with lower surface area (315 m² g⁻¹) prepared from cellulose-[Amim][Cl] have been reported by Tsiptsias et al. [20] for a concentration range of 2 to 3 wt%. Higher area values were reported in the work from Aaltonen [18] with cellulose-[Bmim][Cl] (539 m² g⁻¹ for 3 wt% and 213 m² g⁻¹ for 4 wt%). The different conditions of coagulation and drying used in those two studies could have influenced the properties of the aerogels. In this work, similar properties were obtained with [Amim][Cl] and [Bmim][Cl] for cellulose concentration of 2 wt%. In contrast, much lower surface area (154 m² g⁻¹) was obtained in run 8 using a different IL (2 wt% cellulose-[HOemim][Cl]). The surface area in this experiment could have been affected by the low ability of the [HOemim][Cl] ionic liquid to dissolve cellulose. Hydroxyl group in [HOemim][Cl] alkyl side chain makes it a lower hydrogen-bond basicity ionic liquid [29], and thus lowers its cellulose solvation capacity.

The lower surface area from run 10 (282 m² g⁻¹) was expected as cellulose concentration was increased in this experiment to 2 wt%. Indeed, Sescousse et al. [21] reported a surface area variation from 230 m² g⁻¹ for the aerogel from a 3 wt% cellulose-[Emim][Ac] solution to 130 m² g⁻¹ for a 15 wt% solution. This trend was confirmed by the experiments with [Amim][Cl] (1, 2 and 4 wt%) that showed a decrease of surface area with biopolymer concentration from 434 to 278 m² g⁻¹. Similar ranges of surface area have been reported before with other solvents, e.g. 200 – 300 m² g⁻¹ in NaOH aqueous solutions at lower temperatures [30] and 100 – 400 m² g⁻¹ in N-methyl-morpholine-N-oxide (NMMO) [31]. In the same study, it was found that the internal surface area was mainly influenced by choosing the appropriate regeneration and critical drying conditions instead of the initial cellulose concentration, contrary to the observations in this work that identify cellulose concentration as the key process parameter determining the textural properties.

The aerogels from run 1, 2, 7 and 9 were highly fragile not allowing further analysis and characterization.

Fig. 3 compares the DSC of a typical (run 4) cellulose aerogel prepared in [Amim][Cl] and the DSC of pure [Amim][Cl]. The last one shows a peak at 55°C that corresponds to the melting point of [Amim][Cl]. The DSC of the aerogel (solid line) does not have this peak, indicating a successful IL removal, but presents a small weight loss below 100°C, which could be due to evaporation of adsorbed water. Furthermore, the endothermic peak observed at 310°C corresponds to the decomposition of cellulose [32].

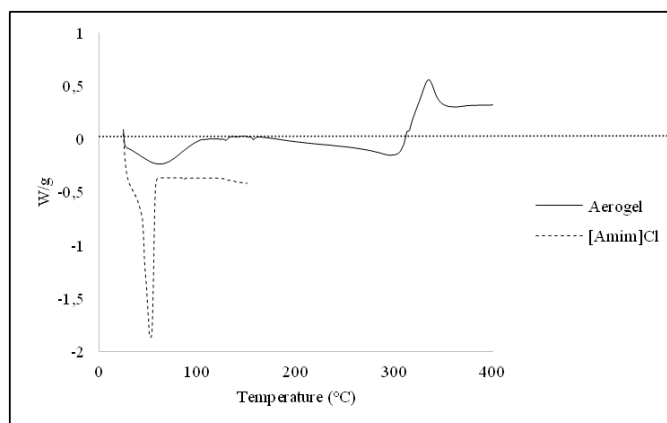


Fig. 3 Comparison of DSC between cellulose aerogel (run 4) and pure [Amim][Cl]

Ionic liquids [Emim][Ac] and [Emim][DEP] have lower melting points and viscosities than those derived from imidazolium chloride. Furthermore they are able to dissolve cellulose at lower temperatures [33]. Nevertheless in these ILs much lower surface areas were obtained compared to those from imidazolium chloride ILs for the same concentrations of cellulose and dissolution temperature.

In the case of [Emim][DEP], aerogels prepared by dissolving cellulose at different temperatures were compared. When cellulose was dissolved at 80°C (run 11) a higher surface area (326 m² g⁻¹) and lower pore volume (1.4 cm³ g⁻¹) and pore size (18 nm) were obtained compared to run 12 where cellulose was dissolved at 40°C. After the dissolution at 40°C, cellulose aerogels could be less amorphous [10] in comparison to that recovered from the one dissolved at 80°C which may have contributed in slowing down the gelation process, thus not improving the surface area.

The aerogel produced from a 2 wt% solution of cellulose in [Emim][DEP] showed different results also with different coagulation conditions. In order to simplify the coagulation step absolute ethanol (run 13) was used. This procedure caused an increase in surface area, pore volume and pore size. Thus, employing higher dissolution temperature and a coagulation bath of absolute ethanol, aerogels produced in [Emim][DEP] show higher values of all the textural properties analyzed (surface areas, pore volume, pore size). Aerogels prepared with [Emim][Ac] (run 10) showed the same properties of aerogels from [Emim][DEP] with cellulose dissolved at 40°C (run 12)

SEM images of aerogels obtained in experiments with 2 wt % cellulose in [Bmim][Cl], [HOemim][Cl], [Emim][Ac] and [Emim][DEP] (Fig. 4) show the same strand structure found in MCC-based aerogel reported by Gavillon & Budtova [30].

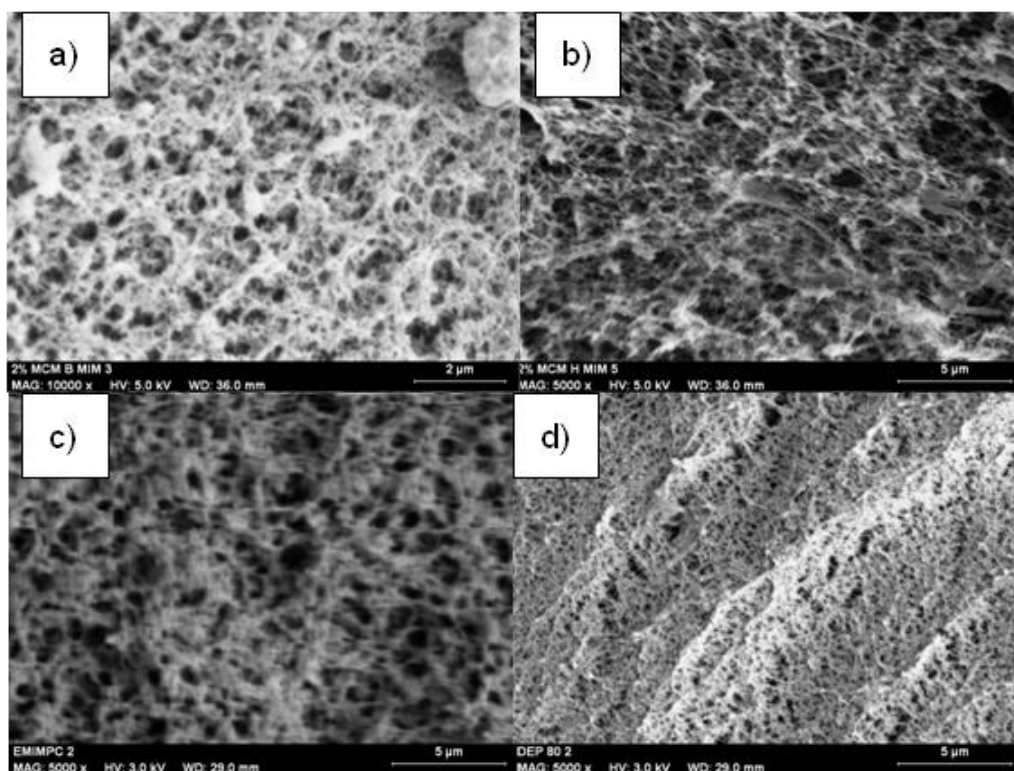


Fig. 4 SEM images of the a) run 6 ([Bmim][Cl]), b) run 8 ([HOemim][Cl]), c) run 10 ([Emim][Ac]) and d) run 11 ([Emim][DEP])

As presented in

Fig. 5, the alcogels from different ILs were transparent. After SC drying all the aerogels were sticky (due to static electricity) with a white opaque appearance.

Furthermore, In row a) it is observed that aerogels shrinkage is less pronounced with increasing cellulose concentrations (0.5, 2 and 4 wt% in [Amim][Cl]). Row b) presents a comparison of aerogels prepared from 2 wt% cellulose/[Emim][EDP] using different parameters: reduction of the dissolution temperature from 80 to 40°C and change of the coagulation conditions. Shrinkage was observed with decreasing dissolution temperature. The row c) shows an aerogel with a rough surface obtained from [Emim][Ac] solutions.

Although SC drying maintains the pore structure, some shrinkage is always present. Shrinkage is associated to the level of chains entanglement in the hydrogel. The shrinkage is more pronounced when cellulose concentration increased from 1 wt% to 2 wt% which agrees with the results reported for natural polymer hydrogel [34]. Similar behavior was observed with run 2. As can be observed in Fig. 6 the shrinkage of the cellulose aerogels produced from alcogels that coagulated solely in pure ethanol (run 13) was more pronounced in comparison to the aerogels produced from the alcogels coagulated successively in ethanol solution (run 12), as shown in Figure 5 b).

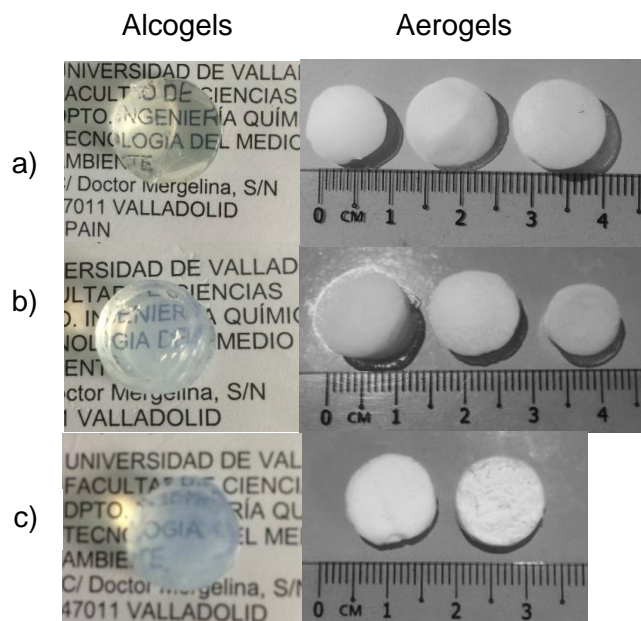


Fig. 5 Cellulose alcogels and cellulose aerogels: a) [Amim][Cl] run 3, 4, 5; b) [Emim][DEP] run 11, 12, 13; c) [Emim][Ac] run 10

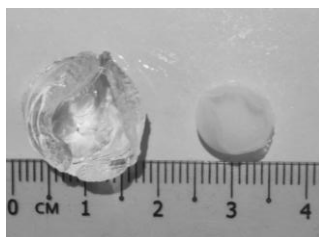


Fig. 6 Comparison of the size of alcogel (run 13) and the aerogel

3.2. Supercritical impregnation onto cellulose aerogels

Table 12 Loading capacity of cellulose aerogels impregnated with phytol by supercritical CO₂

Aerogels regenerated: Ionic liquid / wt% cellulose	*Specific surface area, m ² /g	*Pore volume (cm ³ /g)	*Pore size (nm)	Loading, %L	References
[Amim][Cl] / 2%	426	0.8	9.4	48.7 ± 0.5	This work
[Amim][Cl] / 4%	278	2.4	34	52.3 ± 0.9	This work
[Emim][DEP] / 2%	326	1.4	18	55.4 ± 0.3	This work
Silica aerogels	882	2.9	12.9	30.1 ± 0.6	Mustapa, Martin, Sanz-Moral, Rueda and Cocero [26]
Alginate aerogels	126	0.8	25.5	22.1 ± 0.2	Mustapa, Martin, Sanz-Moral, Rueda and Cocero [26]

* Porosimetry before the SC impregnation

Impregnation of phytol as model bioactive compound was performed to determine the loading capacity of the produced cellulose aerogels. The impregnation was performed using SC-CO₂ at 100 bar and 40°C during 24 h. The amount of phytol employed for impregnation is based on its solubility in SC-CO₂ reported by Lazo [35]. The mass ratio of cellulose aerogels/phytol was maintained constant at 0.1 for all the impregnation series. It was shown that increasing the cellulose concentration resulted in a decrease of the specific surface area of the cellulose aerogels and increase in aerogel pore size and pore volume. However, the loading capacity of the aerogels was higher with the increase of the cellulose concentration for the same IL. As indicated in the Table 12, the aerogels produced from 2 wt% cellulose solution in [Amim][Cl] with a surface area of 426 m²/g yielded lower loading with 48.9 ± 0.5wt% of phytol compared to the ones produced in 4 wt% cellulose solution in [Amim][Cl] with 278 m²/g surface area. Higher phytol loading of 52.3 ± 0.9wt% in aerogel produced from 4 wt% cellulose solution in [Amim][Cl] could be due to the larger pore volume and size in comparison to the one produced in 2 wt% cellulose solution in [Amim][Cl], which enhance the penetration of SC-CO₂ into the inner parts of the cellulose aerogels. On the other hand, aerogels made from 2 wt% cellulose solution in [Emim][DEP], exhibited little higher loading capacity with 55.4 ± 0.3 wt% of phytol compared to the loading in cellulose aerogels regenerated from 2 and 4 wt% cellulose solutions in [Amim][Cl]. Although the latter has the highest surface area, its lower pore volume and pore size reduced the drug load capacity. This indicates that pore volume and pore size are the properties

with a stronger influence on the compound loading into aerogels by SC-CO₂ impregnation. Furthermore, lower phytol loading content was achieved in the aerogel produced from 2 wt% cellulose solution in [Amim][Cl] than in the one generated from 2 wt% cellulose solution in [Emim][DEP] with a lower surface area. Nevertheless the behavior of these effects needs further investigation for different polymer or biopolymer materials. The reason for the variation of loading capacity for different regenerated cellulose by IL is still unknown and to the best of our knowledge there is no literature on these aspects. In contrast, Mustapa, Martin, Sanz-Moral, Rueda and Cocero [26] who performed SC impregnation of phytol at 200 bar and 40°C obtained loading of 20.1 ± 0.2 to 30.1 ± 0.6 wt% for alginate and silica aerogels, respectively. The phytol loading in silica and alginate aerogel are lower even though the impregnation was performed at higher pressure and in the case of silica aerogel pore volume and pore size are higher than of cellulose ones. Thus, higher loading in cellulose aerogel could be due to different biopolymer materials used that lead to different affinity of the compound for the materials.

The IR spectrum of the non- and impregnated aerogels regenerated from 2 wt% cellulose solution in [Amim][Cl] are presented in Fig.7. The appearance of the vibration peak at 2900 cm⁻¹ that corresponds to the -CH groups and the increment of the absorbance intensity at 1380, 1440 and 3400 cm⁻¹ due to the vibration band of C-H, C-C and -OH, respectively indicates the presence of phytol loaded in the cellulose aerogels. In addition, all the cellulose aerogels produced in this work shown a similar IR spectrum after impregnation with phytol, indicating that the phytol has similar interaction with the cellulose material regardless the type of IL used in the regeneration process.

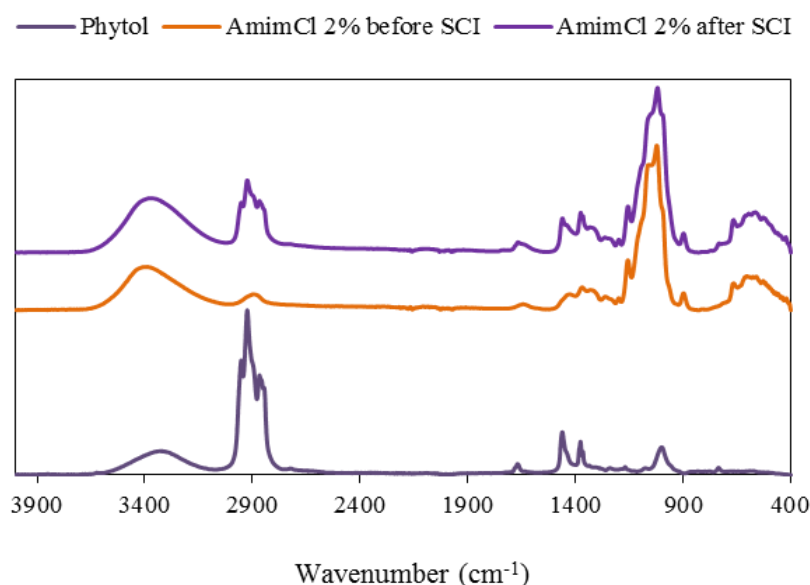


Fig.7 FTIR spectrum of non- and impregnated cellulose aerogels regenerated with phytol by supercritical CO₂ at 100 bar and 40°C

In Fig. 8, the SEM images of non- impregnated and impregnated cellulose aerogels formed from 2 wt% cellulose solution in [Amim][Cl] are presented. It can be seen that the pore morphology became coarser after the impregnation with phytol. Furthermore, it is observed that the morphology of cellulose fibrils was maintained indicating that the high impregnation yield of phytol (from 48.7 ± 0.5 to 55.4 ± 0.3 wt%) by SC-CO₂ did not change or swell the surface morphology of the biopolymer. In a previous work [36], in which cellulose acetate with thymol was impregnated by SC-CO₂ at 100 bar and 35°C in 24h, it was demonstrated that after impregnation the morphology of the biopolymer significantly changed by swelling and melting, especially when the impregnation yield was increased, due to the impact of thymol on the structure of cellulose acetate. This work also showed that the yields varied from 42.86 ± 1.14 % to 55.31 ± 1.36 % depending on the cellulose acetate/thymol mass ratio from 1 to 0.33 at 100 bar and 35°C.

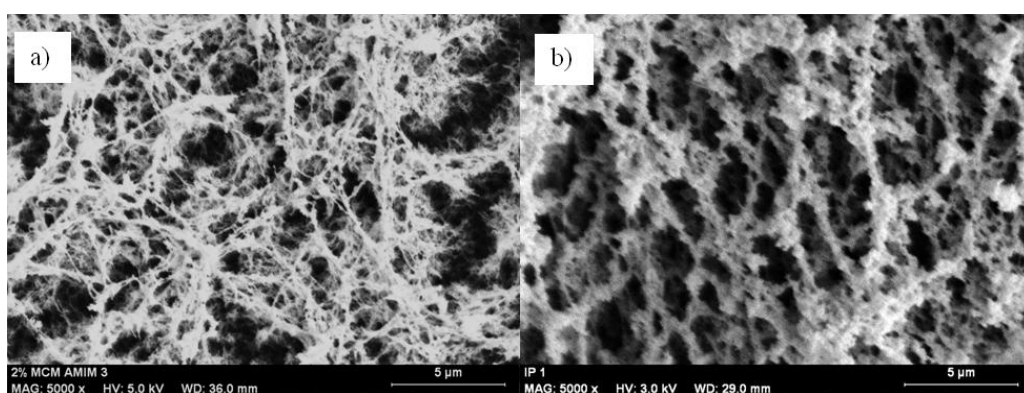


Fig. 8 SEM images of the a) non- and b) impregnated cellulose aerogels regenerated from 2% cellulose solution in [Amim][Cl]

4. Conclusions

The properties of cellulose aerogels prepared from a solution of microcrystalline cellulose and alkylmethylimidazolium ionic liquids can be tuned using different ionic liquids with different anions and cations, and at different dissolution temperature, concentration of cellulose and composition of the coagulation bath. Optimal cellulose concentrations in aerogel preparation are 1-2 wt%. In this concentration range the aerogels prepared from imidazolium chloride ionic liquids have higher surface areas than those obtained from other cellulose dissolving ILs with lower viscosities and melting points. Reducing dissolution temperature decreased the surface area of aerogels but increased pore volume and pore size, although more experimental data is needed in this matter. The same applies to the use of absolute ethanol as coagulant to improve surface area, pore volume and pore size of aerogels.

The aerogel was loaded with phytol as a model compound, obtaining loads of approximately 50 wt%. These values are much higher than loadings in phytol of SiO₂ or alginate aerogels achieved in previous works. The drug loading capacity of the cellulose aerogels was positively influenced by the pore size and volume. Results of IR spectra showed that the cellulose aerogels regenerated from different IL has similar interaction with the phytol model compound.

Acknowledgments

Authors thank the Marie Curie Program for the Project DoHip “Training program for the design of resource and energy efficient products for high pressure process”, the Junta de Castilla y León for funding through the project VA295U14 . MDB thank the Spanish Ministry of Economy and Competitiveness for the Ramón y Cajal research fellowship. Ana N. Mustapa acknowledges a sponsorship of the program from Ministry of Education (MOE), Malaysia, supported together with Universiti Teknologi MARA (UiTM), Faculty of Chemical Engineering Shah Alam, Selangor.

References

1. García-González, C.A., M. Alnaief, and I. Smirnova, Polysaccharide-based aerogels—Promising biodegradable carriers for drug delivery systems. *Carbohydrate Polymers*, 2011. 86(4): p. 1425-1438.
2. Wang, S., A. Lu, and L. Zhang, Recent advances in regenerated cellulose materials. *Progress in Polymer Science*, 2016. 53: p. 169-206.
3. Hüsing, N. and U. Schubert, Aerogels—Airy Materials: Chemistry, Structure, and Properties. *Angewandte Chemie International Edition*, 1998. 37(1-2): p. 22-45.

4. Haimer, E., M. Wendland, K. Schluffer, K. Frankenfeld, P. Miethe, A. Potthast, T. Rosenau, and F. Liebner, Loading of Bacterial Cellulose Aerogels with Bioactive Compounds by Antisolvent Precipitation with Supercritical Carbon Dioxide. *Macromolecular Symposia*, 2010. 294(2): p. 64-74.
5. Oshima, T., T. Sakamoto, K. Ohe, and Y. Baba, Cellulose aerogel regenerated from ionic liquid solution for immobilized metal affinity adsorption. *Carbohydrate Polymers*, 2014. 103: p. 62-69.
6. Jin, C., S. Han, J. Li, and Q. Sun, Fabrication of cellulose-based aerogels from waste newspaper without any pretreatment and their use for absorbents. *Carbohydrate Polymers*, 2015. 123: p. 150-156.
7. Huang, H.-D., C.-Y. Liu, D. Zhou, X. Jiang, G.-J. Zhong, D.-X. Yan, and Z.-M. Li, Cellulose composite aerogel for highly efficient electromagnetic interference shielding. *Journal of Materials Chemistry A*, 2015. 3(9): p. 4983-4991.
8. Mikkonen, K.S., K. Parikka, A. Ghafar, and M. Tenkanen, Prospects of polysaccharide aerogels as modern advanced food materials. *Trends in Food Science & Technology*, 2013. 34(2): p. 124-136.
9. Hallett, J.P. and T. Welton, Room-Temperature Ionic Liquids: Solvents for Synthesis and Catalysis. 2. *Chemical Reviews*, 2011. 111(5): p. 3508-3576.
10. Zhao, D., H. Li, J. Zhang, L. Fu, M. Liu, J. Fu, and P. Ren, Dissolution of cellulose in phosphate-based ionic liquids. *Carbohydrate Polymers*, 2012. 87(2): p. 1490-1494.
11. Xu, A., Y. Zhang, Y. Zhao, and J. Wang, Cellulose dissolution at ambient temperature: Role of preferential solvation of cations of ionic liquids by a cosolvent. *Carbohydrate Polymers*, 2013. 92(1): p. 540-544.
12. Wang, X., H. Li, Y. Cao, and Q. Tang, Cellulose extraction from wood chip in an ionic liquid 1-allyl-3-methylimidazolium chloride (AmimCl). *Bioresource Technology*, 2011. 102(17): p. 7959-7965.
13. Swatloski, R.P., S.K. Spear, J.D. Holbrey, and R.D. Rogers, Dissolution of Cellulose with Ionic Liquids. *Journal of the American Chemical Society*, 2002. 124(18): p. 4974-4975.
14. Ohno, E. and H. Miyafuji, Reaction behavior of cellulose in an ionic liquid, 1-ethyl-3-methylimidazolium chloride. *Journal of Wood Science*, 2013. 59(3): p. 221-228.
15. Takegawa, A., M.-a. Murakami, Y. Kaneko, and J.-i. Kadokawa, Preparation of chitin/cellulose composite gels and films with ionic liquids. *Carbohydrate Polymers*, 2010. 79(1): p. 85-90.

16. Liu, W. and T. Budtova, Ionic liquid: A powerful solvent for homogeneous starch–cellulose mixing and making films with tuned morphology. *Polymer*, 2012. 53(25): p. 5779-5787.
17. Paakko, M., J. Vapaavuori, R. Silvennoinen, H. Kosonen, M. Ankerfors, T. Lindstrom, L.A. Berglund, and O. Ikkala, Long and entangled native cellulose I nanofibers allow flexible aerogels and hierarchically porous templates for functionalities. *Soft Matter*, 2008. 4(12): p. 2492-2499.
18. Aaltonen, O. and O. Jauhiainen, The preparation of lignocellulosic aerogels from ionic liquid solutions. *Carbohydrate Polymers*, 2009. 75(1): p. 125-129.
19. Li, J., Y. Lu, D. Yang, Q. Sun, Y. Liu, and H. Zhao, Lignocellulose Aerogel from Wood-Ionic Liquid Solution (1-Allyl-3-methylimidazolium Chloride) under Freezing and Thawing Conditions. *Biomacromolecules*, 2011. 12(5): p. 1860-1867.
20. Tsiptsias, C., A. Stefopoulos, I. Kokkinomalis, L. Papadopoulou, and C. Panayiotou, Development of micro- and nano-porous composite materials by processing cellulose with ionic liquids and supercritical CO₂. *Green Chemistry*, 2008. 10(9): p. 965-971.
21. Sescousse, R., R. Gavillon, and T. Budtova, Aerocellulose from cellulose–ionic liquid solutions: Preparation, properties and comparison with cellulose–NaOH and cellulose–NMMO routes. *Carbohydrate Polymers*, 2011. 83(4): p. 1766-1774.
22. Wang, H., Z. Shao, M. Bacher, F. Liebner, and T. Rosenau, Fluorescent cellulose aerogels containing covalently immobilized (ZnS)_x(CuInS₂)_{1-x}/ZnS (core/shell) quantum dots. *Cellulose*, 2013. 20(6): p. 3007-3024.
23. Demilecamps, A., C. Beauger, C. Hildenbrand, A. Rigacci, and T. Budtova, Cellulose–silica aerogels. *Carbohydrate Polymers*, 2015. 122: p. 293-300.
24. Lu, Y., Q. Sun, D. Yang, X. She, X. Yao, G. Zhu, Y. Liu, H. Zhao, and J. Li, Fabrication of mesoporous lignocellulose aerogels from wood via cyclic liquid nitrogen freezing–thawing in ionic liquid solution. *Journal of Materials Chemistry*, 2012. 22(27): p. 13548-13557.
25. Pantić, M., Ž. Knez, and Z. Novak, Supercritical impregnation as a feasible technique for entrapment of fat-soluble vitamins into alginate aerogels. *Journal of Non-Crystalline Solids*, 2016. 432, Part B: p. 519-526.
26. Mustapa, A.N., A. Martin, L.M. Sanz-Moral, M. Rueda, and M.J. Cocero, Impregnation of medicinal plant phytochemical compounds into silica and alginate aerogels. *The Journal of Supercritical Fluids*.

27. Lopes, J.M., F.A. Sánchez, S.B.R. Reartes, M.D. Bermejo, Á. Martín, and M.J. Cocero, Melting point depression effect with CO₂ in high melting temperature cellulose dissolving ionic liquids. Modeling with group contribution equation of state. *The Journal of Supercritical Fluids*, 2016. 107: p. 590-604.
28. Lopes, J.M., S. Kareth, M.D. Bermejo, Á. Martín, E. Weidner, and M.J. Cocero, Experimental determination of viscosities and densities of mixtures carbon dioxide + 1-allyl-3-methylimidazolium chloride. Viscosity correlation. *The Journal of Supercritical Fluids*, 2016. 111: p. 91-96.
29. Zhang, S., X. Qi, X. Ma, L. Lu, Q. Zhang, and Y. Deng, Investigation of cation–anion interaction in 1-(2-hydroxyethyl)-3-methylimidazolium-based ion pairs by density functional theory calculations and experiments. *Journal of Physical Organic Chemistry*, 2012. 25(3): p. 248-257.
30. Gavillon, R. and T. Budtova, Aerocellulose: New Highly Porous Cellulose Prepared from Cellulose–NaOH Aqueous Solutions. *Biomacromolecules*, 2008. 9(1): p. 269-277.
31. Innerlohinger, J., H.K. Weber, and G. Kraft, Aerocellulose: Aerogels and Aerogel-like Materials made from Cellulose. *Macromolecular Symposia*, 2006. 244(1): p. 126-135.
32. Yang, H., R. Yan, H. Chen, D.H. Lee, and C. Zheng, Characteristics of hemicellulose, cellulose and lignin pyrolysis. *Fuel*, 2007. 86(12–13): p. 1781-1788.
33. Wang, H., G. Gurau, and R.D. Rogers, Ionic liquid processing of cellulose. *Chemical Society Reviews*, 2012. 41(4): p. 1519-1537.
34. Shen, X., J.L. Shamshina, P. Berton, J. Bandomir, H. Wang, G. Gurau, and R.D. Rogers, Comparison of Hydrogels Prepared with Ionic-Liquid-Isolated vs Commercial Chitin and Cellulose. *ACS Sustainable Chemistry & Engineering*, 2016. 4(2): p. 471-480.
35. Lazo, C., Measuring and modeling of mixed adsorption isotherms for supercritical fluid chromatography. 2000, Technische Universität Hamburg (TUHH): Germany.
36. Milovanovic, S., M. Stamenic, D. Markovic, J. Ivanovic, and I. Zizovic, Supercritical impregnation of cellulose acetate with thymol. *The Journal of Supercritical Fluids*, 2015. 97: p. 107-115.

Conclusions and Future Work

In this thesis the influence of CO₂ in different aspects of cellulose processing using ILs has been thoroughly analysed, obtaining the following conclusions:

Part II. Property determination of mixtures CO₂ + Ionic Liquids, in the part II of the thesis:

1. Physical properties of relevancy for biomass processing media CO₂ + ionic liquids were determined and modelled: Melting points of different alkylimidazolium ionic liquids with chloride anions in presence of CO₂ were experimentally determined by the first melting point method. It was found that all the ionic liquids presents melting points depressions lower than 10K at moderated pressures of CO₂ (around 10 MPa). This is relatively low compared to those produced by CO₂ in ionic liquids of other families such as those with alkylimidazolium cation.
2. Parameters of the Group Contribution EoS (GC-EoS) developed by Skjold-Jørgensen were adjusted for the group 1-alkyl-3-methylimidazolium chloride. Thus now, using this EoS is possible to predict phase equilibrium of ionic liquids of the alkylimidazolium chloride family without additional experimental data. Among other data, solubilities of CO₂ in these ionic liquids can be estimated.
3. The melting point depression caused by CO₂ has been calculated using the GC-EoS, and it can be qualitatively described. Better results are achieved after the correlation of the change in the pure IL volume during melting
4. The viscosities and densities of mixture CO₂ + [Amim][Cl] with molar fractions up to 0.25 and temperatures in the range 333-372 K were measured.
5. Densities were used to calculate excess molar values that resulted strongly negative. This indicates that the CO₂ + [Amim][Cl] mixtures present a highly packed structure and can confirm the generally accepted theory that CO₂ is dissolved in the free spaces of ionic liquids and that the expansion of the ionic liquid induced by the presence of CO₂ is very small.
6. Viscosities were correlated as a function of temperature and carbon dioxide molar fractions with an average relative error of 2.5%. The viscosities of other mixtures CO₂ + ionic liquids were also correlated for ionic liquids of other families using literature data.
7. In general [Amim][Cl] and the other ionic liquids present a linear decrease of viscosity with CO₂ molar fractions up to around 0.5 mol that is more pronounced at lower temperatures, and can reach between 60-100% viscosity reduction with respect the viscosity of the pure ionic liquid, making the CO₂ a promising co-solvent for viscosity reduction in process with ionic liquids.

Part III. The influence of CO₂ in reactions systems related with biomass processing, the conclusions are the following:

1. The influence of CO₂ in the solvation rate of cellulose in different ionic liquids at lower pressures was experimentally investigated, obtaining a slight increase in the rate of cellulose dissolution in different ILs in the presence of CO₂ somewhat higher at lower temperature of 50°C, reaching 50% of cellulose dissolved in 30 minutes.
2. The synthesis of cellulose acetate in imidazolium chloride ionic liquids was thoroughly analyzed both by revising literature data as well as by making new experiments. Cellulose acetate was degree of substitution in general improves with temperature, reaction time and excess of acylating reagent.
3. A mathematical model describing the reactions was developed. The model describes experimental data with an average deviation of 14%. To the best of our knowledge is the first kinetic model proposed to describe the process in literature. The parameters used to describe the reaction in [Amim][Cl] cannot describe the reaction in other ILs of the same family suggesting an important role of the IL in the reaction.
4. Experimentally, new reactions were performed in the IL [Amim][Cl], at temperatures from 40 to 80°C covering temperatures lower than those usually studied in the system. It was found that at 40°C degrees of substitution lower than DS=2 are obtained after 24 h reaction while at 80°C reaction can be almost complete at 6 h being the last steps if substitution very slow. These results are consistent with other authors' observations.
5. The influence of catalyst scandium III triflate, previously used for acetylating of other substances in IL was tested for first time for cellulose acetylation. It was found a non significant influence.
6. The acetylation reaction was performed under 80 bar pressure of CO₂. Analysis indicates degrees of substitution much higher than the maximum. This suggests that CO₂ can be incorporating to the resulting polymer in an unexpected way.

Part IV of the thesis, about producing aerogels from cellulose coagulated from an IL solution and drying by sc-CO₂, the conclusions were:

1. The properties of cellulose aerogels prepared from a solution of microcrystalline cellulose in alkylmethylimidazolium ionic liquids can be tuned using different anions and cations and as well different dissolution temperature, concentration of cellulose and composition of coagulation bath.

2. Optimal cellulose concentrations in aerogel preparation are 1-2% w/w. Imidazolium chloride ionic liquids present higher surface areas than other cellulose dissolving ILs with lower viscosities and melting points

3. The drug loading capacity of the cellulose aerogels was positively influenced by their porosity properties.

4. Cellulose aerogels produced in this way absorbed more model compound (phytol) than other aerogels tested in literature, even when some of them presented better porosity properties. This indicates a positive effect of the material. In general it can be concluded that CO₂ could be an interesting co-solvent in cellulose processing in ILs because it can reduce viscosities as much as 43% without causing cellulose precipitation in imidazolium chloride ILs. Nevertheless, the effect found in cellulose solvation was very small and the effect on cellulose substitution reaction was unexpected and further investigation is necessary to identify the resulting polymer.

In relation to the production of aerogels from cellulose dissolved in ionic liquids and dried with supercritical CO₂ it can be concluded that high quality aerogels can be obtained, and that are promising for the absorption of natural substances such as phytol, but further studies of absorption and release of different substances must be made.

Future Work

During this doctoral thesis was developed an investigation on ionic liquids for the efficient dissolution and transformation of lignocellulose into value-added products. This work has demonstrated a sustainable way of biomass processing for support of the industry in the design and implementation of a clean chemical process. It is known that high cost and high viscosity of ILs have been delaying their use in industrial cellulose processing. Carbon dioxide as been proved to be an alternative solvent for melting point and viscosity reduction with the new thermodynamic data on ILs field (Imidazolium chloride family) proposed in this work. Thus, now using this EoS is possible to predict phase equilibrium of ionic liquids of the alkyimidazolium chloride family without additional experimental data, it would be convenient to generate additional equilibrium data of other ionic liquids of the same family in order to further validate the model, and also to extent it to other cellulose dissolving ionic liquids such as the imidazolium alkyl-phosphate ionic liquids.

The measurement of experimental viscosities of the mixture cellulose + ionic liquid + CO₂ could be complementary step for the work on thermophysical properties developed in this thesis.

It has been studied the reaction of cellulose acetylation: degree of substitution (reaction conversion) and reaction yield. However, substituted positions using NMR analysis and the influence of CO₂ on the molecular mass of cellulose esters need to be studied.

Cellulose aerogels from ionic liquid showd their potential uses in the pharmaceutical or medical industry thus a study on the influence of the ILs on the porosity and on drug loading capacity using alkylimidazolium-based ILs is needed.

Resumen

Estudio de la mejora de procesamiento de celulosa en líquidos iónicos por utilizando dióxido de carbono

La capacidad de los líquidos iónicos de disolver altas concentraciones de celulosa y / o lignina a temperaturas relativamente bajas los hace disolventes prometedores para el aprovechamiento de residuos de biomasa lignocelulósica. Se han propuesto muchas aplicaciones en los últimos años: pre-tratamiento para procesos de fermentación, transformaciones químicas para la obtención de químicos y combustibles y reacciones de sustitución para la obtención de polímeros de celulosa derivada entre otros. El uso de líquidos iónicos tiene una serie de ventajas determinadas por la combinación única de sus propiedades. Los líquidos iónicos son un grupo de sales que existen como líquidos a temperaturas relativamente bajas (<100 ° C). Sus propiedades se pueden ajustar por selección apropiada de catión y el anión, y tienen una presión de vapor inconmensurablemente baja que les hace ser considerados disolventes verdes.

En el estado del arte se han revisado y analizado varios aspectos del procesado de celulosa en líquidos iónicos. Las ventajas y desventajas del uso de líquidos iónicos en la producción de derivados de celulosa se discutieron para la esterificación y eterificación de celulosa. La principal limitación de estos procesos es la alta viscosidad que aumenta cuando se disuelve celulosa. Se sabe que cuando los líquidos iónicos disuelven pequeñas cantidades de disolventes moleculares su viscosidad se disminuye drásticamente. Sin embargo, el uso de estos disolventes está limitado por el hecho de que no causen la precipitación de celulosa (como agua o otros disolventes próticos) y que se puede recuperar fácilmente.

El dióxido de carbono se presenta como un co-disolvente prometedor para el procesado de lignocelulosa en líquido iónico ya que es un gas inerte sin limitación ambiental que presenta altas solubilidades en líquidos iónicos incluso a bajas presiones, y se puede separar fácilmente de la mezcla por despresurización. El objetivo de este trabajo es estudiar cómo el CO₂ puede mejorar diferentes aspectos del procesado de biomasa utilizando líquidos iónicos. Para lograr el objetivo de esta tesis varios aspectos se han tenido en cuenta

- 1) Efecto del CO₂ en las propiedades de las mezclas CO₂ + ILs: equilibrio de fases, puntos de fusión puntos, viscosidades y densidades.
- 2) Análisis de la influencia de CO₂ en procesos de reacción, específicamente en reacciones de sustitución con el fin de producir polímeros derivados de la celulosa. Para ello la síntesis bien conocida de acetato de celulosa se elige como modelo de reacción.
- 3) Estudiar la aplicación de CO₂ en la recuperación de materiales valiosos derivados de la celulosa. Para lograr este objetivo se obtiene la preparación de aerogeles de celulosa a partir de los líquidos iónicos mediante secado supercrítico.

Con el fin de alcanzar los objetivos del trabajo se estructura en cuatro partes:

En la primera parte, se revisa el estado de la arte en el **Capítulo 1** "Líquido iónico como medio de reacción para la producción de polímeros derivados de la celulosa a partir de subproductos de biomasa celulósica" donde los temas del mecanismo de disolución de la celulosa, el uso de líquidos iónicos en el pretratamiento y reacciones de sustitución se revisan a fondo. Además

otros temas no tan directamente relacionados, como la toxicidad y reciclado de los líquidos iónicos se consideran porque no son importantes para el desarrollo comercial de estos procesos. Las ventajas y desventajas del uso de líquidos iónicos en la síntesis de derivados de celulosa se discuten para la esterificación y eterificación de celulosa. Sin embargo, los problemas clave como el alto costo y alta viscosidad de líquidos iónicos han retrasado su uso en el procesamiento de celulosa industrial. Además, también se requiere mejorar la eficacia del reciclado y la reutilización de los líquidos iónicos para la aplicación industrial. La mayoría de los líquidos iónicos utilizados para el procesamiento de la celulosa presentan toxicidad y ecotoxicidad baja o moderada, pero se deben hacer estudios adicionales debido a posibles trazas residuales en los materiales y derivados de celulosa regenerada.

En la **Parte II** de propiedades de parte de las mezclas de CO₂ + líquidos iónicos capaces de disolver celulosa objetos de estudio. Esta parte consta de dos capítulos:

En el **Capítulo 2** "Efecto del CO₂ en la disminución del punto de fusión en líquidos iónicos con alta temperatura de fusión capaces de disolver celulosa. Modelado con la ecuación de estado de contribución de grupos "el efecto del dióxido de carbono presurizado en la depresión del punto de fusión (MPD) de algunos líquidos iónicos capaces de disolver biopolímeros se determina experimentalmente usando el método del primer punto de fusión de la superficie del sólido. Se estudiaron cinco ILs diferentes en contacto con dióxido de carbono usando una celda visual de alta presión, hasta 10 MPa. Los resultados experimentales se muestran en la tabla 1.

Tabla 1. Datos experimentales de temperaturas de fusión a diferentes presiones de CO₂

IL	P_{CO_2} (bar)	T_m (K)
[Amim][Cl]	vacuum	311.4 ± 1.3
	10.6 ± 0.5	311.2 ± 0.6
	20.3 ± 0.2	309.3 ± 0.1
	30.9 ± 0.2	306.6 ± 0.6
	41.9 ± 1.4	303.5 ± 0.6
[C ₂ mim][Cl]	Vacuum	341.1 ± 0.6
	12.3 ± 1	341.3 ± 0.2
	20.2 ± 0.3	340.6 ± 0.1
	31.5 ± 1.1	340.6 ± 0.3
	42.1 ± 2.4	339.9 ± 0.2
	50.9 ± 1.1	338.0 ± 1.0
[C ₄ mim][Cl]	100.7 ± 0.4	329.1 ± 0.5
	Vacuum	335.3 ± 2.0

	11.7 ± 0.7	335.2 ± 0.1
	21.7 ± 0.1	333.1 ± 0.1
	41.2 ± 1.1	334.5 ± 0.5
	51.2 ± 1	332.3 ± 0.1
	100.5 ± 0.4	325.3 ± 0.1
<hr/>		
[C ₂ OHmim][Cl]	Vacuum	349.3 ± 0.4
	11.2 ± 1.3	349.5 ± 0.2
	20.7 ± 0.4	349.1 ± 0.5
	41 ± 0.4	348.5 ± 0.4
	52.3 ± 0.1	349.1 ± 1.7
	101.6 ± 1	343.5 ± 0.1
<hr/>		
[Cho][DHP]	Vacuum	385.4 ± 0.3
	20.3 ± 0.3	361.9 ± 1.7
	31 ± 1.2	360.0 ± 1.2
	40.9 ± 0.5	354.1 ± 0.5
	50.1 ± 0.1	352.6 ± 1.0
	100.6 ± 0.2	352.2 ± 0.3

Para correlacionar el MPD de líquidos iónicos de cloruro de imidazolio los parámetros de la ecuación de contribución de grupos de Estado de Skold Jorgensen se ajustaron utilizando datos de la literatura de vapor de líquido y coeficiente de actividad y dilución infinita. De esta manera se obtuvo una correlación predictiva para calcular la solubilidad del CO₂ en diferentes líquidos iónicos de la familia de cloruro de alquilimidazolio. La Fig. 1 muestra la predicción de la solubilidad del CO₂ en otros líquidos iónicos a base de cloruro de imidazolio tratadas en este trabajo evaluado a la temperatura de fusión de cada IL. El modelo predice la solubilidad más grande para CO₂ en [Amim][Cl], y, al mismo tiempo, este es el sistema que muestra la mayor MPD.

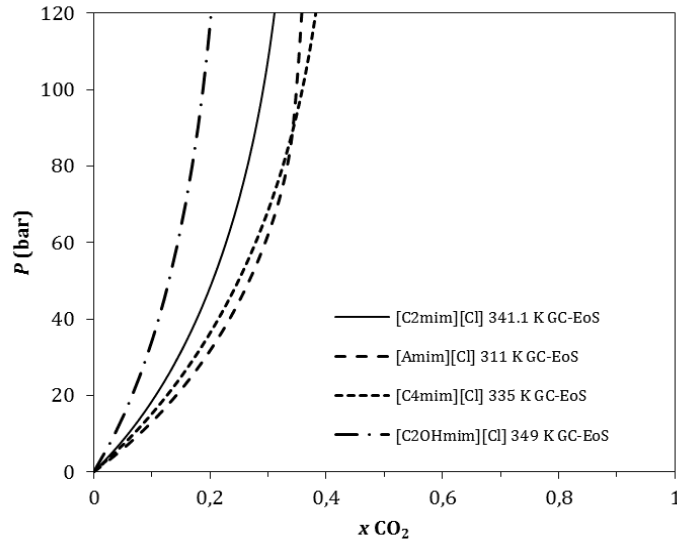


Fig. 1 Comparación de la solubilidad predicha de CO₂ en los líquidos iónicos a base de cloruro de alkylmethylimidazolium utilizados en este trabajo en el punto de fusión de vacío se indica en la Tabla 7. [C2mim] [Cl] (línea continua), [Amim] [Cl] (línea discontinua), [C4mim] [Cl] (línea de puntos) y [C2OHmim] [Cl] (línea discontinua de puntos).

En el **Capítulo 3** "Determinación experimental de viscosidades y densidades de dióxido de carbono + mezclas de cloruro de 1-alil-3-metilimidazolio. Correlación de la viscosidad " se presenta el estudio del efecto de CO₂ de la viscosidad y la densidad del líquido iónico [Amim] Cl. Las viscosidades se correlacionan como en función de la temperatura y fracciones molares CO₂. Las viscosidades de otras mezclas CO₂ + líquidos iónicos también se correlacionaron para otros líquidos iónicos. En general [Amim] Cl y los demás líquidos iónicos presentan una disminución lineal de la viscosidad con fracciones molares CO₂ hasta alrededor de 0,5 mol que más pronunciada a temperaturas más bajas y depende de cada líquido iónico, y pueden alcanzar reducciones de viscosidad desde 60 hasta 100% con respecto la viscosidad del líquido iónico puro. Las viscosidades predichas de varias mezclas AmimCl + CO₂ predichas por la correlación de agua se representan en la Fig. 2 como una función de la presión y de la fracción de CO₂ molar. Hay que tener en cuenta que las fracciones molares de CO₂ en el líquido iónico que corresponden a una determinada presión y temperatura se calcularon con los GC-EOS. Las viscosidades se pueden predecir con desviaciones medias de 4 a 13% y las desviaciones máximas de 15 a 46%.

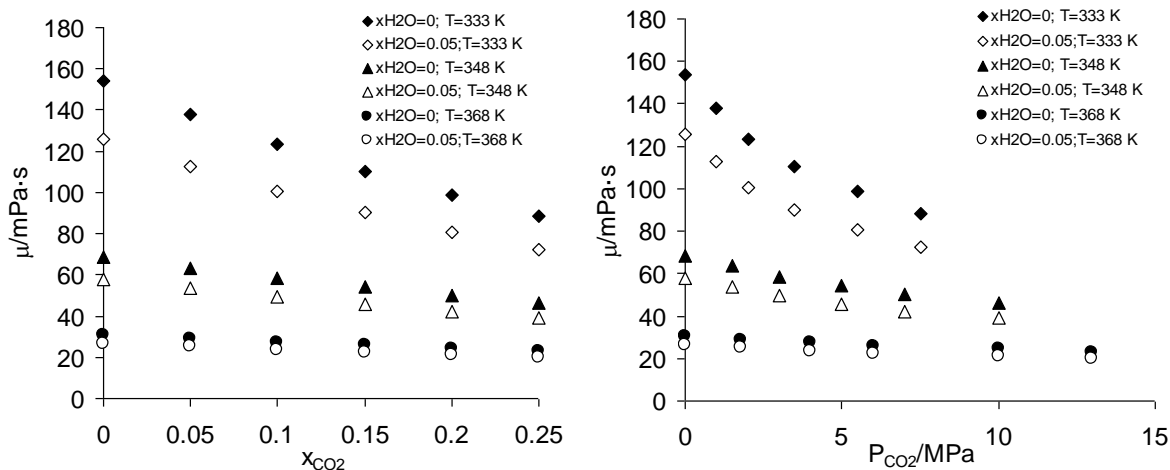


Fig. 2. Viscosidad predicha por la correlación en función de la fracción molar de CO₂ y la presión de CO₂ para diferentes temperaturas y concentraciones iniciales de agua del líquido iónico [Amim][Cl]

En la **Parte III** de la tesis, se pone el foco en la reacción de acetilación de celulosa en líquidos iónicos de cloruro de imidazolio. Consiste en el capítulo 4 "Análisis de la síntesis de acetato de celulosa en líquidos iónicos. Estudio experimental, modelado y uso de aditivos y codisolventes", donde se analiza la síntesis de acetato de celulosa en líquidos iónicos. Para ello, el grado de sustitución de celulosa acetilada se han medido experimentalmente para 40, 60 y 80°C y tiempos de residencia entre 1 y 24 h en el líquido iónico AmimCl, que comprende de este modo un rango de temperatura (inferior a 60°C) poco estudiado en la literatura. Además se investigaron las influencias de aditivos como el escandio III triflato y el CO₂. Se analizaron también otros factores como la utilización de líquidos iónicos de diferentes proveedores y el contenido de agua. Un modelo matemático fue desarrollado utilizando datos de literatura y datos experimentales, obteniendo parámetros cinéticos parámetros. En la Fig. 3 se muestran las predicciones de la evolución de reacción durante 60 y 80°C y para 4,5 mol de reactivo por mol de AGU.

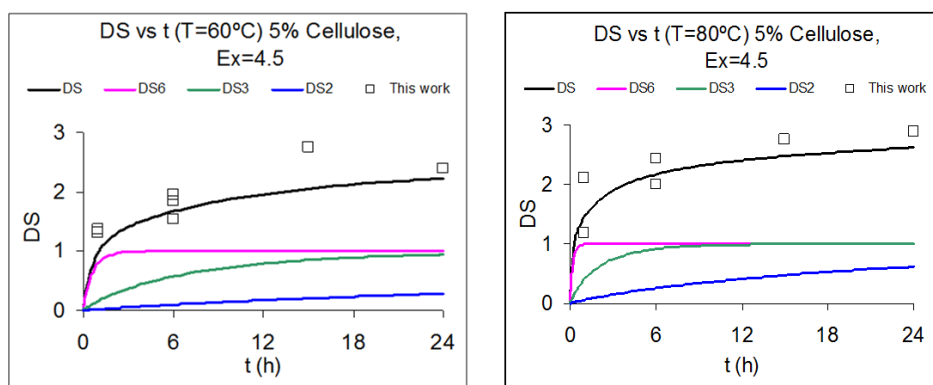


Fig. 3 Comparison of DS prediction by the model and experimental data from this work for reaction at 60 and 80°C

En la Fig. 4 la influencia de la relación de anhídrido acético / AGU de acuerdo con el modelo se muestra y se compara con diferentes datos experimentales.

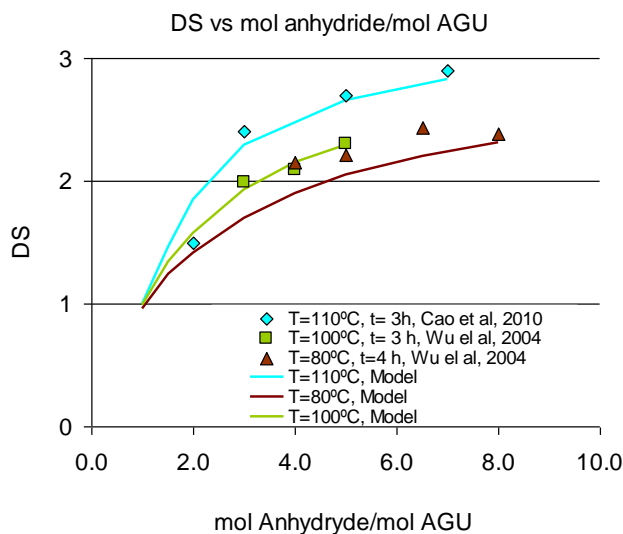


Fig. 4 Relación entre mol de anhídrido acético / AGU mol y el grado de sustitución

La **Parte IV** de la tesis está dedicada a la obtención de materiales de alto valor a partir de la celulosa. Consiste en el **Capítulo 5** "Aerogeles de celulosa regenerada a partir de celulosa microcristalina + solución de líquido iónico: propiedades y estudio de la capacidad de carga de fármaco" en el que se presenta el estudio sobre la influencia de los líquidos iónicos, temperatura de disolución y baño de coagulación en el área superficial, el volumen y el tamaño de poro de los aerogeles de celulosa producidos mediante secado por CO₂ supercrítico. Los aerogeles de celulosa a partir de soluciones de celulosa en líquidos iónicos se prepararon con cinco líquidos iónicos con catión derivado del alquilmetilimidazolio diferentes. Las concentraciones de celulosa óptimas para la preparación de aerogel son 1-2% w / w. El aerogel se cargó con fitol como un compuesto modelo de la obtención de cargas de alrededor de 50% w / w. La capacidad de carga de fármaco de los aerogeles de celulosa fue influenciada positivamente por sus propiedades de porosidad y resultó ser mucho mejor que los aerogeles de diferentes materiales probadas en literatura. Las mayores áreas superficiales se obtuvieron usando 1% en peso de celulosa disuelto en [Amim][Cl] (434 m² g⁻¹). Las diferentes condiciones de coagulación y secado crítica utilizados influyeron en las propiedades de los aerogeles. En este trabajo propiedades similares se obtuvieron con [Amim][Cl] y [Bmim][Cl] para la concentración de celulosa de 2% en peso. Los aerogeles preparados con la concentración más baja (0,2%) no se secaron debido al gel de alta fragilidad. Los líquidos iónicos [Emim][AC] y [Emim][DEP] presentan un punto de fusión y viscosidad menores que las de otros derivados de imidazolio y son capaces de disolver celulosa a temperaturas más bajas. La solución 2% en peso de celulosa en [Emim][DEP] mostró resultados diferentes, así como con diferentes

condiciones de coagulación. Los aerogeles preparados con [Emim][Ac] mostraron las mismas propiedades de [Emim][DEP] en que se disolvió la celulosa a 40°C.

Tabla 2. Comparación de la carga de fitol en diferentes aerogeles

Aerogels regenerated: Ionic liquid / wt% cellulose	*Specific surface area, m ² /g	*Pore volume (cm ³ /g)	*Pore size (nm)	Loading, %L	References
[Amim][Cl] / 2%	426.3	0.8	9.4	48.7 ± 0.5	This work
[Amim][Cl] / 4%	278.4	2.4	34	52.3 ± 0.9	This work
[Emim][DEP] / 2%	326.2	1.4	18	55.4 ± 0.3	This work
Silica aerogels	881.5	2.9	12.9	30.1 ± 0.6	[34]
Alginate aerogels	125.9	0.8	25.5	22.1 ± 0.2	[34]

* Porosimetry before the SC impregnation

Tabla 4 Capacidad de carga de los aerogeles de celulosa impregnada con fitol por CO₂ supercrítico

Los aerogeles producidos con una concentración del 2% de celulosa en AmimCl tienen un área superficial de 426.3 m² / g y un rendimiento de carga de 48,7 ± 0,5% en peso de fitol en comparación con los producidos con un 4% de celulosa en AmimCl que tiene 278,4 m² / g superficie (Tabla 2). Se produjo mayor carga fitol con 52,3 ± 0.9wt% en los aerogeles de celulosa preparados AmimCl con un 4% de celulosa. Esto podría ser debido a al mayor volumen de poro y tamaño en comparación con los aerogeles de celulosa preparados con AmimCl al 2%, que mejora la penetración de SC-CO₂ en la parte interior de los aerogeles de celulosa Además, una mayor área superficial de los aerogeles producidos en Emim[DEP] da como resultado un contenido de fitol más alto.

En esta tesis la influencia de CO₂ en diferentes aspectos del procesado de celulosa usando líquidos iónicos se ha analizado, obteniendo las siguientes **conclusiones**:

Las propiedades físicas de relevancia para el procesado de biomasa en mezclas CO₂ + líquidos iónicos se determinaron y modelaron. Los puntos de fusión de diferentes líquidos iónicos alquilimidazolio con aniones cloruro en presencia de CO₂ se determinaron experimentalmente por el método del primer punto de fusión. Se encontró que todos los líquidos iónicos presentan disminuciones de puntos de fusión menores 10K a presiones moderadas de CO₂ (alrededor de 10 MPa). Esto es relativamente bajo en comparación con los producidos por CO₂ en líquidos iónicos de otras familias con cationes alquilimidazolio. Se ajustaron parámetros de la EOS

contribución de grupos (GC-EOS) desarrollada por Skjold-Jørgensen para líquidos iónicos de la familia cloruro de 1-alkil-3-metilimidazolium. Por lo tanto ahora, usando esta EoS es posible predecir equilibrio de fases de líquidos iónicos de la familia de cloruro de alquilimidazolio sin datos experimentales adicionales. Entre otros datos, se pueden estimar solubilidades de CO₂ en estos líquidos iónicos. La depresión del punto de fusión causado por el CO₂ se ha calculado utilizando la GC-EOS, y puede ser descrito cualitativamente. Se obtienen mejores resultados después de la correlación de la variación en el volumen del líquido iónico puro durante la fusión

Se midieron las viscosidades y densidades de la mezcla CO₂ + [Amim] Cl con fracciones molares de hasta 0,25 y temperaturas en el rango de 333 a 372 K. Las densidades se utilizaron para calcular los valores molares en exceso que resultaron fuertemente negativos. Esto confirma la teoría generalmente aceptada de que el CO₂ se disuelve en los espacios libres de los líquidos iónicos y que la expansión del líquido iónico inducido por la presencia de CO₂ es muy pequeña. Las viscosidades se correlacionaron en función de la temperatura y de la fracción molar de dióxido de carbono con un error relativo promedio de 2,5%. Las viscosidades de otras mezclas de CO₂ + líquidos iónicos también se correlacionaron para líquidos iónicos de otras familias usando datos de la literatura. En general [Amim] Cl y los demás líquidos iónicos presentan una disminución lineal de la viscosidad con fracciones molares CO₂ hasta alrededor de 0,5 mol que es más pronunciada a temperaturas más bajas, y pueden alcanzar reducciones de la viscosidad desde 60 hasta 100% respecto de la viscosidad del líquido iónico puro, haciendo que el CO₂ de un co-disolvente prometedor para la reducción de la viscosidad en proceso con líquidos iónicos.

La influencia de CO₂ en la velocidad de solvatación de la celulosa en varios líquidos iónicos a presiones más bajas se investigó experimentalmente. Se observó un ligero aumento en la velocidad de disolución de celulosa en diferentes líquidos iónicos en presencia de CO₂, algo superior a 50°C, alcanzando 50% de celulosa disuelta en 30 minutos.

La síntesis de acetato de celulosa en líquidos iónicos de cloruro de imidazolio se analizó a fondo tanto mediante la revisión de datos de la literatura, como con nuevos experimentos. El grado de sustitución de acetato de celulosa en general mejora con la temperatura, tiempo de reacción y el exceso de reactivo acilante. Se desarrolló un modelo matemático que describe las reacciones. El modelo describe los datos experimentales con una desviación media del 14%. Por lo que sabemos es el primer modelo cinético propuesto para describir el proceso en la literatura. Los parámetros utilizados para describir la reacción de [Amim] Cl no pueden describir la reacción en otros líquidos iónicos de la misma familia que sugieren un importante papel del IL en la reacción. Experimentalmente, las nuevas reacciones se realizaron en el IL [Amim] Cl, a temperaturas de 40 a 80°C que cubren temperaturas más bajas que las habitualmente estudiado en el sistema. Se encontró que a 40 ° C los grados de sustitución eran inferiores a DS = 2 después de la reacción 24 h mientras que en la reacción 80 ° C puede ser casi completada en 6 h siendo los últimos pasos de la sustitución muy lentos. Estos resultados son consistentes con las observaciones de otros autores. La influencia del escandio de triflato III, utilizado anteriormente como catalizador para la acetilación de otras sustancias en LIs fue probado por primera vez para la acetilación de celulosa. Se encontró una ligera influencia positiva, difícil de discriminar del error experimental. La reacción de acetilación se realizó a 80

bar de presión de CO₂. Los análisis indican grados de sustitución mucho más altos que el máximo. Esto sugiere que el CO₂ se puede incorporar al polímero resultante de una manera inesperada.

Las propiedades de los aerogeles de celulosa preparados a partir de una solución de celulosa microcristalina en los líquidos iónicos alkylmethylimidazolium se pueden sintetizar utilizando diferentes LIs con diferentes aniones y cationes, diferentes temperaturas de disolución, concentraciones de celulosa y composiciones del baño de coagulación. Las concentraciones de celulosa óptimas en aerogeles son 1-2% w / w en líquidos iónicos de cloruro de imidazolio. Presentan áreas superficiales más altas que los precipitados de otros líquidos con viscosidades y puntos de fusión menores. La capacidad de carga de fármaco de los aerogeles de celulosa fue influenciada positivamente por sus propiedades de porosidad. Los aerogeles de celulosa producidos de esta manera absorben más compuesto modelo (fitol) que otros aerogeles probados en la literatura, cuando algunos de ellos presentan mejores propiedades de porosidad. Esto indica un efecto positivo del material.

En general se puede concluir que el CO₂ podría ser un interesante co-disolvente en el procesado de la celulosa en líquidos iónicos ya que puede reducir viscosidades un 43% sin causar la precipitación de celulosa en líquidos iónicos de cloruro de imidazolio. Sin embargo, el efecto que se encuentra en la solvatación de celulosa era muy pequeño y el efecto sobre la reacción de sustitución de celulosa fue inesperado es necesario mayor investigación acerca del polímero obtenido. En relación con la producción de aerogeles de celulosa disuelta en líquidos iónicos y secados con CO₂ supercrítico se puede concluir que se pueden obtener aerogeles de alta calidad prometedores para la absorción de sustancias naturales tales como fitol.

Aerogeles de celulosa de líquido iónico enseñó sus posibles usos en la industria farmacéutica o médica tanto, se necesita un estudio sobre la influencia de los líquidos iónicos en la porosidad y en la capacidad de carga de fármaco utilizando líquidos iónicos basados en alquilimidazolio.

Acknowledgements

First I would like to express my sincere gratitude to the head of the High Pressure Processes Group, Prof. María José Cocero Alonso for the continuous support of my PhD study for her motivation, enthusiasm and knowledge.

I would like to thank to Dr. María Dolores Bermejo for her support and her patience. Her guidance helped me throughout the thesis in all the time of research and writing.

I would like to thank Dr. Ángel Martín as well for all his help and ideas.

I thank Prof. Weidner and Dr Sabine Kareth for the research opportunity at Ruhr University Bochum and leading me on an exciting project.

I thank Prof. Knez and Prof. Zoran Novak for offering a work opportunity in their research group at the University of Maribor.

I thank Prof. Edward Lack and Martin Sova for the internship at Natex and for the glimpse of the industrial professional world.

I thank my fellow DoHippies: Gyory Levai, Daniel Varga, Candela Domingues, Elvira Mateos, Sara Marcos, Luca Davico, Alejandro Bartolome, Milica Pantic, Markus Mayer, Amit Zodge and Alba Calvo for all the fun we have had in the last three years.

I would like to thank my fellow labmates: LuisMi, Miriam, Gerardo, Victoria, Yoana, María, Sandra, María José, Sergio, Marta, Alberto, Vanessa, Alvaro, Víctor, Gianluca, Nerea, Nuria, Reinaldo, Rut, Ana Alvarez, Celía, Daniel, Laura, Jorge e Raffaella.

I thank to Ana Najwa for the endless afternoons we were working together, for all the fun we have had and especially for your friendship.

I would like to thank my friends and former coworkers from Universidade Nova de Lisboa: Rita Maduro, Gosia, Ana Nunes, Vesna and Prof. Nunes da Ponte for all the support since the beginning of this journey.

I thank Ana Inês Paninho for her enthusiasm, joy and friendship. I could not have imagined having a better friend helping me when I needed the most.

Last but not the least, I would like to thank my family: Manuela, António Pedro, Paulo e Sofia obrigada pelo vosso carinho. Quero agradecer à Teresa e ao João Reis a vossa amizade e todo o apoio todos estes anos. Agradeço à Amélia pela tua boa disposição e o carinho. À Raquel e Tânia agradeço a vossa amizade. Quero agradecer à minha querida avó Flora por me telefonar (quase) todas as semanas, à minha linda tia Lília pelo carinho e pela companhia mesmo que por skype, ao Zé Pedro e à minha mãe Ermelinda Lopes pelo apoio e carinho.

Finalmente quero agradecer ao Ricardo que me deu força para continuar com o seu amor durante estes anos.

Esta tesis doctoral ha sido financiada a través del programa Marie Curie Proyecto DoHip “Training program for the design of resource and energy efficient products for high pressure process”, y por la Junta de Castilla y León Proyecto VA295U14.

About the author

Joana M. Lopes was born in Lisbon, Portugal. She finished a M. S. in Chemical Engineering at the Universidade Nova de Lisboa, (UNL) Portugal in 2010. After graduation she worked as research fellow at the Laboratory of Thermodynamics of Liquid Solutions and on Supercritical Fluid Extraction at UNL. In July 2013 she was awarded a Marie Curie fellowship to work under the European project DoHip at the University of Valladolid. In July 2013 she started her Ph.D. Thesis at the High Pressure Processes Group. During the Ph.D. the author completed its research work with two secondments: one at the Ruhr-University Bochum in Germany and the other at the University of Maribor in Slovenia.

List of Publication

Joana M. Lopes, Sabine Kareth, M^a Dolores Bermejo, Ángel Martín, Eckhard Weidner, M^a José Cocero, Experimental determination of viscosities and densities of mixtures carbon dioxide + 1-allyl-3-methylimidazolium chloride. Viscosity correlation, *Journal of Supercritical Fluids*, 111 (2016), 91-96.

Joana M. Lopes, Francisco A. Sánchez, S. Belén Rodríguez Reartes, M. Dolores Bermejo, Ángel Martín, M. José Cocero, Melting point depression effect with CO₂ in high melting temperature cellulose dissolving ionic liquids. Modeling with group contribution equation of state, *Journal of Supercritical Fluids*, 107 (2015), 590-604.

Joana M. Lopes, Ana V. M. Nunes, Manuel Nunes da Ponte, Zoran P. Visak, Vesna Najdanovic-Visak, Performance of sodium chloride versus commercial ionic liquid as salting-out media for the separation of nicotine from its aqueous solutions. *Industrial & Engineering Chemistry Research*, 53 (2014), 9883-9888.

Joana M. Lopes, Ana B. Paninho, Marta F. Mólho, Ana V. M. Nunes, Angelo Rocha, Nuno M. T. Lourenço, Vesna Najdanovic-Visak, Biocompatible choline based ionic salts: Solubility in short-chain alcohols, *Journal of Chemical Thermodynamics*, 67 (2013), 99-105.

Malgorzata E. Zakrzewska, Ana B. Paninho, Marta F. Mólho, Ana V. M. Nunes, Carlos A. M. Afonso, Andreia A. Rosatella, Joana M. Lopes, Vesna Najdanovic-Visak, Solubility and phase behavior of binary systems containing salts based on transitional metals, *Journal of Chemical Thermodynamics*, 63 (2013), 123-127.

Joana M. Lopes, Zeljko Petrovski, Rafal Bogel-Lukasik, Ewa Bogel-Lukasik, Heterogeneous palladium-catalyzed telomerization of myrcene with glycerol derivatives in supercritical carbon dioxide: a facile route to new building blocks, *Green Chemistry*, 13 (2011), 2013-2016

Submitted

Joana M. Lopes, M^a Dolores Bermejo, Ángel Martín, M^a José Cocero. Ionic liquid as reaction media for the production of cellulose-derived polymers from cellulosic biomass byproducts. Review.

Joana M. Lopes, Ana M. Mustapa, Milica Pantić, M^a Dolores Bermejo, Ángel Martín, Zoran Novak, Željko Knez, M^a José Cocero. Cellulose aerogels prepared from microcrystalline cellulose + ionic liquid solution: properties and drug loading capacity study.

Oral Presentation:

J. M. Lopes, M.D. Bermejo*, A. Martín, F. A. Sánchez, S. B. Rodríguez Reartes, S. Kareth, E. Weidner, M. J. Cocero "Microcrystalline cellulose processing with supercritical CO₂ in alkylmethylimidazolium chloride ionic liquids", 15th European Meeting on Supercritical Fluids, Essen, Germany, 8-11 May 2016, Essen (Germany) (SPEAKER)

J.M. Lopes, M.D. Bermejo, A. Martín, M.J. Cocero, "Improvement of Cellulose Processing in High Melting Point Ionic Liquids by Using Carbon Dioxide", 10th European Congress of Chemical Engineering, (ECCE10) Nice, France, 27th Sep -1st Oct 2015, Nice (France) (SPEAKER)

J. M. Lopes, F. A. Sánchez, S. B. Rodríguez Reartes, M D. Bermejo, Á. Martín, M^a José Cocero, "Melting Point Depression Effect with CO₂ in High Melting Temperature Cellulose Dissolving Ionic Liquid", Equifase 2015, 28th Junio-1 Julio, 2015 Alicante, Spain

Poster:

Joana M. Lopes, María D. Bermejo, Ángel Martín, María J. Cocero, "Improvement of cellulose processing in high melting point ionic liquids by using carbon dioxide", 2nd EuChemMS Congress on Green and Sustainable Chemistry, 4-7 October, 2015, Lisbon (Portugal)

J. M. Lopes, C. Jiménez, M. D. Bermejo, Á. Martín, M. J. Cocero, Analysis of the Advantages of Using CO₂ as a co-solvent in Cellulose Processing in High Melting Point Ionic Liquids, Iberoamerican Meeting on Ionic Liquids (IMIL15), July 2-3, 2015, Madrid (Spain)

J. M. Lopes, F. A. Sánchez, S. B. Rodríguez Reartes, M D. Bermejo, Á. Martín, M^a José Cocero, Experimental Determination of Melting Point Depression Induced by CO₂ in High Melting Temperature Cellulose Dissolving Ionic Liquid. Modeling with GC-EoS", Iberoamerican Meeting on Ionic Liquids (IMIL15), July 2-3, 2015, Madrid (Spain)

J. M. Lopes, M.D. Bermejo, M.J. Cocero, "Improvements of Cellulose Processing in ionic liquids by using carbon dioxide" 10th International Conference on Renewable Resources and Biorefineries, June 2014, Valladolid (Spain)

J. Lopes, M.D. Bermejo, A. Martín, M.J. Cocero, "Intensified Cellulose Conversion in an Ionic Liquid with Supercritical CO₂", EXIL Workshop on ionic liquids, April 2014, Strasbourg (France)

Joana M. Lopes, Małgorzata E. Zakrzewska, Ana V. M. Nunes, Carlos A. M. Afonso, Andreia A. Rosatella, Nuno Torres Lourenço, Ângelo M. R. Rocha, Manuel Nunes da Ponte, Vesna Najdanovic-Visak Solubility and Phase Behaviour of Binary Systems Containing Choline-Derived Salts, 5th International Congress on Ionic Liquids (COIL-5), April 2013, Vilamoura (Portugal)